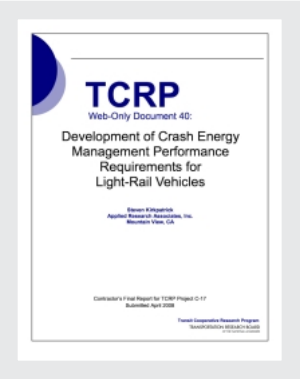

Development of Crash Energy Management Performance Requirements for Light-Rail Vehicles

DETAILS

0 pages | | PAPERBACK
ISBN 978-0-309-43194-1 | DOI 10.17226/22021

AUTHORS

ACKNOWLEDGMENT

This work was sponsored by the Federal Transit Administration (FTA) in cooperation with the Transit Development Corporation. It was conducted through the Transit Cooperative Research Program (TCRP), which is administered by the Transportation Research Board (TRB) of the National Academies.

THE NATIONAL ACADEMIES

Advisers to the Nation on Science, Engineering, and Medicine

The **National Academy of Sciences** is a private, nonprofit, self-perpetuating society of distinguished scholars engaged in scientific and engineering research, dedicated to the furtherance of science and technology and to their use for the general welfare. On the authority of the charter granted to it by the Congress in 1863, the Academy has a mandate that requires it to advise the federal government on scientific and technical matters. Dr. Ralph J. Cicerone is president of the National Academy of Sciences.

The **National Academy of Engineering** was established in 1964, under the charter of the National Academy of Sciences, as a parallel organization of outstanding engineers. It is autonomous in its administration and in the selection of its members, sharing with the National Academy of Sciences the responsibility for advising the federal government. The National Academy of Engineering also sponsors engineering programs aimed at meeting national needs, encourages education and research, and recognizes the superior achievements of engineers. Dr. Charles M. Vest is president of the National Academy of Engineering.

The **Institute of Medicine** was established in 1970 by the National Academy of Sciences to secure the services of eminent members of appropriate professions in the examination of policy matters pertaining to the health of the public. The Institute acts under the responsibility given to the National Academy of Sciences by its congressional charter to be an adviser to the federal government and, on its own initiative, to identify issues of medical care, research, and education. Dr. Harvey V. Fineberg is president of the Institute of Medicine.

The **National Research Council** was organized by the National Academy of Sciences in 1916 to associate the broad community of science and technology with the Academy's purposes of furthering knowledge and advising the federal government. Functioning in accordance with general policies determined by the Academy, the Council has become the principal operating agency of both the National Academy of Sciences and the National Academy of Engineering in providing services to the government, the public, and the scientific and engineering communities. The Council is administered jointly by both the Academies and the Institute of Medicine. Dr. Ralph J. Cicerone and Dr. Charles M. Vest are chair and vice chair, respectively, of the National Research Council.

The **Transportation Research Board** is one of six major divisions of the National Research Council. The mission of the Transportation Research Board is to provide leadership in transportation innovation and progress through research and information exchange, conducted within a setting that is objective, interdisciplinary, and multimodal. The Board's varied activities annually engage about 7,000 engineers, scientists, and other transportation researchers and practitioners from the public and private sectors and academia, all of whom contribute their expertise in the public interest. The program is supported by state transportation departments, federal agencies including the component administrations of the U.S. Department of Transportation, and other organizations and individuals interested in the development of transportation. **www.TRB.org**

www.national-academies.org

CONTENTS

LIST OF FIGURES

LIST OF TABLES

ACKNOWLEDGEMENTS

The results presented in this report are from the analysis efforts at Applied Research Associates, Inc. (ARA). In addition to the author, Robert MacNeill, Claudia Northrup, and Gary Gauthier of the ARA staff made significant technical contributions. However, this study could not have been performed without the support and collaboration of additional organizations. The author would like to acknowledge those people and organizations that contributed directly to the success of this project.

This study would never have been performed without the commitment and support of the members of the American Society of Mechanical Engineers (ASME) Rail Transit (RT) Committee who are working to develop a set of safety standards for light rail vehicles. The current chair of the ASME RT Committee, Martin Schroeder, has been a strong advocate for the development of the light rail vehicle (LRV) safety standards and recognized the need for supporting analyses to complete these standards. Subsequently, Chris Jenks of the Transportation Research Board provided the leadership of this project under the Transit Cooperative Research Program.

Obviously the key aspect of this study is the detailed LRV crash analyses that could not have been performed without the support and models provided by the LRV Manufacturers. Siemens Transportation Systems, Inc. was a strong supporter of this effort and provided models for multiple LRV designs. In addition to the LRV models, Siemens provided engineering support and analyses contributing to the effort to modify two LRV designs for a lower buff strength requirement. In particular, Glenn Gough and Emil Hice provided significant support to this effort.

In addition, Bombardier Transportation also supported this effort by provided a finite element model of one of their LRV designs for use in this study. This alternate vehicle design developed by a second vehicle design team provided additional diversity in the LRV car body structures that significantly improved the confidence in the resulting findings.

Finally, the collisions between LRVs and highway vehicles were performed using models developed under Federal Highway Administration (FHWA) and/or National Highway Traffic Safety Administration (NHTSA) sponsorship and maintained at the FHWA/NHTSA National Crash Analysis Center at the George Washington University. These models are continuously updated by the highway crash analysis community to improve their capabilities in predicting responses in various impact scenarios.

ABSTRACT

This report presents the results of a study to analyze potential crash scenarios for various light rail vehicle designs and apply the results to develop crash energy management guidelines. The crash scenarios involve both collisions between light rail vehicles of identical or dissimilar design and collisions between light rail vehicles and highway vehicles. The analyses were performed using detailed nonlinear dynamic finite element simulations of the collisions between the various vehicle types. Collision responses such as the crash force levels and crush lengths in the colliding light rail vehicles or the maximum crush in the struck highway vehicles were determined and can be used to define crash energy management requirements in a light rail safety standard.

EXECUTIVE SUMMARY

Traditional North American light rail vehicle (LRV) designs have relied on the vehicle's overall static strength to protect occupants in a collision. Although this design approach can be effective in limiting penetration from end collisions, it may lead to heavier vehicle designs and does not assure controlled energy dissipation behaviors that result in crash safety improvements. More modern LRV design methodologies incorporate crash energy management (CEM) strategies. The CEM approach specifies a crash response that absorbs impact energy and smoothly decelerates the vehicle and its occupants with controlled deformation that protects the occupied volume.

In an effort to ensure safety of LRV operations in the United States, The American Society of Mechanical Engineers (ASME) RT-1 Committee is developing a structural safety standard incorporating the CEM design approach. However, the ASME Committee has not reached a consensus on the CEM requirements to include in the safety standard. A series of technical unknowns identified by the ASME RT-1 Committee included:

1. The crash performance of current and past LRVs and variation in performance among vehicles in service.
2. The potential correlation between static buff-strength and crush-strength (dynamic strength).
3. The extent of problems that may exist because of strength incompatibility between colliding LRVs.
4. The appropriate collision speeds or crash energy parameters for the CEM requirements for LRV safety.
5. The relative benefits of collision scenarios specified in previous design requirements for various LRVs.
6. The appropriate CEM specifications for collisions between LRVs and passenger cars.
7. Appropriate strength specifications for protection of low floor LRV occupants from intrusion in side impact by automobiles and light trucks.

These unknowns were an impediment to the development of the ASME RT-1 safety standard for LRVs and served as a justification for this study.

In the initial phase of the study, available data was collected on LRV crashworthiness and safety. The accident data clearly indicated that the vast majority of the injuries and fatalities associated with LRV collisions were a result of collisions between LRVs and highway vehicles (and to a lesser extent with pedestrians and bicyclists). The accident data and collision analyses in this study indicate that the CEM requirements with the highest potential for safety improvements are in the specification of the LRV front-end characteristics to reduce the aggressivity in collisions with highway vehicles. However, there is general agreement that the collisions between two LRVs represent a severe collision condition that can’t be neglected.

The primary tasks in this study were to perform detailed crash analyses for various LRV designs and collision conditions. Results of these analyses were used to demonstrate the level of crashworthiness of current equipment and develop supporting information for the development of an LRV safety standard. The analyses used detailed models of the various LRV and highway vehicle designs in advanced nonlinear dynamic finite element analyses.

The first series of these analyses was the evaluation of the collision response for compatible collisions between two identical LRVs at various collision speeds. In the compatible collision simulations, the bullet (moving) LRV was initialized at the desired collision speed and the target LRV was stationary. Impact simulations were performed for a range of collision speeds (e.g. 5, 10, 15, 20, 25, and 30 mph). The analyses of different severity collisions allowed for the assessment of the range of outcomes for different collision conditions. These analyses establish the expected range of collision behaviors of current equipment. This range of collision behaviors can be used to guide the selection of crash scenarios (e.g. closing speeds) and acceptable outcomes (e.g. crush lengths) in the development of the CEM requirements in the LRV safety standard.

Four different LRV models were used for the collision analyses. A summary of critical design information for each of the LRV models is presented in Table 1. The comparison shows that all of the LRVs are between 40,000 and 47,000 kg and designed to specifications that included a 2g buff load requirement. The primary differences in the LRVs result from the different structural designs developed to meet the specifications and the CEM requirements placed in the design specifications. LRVs 1, 2, and 4 are all 70 percent low floor design. LRV 3 is 100 percent high floor. The design Specifications for LRVs 1 and 2 included analysis of a 20 mph collision of two identical LRVs as a CEM requirement. In addition, LRV 2 had a secondary collision scenario of a 20 mph collision with a second LRV design that had an end girder position that was 230 mm higher than in LRV 2. LRV 3 was designed without any CEM requirements in the design specification (only static load case requirements). Finally, LRV 4 had a CEM collision scenario requirement of a 14 mph collision into a flat rigid wall.

Table 1. Summary of the LRV models

Model	Total Mass	Design Buff Load Requirement	LRV Type	CEM Design Analyses
LRV 1	45,126 kg	2g	70% Low Floor	A
LRV 2	43,010 kg	2g	70% Low Floor	A, B
LRV 3	40,822 kg	2g	100% High Floor	None
LRV 4	46,384 kg	2g	70% Low Floor	C

A. Moving LRV colliding with an identical stationary LRV at 20 mph – brakes applied on both.
B. Incompatible collision of moving and stationary LRVs at 20 mph – 230 mm vertical offset of head girders at collision interface.
C. Single LRV colliding with a rigid wall at 14 mph.

A summary of the average LRV crush lengths for the various collision speeds and LRV designs is presented in Table 2. These crush lengths can be used to assess the appropriateness of proposed CEM requirements for LRV collisions such as those in Table 3. The collision analyses demonstrate that most current LRV designs would meet these proposed CEM levels without significant design modifications. The most difficult requirement for some LRV designs may be to maintain the operator survival space as defined in the severe collision CEM scenario.

Table 2. Summary of vehicle crush lengths (in mm) for the compatible collision analyses.

Average Vehicle Crush (in mm)	Collision Speed					
	5 mph	10 mph	15 mph	20 mph	25 mph	30 mph
LRV 1	3	25	75	202	487	520
LRV 2	8	30	89	171	238	278
LRV 3	11	93	236	364	525	666
LRV 4	—	57	158	274	400	556
Ave All LRVs	7	51	140	253	412	505

Table 3. Proposed CEM requirements for collisions between LRVs.

Crash Severity	Collision Conditions	Pass Criteria
Low	Collision between 2 similar LRVs at closing speed of 8 kph (5 mph)	No structural damage to either LRV
Medium	Collision between 2 similar LRVs at closing speed of 24 kph (15 mph)	Permanent crush distance in the cab not to exceed 300 mm (12 in)
High	Collision between 2 similar LRVs at closing speed up to 40 kph (25 mph)	Crush damage shall be limited to the front cab sections of both colliding vehicles. A 750 mm (30 in) operator's survival space shall be maintained.

The calculated force-crush curves for all of the LRV designs in the 25 mph collision are shown in Figure 1. The comparison shows that the different LRV designs have significantly different force-crush profiles even though they are all designed with a 2g buff strength requirement. This illustrates that the buff strength represents a static proof load and establishes only an initial lower bound in the longitudinal force before significant crushing can be initiated. Beyond the onset of plasticity, there is no direct relationship between the buff strength and the crush strength. The details of the force crush behavior are controlled by the geometry of the structural members in the forward cab and the corresponding crush modes that develop in those structures.

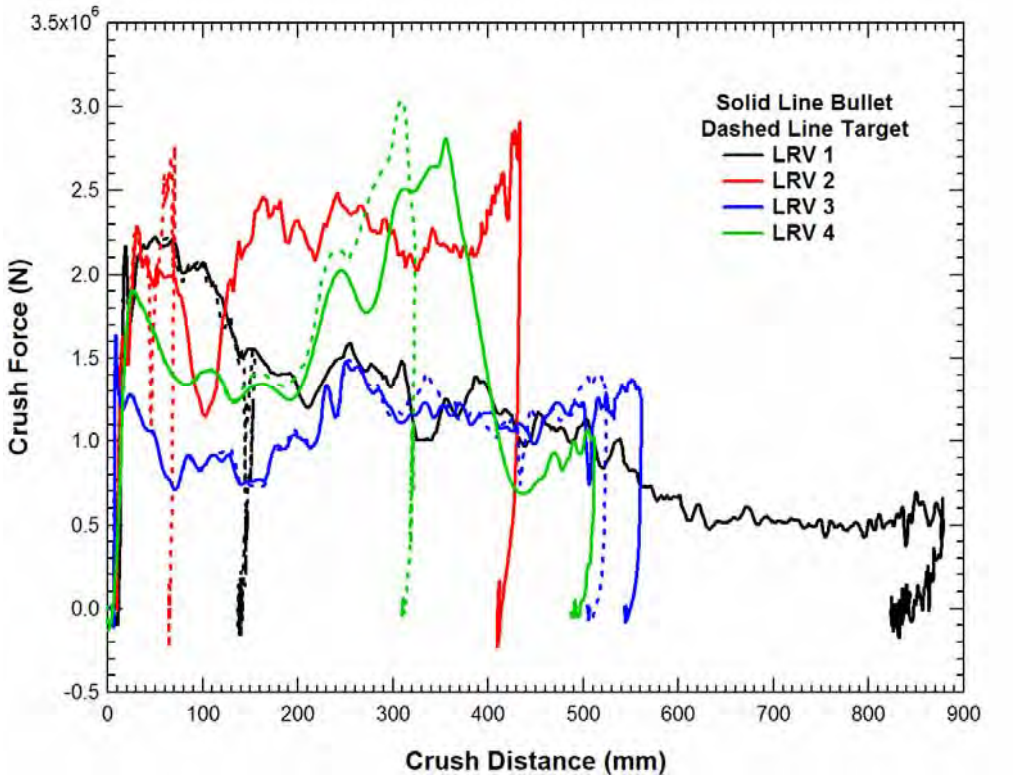

Figure 1. Force-Crush Plots for all the LRVs in the 25 mph Compatible Collisions.

An estimate of the crash decelerations can be obtained by normalizing the crush forces for each LRV by the corresponding vehicle mass. The resulting normalized force-crush curves for all of the LRV designs in the 25 mph collision are shown in Figure 2. All of the LRVs have an initial normalized force above 4g before significant crushing is initiated (note that all of these initial forces are at least twice the 2g buff strength). Subsequently the steady state normalized crush strengths are primarily in the range between 2g and 6g. The two stronger vehicles (LRV 2 and LRV 4) both have a maximum normalized crush force of approximately 7g at a crush displacement of approximately 300-400 mm.

The consequences of these crash acceleration levels on occupant injury potential in LRVs are difficult to assess quantitatively. The accelerations are much lower than those in highway vehicles and lower than expected for many commuter rail cars. In addition, collisions between LRVs that would result in significant crash acceleration pulses are very rare and result in a small fraction of passenger injuries in LRV collisions. As a result, the greatest potential for reducing LRV passenger injuries would be from improving interior crashworthiness rather than limiting crush strengths (e.g. improving crash padding, seating arrangements grab rails, etc.).

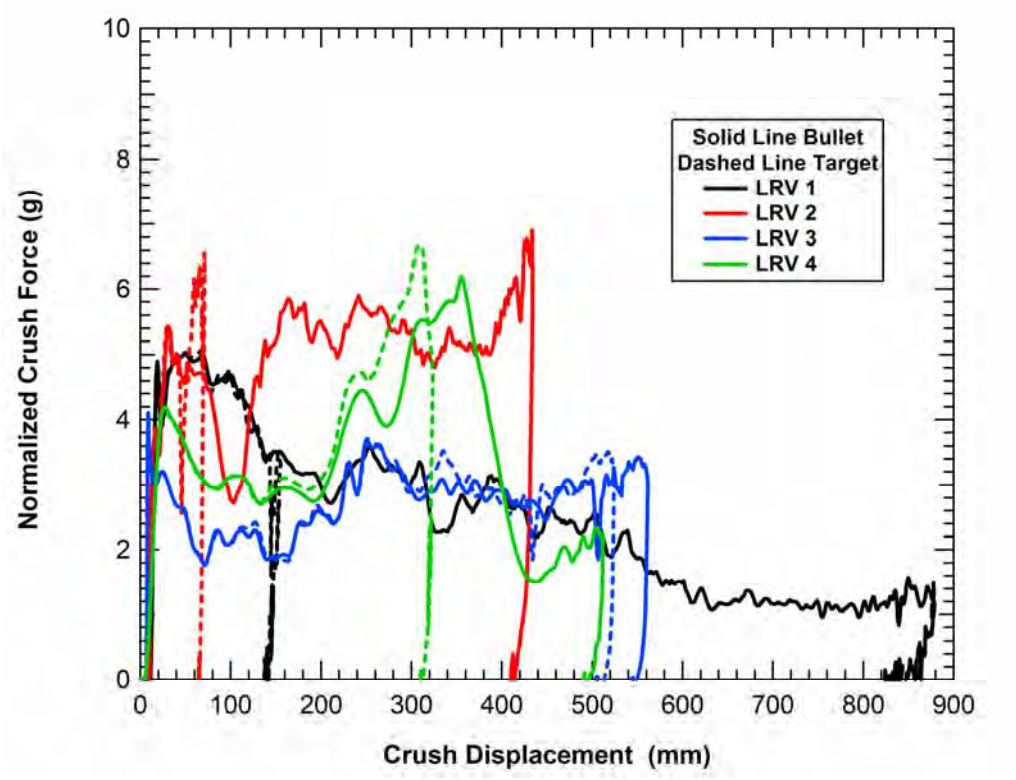

Figure 2. Normalized Crush Forces for the LRVs in the 25 mph Compatible Collisions.

The second set of LRV collision calculations performed were the incompatible collisions between different LRV designs. These analyses are important for understanding the issues associated with the compatibility of vehicles built to a new safety standard with existing vehicles. To assess compatibility concerns, we need to establish the compatibility of the current fleet of vehicles that could be operating together as well as the compatibility of different vehicles built to the same specification under the current state of practice.

The first set of incompatible collision analyses was performed with the two designs with the overall lowest average crush strength (LRV 1 and LRV 3). The comparison of crush strength for these two vehicles in Figure 1 shows that during the initial 200 mm of crush, LRV 1 is significantly stronger than LRV 3. Subsequently, the two have similar crush strengths. However, the high initial crush strength of LRV 1 is higher than the entire curve of LRV 3 out to the crush displacements of 700 mm.

A summary of vehicle force-crush behaviors for the vehicles in the LRV 1 to LRV 3 incompatible collisions is shown in Figure 3. The LRV 1 to LRV 3 incompatible collisions were performed at closing speeds between 5 and 25 mph. The crush curves clearly indicate that the vast majority of the crush occurred in LRV 3 with very little damage to LRV 1. Even at the 25 mph closing speed the LRV 1 damage was limited to 14 mm of crush in the nose of the head girder. A similar behavior would be expected for collisions of either LRV 2 or LRV 4 against

LRV 3 based on the comparison of the crush curves and the relatively high strengths of the other vehicles compared to LRV 3.

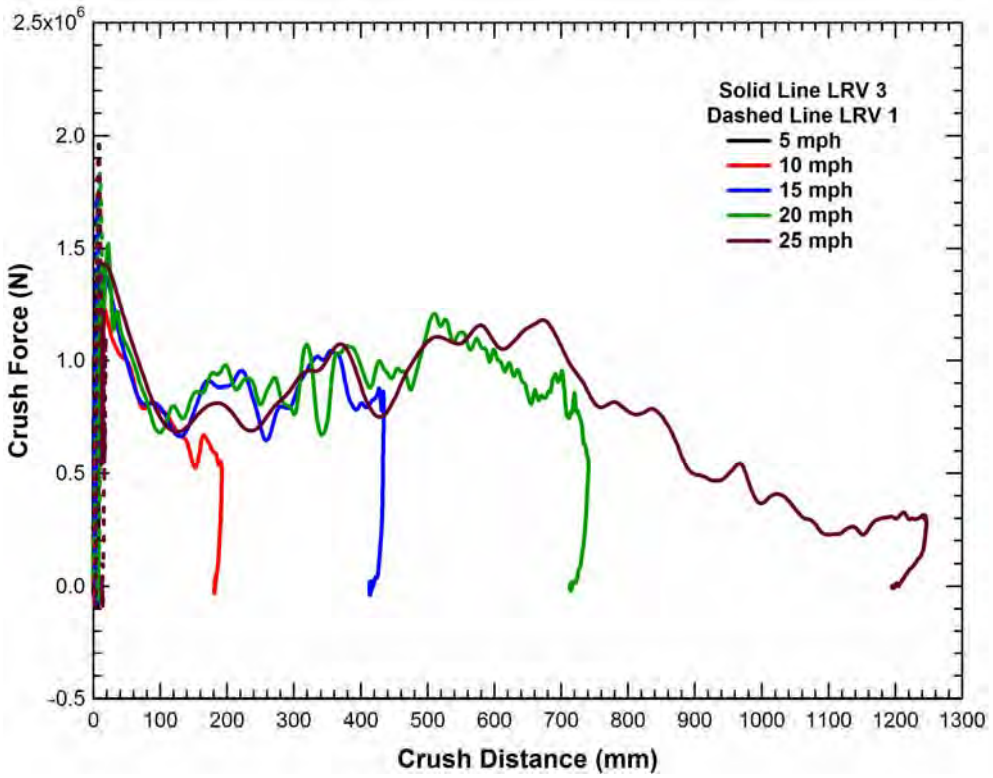

Figure 3. Force-Crush Behaviors for the LRV 1 to LRV 3 Incompatible Crash Analysis.

The subsequent set of incompatible collision analyses was performed with the other two designs (LRV 2 and LRV 4). These two vehicles were designed with very similar specifications on crash safety including both a 2g buff strength and a compatible crash scenario at a closing speed of 15-20 mph. The comparison of the vehicle crush strengths in Figure 1 shows that the two vehicles have both a similar strength in the initial portion of the crush response and the peak crush forces that occur between 300 and 400 mm of crush. However, between 100 and 300 mm of crush, LRV 2 is the stronger of the two vehicles.

A summary of vehicle force-crush behaviors for the vehicles in the LRV 2 to LRV 4 incompatible collisions is shown in Figure 4. These analyses were performed at closing speeds between 20 and 30 mph. The crush distances are more balanced than in the incompatible collisions between LRV 1 and LRV 3. However there is still significantly greater crush in LRV 4 than in LRV 2. The crush curves indicate that LRV 2 absorbs part of the energy in a crush length of approximately 200 mm and the remainder of the crush is in LRV 4. For the higher collision speeds, the crush in LRV 4 is significantly larger than in LRV 2.

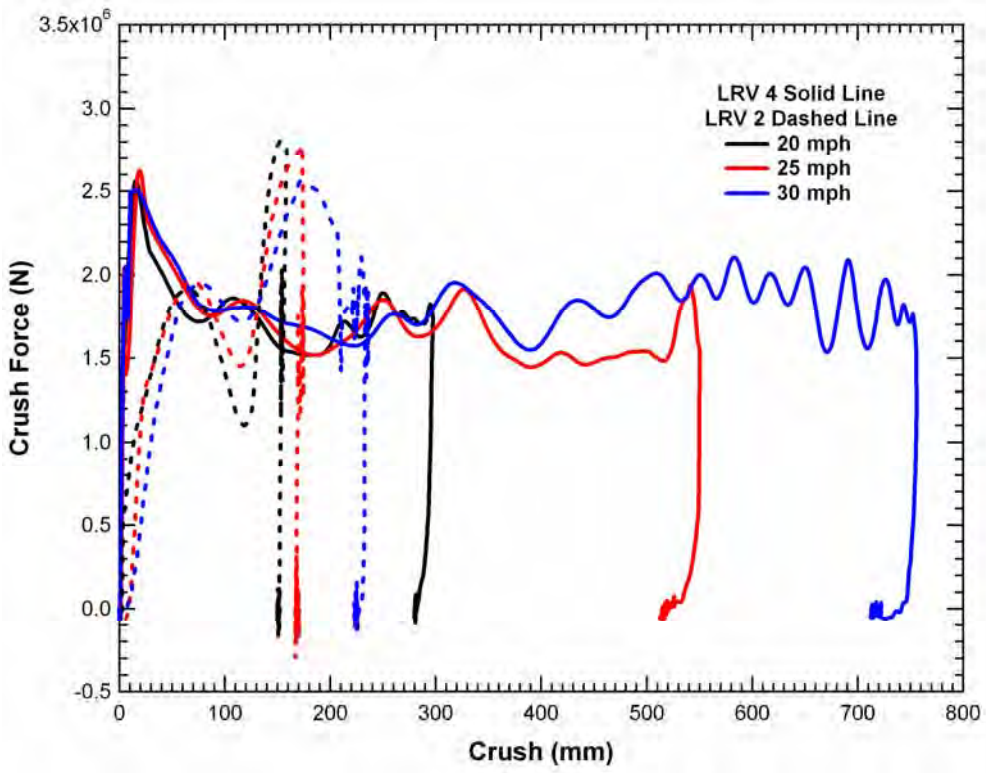

Figure 4. Force-Crush Behavior for the LRV 2 to LRV 4 Incompatible Crash Analysis.

The above summary of the incompatible crash analyses show that the current fleet of LRVs, including vehicles designed to very similar crush strengths, are not sufficiently compatible to obtain a balanced crush in both colliding vehicles. In fact, several of the compatible LRV collision analyses had unbalanced levels of crush in the colliding vehicles. In many of these collisions, the unbalanced crush does not necessarily mean that the collision behaviors obtained are undesirable or result in a greater risk of injuries if the damage remains in unoccupied regions of the vehicle. However, in some cases, the larger crush in one of the vehicles would put the occupants of the cab at a greater risk of injuries. To ensure compatible behavior, much tighter controls on the acceptable force-crush behaviors would be required. Developing these tightly controlled crush behaviors would be very difficult for many existing LRV designs and would add significant cost (and potentially weight) to the LRV designs.

Some specific findings from the LRV collision analyses include:

(1) The various LRV designs that are currently in use have a significant range of crush strengths and collision behaviors. Even vehicles that were designed to nearly identical specifications can have significantly different crush strengths. As a result, current design practice in the United States does not ensure crash compatibility in the existing LRV fleet. The type of incompatibility described here refers to the possibility that most or all of the crush deformation is localized to one of the colliding LRVs. This type of incompatibility is not necessarily a problem for many collisions if the damage remains in unoccupied regions of the vehicle. However, it can lead to higher injury potential in

a more severe collision when the available crush zones in the lower strength vehicle are exhausted.

(2) Some of the LRV designs resulted in asymmetric crush lengths in the two vehicles in the compatible collision scenarios. Greater stability of the crush behavior could be obtained by including specifications on the compatibility of the two LRV crush lengths for these collision scenarios. The most common approach to meet this requirement is to design a crush response with an increasing crush load for larger crush distances. This crush profile is more stable and has been shown to be a favorable behavior for crash safety of rail vehicles. However, the complexity of the LRV cab structures and variations in LRV designs (e.g. rounded cab end structures and variable floor heights) makes the development of a steadily increasing crush strength profile much more difficult than for other rail vehicle types. Given the low probability of these severe LRV collisions the additional requirements on the crush profile may not be justified.

(3) All of the vehicles had minimal damage at the 5 mph collision speed with damage limited to the anticlimber ribs and head girder. This suggests that a 5 mph collision requirement that results in no permanent damage to the vehicle is acceptable. Any energy dissipation requirements at this collision speed could be managed with existing coupler technologies or energy-absorbing bumper systems.

(4) All of the vehicles analyzed had crush behaviors that were generally acceptable up to a collision closing speed above 25 mph. The crush behaviors were all limited to a forward zone in the operator cabin and the average crush lengths in each LRV were approximately 400 mm. This suggests that a 25 mph collision scenario is an achievable level for a high-severity CEM requirement in a safety standard.

To address the influence of buff strength requirements on the collision response, a vehicle design study was performed to modify an LRV with a 2g buff strength design into a vehicle with a 1g buff strength. The design study found that the 50% reduction in the buff strength requirement is expected to produce less than a 20% reduction in the crush strength. This variation in crush strength is significantly less than the difference in strengths typically seen between two different LRV designs with equivalent buff strengths. More importantly, the design study demonstrated that the CEM specifications (collisions at various speeds and acceptable outcomes) provided a much more stringent set of constraints on the crush behavior and vehicle design than the buff load specification. Thus if appropriate CEM requirements are included in a safety specification, the selection of the buff load requirement will have a negligible influence on the crash safety of the resulting LRVs.

The final series of collision scenarios analyzed were between LRVs and highway vehicles. These are important collisions to evaluate since they represent the vast majority of LRV collisions and result in the majority of injuries and fatalities for LRV operations. A significant portion of the fatalities and serious injuries attributed to transit operation is to the occupants of

the highway vehicles. Incorporating features that can enhance the crash safety in these collision scenarios can result in large overall improvements to transit system safety.

Primary modifications that can be made to improve compatibility in collisions with automobiles are to eliminate features in the LRV front end geometry that make it aggressive. These measures include (1) adopting retractable or fold-away couplers at the ends of the LRV, (2) enclosing the front end of the vehicle and having a sufficiently low nose to prevent override of cars, and (3) including energy absorbing elements in the front-end designs of LRVs.

Collision simulations of between LRVs and automobiles were used in this effort to quantify the potential safety improvements that can be obtained by adding appropriate crash safety features to the LRV. The base LRV model used for the collision analyses was LRV 2. Two different highway vehicles were used in the collision analyses as shown in Figure 5. Highway vehicle 1 (HV 1) is the Dodge Neon, selected to be representative of a small passenger vehicle with greater height and weight differences in a collision with an LRV. Highway vehicle 2 (HV 2) is the Ford Explorer, selected to be representative of the light truck and sport utility vehicle (SUV) class of passenger vehicles which are very common in the highway vehicle fleet.

The collisions were performed at a range of speeds between 10 mph and 30 mph. Two different impact orientations were used as shown in Figure 6. The first is a normal (90 degree) impact of the LRV into the side of the highway vehicle passenger compartment and the second is an oblique impact of the corner of the LRV into the highway vehicles at a 45 degree angle relative to the LRV axis.

A side view of the impact interface between HV 1 and LRV 2 with the different modifications to the front end geometry is shown in Figure 7. The impact geometry clearly illustrates the potential geometric incompatibility of the two vehicles that introduce a significant injury risk to the occupants of the highway vehicle. The impact point of the head girder is close to the bottom of the side window. Such an impact would result in large intrusions close to the upper thorax of an occupant, leading to a high potential of a head impact against the LRV front end structures. The potential safety features illustrated in Figure 7 include a rigid bumper enclosure that provides a larger smooth impact patch on the highway vehicle and a simple pilot beam that is designed to engage the lower structures on the struck highway vehicles. The bumper enclosure extends in height from approximately 300 mm to slightly over a meter above top of rail. The center height of the pilot beam is approximately 480 mm above top of rail. The primary pilot beam structure is constructed with a steel box section tube approximately 80 mm in height and width. This is a narrow profile for a pilot beam and would not be expected to provide an optimum level of protection compared to a pilot beam that has a greater height and extending lower toward the top of the rail.

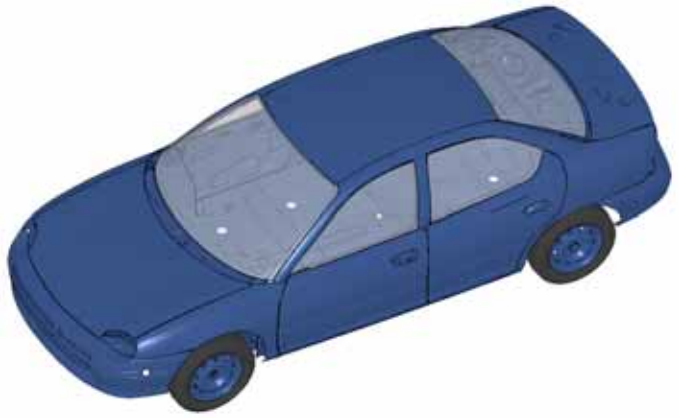

(a) Highway Vehicle 1 - Dodge Neon

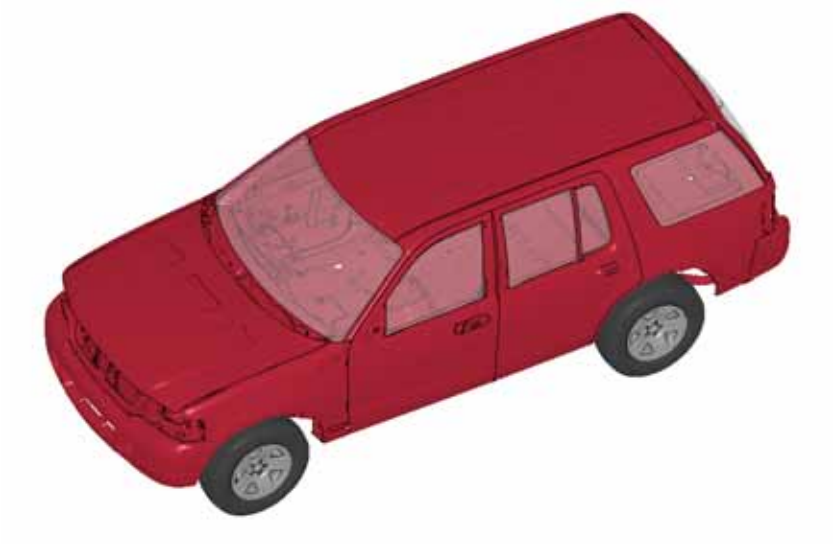

(b) Highway Vehicle2 - Ford Explorer

Figure 5. Finite Element Models for the Highway Vehicles used in the crash analyses.

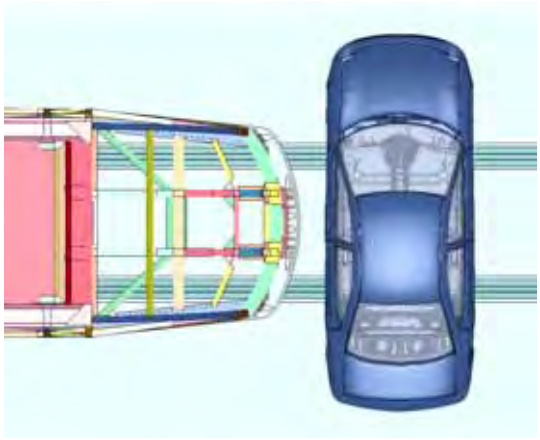

(a) 90 degree Collision Interface

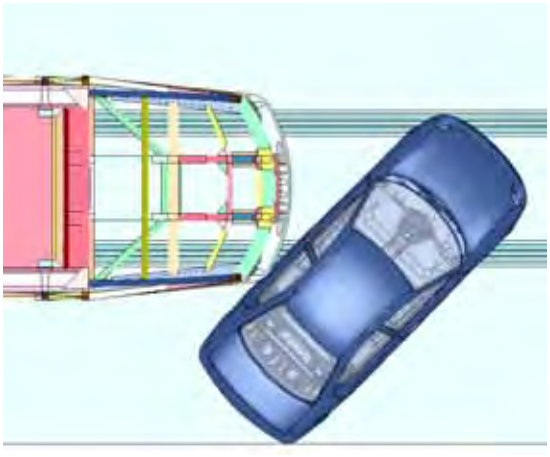

(b) 45 degree Collision Interface

Figure 6. Collision Interface conditions for LRV 2 and Highway Vehicle 1.

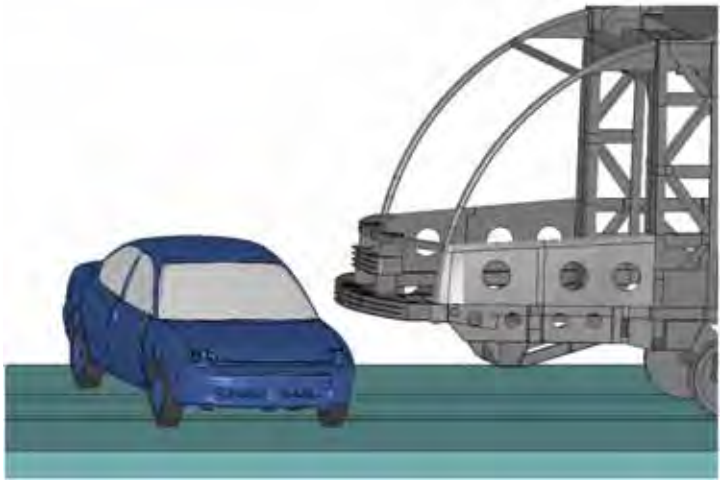

(a) LRV without any Safety Features

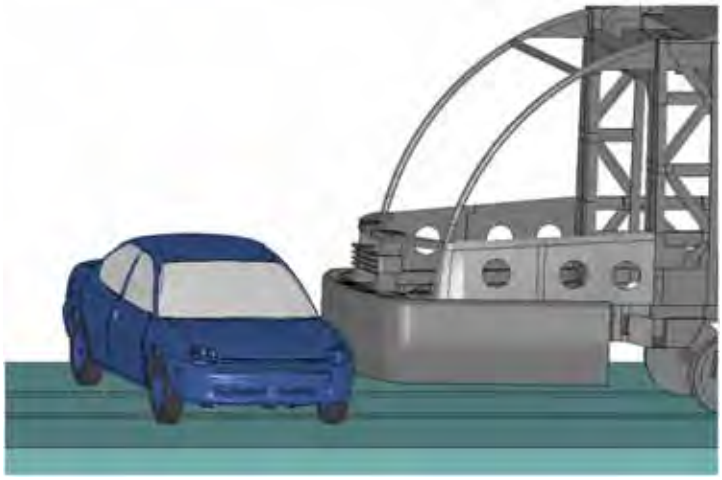

(b) LRV with Rigid Bumper

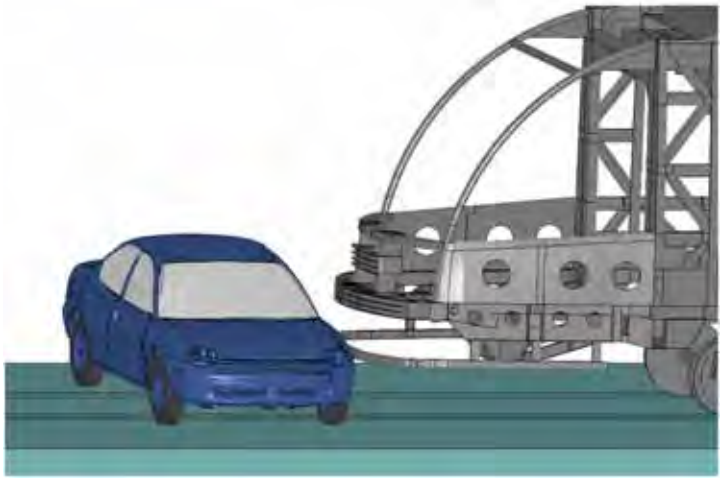

(c) LRV with a Pilot Beam

Figure 7. Collision Interface with Different LRV Front End Features.

The calculated 20 mph crash behavior of the LRV without any front end safety features into the side of HV 1 (90 degree) is shown in Figure 8. The head girder overrides much of the HV 1 side protective structures and intrudes significantly into the occupant volume. The high location of the impact also rotates the struck HV 1 lifting the wheels on the impact side off the ground. The response illustrated the significant incompatibility of the two vehicles in the collision and the potential for the LRV to override the highway vehicle and cause significant injuries to the occupants.

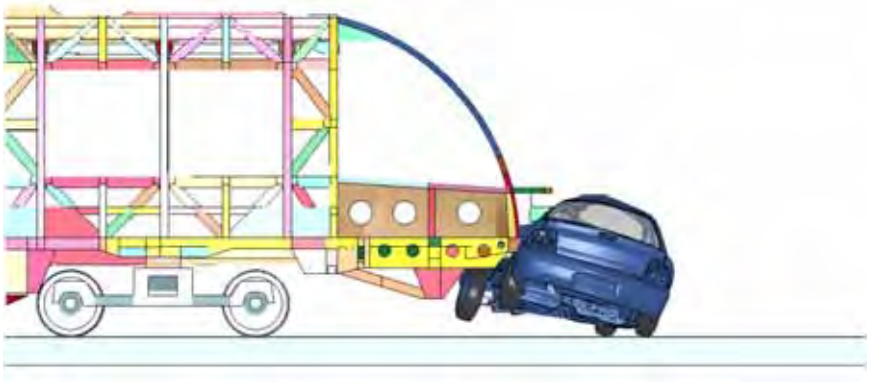

(a) Side View

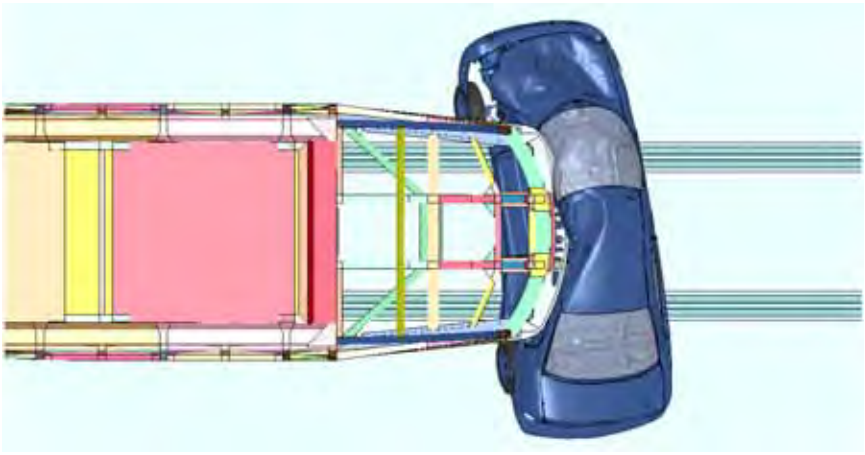

(b) Top View

Figure 8. Simulation of the 90 degree, 20 mph Collision with HV 1 (LRV without a Bumper).

The calculated 20 mph crash behavior of the LRV with a bumper enclosure into the side of HV 1 (90 degree) is shown in Figure 9. The bumper engages much of the HV 1 side protective structures and the crash response is significantly modified. The lower height of the impact loads pushes HV 1 laterally in the direction of the LRV movement. The motion is primarily a translation without the large roll of HV 1 seen when impacted without the bumper. The bumper also significantly reduces the crush intrusions of the LRV into HV 1.

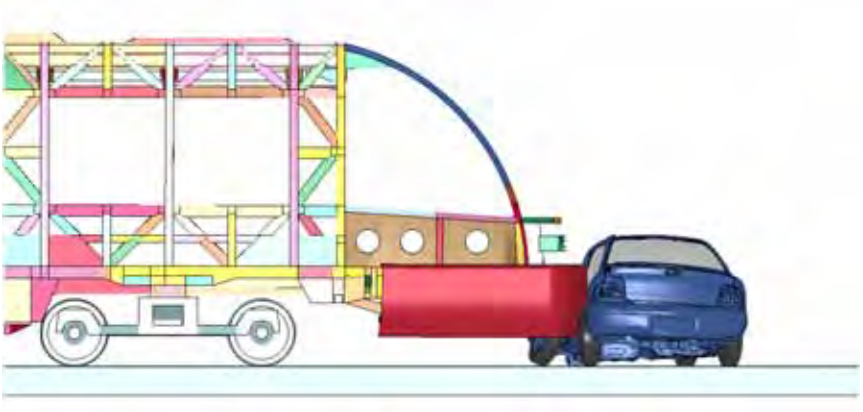

(a) Side View

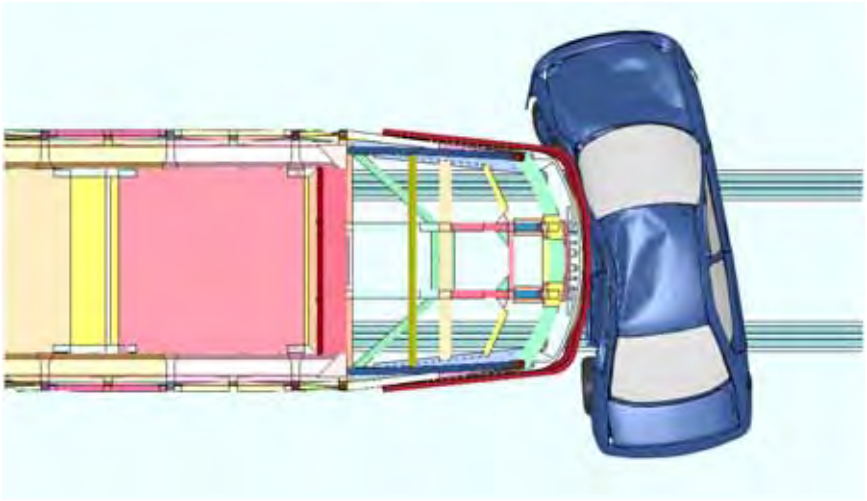

(b) Top View

Figure 9. Simulation of the 90 degree, 20 mph Collision with HV 1 (LRV Fitted with a Bumper).

The corresponding crush intrusions in the Dodge Neon for the 20 mph collisions with different LRV front end features are shown in Figure 10. The differences in the crush intrusions are significant. The maximum crush without the bumper enclosure was approximately 670 mm and located relatively high on the occupant compartment of the car. With the bumper enclosure, the maximum crush in the occupant compartment was reduced to approximately 450 mm and is more uniform over the center portion of the door. The maximum crush with the pilot beam was approximately 490 mm and located close to the bottom of the doors. Thus adding either a bumper or pilot beam is a significant improvement in both the magnitude and location of crush intrusions in the highway vehicle.

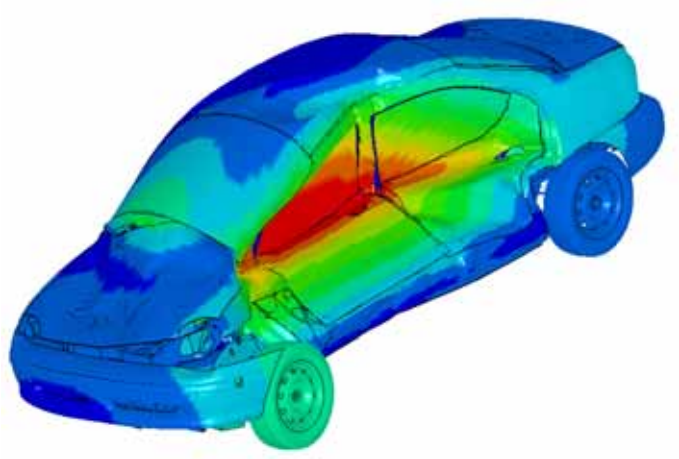

(a) Without Bumper (Maximum Crush 670 mm)

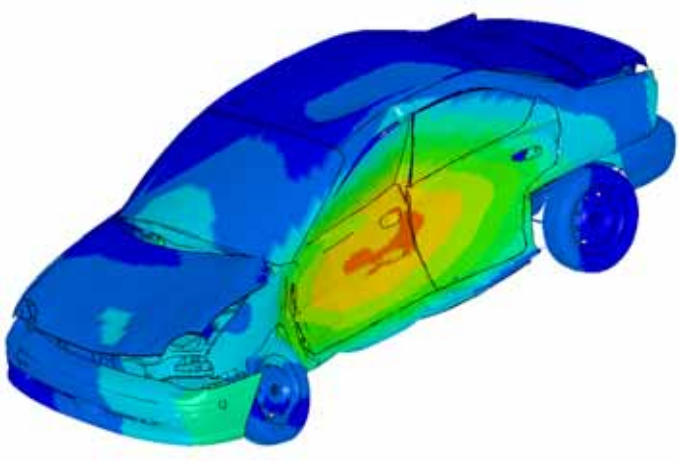

(b) With bumper (Maximum Crush 450 mm)

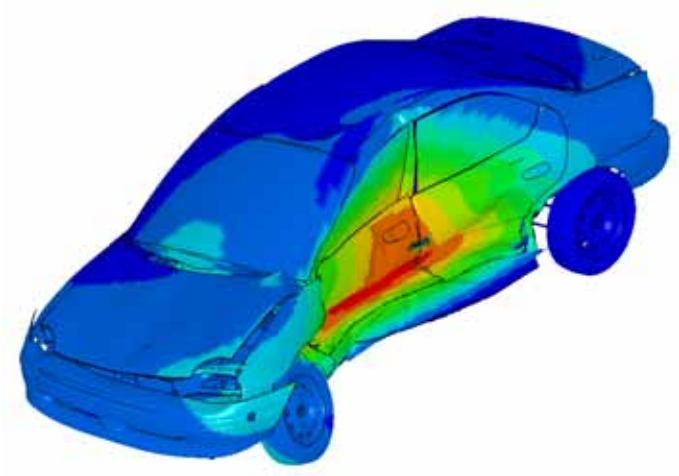

(c) With Pilot Beam (Maximum Crush 490 mm)

Figure 10. Calculated Crush for HV 1 in the 90 degree, 20 mph Collisions.

The level of automobile injury potential resulting from inclusion of the bumper enclosure can be estimated from research on side impact safety of automobiles provided by the National Automotive Sampling System (NASS), which reports statistics of injury. Data from NASS correlates injury probability to the physical intrusion into the vehicle. As a result of adding bumpers, the probability of a fatal injury is reduced from 73% without the bumper enclosure down to approximately 39% with the enclosure and 45% with the pilot beam. Similarly the probabilities of serious injuries are reduced from 94% to 69% with the bumper and 75% with the pilot beam. These injury probabilities are based on measurements of a large number of vehicles impacted in automotive accidents so that they will not necessarily incorporate the additional reduction in injury probability obtained by lowering the position of the maximum crush in the highway vehicle.

Collision analyses with the Ford Explorer model (HV 2) found very similar trends. The calculated 20 mph crash behavior of the LRV without any front-end safety features into the side of HV 2 (90 degree) is shown in Figure 11. The head girder overrides much of the HV 2 side protective structures and intrudes significantly into the occupant volume. The high location of the impact also rotates the HV 2 lifting the wheels on the impact side off the ground. When the bumper is added to the LRV, the collision engages much of the HV 2 side protective structures and the crash response is significantly modified. The bumper significantly reduces the crush intrusions of the LRV into HV 2 the motion is primarily a translation without the large roll seen when impacted without the bumper.

An important result of the analyses of collisions between LRVs and highway vehicles is the assessment of the side force crush characteristics of the highway vehicles. This information can be used to determine effective bumper energy absorbing characteristics to protect occupants of automobiles struck by an LRV. The force-crush characteristics for both HV 1 and HV 2 impacted at 20 mph by the LRV with the rigid bumper system at 90 degree and 45 degree orientations are shown in Figure 12. For the 90 degree collisions, the crush forces remain below approximately 100 KN until a crush intrusion of 300-400 mm. The forces then increase to a maximum of 150 KN for HV1 and 220 KN for HV 2 at crush intrusions between 400 and 500 mm. For the 45 degree collisions, the crush forces remain below approximately 40 KN for HV 1 and 75 KN for HV 2 until a crush intrusion of greater than 500 mm. The peak crush force for either vehicle in the 45 degree collisions remains below 100 KN.

The comparison of the highway vehicle force-crush behaviors illustrates the difficulty of defining an energy-absorbing bumper for LRVs that reduces injury to automobile occupants and is still effective for LRV operations. Unless the force for bumper activation is significantly below 100 KN, the energy absorption mechanisms will not be activated in oblique impacts. If the system has 200 mm of travel at an average force of 50 KN, the energy absorbed would be 10 KJ. In the 90 degree impacts at 20 mph, this would reduce the crush by approximately 15%. By comparison, the addition of the rigid bumper enclosure reduced the crush by approximately 35 % in HV 1 and nearly 50% in HV 2.

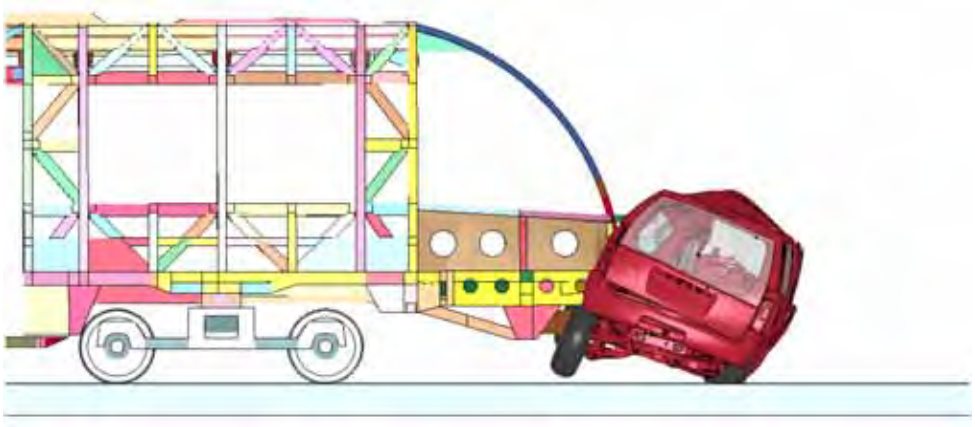

(a) Side View

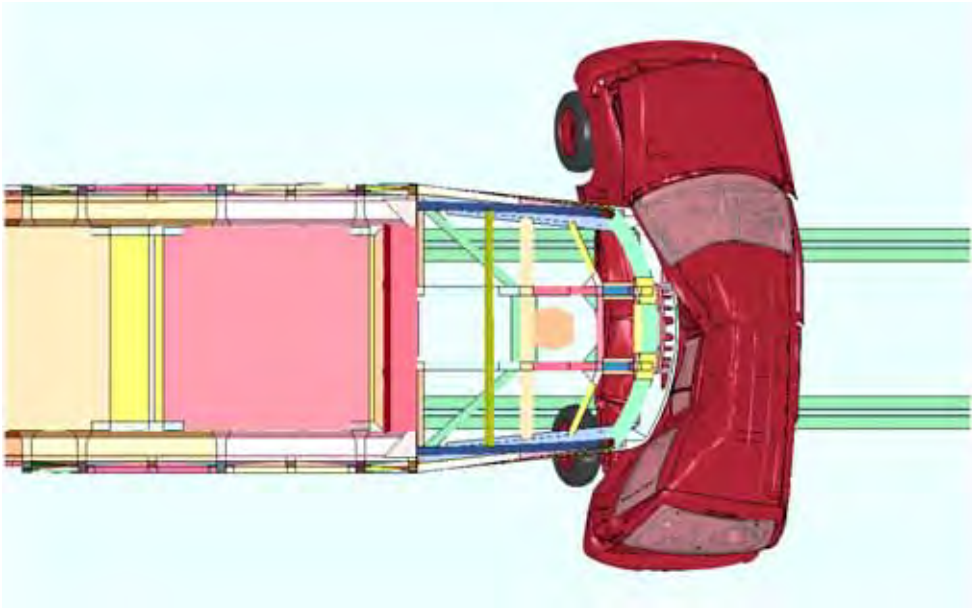

(b) Top View

Figure 11. Simulation of the 90 degree, 20 mph Collision with HV 2 (LRV without a Bumper).

In addition, the 10 KJ of energy dissipation in the bumper is only about one third of the energy dissipation needed for the 5 mph collision between two similar LRVs. As a result, it is difficult to develop a bumper system that will both dissipate a significant amount of energy in collisions with automobiles but still be suitable for preventing damage in the 5 mph collision between two identical LRVs.

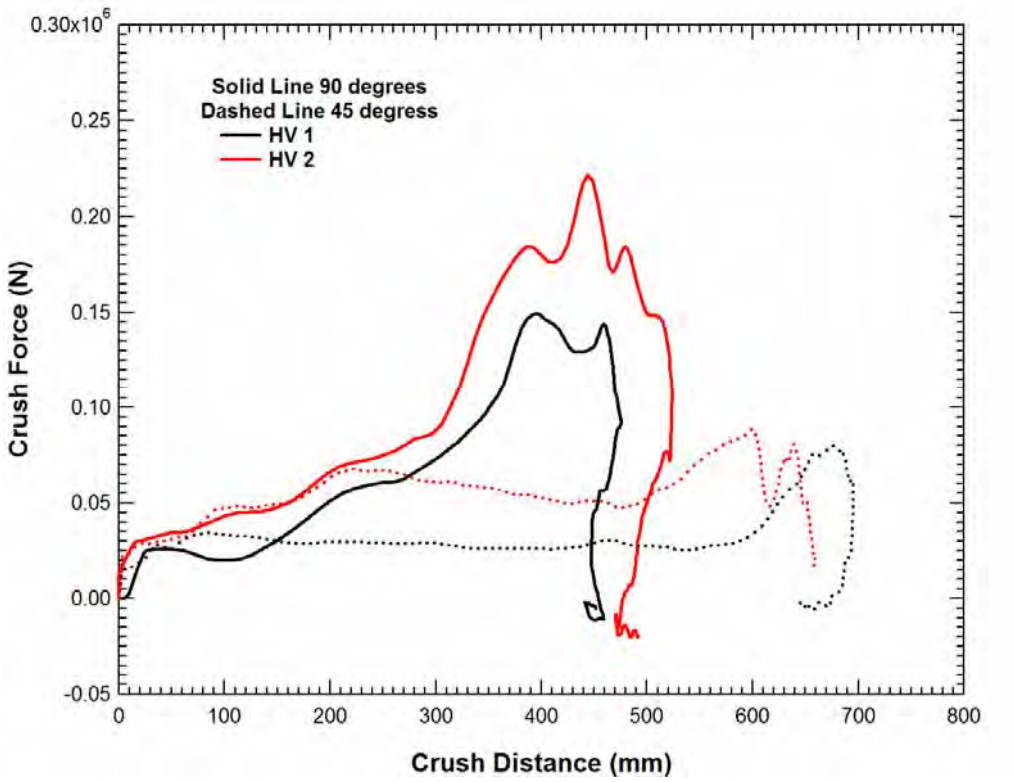

Figure 12. Force-Crush Profiles for the 45 and 90 degree, 20 mph Collisions (LRV Fitted with Bumper)

Some specific findings from the collision analyses between LRVs and highway vehicles include:

(1) The addition of a bumper enclosure, resulting in a smooth LRV front-end profile and lower contact zone between the LRV and the automobile, has a significant potential for reducing injuries and fatalities in side collisions. Although further research into methodologies and equipment to protect automobile occupants in these collisions would be warranted, the analyses in this study suggest that modifications to the LRV geometric profile has the greatest potential for reducing the number of fatalities and severity of injuries in these collisions.

(2) In scenarios where a bumper enclosure is not compatible with the operational requirements, a pilot beam or other structures to engage the highway vehicle at a lower position in a collision was shown to have a significant safety benefit.

(3) An energy-absorbing bumper system that protects against a 5 mph LRV collision does not appear to offer much advantage in collisions with automobiles over the performance of a rigid bumper enclosure. The side crush strengths of automobiles, particularly for the oblique impact conditions, are sufficiently low that the energy absorbers would not be activated. Designing an energy-absorbing bumper to protect the automobile would require low force levels and a large stroke length for significant safety improvements.

CHAPTER 1. Research Plan

1.1. Introduction

Traditional North American LRV designs have relied on the vehicle's overall static strength to protect occupants in a collision. This requires a vehicle structure to withstand a set of proof loads including an end-to-end compressive force, often equal to twice its weight (2g buff load design). This approach requires the structural frame to be sufficiently strong to resist this force, potentially resulting in a vehicle weight penalty and larger crash decelerations in the passenger compartment that may prove detrimental to passenger safety. Although this design approach can be effective in limiting penetration from end collisions, it may lead to heavier vehicle designs and does not assure controlled energy dissipation behaviors that result in crash safety improvements.

In Europe and elsewhere, modern LRV design incorporates CEM strategies. The CEM approach specifies a crash response that absorbs impact energy and smoothly decelerates the vehicle and its occupants with controlled deformation that protects the occupied volume. Strength requirements are no longer the primary design factor for occupant protection and specifications typically have lower buff strength requirements; commonly equal to the vehicle's weight (1g) or less. The CEM requirements for LRVs still require sufficient strength of the passenger compartment to preserve volume in the passenger compartment during a severe collision. This CEM approach has already become part of some current LRVs designed for United States markets. However, it is often adapted while maintaining a higher buff load requirement than in European specifications. Additionally, a more general CEM approach would typically include provisions for collisions with highway vehicles. The intended result is less damage, and reduced occupant injury potential, associated with both vehicles.

In an effort to improve safety of LRV designs in the United States, while allowing for lighter vehicle designs, The American Society of Mechanical Engineers (ASME) RT-1 Committee is considering the CEM design approach with reduced buff load requirements. However, the Committee has not reached a consensus as a result of concerns over compatibility with older vehicles and assuring that the CEM approach provides equal or better protection for occupants than using the approach with a high static buff strength. As a result, the Committee had reached an impasse trying to decide which basic design format to adopt; high end-to-end static strength or controlled crash energy management with lower end-to-end static strength.

A series of technical unknowns identified by the ASME RT-1 Committee, and the Crash Energy Management (CEM) Subcommittee, included:

1. The crash performance of current and past LRVs and variation in performance among vehicles in service.
2. The potential correlation between static buff-strength and crush-strength (dynamic strength).

3. The extent of problems that may exist because of strength incompatibility between colliding LRVs.
4. The appropriate collision speeds or crash energy parameters for the CEM requirements for LRV safety.
5. The relative benefits of collision scenarios specified in previous design requirements for various LRVs.
6. The appropriate CEM specifications for collisions between LRVs and passenger cars.
7. Appropriate strength specifications for protection of low floor LRV occupants from intrusion in side impact by automobiles and light trucks.

These unknowns were an impediment to the development of the ASME RT-1 safety standard for LRVs and served as a justification for this study.

Crashworthiness, in the modern sense of the word, is a relatively new development. However, rail vehicle crashworthiness is underpinned by a long history of main line railroad and transit operational experience specifications which dictated various structural strength levels and vehicle construction materials. Traditional static criteria originally evolved from over 130 years of main line railroad experience and more recently over 30 years of LRV experience. The static buff load values most commonly used for LRV car shell designs appear to be somewhat arbitrary and not necessarily directly related to passenger and operator safety, but have nonetheless created a perceived level of safety no one wants to sacrifice. Over the last two decades, new analytic tools and computer systems have become available for crashworthiness engineering. These developments were primarily developed in automotive crashworthiness applications and then transferred to applications in rail vehicle structural designs to create high levels of passenger and operator safety.

Traditional car shell design is based upon static design criteria where the application of a set of static forces defines the structural system, with no reference to what occurs in a collision. This is verified by finite element analysis (FEA) and static testing. Conversely, CEM design uses collision scenarios and corresponding crash responses (e.g. length of crush zone) to define the performance of the car shell structure. The difficulty is that there is no clear correlation between the two design approaches. Thus there is resistance to modify the current US design approach without a clear demonstration that it will lead to equal or better LRV safety.

Analyses are needed to establish current levels of crashworthiness for existing vehicles and to determine their crush characteristics (i.e., crash energy absorption). This should include older LRVs designed with traditional static criteria, as well as the latest designs which include CEM measures. The relevant information on LRV accident data and European LRV crashworthiness requirements should then incorporated. Based on the combined information, values for collision speed and crush distance can be selected.

1.2. Objectives

The objective of the RT-1 Standard is to enable the development of LRVs that will be as safe or safer than current designs and potentially lighter and more energy efficient. Safer designs reduce the risk of injury resulting from primary and secondary collisions caused by either vehicle intrusions or high levels of crash deceleration. This will be achieved in LRVs by basing the design on CEM principals rather than older design practice based on static strength requirements. The intent is to incorporate safety features that mitigate injuries from the more common low severity LRV accidents while maintaining sufficient vehicle strength needed to preserve volume in the passenger compartment in the much less frequent higher severity accidents. Vehicles designed with this approach will also help to mitigate injuries to passengers of automobiles and trucks in street running collisions.

Vehicle designs that are built to absorb energy in a collision and control deformations has been used extensively in the automotive industry and more recently in rail vehicle designs. The application of these modern crashworthiness (CEM) design principles to LRVs can potentially reduce vehicle weight while improving overall crash safety. These improvements are possible since the traditional design practice for rail vehicles specified static strength and typically did not lead to an optimized use of structural components for both service and crash conditions.

The ASME RT-1 Committee is in general agreement that the safety standard should incorporate appropriate CEM requirements for LRVs. However, there was not general agreement about what CEM requirements are appropriate and there was insufficient data on LRV crash behaviors to resolve the questions. The objectives of this Transit Cooperative Research Program (TCRP) Project C-17 are to collect the supporting information and perform the necessary analyses to allow the ASME committee to complete the CEM requirements in the RT-1 Standard.

1.3. Approach

The overall program was performed in two phases and divided into the following nine tasks:

Phase I:

- Task 1 – Identify and Evaluate Research Approach
- Task 2 – Collect LRV Crashworthiness Information
- Task 3 – Develop Detailed Work Plan
- Task 4 – Describe Analysis Techniques
- Task 5 – Prepare Working Paper
- Task 6 – Phase II Work Plan
- Task 7 – Interim Report

Phase II:

- Task 8 – Execute Phase II Work Plan
- Task 9 – Final Report

The research approach was identified through a combined survey and interview of the interested parties in the ASME RT-1 Committee and the TCRP Project Panel. The results were used to rank the issues that need to be resolved and develop proposed methodologies to address the issues. LRV manufacturers were contacted and relevant crash information was collected for various LRV designs. Wherever possible, crash models of LRV designs were obtained. The combination of proposed methodologies and available models were incorporated into the working paper that was submitted to the TCRP Project team for review and comment. The review comments were incorporated and expanded into the detailed Phase II research work plan.

The critical efforts identified for the Phase II research plan included:

- Collision analyses between two LRVs. The primary objective of these analyses was to provide supporting information to determine appropriate collision scenarios to include in the CEM requirements for the RT-1 Standard. Secondary objectives were to address issues of crash compatibility and the influence of specifications (e.g. buff load magnitude) on crash behavior.
- Collision analyses between LRVs and automobiles. The objective was to provide information to support the determination of magnitudes for the crash features designed to protect automobile occupants in a collision. These included the geometry and potentially energy absorption characteristics of a bumper system.
- Perform an analysis of the available LRV transit system safety statistics to assess the influence of variations in current LRV front end designs on system crash safety. This assessment supported the decision making on the front end requirements in the LRV safety standard.

Additional details on the specific Phase II tasks are described below.

1.4. Phase II Work Plan

The work plan and the comments from the TCRP C-17 panel have been incorporated into the detailed Phase II research plan. The tasks are split out in more detail below:

Phase II Task 1 - Prepare LRV Models

The first task was to prepare the LRV models that were made available for the various crash analyses in this study. This task included conversion to LS-DYNA format (if necessary) with all of the appropriate nonlinear material specifications, etc. The second modification to the models was to build in a series of force cross-sections. Specific cross-section planes were defined at various locations in the structure to show the load paths through the structure and the redistribution of loads as the crush behavior develops.

Phase II Task 2 - Symmetric Collisions between Identical LRVs

A common approach for CEM design is to select collision scenarios and specify the corresponding vehicle crash performance. One of the primary collision scenarios proposed for the RT-1 Standard (and commonly found in rail crash specifications) is the symmetric collision between two LRVs. However, determination of appropriate speeds and collision outcomes are still being developed. The CEM subcommittee requested that project C-17 perform symmetric collision simulations on existing designs to determine the appropriate collision speeds to be included in the standard. This task used each of the available LRV models in a series of collision analyses between identical vehicles at a range of collision speeds (i.e. 5mph, 10 mph, 15 mph, 20 mph, 25 mph, and 30 mph). The objective was to support the selection of appropriate collision scenarios (load cases) and acceptable crash responses (acceptance criteria) to add to the RT-1 Standard. Evaluating the crash performance of existing vehicle designs will assist in determining these collision scenarios.

The analysis technique for these compatible LRV collisions was as follows:

1) Calculations were for a collision between two single identical LRVs. The bullet LRV was moving at the desired collision speed and the target LRV was stationary. The brakes were applied on both vehicles.

2) Impact simulations were performed for a range of collision speeds (e.g. 5, 10, 15, 20, 25, and 30 mph). The analyses of different severity collisions allow assessment of the range of outcomes for different collision conditions.

3) Fully dynamic nonlinear analysis methodologies were applied. The explicit nonlinear dynamic finite element code LS-DYNA was used. Elastic-plastic constitutive models were used for metals.

4) The primary outputs were plots of collision force versus crush displacement.

5) Additional information included visualization of the deformation modes at various times during the simulation.

6) Crush distance was defined as relative displacements between a reference point on the LRV (e.g., a point at the back of the cab or the front truck connection point) and the nose of the LRV.

7) The crush force was obtained directly from a force cross-sectional plane defined at the back of the cab structures behind the crush zone. This methodology has the benefit of eliminating the inertial effects on the force and more clearly defining the structural crush strength.

For each of the LRV designs, a series of 4-6 calculations were performed. The starting calculation was typically the 5 mph impact and the calculation was repeated increasing the collision speed by 5 mph increments until an unstable collision behavior or a 30 mph maximum

collision speed was reached. Note that the 30 mph collision between two identical vehicles is the same collision energy severity as a 15 mph collision of a single LRV into a rigid wall. However, the vehicle to vehicle simulation adds an additional assessment of the stability of the crash response that is potentially suppressed in a rigid wall collision analysis.

Phase II Task 3 - Collisions between Different LRV Designs

The symmetric collision behaviors establish a baseline behavior for the different LRV designs. However, one of the difficult technical challenges is assessing the potential consequences of vehicle incompatibilities that might result from different design standards. The concern is the differences between a 2g LRV designed to a strength-based specification and various CEM designs.

Before assessing the potential consequences of the requirements that would be incorporated in the ASME RT-1 Standard, the first step is to establish the range of incompatibility of LRV designs developed under current design practice and specifications within the US market. In this task, a series of calculations were performed where the different LRV types are collided with each other at various speeds. Some modification of the LRV models was necessary for these analyses. Primarily, the LRVs were shifted vertically so that the end beams (head girders) are at the same height and the anticlimber ribs engage. It is expected that this level of geometric compatibility would be present on any given transit system.

The incompatible collision calculations were performed similar to the compatible collisions. Analyses were performed at a range of speeds until an unstable collision behavior or a 30 mph maximum collision speed was reached. Because of the incompatibilities in structural designs, it was expected that the unstable crush modes (or disproportionate crush magnitudes in the collision partners) would occur at lower closing speeds than the in the symmetric collision simulations in Task 1.

Phase II Task 4 - Modify LRV Models

The objective of this task was to modify the existing designs in order to represent a car body design built to an alternate design specification not covered by the current set of vehicle models. For example, the thickness of the members in the cab underframe can all be slightly reduced to be more representative of an LRV designed to a specification with a 1g buff load requirement.

The current models span a range of design practice. Two of the LRV designs were designed to satisfy a 2g buff load condition and include CEM features based on a single symmetric collision scenario. However, the two vehicles were designed by different manufacturers and have very different structural arrangements in the cab. Alternatively, the third LRV was designed to a strength-based specification that included a 2g buff load but without and CEM collision scenarios analyzed.

The final LRV design is somewhat unique in that multiple CEM requirements were considered. The unique design considerations arose since the end frame of the LRV design was approximately 12 inches lower than the older vehicles in operation on the system. As a result, the design was developed with CEM considerations for both the symmetric and incompatible collision scenarios. This resulted in some unique modifications to the design to obtain the desired crash energy dissipation and to maintain controlled stable crush modes.

A significant design alternative missing from the above model set is a vehicle designed to a lower buff strength requirement. A model for an LRV designed to a lower buff strength was not obtained for use in this study. As a result, this task was to modify a 2g CEM design to be a 1g CEM design.

The design changes in this task were made in collaboration with the designer. In addition, static analyses of the 2g and 1g static buff loads on the original and modified LRV models were performed to confirm the relative stress magnitudes in the modified structural elements designed to meet the different static proof load levels.

Phase II Task 5 - Collisions between Original and Modified LRVs

The objective of this task is to quantify the effect of the design modifications in the similar LRV collisions. The task was to perform a series of collision analyses between the original and modified LRV designs from Task 4 (2g and 1g, respectively). Quasi-symmetric analyses were performed using the same methodology as in Task 1. The asymmetry of the crush behaviors and strengths resulting from the design modifications were quantified and compared to the similar behaviors from the crash analyses in Tasks 1 and 2.

Phase II Task 6 - Evaluation of LRV Front End Specifications

The analysis of collisions between LRVs and highway vehicles are important since these scenarios represent the large majority of the LRV collisions in service. These collisions also result in a large percentage of the overall injuries resulting from light rail transit operations. A large body of research on crashworthiness of highway vehicles is available to assist in this effort. These include analyses of the effects of vehicle strengths, geometry, and impact orientations on injury potential. These methodologies can be applied to determine the range of CEM features for protection in collisions between LRVs and highway vehicles such as bumper height and energy absorption characteristics.

Data collection and analysis were needed to develop LRV front-end requirements and appropriate standards for LRVs colliding with automobiles. Analysis of transit accident data [1-5] may provide some of the needed information about the safety effects of enclosing the vehicle front end and eliminating a protruding coupler. The accident data analysis effort is described in Task 7 below. The objective of this task is to analyze the collisions between LRVs and automobiles to develop information about the requirements on associated safety standards.

The proposed low energy CEM specifications have potentially conflicting energy dissipation goals for a bumper system. The safety benefit of including a lower force level for bumper activation in collisions with automobiles was not quantified. Analyses were needed to assess the optimized bumper energy absorption requirements and activation force levels for these collisions. One possibility is that an enclosed geometry will provide the primary protection for automobile collisions while the bumper energy absorption characteristics are designed for the 5 mph LRV-to-LRV collision.

The analysis approach selected to evaluate bumper characteristics was to perform explicit impact simulations of various LRV front-end profiles into existing models for different types of automobiles. Although these detailed simulations were not included in the original scope, this approach was adopted because it was both more accurate and less expensive than alternate analysis methodologies. An example of the calculated damage to a Chevrolet C2500 pickup from a side impact of an LRV at 20 mph is shown in Figure 13. In this case, the LRV model did not include either a bumper or extended coupler. The collision of the end beam into the side of the pickup results in significant intrusions into the pickup cab.

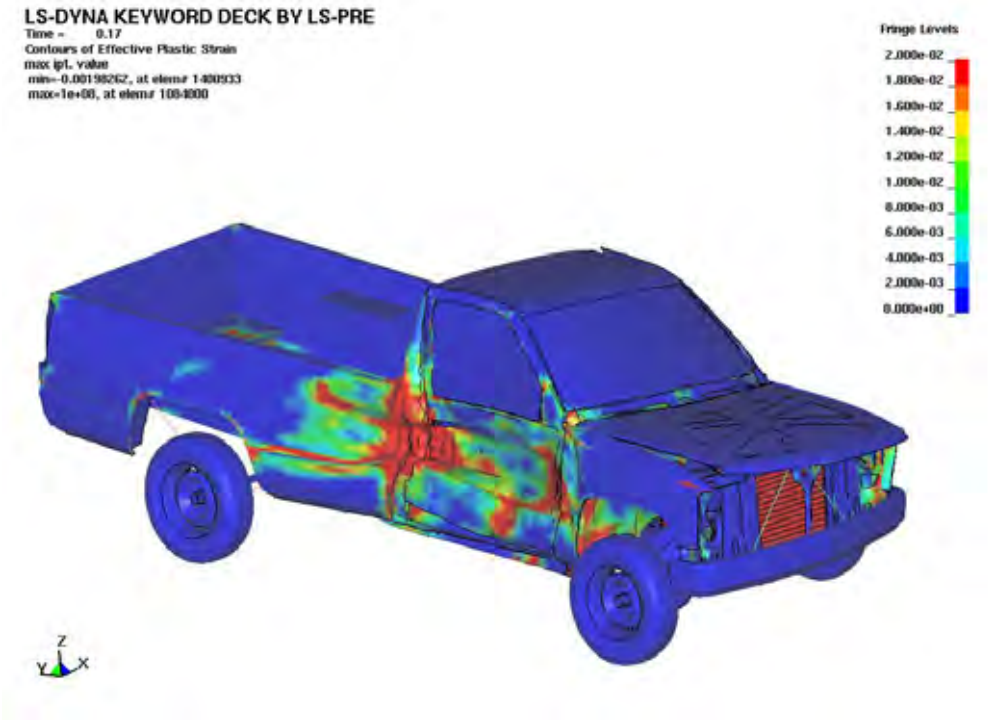

Figure 13. Damage to a Full size pickup from a 20 mph LRV side impact.

In this task, a simple bumper system was developed and adapted to one of the LRV models. Variations in the bumper design and collision conditions were used to assess the performance for protecting occupants of the automobile. High-fidelity models of both a sport utility vehicle (SUV) and a typical small passenger car were used in the study.

The matrix of calculations included:

1. Two different highway vehicles (e.g. SUV and Dodge Neon).
2. Two impact locations (90 degree side impact and 45 degree corner impact).
3. Various collision speeds.

The calculated crush forces and vehicle intrusions for each simulation was determined. The primary measurement of effectiveness was the maximum lateral crush of the highway vehicles. This is shown to have a strong correlation to injury severity as shown in Figure 14 [6].

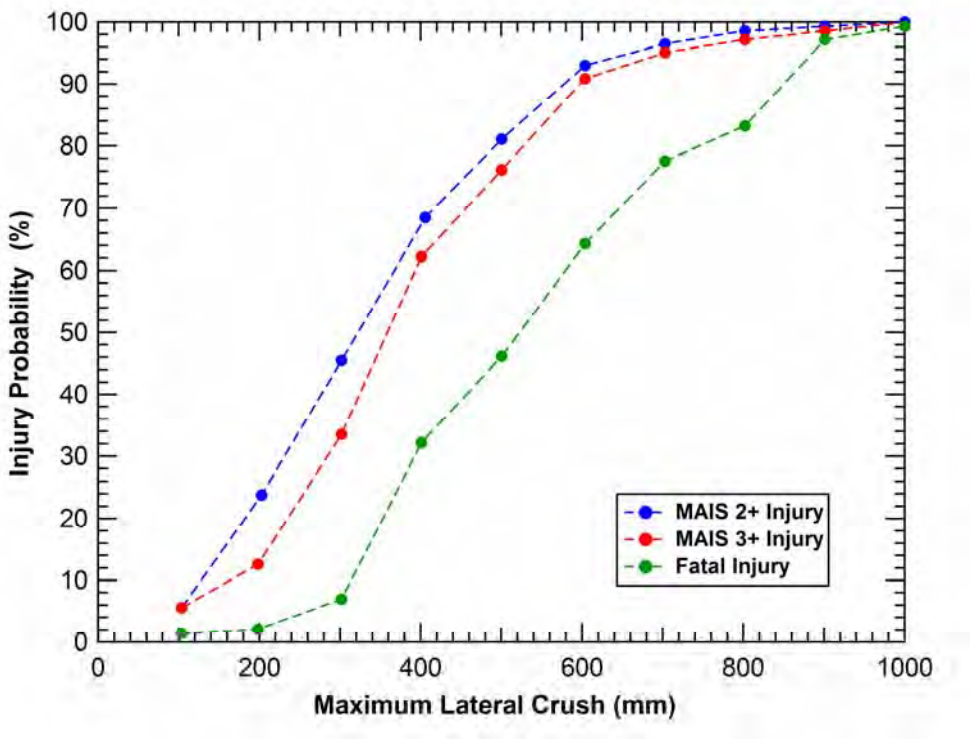

Figure 14. Injury probability in side impacts as a function of the vehicle crush.

Phase II Task 7 - Evaluation of LRV Side Impact Specifications

A major objective in the development of LRV safety standards is to provide sufficient strength of the passenger compartment to preserve volume in the passenger compartment during collisions. There has been growing concern in the LRV crash safety community that the past design practices may not be sufficient to protect against impacts by large SUVs or trucks against the LRV side, particularly for vehicle regions with a low floor. It is especially important due to the growing trends of lowering floors in newly designed LRVs combined with the increase in the US automotive fleet of larger, heavier, and higher trucks and SUVs.

Past practice to protect against this collision scenario is the application of static design loads on the side wall. Under this load case, the acceptance criterion is that no yielding of car body structure occurs. An alternate requirement would be to define a residual space for the passenger compartment that shall not be compromised during specified accident scenarios. However, this

second approach is more difficult evaluate and may add cost to the design process. The objective of this task was to use a SUV or a pickup truck model to assess possible penetration into the passenger residual space and the effectiveness of the current practice for these collisions.

In this task, the SUV model was used for side impact analyses against an LRV model. The primary parameter that was varied was the impact speed (20-35 mph). These analyses are to determine the adequacy of the current design methodologies on side impact structural integrity.

Phase II Task 8 - Data Analysis of Collisions between LRVs and Automobiles

Accident statistics show that the vast majority of collisions involving an LRV do not involve another LRV. An automobile or truck was involved in 62% of cases reported to the Transit Cooperative Research Program [1], and pedestrians and cyclists were involved in 38% of cases. Slightly more pedestrians/cyclists than occupants of highway vehicles were killed. LRV to LRV collisions are so rare that they do not even figure in the statistics. It is probable that they do happen, but at relatively low speeds in the maintenance facility, when no passengers are on board.

An analysis method was identified to evaluate approaches for addressing the collisions with automobiles in the RT-1 Standard. In order to quantify the relationship between highway vehicle design and collision fatalities, automotive researchers defined the “aggressivity index” [7]. This index is the ratio of ‘Driver Fatalities in Collision Partners’ to ‘Number of Crashes of Subject Vehicle’. A summary of the highway vehicle aggressivity as a function of vehicle class is shown in Figure 15. The figure shows that the most aggressive vehicles were full size vans with a rating of 2.47, followed by full-sized pickups with a rating of 2.31. Midsize cars had a rating of 0.70.

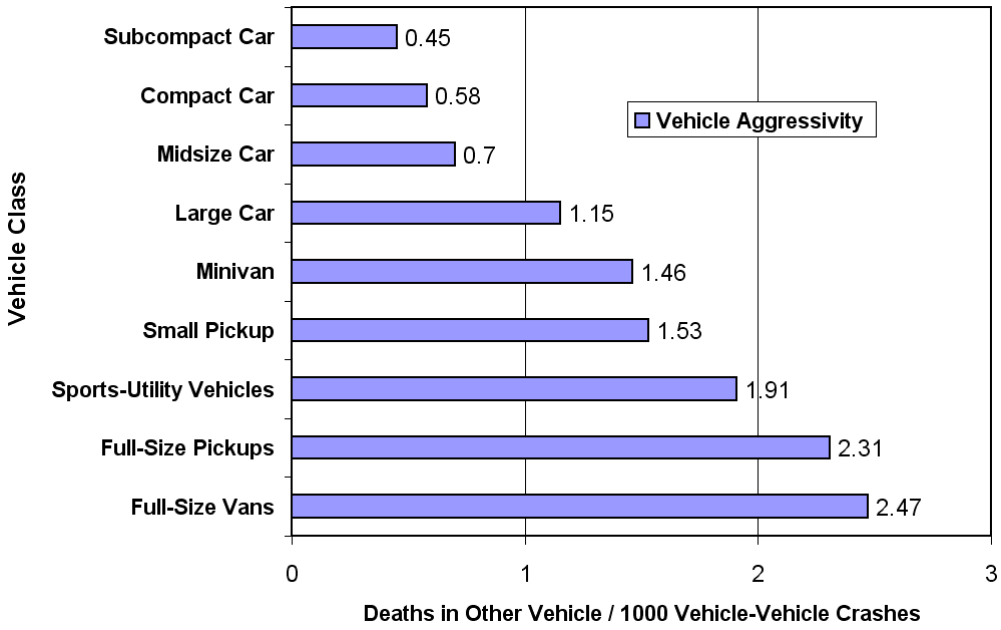

Figure 15. Vehicle Aggressivity for Side Impacts of Automobiles [7].

In this task, the same statistical analysis methodology, suggested by Figure 15, was applied for LRVs to determine the relative safety of different LRV designs in collisions with automobiles. The transit accident data collected in the US over the last decade should contain the information necessary to perform an assessment of the aggressivity of different LRV designs [1-5]. The objective was to compare the aggressivity of LRVs with an enclosed front end design (e.g. Houston, Phoenix, Portland Streetcar) with that of LRVs with open front end designs and exposed couplers (e.g. Denver, Sacramento, San Jose), or those of hybrid geometry, such as Minneapolis, that have an enclosed rounded front end, but an exposed coupler. Using the relative aggressivity of different designs with the overall crash statistics of the industry would allow us to determine the number of lives that can potentially be saved by modifying the standards for vehicle front end profiles.

This data is collected as part of the State Safety Oversight program [4]. Initially, the data extracted from the annual reports from this program do not split out the data sufficiently for the assessment of aggressivity. However, we were able to obtain the raw data separated by transit authority reporting. The subsequent evaluation of the raw data indicated that the data collection and reporting methodologies applied across different transit authorities was not of sufficient uniformity to produce statistically significant conclusions. Modifications to the data collection and reporting procedures are recommended to allow for this type of safety assessment in the future.

CHAPTER 2. Phase II Research

2.1. Introduction

In this section, the results of the Phase II research are presented. Wherever possible, the implications of the analyses on safety standards are described.

The detailed collision analyses performed in the Phase II research used the LS-DYNA finite element code (LS-DYNA Version 971). LS-DYNA is a commercially available nonlinear explicit finite element code for the dynamic analysis of structures [8]. The initial foundation of LS-DYNA was the public domain DYNA3D finite element code developed at the Lawrence Livermore National Laboratory [9]. Since 1987, the code has been extensively developed and supported by the Livermore Software Technology Corporation (LSTC) and is used for a wide variety of crash, blast, and impact applications.

The impact analyses described in this report used a variety of capabilities and algorithms in LS-DYNA. A brief description of these capabilities is described in this section. A significantly detailed description of the analysis methods is provided in the LS-DYNA Theoretical Manual [10].

The LRV structural components were typically modeled using Belytschko-Lin-Tsay shell elements. These are four node shell elements with single point integration. The Belytschko-Lin-Tsay element is a computationally efficient alternative to the Hughes-Liu element in LS-DYNA and is a widely used shell element formulation within LS-DYNA for crash, impact, and metal forming applications. Results generated with the Belytschko-Lin-Tsay element typically agree with those generated using the Hughes-Liu element.

Damage and failure were included through the constitutive algorithms and element erosion. This is a common approach to introducing damage and failure. Damage criteria (maximum plastic strain) were tracked for each element within the constitutive model evaluation, and elements were eroded when the failure criteria were exceeded. This allowed for a direct evaluation of damage and failure within the impact simulations. The eroded elements allowed for the initiation and extension of fracture in the model.

Overall contact in the impact analyses was modeled using the automatic single surface contact algorithms in LS-DYNA. Interacting components were defined by a material list, and contact segments were automatically generated by LS-DYNA. This greatly simplified the specification of contact between various components in crash analyses. The type 1 soft constraint option was used in the contact algorithm that determined the contact stiffness based on stability considerations, time step size, and nodal mass. This soft constraint option was found to be more robust than the default penalty formulation for modeling the complex contact behaviors in large impact and crash simulations.

These modeling methodologies have been applied extensively for various crash and impact simulations and validated against test data. For example, these techniques were used to model the impact of a Pioneer rail coach car on a concrete barrier [11]. In this simulation, a model of an entire rail passenger car was developed to predict the car crush, the three-dimensional gross motions of the car, and its vertical, lateral, and longitudinal accelerations. The finite element model of the Pioneer car is shown in Figure 16. The measured and calculated collision response for a 35-mph impact into a rigid wall is shown in Figure 17. The model was able to accurately reproduce the crush behavior and vehicle motions as measured in the test. The corresponding measured and calculated crush force-displacement curves are shown in Figure 18 showing that the model is capable of reproducing the complex impact force history against the wall.

Figure 16. Detailed finite Element Model of a Pioneer Passenger Coach Car.

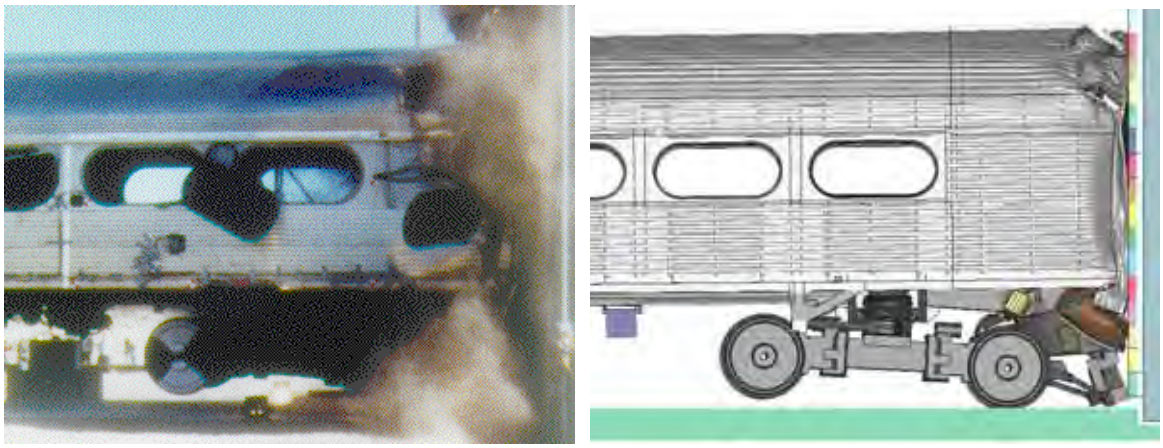

Figure 17. Comparison of the Measured and Calculated Collision Response.

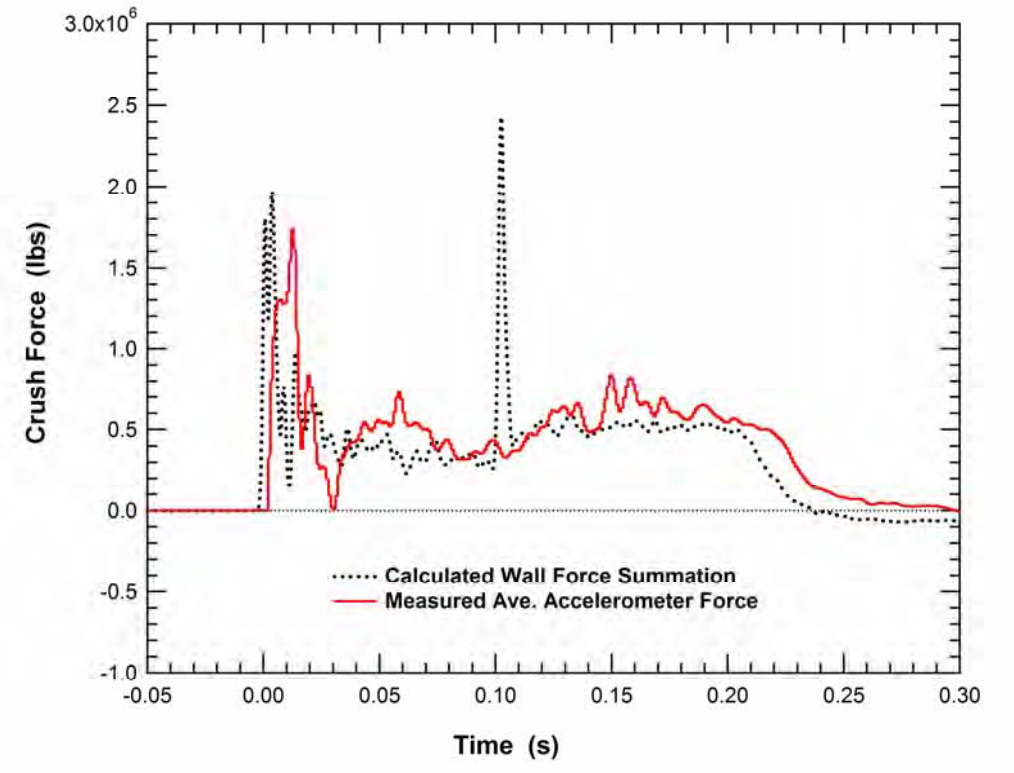

Figure 18. Comparison of the Measured and Calculated Impact Force Histories.

2.2. Summary of Analysis Results for Compatible LRV Collisions

The first set of LRV simulations were of compatible collisions between two identical vehicles (Phase II Task 2). These analyses are important for the development of an LRV safety standard since the proposed CEM requirements include assessment of compatible LRV collisions at one or more closing speeds. The crash performance of current LRVs must be established to ensure that the proposed collision scenarios and CEM performance requirements in the LRV safety standard are achievable and appropriate.

In the compatible collision simulations, the bullet (moving) LRV was initialized at the desired collision speed and the target LRV was stationary. Impact simulations were performed for a range of collision speeds (e.g. 5, 10, 15, 20, 25, and 30 mph). The analyses of different severity collisions allowed for the assessment of the range of outcomes for different collision conditions.

Four different LRV models were used for the collision analyses. A summary of critical design information for each of the LRV models is presented in Table 4. The details of the individual LRV models and collision analyses are presented in the following sections. The comparison shows that all of the LRVs are between 40,000 and 47,000 kg and designed to specifications that included a 2g buff load requirement. The primary differences in the LRVs result from the different structural designs developed to meet the specifications and the CEM

requirements placed in the design specifications. LRVs 1, 2, and 4 are all 70 percent low floor design. LRV 3 is 100 percent high floor. The design Specifications for LRVs 1 and 2 included analysis of a 20 mph collision of two identical LRVs as a CEM requirement. In addition, LRV 2 had a secondary collision scenario of a 20 mph collision with a second LRV design that had an end girder position that was 230 mm higher than in LRV 2. LRV 3 was designed without any CEM requirements in the design specification (only static load case requirements). Finally, LRV 4 had a CEM collision scenario requirement of a 14 mph collision into a flat rigid wall.

Table 4. Summary of the LRV models

Model	Total Mass	Design Buff Load Requirement	LRV Type	CEM Design Analyses
LRV 1	45,126 kg	2g	70% Low Floor	A
LRV 2	43,010 kg	2g	70% Low Floor	A, B
LRV 3	40,822 kg	2g	100% High Floor	None
LRV 4	46,384 kg	2g	70% Low Floor	C

A. Moving LRV colliding with an identical stationary LRV at 20 mph – brakes applied on both.
B. Incompatible collision of moving and stationary LRVs at 20 mph – 230 mm vertical offset of head girders at collision interface.
C. Single LRV colliding with a rigid wall at 14 mph.

A summary of the LRV crush lengths for the various collision speeds and LRV designs is presented in Table 5. For each of the designs and collision speeds, the crush in each of the vehicles is presented along with the average in both vehicles. A big difference in the crush lengths of the two colliding vehicles is an indication of a less stable crash deformation mode, typically caused by a softening behavior in the force-crush characteristics. This is not necessarily a problem for crash safety since the crash accelerations and energy dissipation is governed by the total crush in the two colliding vehicles. As long as the deformations are occurring in unoccupied crush zones, the unbalanced crush lengths across the collision interface will not significantly increase the injury potential. However, at higher speeds when the desired crush zones are completely exhausted, the unbalanced behavior can produce increased injuries.

A proposed CEM requirement for the low severity impact scenario is a closing speed between two like LRVs of 8 km/h (5 mph) that must result in no structural damage. This is a typical CEM requirement that has been used for both heavy and light rail applications. As shown in Table 5, all of the designs have a crush length of 11 mm or less (less than 0.5 inches) for the 5 mph impacts. This is for exposed cab end structures without couplers, bumpers or other enclosures (direct contact of head girders and anticlimbers). With relatively simple and established design methodologies, this type of low severity CEM requirement should be easily obtained.

Table 5. Summary of vehicle crush lengths (in mm) for the compatible collision analyses.

Vehicle Crush (in mm)		Collision Speed					
		5 mph	10 mph	15 mph	20 mph	25 mph	30 mph
LRV 1	Bullet	3	24	84	77	835	505
	Target	3	26	66	327	140	535
	Average	**3**	**25**	**75**	**202**	**487**	**520**
LRV 2	Bullet	8	36	144	291	411	327
	Target	8	24	34	51	65	230
	Average	**8**	**30**	**89**	**171**	**238**	**278**
LRV 3	Bullet	11	37	255	377	544	650
	Target	11	150	218	352	506	682
	Average	**11**	**93**	**236**	**364**	**525**	**666**
LRV 4	Bullet	—	70	110	327	490	679
	Target	—	45	207	220	310	434
	Average	—	**57**	**158**	**274**	**400**	**556**
Ave All LRVs		**7**	**51**	**140**	**253**	**412**	**505**

A proposed CEM requirement for the medium severity impact scenario is a collision between two like LRVs at 24 km/h (15 mph) that must result in a permanent crush distance in the cab not to exceed 300 mm (12 in) and no visible damage to the passenger compartment. The force-crush curves for all of the LRV designs in the 15 mph collision are shown in Figure 19. The figure shows that there are significant differences in the force crush characteristics of the various LRV designs. However, all of the designs would have met this medium severity impact requirement. From Table 5, the LRV crush lengths for the 15 mph collision are between 50 and 260 mm.

The proposed CEM requirement for the high severity impact scenario is a closing speed between two like LRVs of 40 km/h (25 mph) that must result in crush damage limited to the front cab sections of both colliding vehicles. In addition, a 750 mm (30 in) operator's survival space shall be maintained in the direction of collapse. Finally, there is to be no loss of volume for the passenger compartment (some local plastic deformations allowed).

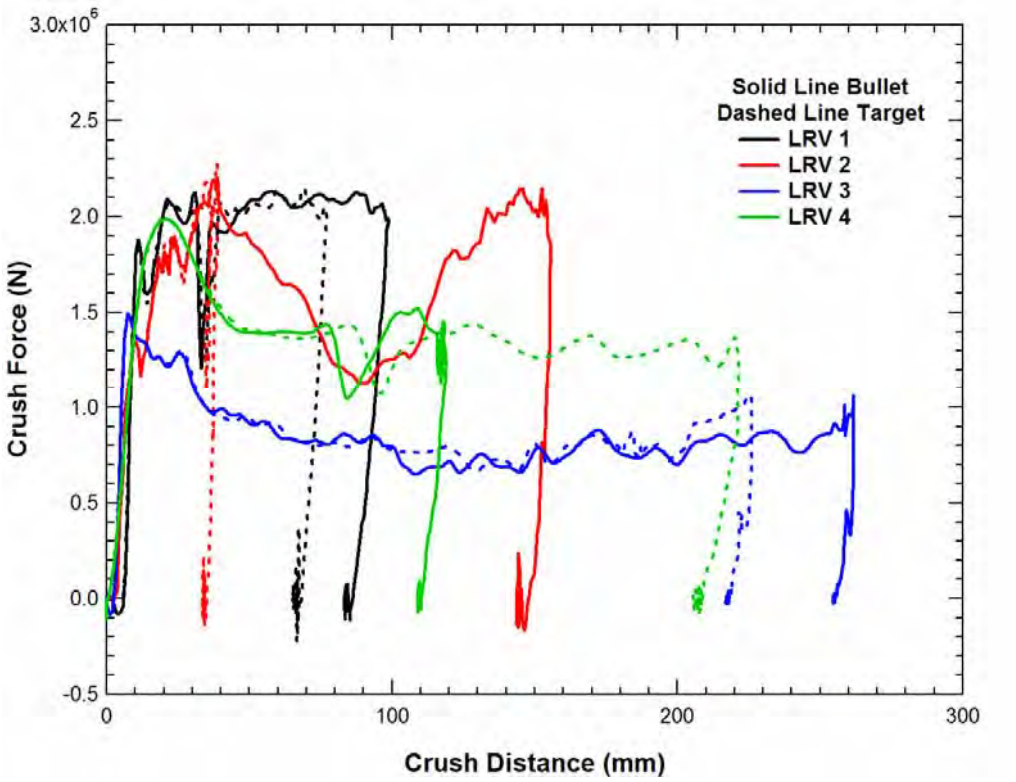

Figure 19. Force-Crush Plots for all the LRVs in the 15 mph Compatible Collisions.

All of the designs would have met the requirements for maintaining crush at the front of the LRV cab and no loss of volume in the passenger compartment for the high severity impact scenario. The corresponding force-crush curves for all of the LRV designs in the 25 mph collision are shown in Figure 20. The difficult requirement for some LRV designs may be to maintain the operator survival space as defined in the requirement. The average LRV crush for the LRV designs in this 25 mph collision is 412 mm. Many of these vehicles have a relatively short cab and the LRV length is limited by operational considerations. Therefore, maintaining the full 750 mm operator survival space in addition to the vehicle crush distance may require that some of the space behind the cab, currently used for passengers, be converted to operator survival space. Alternative requirements such as providing for rapid operator egress could also be considered.

A potential question for the development of a high severity collision CEM requirement is whether the crush length should be specified. From the table of calculated crush zone lengths, a maximum crush length of approximately 500 mm would be an appropriate level. The vehicle design that did not meet a 500 mm crush length condition based on average crush (LRV 3) would have been able to meet this with some very minor strengthening in the cab structures. The other individual vehicle that did not meet this (LRV 1 Bullet) would be in compliance if the LRV design was modified to obtain a more balanced symmetric crush response of the two colliding vehicles. Alternatively, a maximum crush length of 600 mm

would be achievable by all of the LRV designs if LRV 1 were modified to achieve a more balanced symmetric crush response.

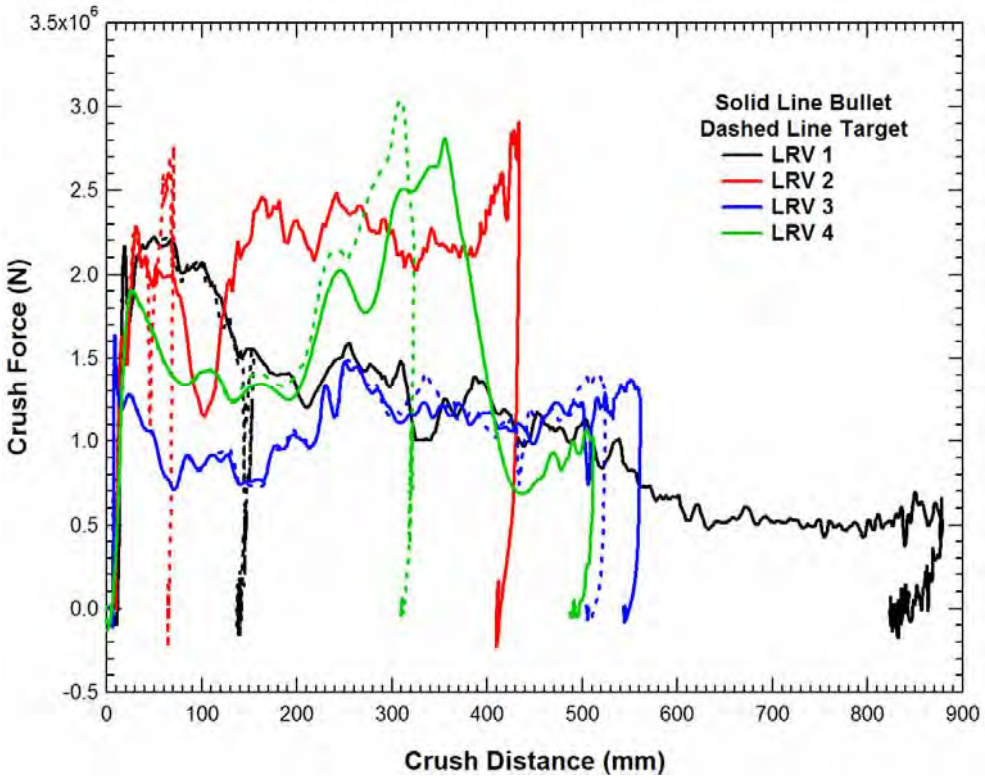

Figure 20. Force-Crush Plots for all the LRVs in the 25 mph Compatible Collisions.

Another factor considered in crash safety is the crash environment for the occupants inside the LRVs. As the crush strength is increased, the corresponding crash decelerations are increased in a collision between two LRVs. An estimate of the crash decelerations can be obtained by normalizing the crush forces for each LRV by the corresponding vehicle mass. The resulting normalized force-crush curves for all of the LRV designs in the 25 mph collision are shown in Figure 21. All of the LRVs have an initial normalized force above 4g before significant crushing is initiated (note that all of these initial forces are at least twice the 2g buff strength). Subsequently the steady state normalized crush strengths are primarily in the range between 2g and 6g. The two stronger vehicles (LRV 2 and LRV 4) both have a maximum normalized crush force of approximately 7g at a crush displacement of approximately 300-400 mm.

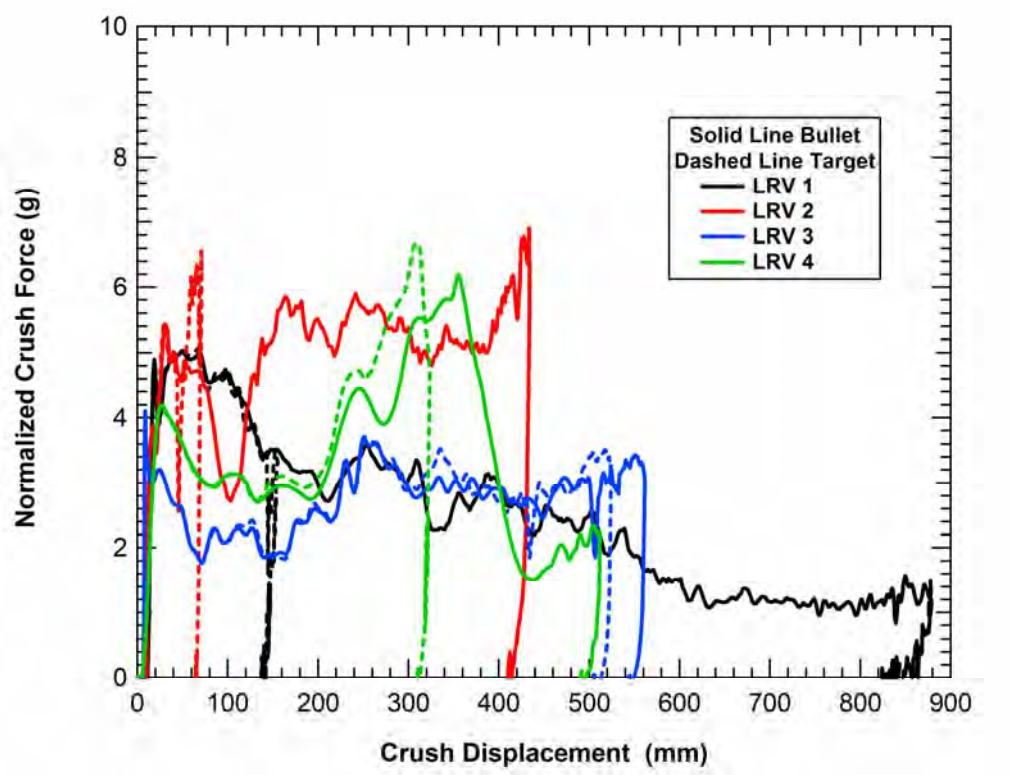

Figure 21. Normalized Crush Forces for the LRVs in the 25 mph Compatible Collisions.

A detailed assessment of the influence of these crash decelerations on occupant protection is beyond the scope of this study. In general, lower crash accelerations can result in lower secondary impact velocities of the occupants with the vehicle interior and lower injury potential from those secondary impacts. However, the lower crash acceleration levels also produce larger crush distances and a greater risk of intruding on an occupant survival volume in a severe collision. In addition, the LRV crash acceleration levels are relatively low compared to other transportation modes. Automobiles commonly have crash acceleration levels in frontal impacts in excess of 20g [12]. As a result, the automotive industry has developed advanced occupant protection strategies including restraints and airbags. Crash tests on current and proposed United States commuter rail vehicle designs have measured crash acceleration levels from 7g to 14g [13].

Additional guidance on occupant protection strategies for LRVs can be obtained from the commuter rail safety studies. These studies have shown that for secondary impact velocities of up to 18 mph, conventional seating systems can be used to prevent fatalities in train collisions [14]. In this study, the most severe collision analyzed (30 mph collision between two LRVs) would result in a maximum secondary impact velocity of 15 mph. LRV accident data shows that the vast majorities occur in accidents where the maximum secondary impact velocity is much lower than 15 mph. These suggests that the approach for light rail occupant protection should place more emphasis on the interior crashworthiness design (crash padding,

grab rails, etc.) and interior seating configurations rather than reducing the LRV crush strengths and corresponding crash acceleration levels.

A typical time history of the car-to-car collision global energy balance is shown in Figure 22. This example corresponds to a 20 mph collision with the LRV 1 design and the energy balance corresponds closely to the idealized behavior of a perfectly plastic collision between two objects. Initial kinetic energy is approximately 1.8 MJ. Of the total energy, approximately half (0.9 MJ) is absorbed as internal energy in the crush zone of the forward LRV structures (distributed between the two car bodies) and the other half remains as residual kinetic energy of the two LRVs after the collision. One can see from the energy plot that the majority of the structural collapse occurs within 0.2 s. The remainder of the calculation captures the rigid body motion of the cars after impact. Approximately 0.2 MJ is absorbed by sliding friction at the end of the simulation (0.7 second), mostly from the wheel and rail frictional interaction. Most of this sliding energy is dissipated at later time after the primary collision response has been completed. Also note that hourglass energy remains small in the calculation.

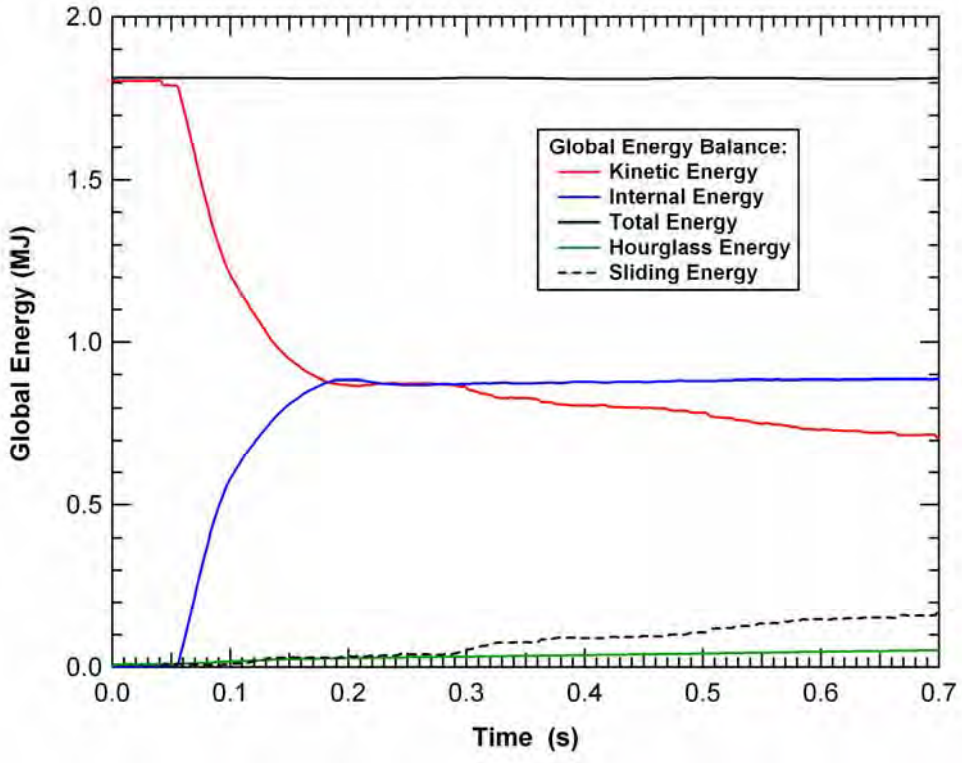

Figure 22. LS-DYNA Simulation Global Energies.

These energy balance plots confirm that the calculations were numerically stable and the collision is behaving as expected, but otherwise did not contribute significant information. As a result, they are not included in the remainder of the report.

2.3. LRV 1 Compatible Collisions

In this section, the compatible collision analyses for the various LRV designs are described in detail.

LRV 1 Model

The mesh for the LRV 1 model was originally developed by the manufacturer in ANSYS format and converted to LS-DYNA format. Further input file modifications were made to: (1) separate rigid bodies, (2) add a rail and ground model, (3) assign appropriate shell thickness values, (4) assign material models, (5) prescribe contact algorithms, (6) add gravity, (7) prescribe initial conditions, and (8) perform other miscellaneous edits to run the model in LS-DYNA. Figure 23 shows the LRV 1 model for the compatible collision analyses after conversion to run with LS-DYNA. Note that only the A-car (leading car section) is explicitly modeled. The B and C cars (trailing and center articulated car sections, respectively) are lumped into a trailing mass coupled to the respective A-car through the articulating joint. All of the crash energy dissipation occurs in the leading A-car structures.

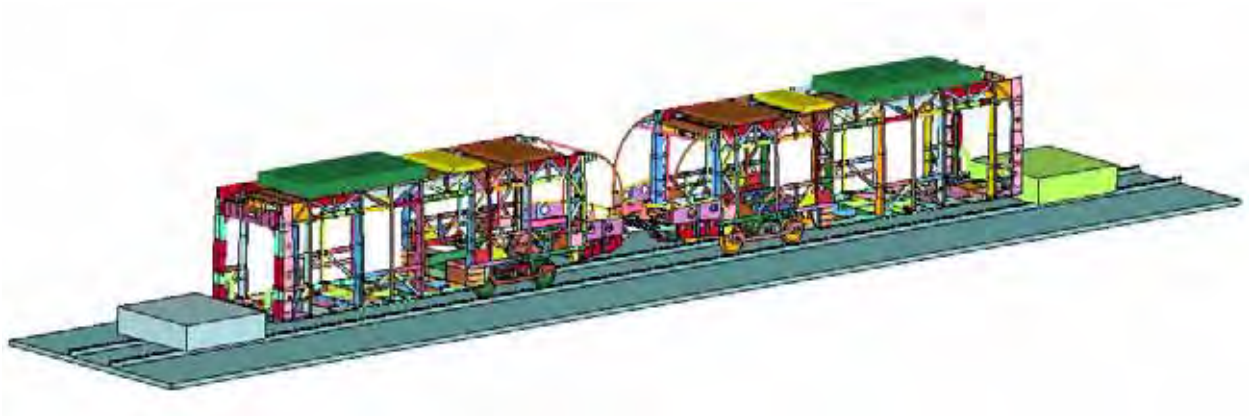

Figure 23. Overview of the 2-LRV Finite Element Model.

Only the structural members are included in the car models; no outer panels, auxiliary equipment, or interior fitments are included. This is a modeling approach that has been traditionally used in the analyses of LRVs where only the primary structural frame is considered. It ignores the secondary structures which are often designed with materials and attachments that are significantly weaker than the primary structural frame. The approach is considered to be conservative since the weight of the secondary components is included in the model but their potential structural reinforcement contributions are neglected. Thus, the actual crush strengths would be expected to be marginally higher than that obtained from these models.

The two impacting LRVs are identical (i.e. reflected LRVs placed on a level track). For this simulation, the car on the left was initially traveling at 20 mph. The impacted car on the right was initially stationary. The wheels on both cars were non-rotating and sliding along the rail

to simulate a condition of fully locked brakes such that the wheels slide along the rails with a frictional coefficient of 0.30. In previous analyses, the magnitude of the friction coefficient was found to have a small effect on the overall crash behaviors (e.g. average crush force and lengths). However, some level of friction is helpful to add unbalanced collision forces that will initiate asymmetric behaviors unless they are controlled by the design.

The collision interface between the two vehicles is shown in Figure 24. The initial collision occurs at the underframe with the primary collision load path transmitted to both vehicles through the head girder (end beam with anticlimber ribs).

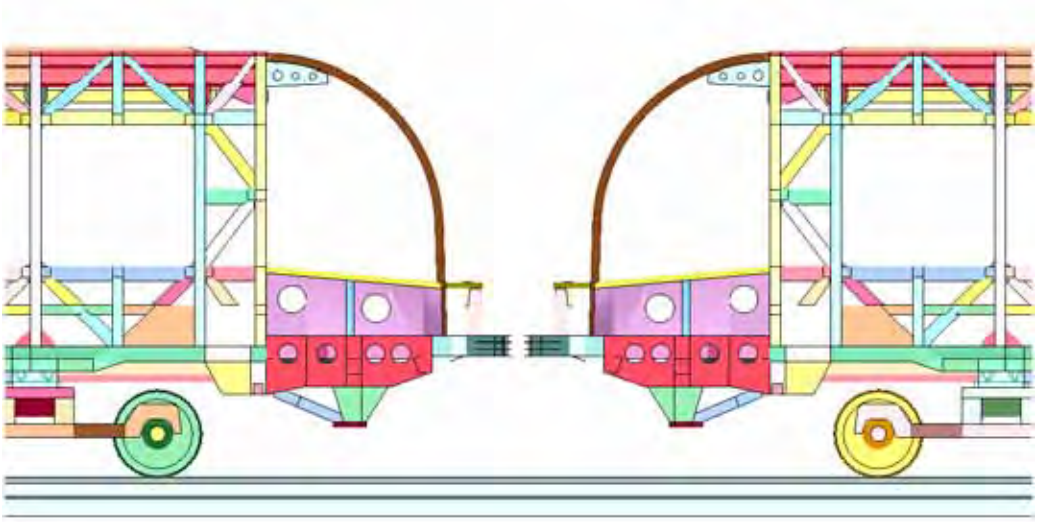

Figure 24. Collision Interface for the LRV 1 Compatible Crash Analysis.

The finite element mesh for LRV 1 was constructed as an assembly of many parts, using a mix of shell, brick, and beam elements. Most of the car model was constructed from 4-node shell elements. Some variation in the mesh resolution was included in various regions of the model. A relatively uniform mesh and fine mesh resolution in the impact zone of the LRV 1 model was used and contributed to a high quality simulation of the collision behavior. The trucks, ground, rail, and trailing masses were modeled with rigid 8-node brick elements. Beam elements were used in the articulating joint and bolster beam parts. These are modeling methodologies that have been previously applied and validated for a wide range of rail and highway vehicle crash analysis applications.

Cross section definitions were added to the model to collect forces through specified planes. This is a convenient way in LSDYNA to capture collision forces throughout the car body. Figure 25 shows the approximate location of each cross section. Four locations were selected for collecting forces:

1) Aft of the crush zone (section definition numbers 101-106),

2) Aft of the operator compartment (section definition number 107),

3) Aft of the bogie (section definition number 108), and

4) Forward of the articulation joint (section definition number 109).

At location 1, several sections were set up to collect total forces (101) and separate component forces (102-106). The components were split into side sills (102), central girders (103), underframe cross bracing (104), window belt and sheeting (105), and corner posts (106).

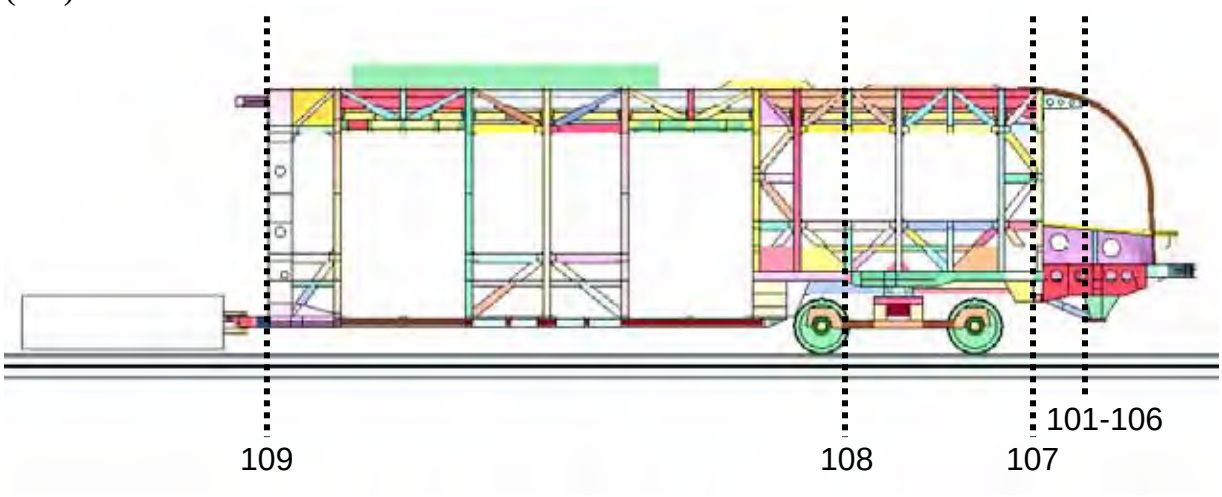

Figure 25. Force Cross Section Plane Locations for the LRV 1 model.

The cars were modeled using properties of Corten-B steel for most of the car body structure with some 70-ksi High-Strength Low Alloy (HSLA-70) steel in the corner posts and structural shelf. These materials were modeled using the bilinear elastic-plastic model *MAT_PLASTIC_KINEMATIC in LS-DYNA. Rigid bodies were given generic steel properties and were modeled with the *MAT_RIGID material in LS-DYNA. Material properties used in this study are summarized in Table 6.

Material densities were adjusted by major component group to match the specified vehicle weight. See Table 7 for breakout of component and total modeled masses compared to design LRV equipment weights.

Table 6. Material Properties Used in the LRV 1 Analyses

Material	Corten-B	HSLA-70	Steel (generic)
LS-DYNA Material	3, Bi-linear E-P	3, Bi-linear E-P	20, Rigid
Young's Modulus (GPa)	210	200	210
Poisson's Ratio	0.30	0.30	0.3
Yield Strength (MPa)	355	482	N/A
Tangent Modulus (MPa)	1403	779	N/A
Material Failure Strain	0.28	0.20	N/A

Table 7. Component Masses in the LRV 1 Model

Component	FEA Model (kg)
A-Car	12,614
Motor Bogie	5,315
Trailing Mass (includes B & C-car, Motor Bogie, and center truck)	27,197
Total	45,126

Material failure was included through element erosion. If an element reaches its critical plastic strain value (e.g. 20% effective plastic strain for HSLA-70), it is deleted from the calculation, creating a void and an area for stress concentration in the mesh (equivalent to setting the residual material strength in the failed element to zero). Failure criteria for the two elastic-plastic materials were chosen based on available material properties and mesh density considerations. This approach is used to identify regions where large scale fractures could eliminate a necessary load path in the stable crush behavior in a collision. In all of the analyses in this study, the failure modeling indicated only local small scale fractures and the complete failure of structural members was not a problem.

Contact between the two impacting cars and the rail was controlled with the LS-DYNA automatic contact algorithm *CONTACT_AUTOMATIC_SINGLE_SURFACE. This contact type is an efficient, robust algorithm recommended by LSTC, the makers of LS-DYNA, for vehicle crashworthiness analysis. The soft constraint option (SOFT=1) was employed within the contact algorithm, which uses a node-to-surface contact search algorithm. This approach works well for vehicle collision analyses over a broad range of speeds and varying material types. Contact within LS-DYNA is treated much like a spring between contacting segments. A restoring force, whose formulation depends on the SOFT option employed, is imposed on the contacting nodes to counteract penetrations between materials. For SOFT=1, the restoring force is based on nodal mass and time step. These contact algorithms and parameters were used for all of the analyses described in this report.

Analysis Results

The compatible collisions analyzed for LRV 1 are at 5, 10, 15, 20, 25, and 30 mph. One vehicle is moving at the collision speed (bullet) and the other is stationary (target). Unless otherwise stated, all figures show the bullet vehicle on the left and the target vehicle on the right. The force crush behaviors calculated for LRV 1 at the various collision closing speeds are shown in Figure 26. The characteristic force-crush behavior shows that the vehicle initially loads up to a crush force of approximately 2.0 MN before the significant crush forces develop. As the crush progresses the steady crush forces drop to a level of approximately 1.3 MN.

For the higher severity collision resulting in greater than 400 mm of crush for at least one of the vehicles, different crush responses can develop. In the 25 mph collision, an asymmetric crush response is obtained where one side has a greater rotation of the head girder and the crush length is significantly greater in one vehicle. In this asymmetric response, the crush forces continue to drop with increasing crush length. However, in the 30 mph collision, a

symmetric crush response is obtained and the crush forces increases to approximately 1.9 MN for crush lengths of 500-600 mm.

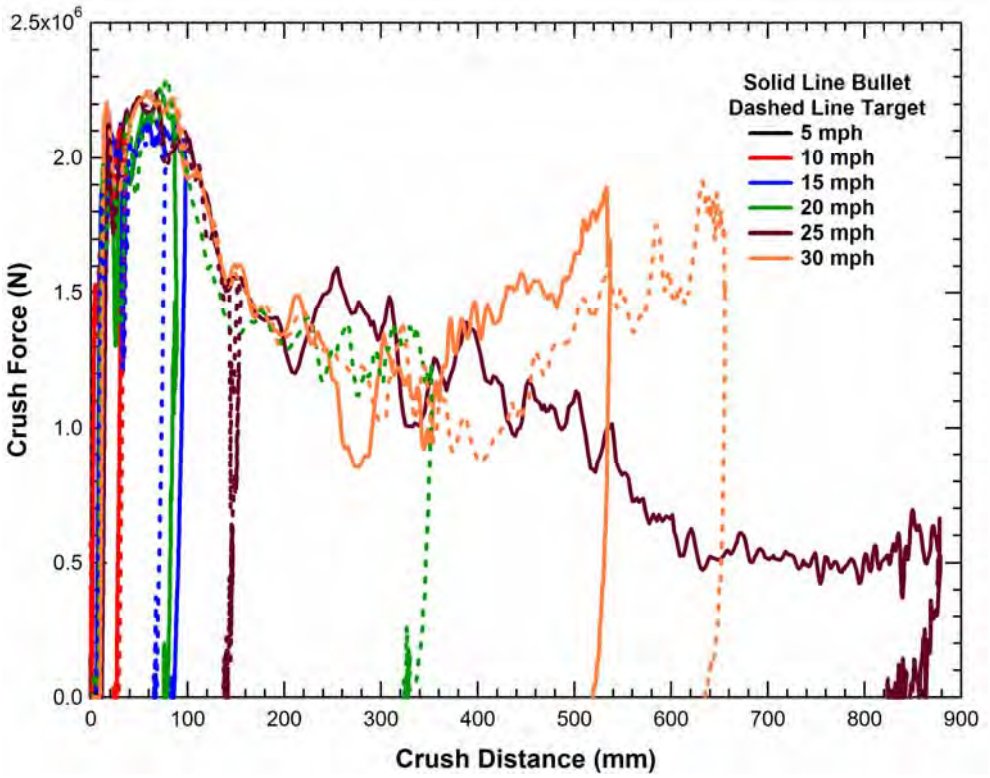

Figure 26. Force-Crush Behavior for all Speeds of the LRV 1 Compatible Crash Analysis.

The crush deformations of LRV 1 at 5 mph were limited to some minor deformations (3 mm) of the anticlimber ribs on the head girder and are therefore not provided in detail. The 5 mph behavior does indicate that a no damage requirement at this collision speed can be easily achieved with some level of energy absorption in either a coupler or bumper assembly.

The crush response of the target LRV 1 for the 10 mph collision is shown in Figure 27. The fringes of crush are reference to a plane at the back of the cab. However, no significant crush deformations occurred in these analyses for structures aft of the cab. There is approximately 25 mm of crush in the target LRV and the response of the bullet vehicle is nearly identical. The crush response is a flattening of the nose of the head girder and a corresponding 15-20 mm of displacement in the structural shelf produced by the strong connection through the collision posts. This crush response is a controlled collapse that occurs in the desired mode developed during the vehicle design effort.

The calculated 15 mph compatible collision behavior of LRV 1 is shown in Figure 28. The bullet vehicle is shown on the left and the target on the right. The crash response at a time of 0.15 s, shown in Figure 28(a), is clearly asymmetric, even at this lower speed. By the time of 0.27 s, shown in Figure 28(b), the collision is over.

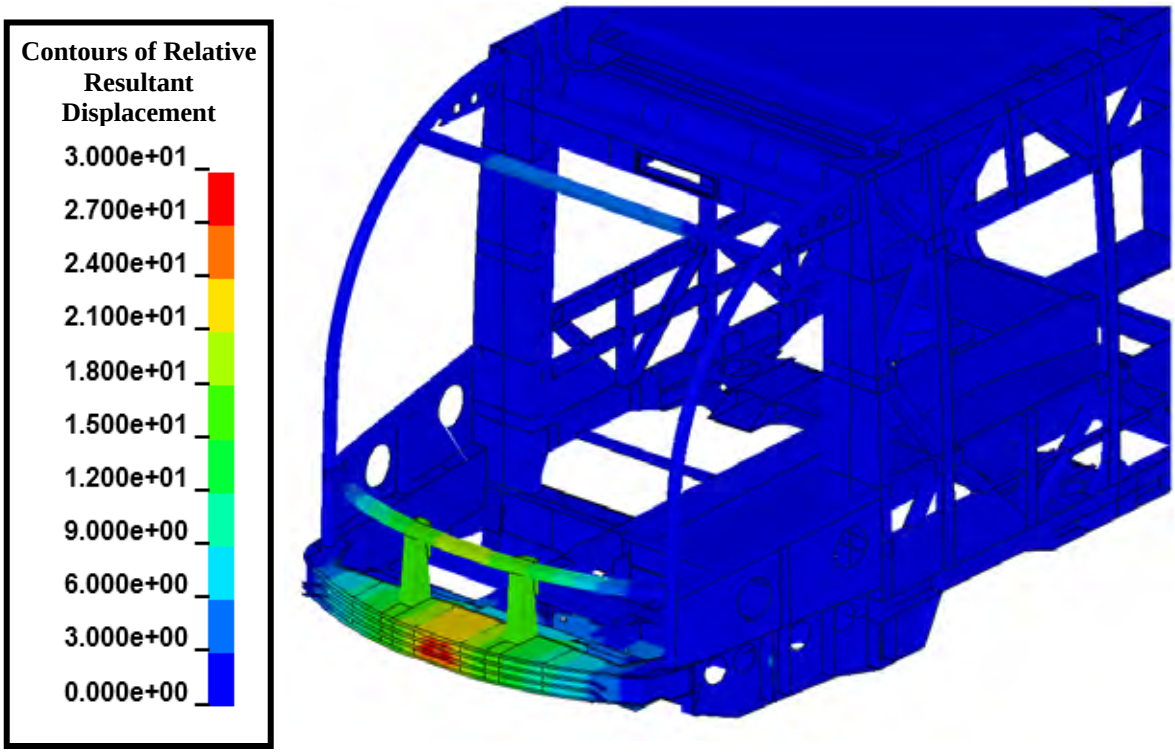

Figure 27. Crush Level (mm) for the LRV 1 Target Car in the 10 mph Compatible Collision.

This asymmetric crush behavior illustrates the significance of performing analyses of the collisions of two vehicles with one vehicle moving and one at rest. Due to the braking forces (frictional sliding of the wheels on the rails), the bullet vehicle has a tendency to pitch downward and the crash forces on the target vehicle will result in an upward pitch motion. These variations in the loading are a significant test of the stability of the crush behavior. If an idealized simulation of a single collision into a rigid wall was used, the development of the asymmetric crash response would not have been identified. Thus, a recommendation of this study is that this type of analysis (moving vehicle colliding with a stationary vehicle, both with brakes applied) be used in the proposed CEM requirements for an LRV safety standard to require that the stability of the crush response be evaluated in the design process.

The crush responses of the bullet and target LRV 1 vehicles for the 15 mph collision are shown in Figure 29 and Figure 30, respectively. The fringes of crush are again referenced to a plane at the back of the cab. There is approximately 80 mm of crush in the target LRV and 100 mm of crush in the bullet vehicle. The crush response is a flattening of the nose of the head girder and a corresponding displacement in the structural shelf produced by the strong connection through the collision posts. Despite the asymmetry of the vehicle responses, the behaviors are both a progressive collapse occurring in a desirable crush mode similar to that developed during the vehicle design effort.

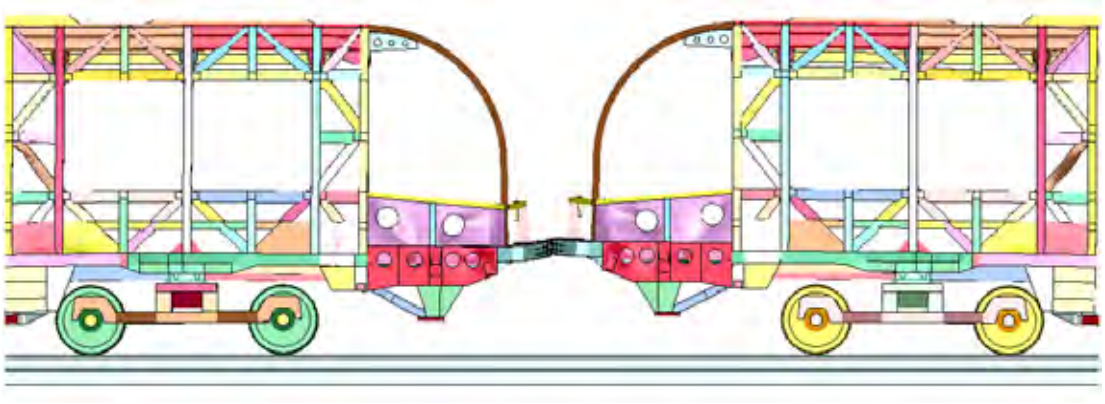

(a) Time = 0.150 s

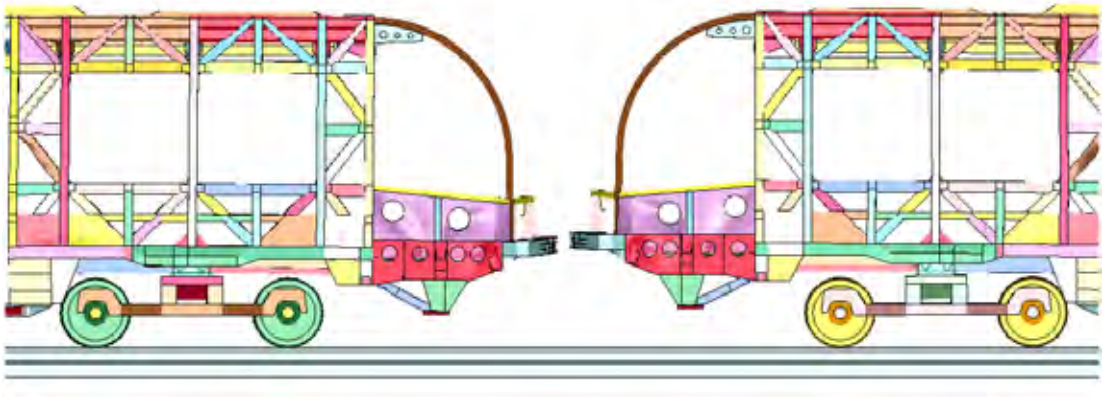

(b) Time = 0.270 s

Figure 28. Simulation of the LRV 1 Compatible Collision at 15 mph.

The calculated 20 mph compatible collision response of LRV 1 is shown in Figure 31. The bullet vehicle is shown on the left and the target on the right and the response is shown at a time where the collision event is over and the vehicles have rebounded from each other. The calculated crush for the LRV 1 bullet and target vehicles in the 20 mph collision are shown in Figure 32 and Figure 33, respectively. The fringes of crush are again referenced to a plane at the back of the cab.

There is approximately 350 mm of crush in the target LRV and 100 mm of crush in the bullet vehicle. The larger crush of the target vehicle is developed through a push back and downward rotation of the head girder and a corresponding crush of the central sills immediately aft of the head girder. A small amount of corresponding crush is also developed in the forward side sills. Despite the asymmetry of the vehicle responses, the behaviors are both a progressive collapse occurring in a desirable crush mode similar to that developed during the vehicle design effort.

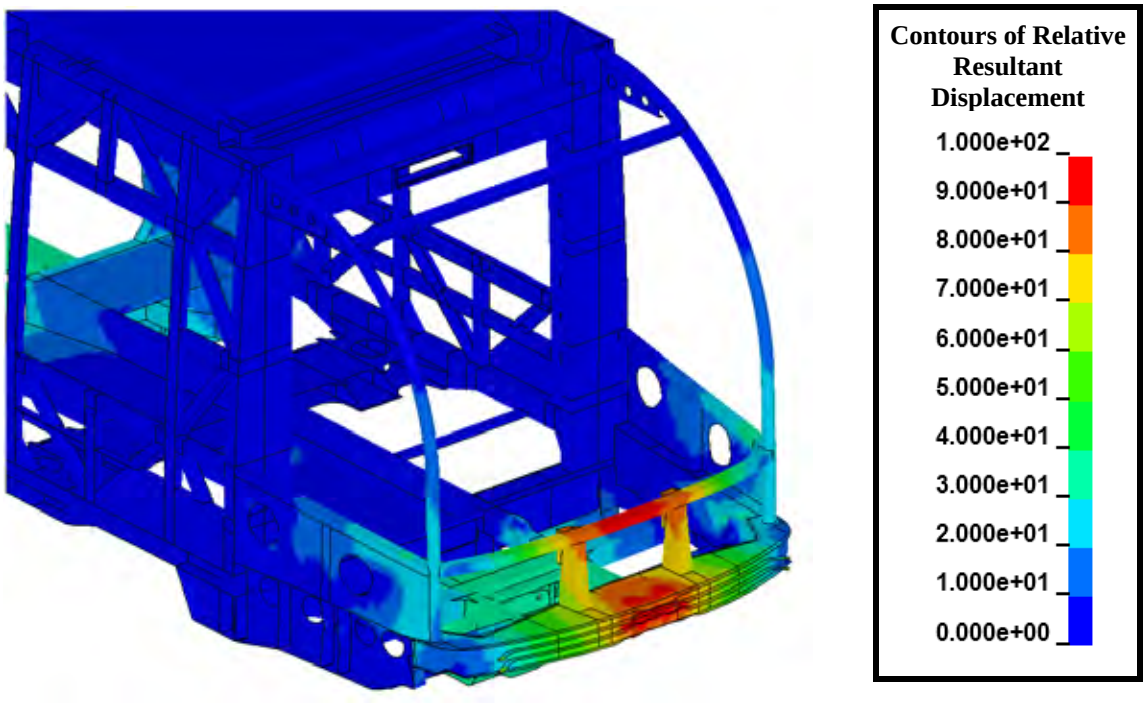

Figure 29. Crush Level (mm) for the LRV 1 Bullet Car in the 15 mph Compatible Collision.

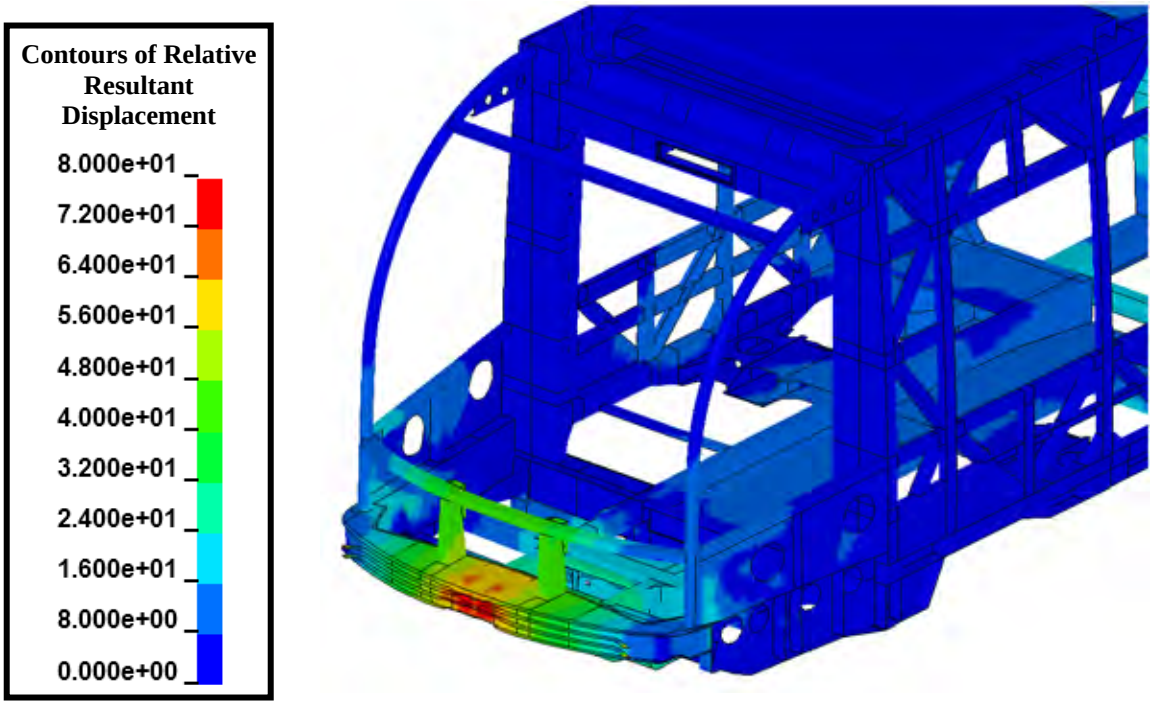

Figure 30. Crush Level (mm) for the LRV 1 Target Car in the 15 mph Compatible Collision.

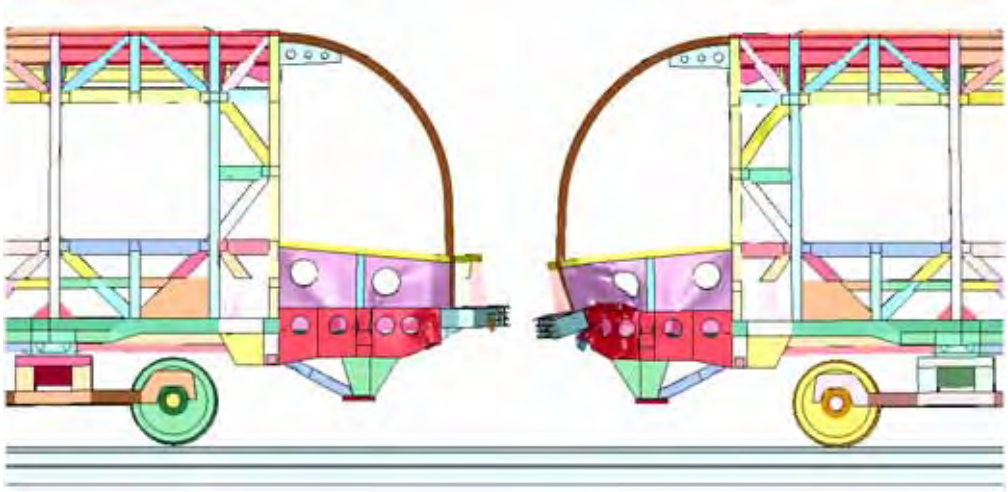

Figure 31. Simulation of the LRV 1 Compatible Collision at 20 mph.

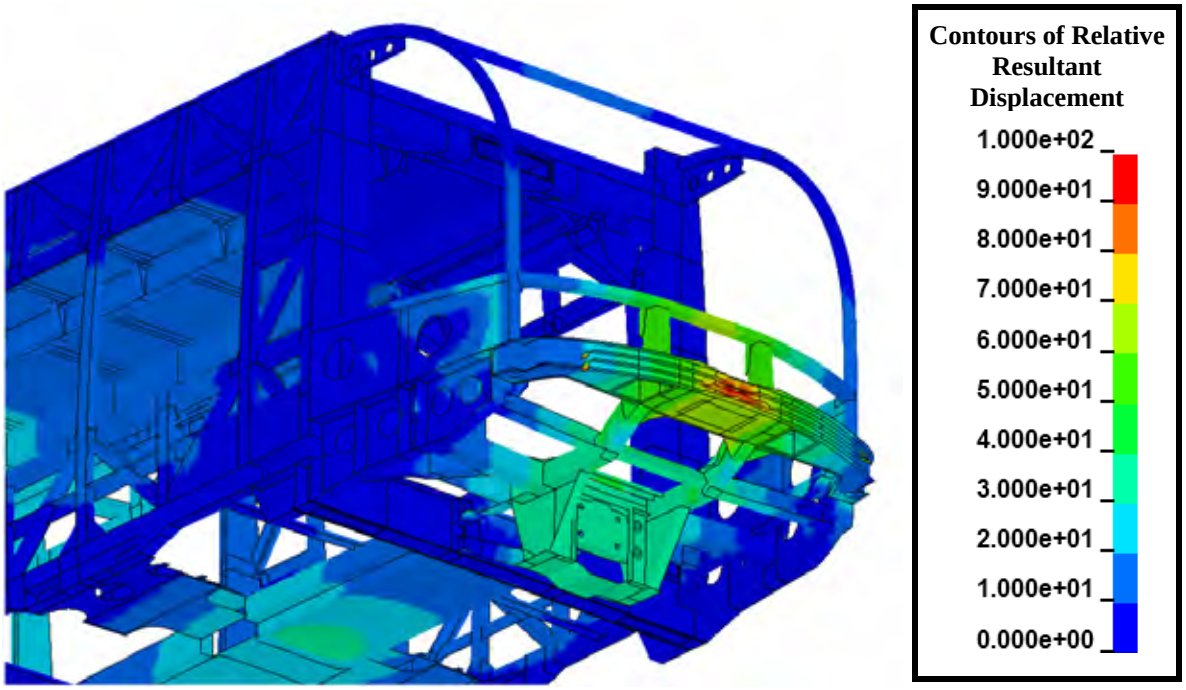

Figure 32. Crush Level (mm) for the LRV 1 Bullet Car in the 20 mph Compatible Collision.

The calculated 25 mph compatible collision response of LRV 1 is shown in Figure 34. The bullet vehicle is shown on the left and the target on the right. The calculated crush for the LRV 1 bullet and target vehicles in the 25 mph collision are shown in Figure 35 and Figure 36, respectively. There is approximately 150 mm of crush in the target LRV and 900 mm of crush in the bullet vehicle. Note that for the 25 mph collision the bullet vehicle now has the larger crush distance of the two vehicles as opposed to the response in the 20 mph collision. This indicates that relatively small variations in the impact conditions can influence the vehicle that experiences the larger crush magnitude.

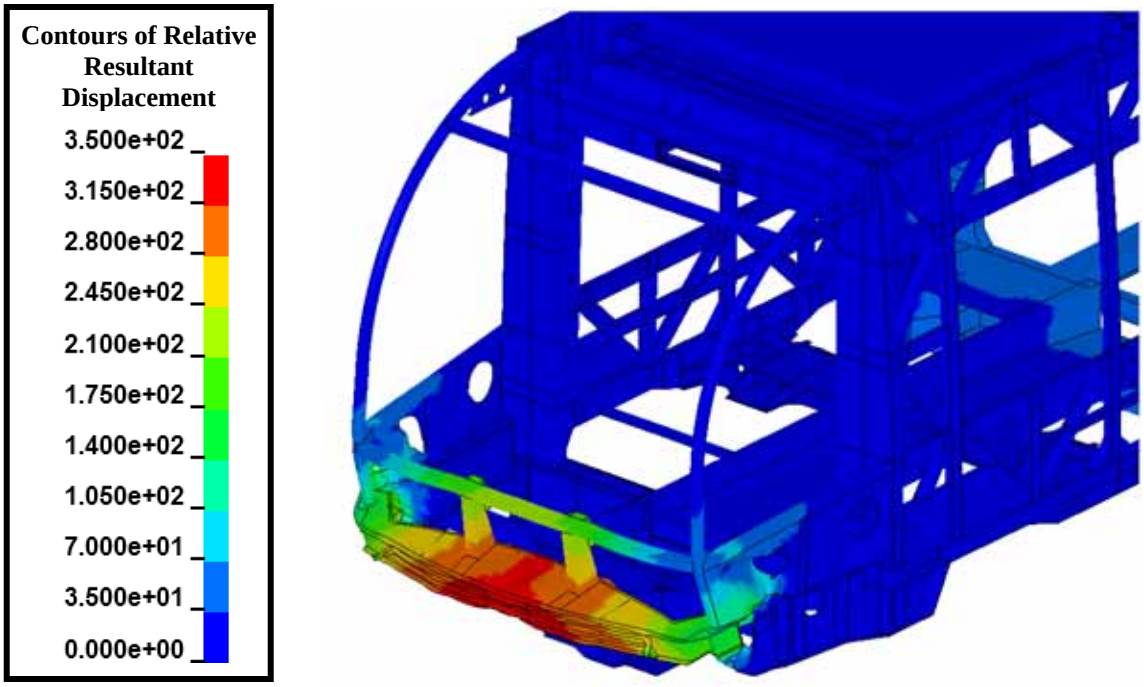

Figure 33. Crush Level (mm) for the LRV 1 Target Car in the 20 mph Compatible Collision.

The larger crush of the bullet vehicle is again developed through a push back and downward rotation of the head girder and a corresponding crush of the central sills immediately aft of the head girder. Corresponding crush is also developed in the forward side sills.

The calculated 30 mph compatible collision response of LRV 1 is shown in Figure 37. The bullet vehicle is shown on the left and the target on the right. The calculated crush for the LRV 1 bullet and target vehicles in the 30 mph collision are shown in Figure 38 and Figure 39, respectively. The fringes of crush are again referenced to a plane at the back of the cab. At this collision speed the crush in both vehicles is relatively symmetric and balanced with approximately 600 mm of crush in both LRVs. The crush mode of both vehicles is again developed through a push back and downward rotation of the head girder and a corresponding crush of the central sills immediately aft of the head girder. Corresponding crush is also developed in the forward side sills. The crush responses are a progressive collapse from the front of the cab as desired for a crashworthy design.

The contributions to the crush force transmitted through the cross section at the back of the cab are plotted against the crush displacements in Figure 40 (cross section definitions 101 through 106 are shown in Figure 25). Initially the central girders carry more than half of the total impact loads and rapidly reach a transmitted force of 1.2 MN before the buckling and crush of the central girders is initiated and the load drops off. As the loads in the central girders are reduced (between 0 and 150 mm of crush), the load is transmitted to the side sills and window belt.

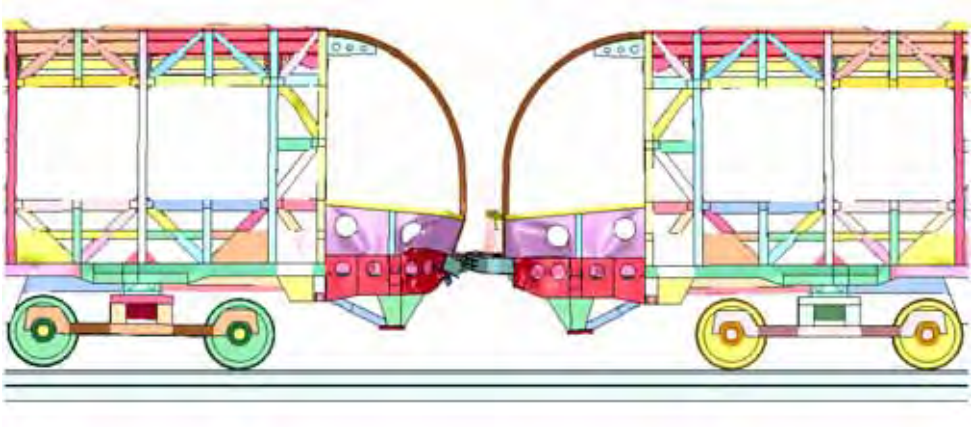

(a) Time = 0.150 s

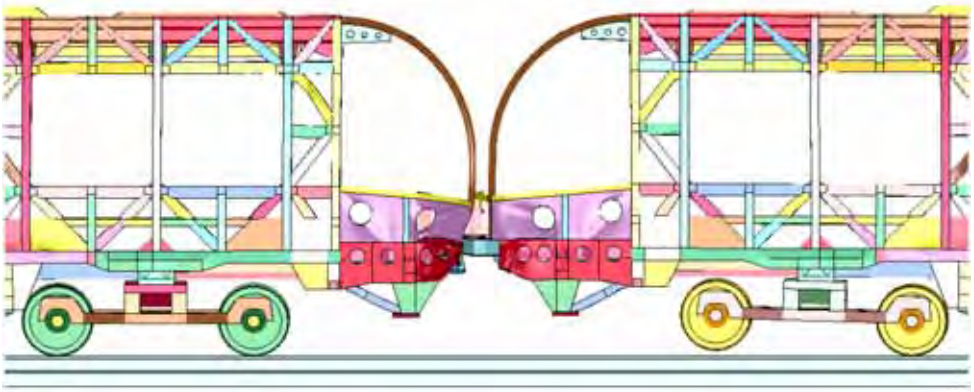

(b) Time = 0.420 s

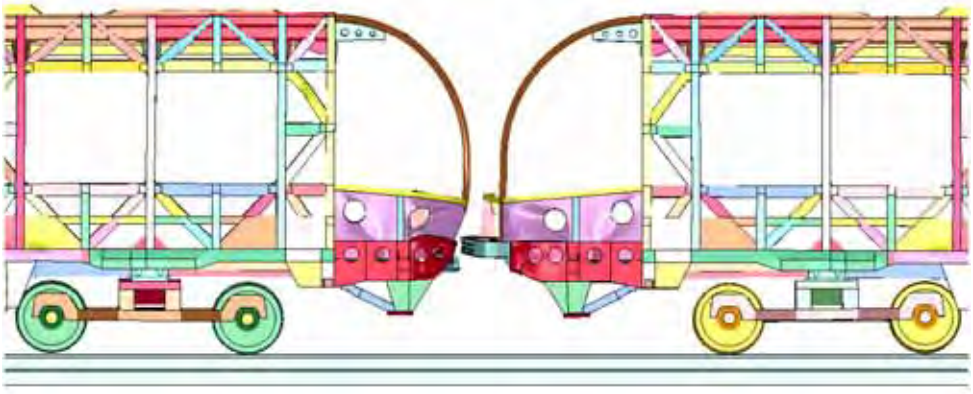

(c) Time = 0.620 s

Figure 34. Simulation of the LRV 1 Compatible Collision at 25 mph.

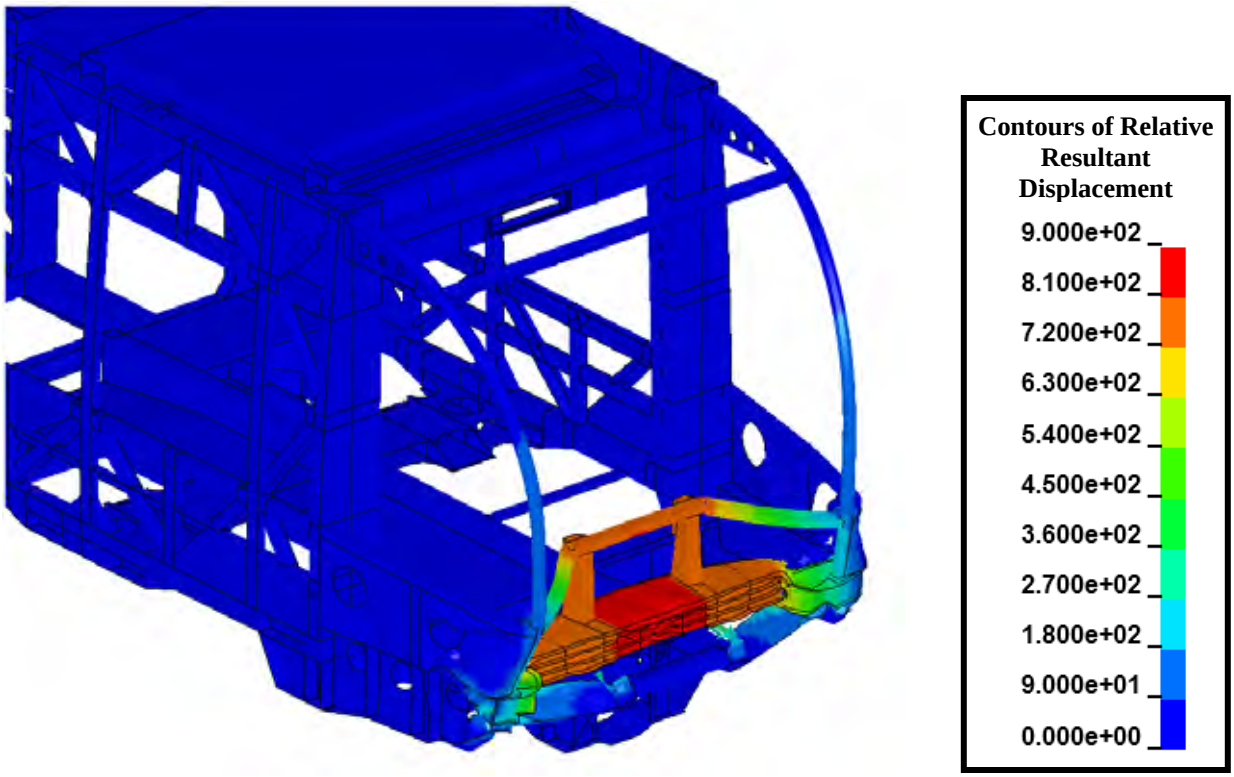

Figure 35. Crush Level (mm) for the LRV 1 Bullet Car in the 25 mph Compatible Collision.

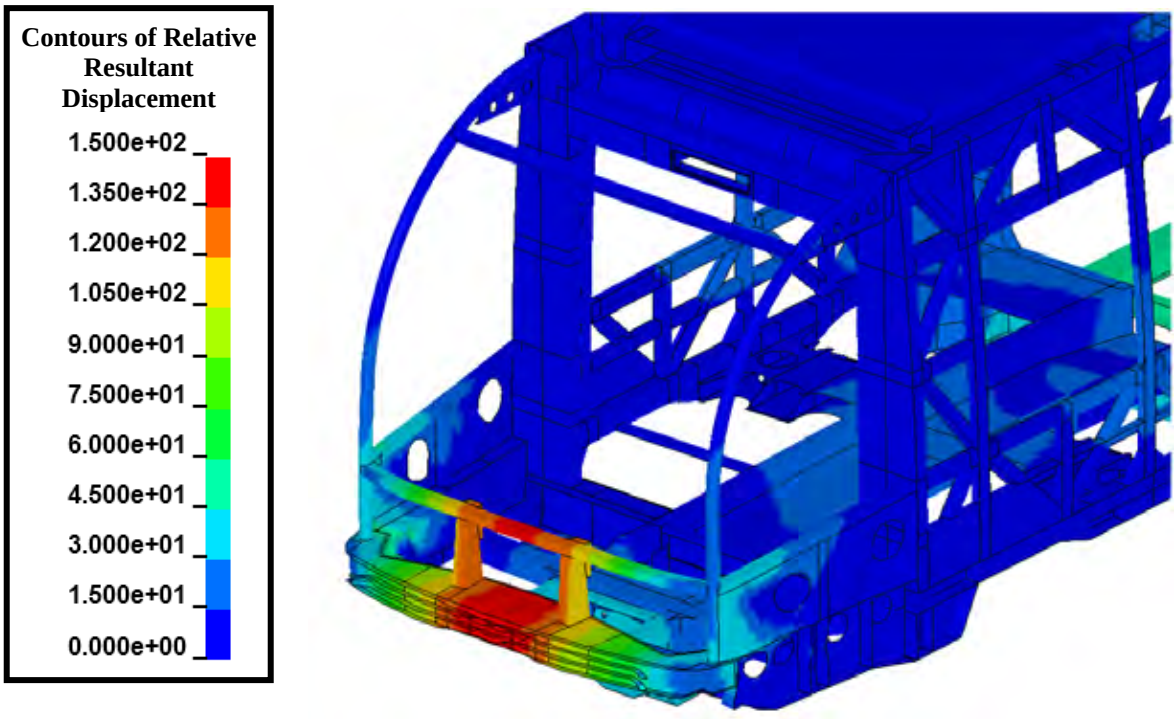

Figure 36. Crush Level (mm) for the LRV 1 Target Car in the 25 mph Compatible Collision.

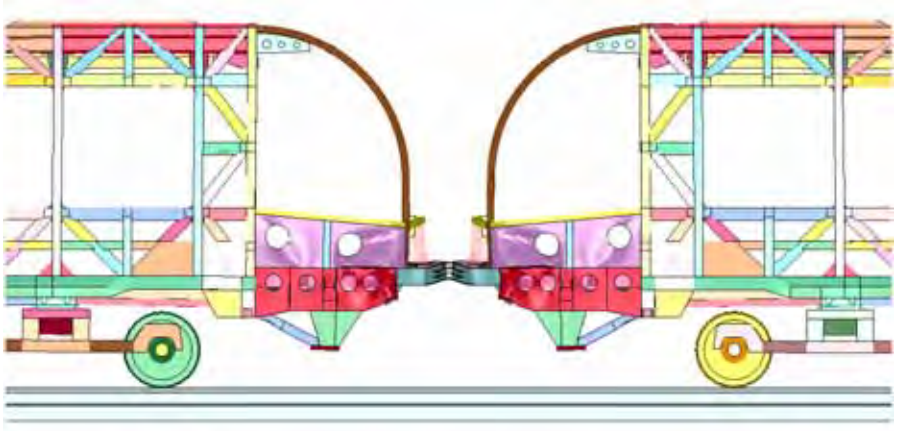

(a) Time = 0.070 s

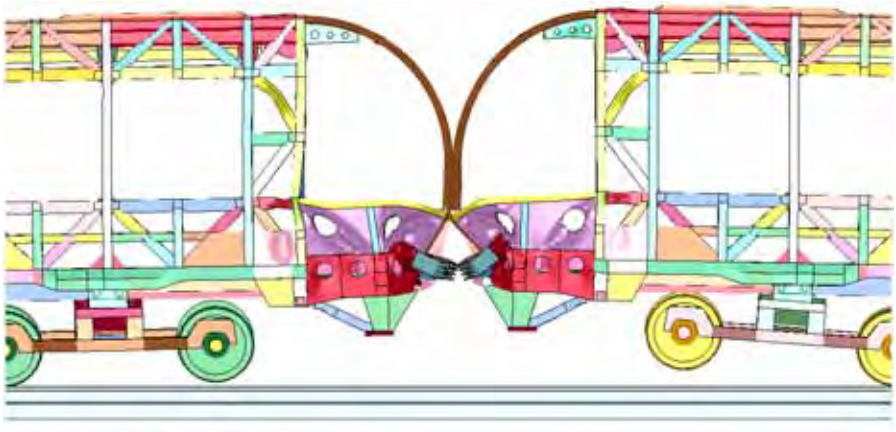

(b) Time = 0.290 s

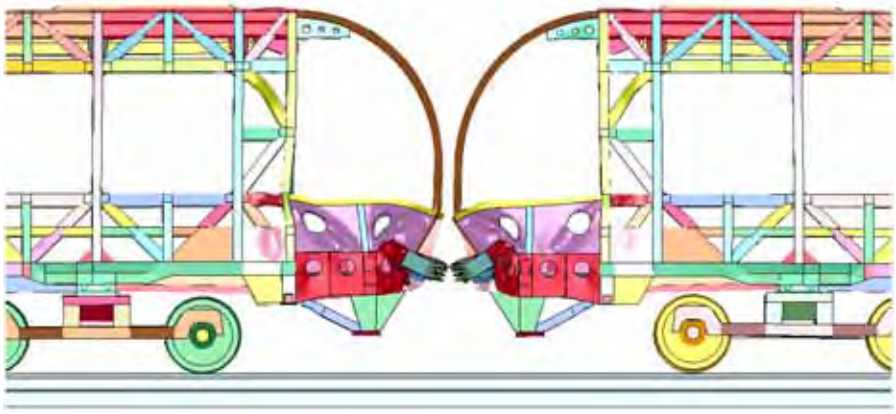

(c) Time = 0.500 s

Figure 37. Simulation of the LRV 1 Compatible Collision at 30 mph.

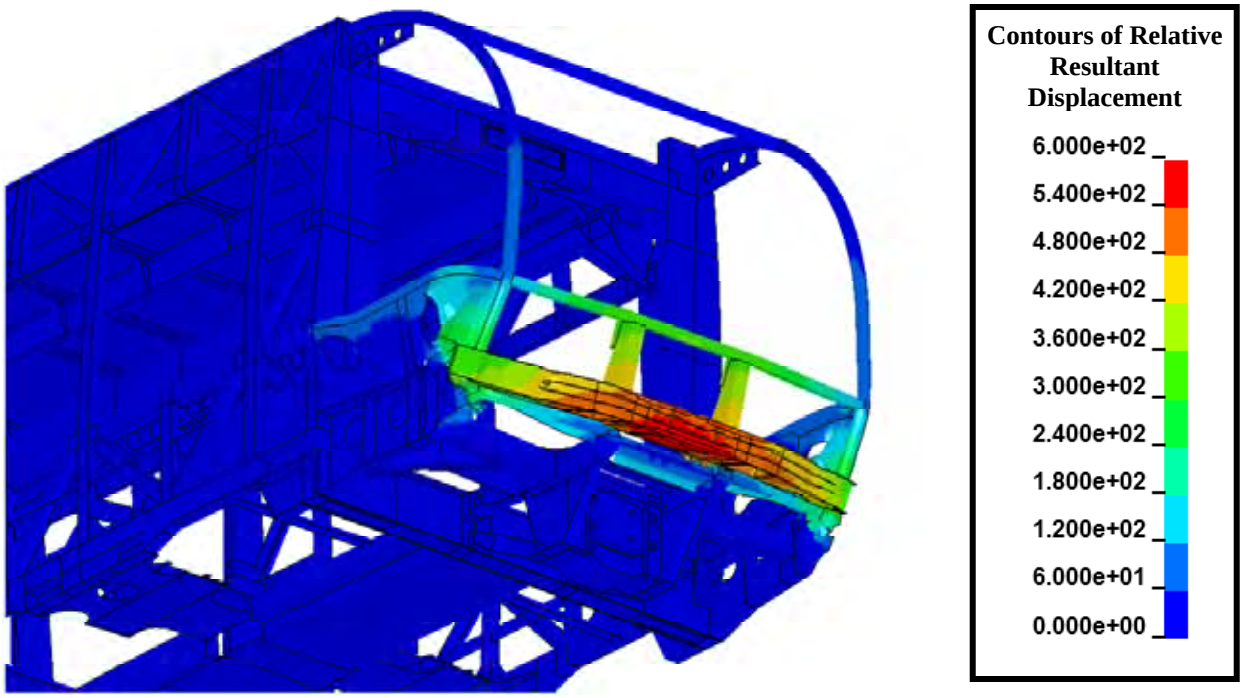

Figure 38. Crush Level (mm) for the LRV 1 Bullet Car in the 30 mph Compatible Collision.

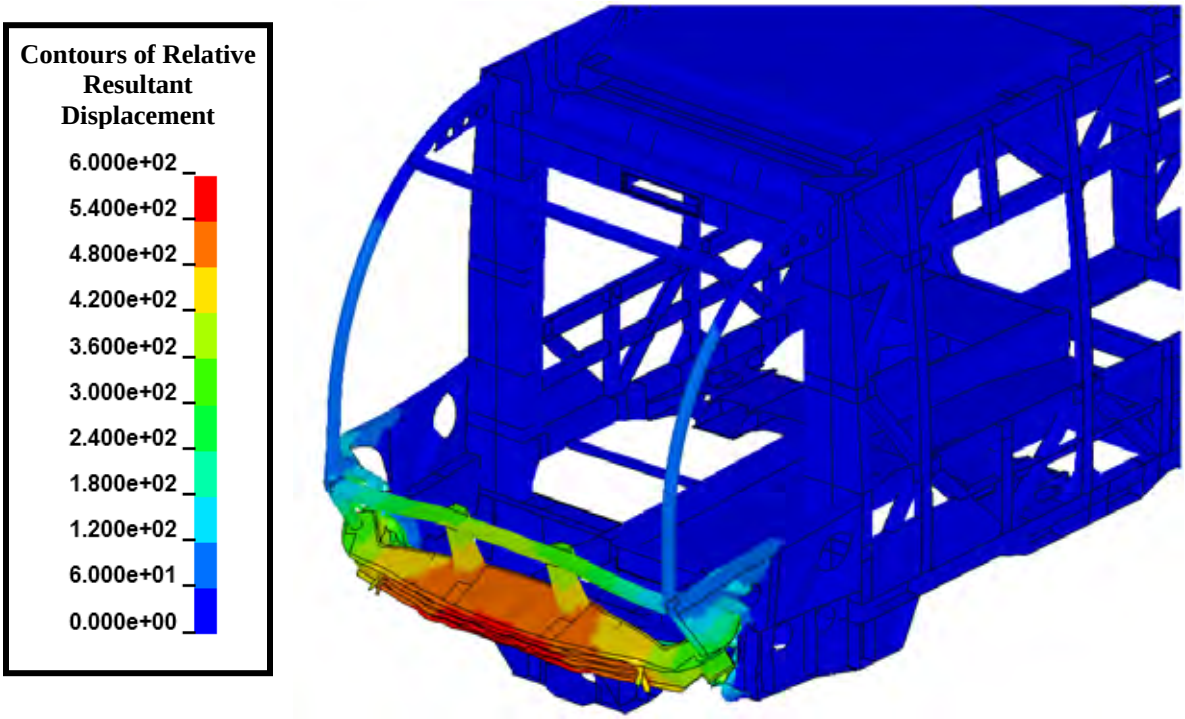

Figure 39. Crush Level (mm) for the LRV 1 Target Car in the 30 mph Compatible Collision.

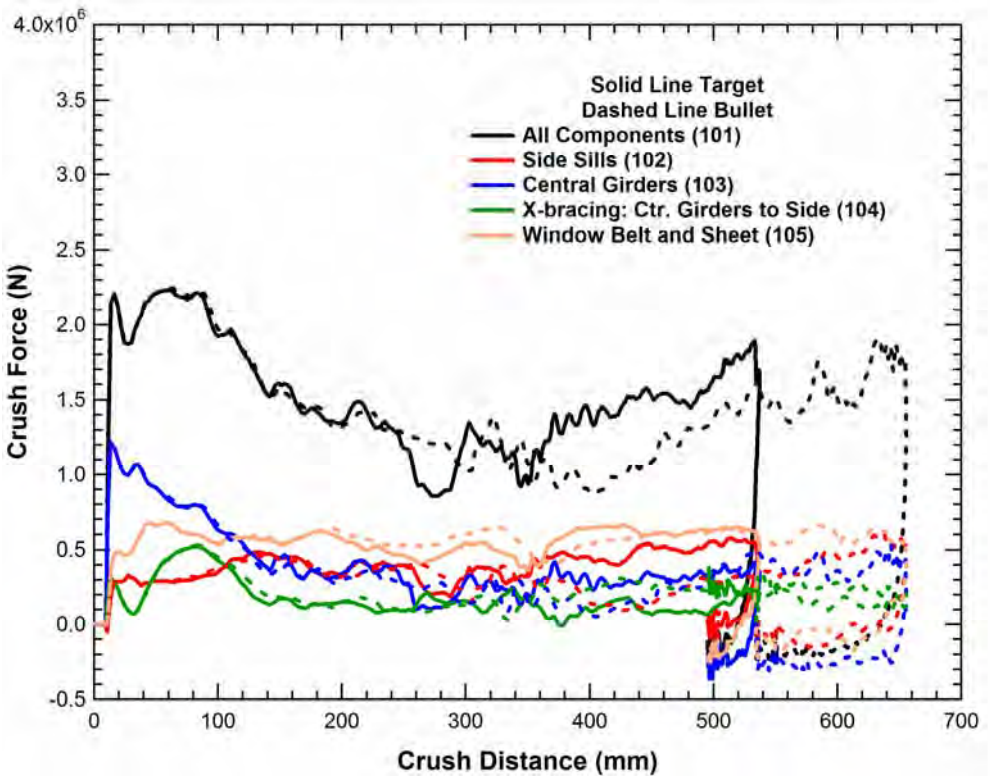

Figure 40. Force-Crush Behavior for the 30 mph LRV 1 Compatible Crash Analysis.

2.4. LRV 2 Compatible Collisions

LRV 2 Model

The mesh for the LRV 2 model was initially developed in ANSYS format and converted to LS-DYNA format. Further input file modifications were made to: (1) separate rigid bodies, (2) add a rail and ground model, (3) assign appropriate shell thickness values, (4) assign material models, (5) prescribe contact algorithms, (6) add gravity, (7) prescribe initial conditions, and (8) perform other miscellaneous edits to run the model in LS-DYNA.

The model for LRV2 after conversion to LS-DYNA format is shown in Figure 41. The force cross section plane definitions are also indicated in the figure. Note that only the A-car is explicitly modeled. The B and C cars are lumped into a trailing mass coupled to the respective A-car through the articulating joint. Only the structural members are included in the car models; no outer panels, auxiliary equipment, or interior fitments are included. The mesh refinement in the forward portion of the cab is shown in Figure 42.

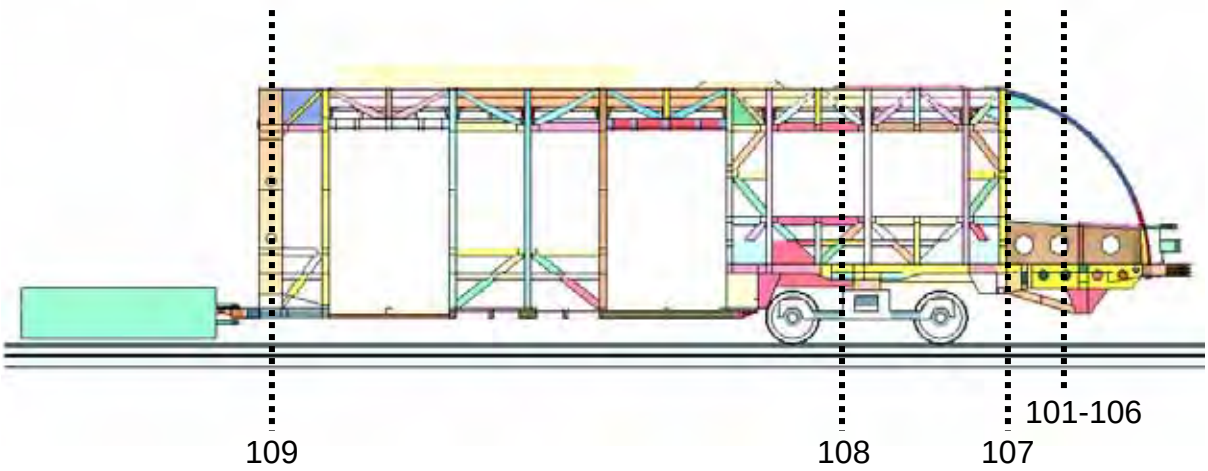

Figure 41. Force Cross Section Plane Locations for the LRV 2 Model.

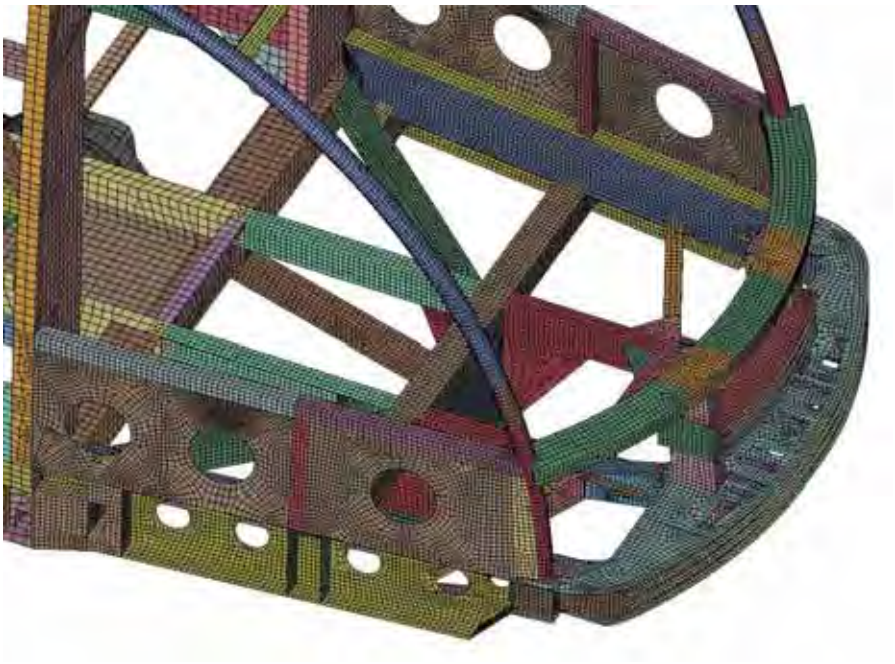

Figure 42. Overview of the Finite Element Model for LRV 2.

The cross section definitions were added to the model to collect forces through specified planes. This is a convenient way in LSDYNA to capture collision forces throughout the car body. Figure 41 shows the approximate location of each cross section. Four locations were selected for collecting forces:

1) Aft of the crush zone (section definition numbers 101-106),
2) Aft of the operator compartment (section definition number 107),
3) Aft of the bogie (section definition number 108), and
4) Forward of the articulation joint (section definition number 109).

At the forward cab location, several sections were set up to collect total forces (101) and separate component forces (102-106). The components were split into side sills (102), central girders (103), underframe cross bracing (104), window belt and sheeting (105), and corner posts (106).

The design of this LRV is unique as a result of a geometric mismatch of the LRV with existing LRVs currently operating on the system. The LRV 2 design is consistent with the ongoing trend in modern LRV designs toward a lower vehicle underframe, fold back couplers, and enclosed front end design. However, older LRVs operating on the system had a higher cab underframe and head girder.

The operational interface between the new and existing LRV designs is shown in Figure 43. The vertical offset between the head girders in the two LRVs is 310 mm. The LRV 2 design incorporated a secondary anticlimber at a height compatible with the older LRV geometry. This secondary anticlimber structure was attached to the collision posts at a position approximately mid-height from the head girder to the structural shelf. Many of the LRV 2 cab structural members were also strengthened to be able to resist the loads from a collision with a vehicle with this vertical offset.

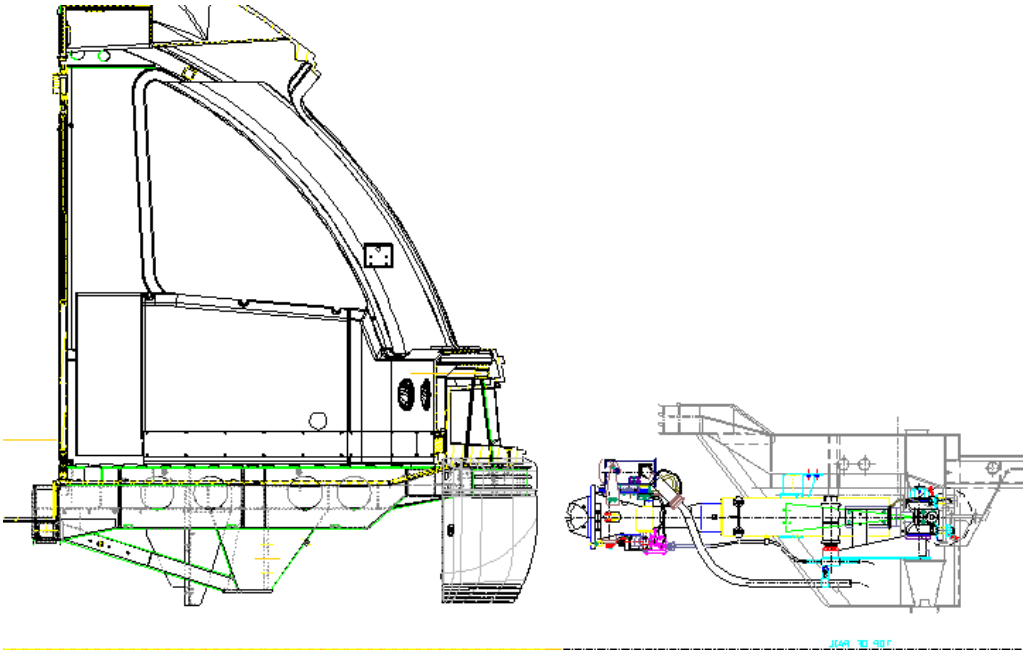

Figure 43. Operational Interface between LRV 2 (left) and an Existing LRV Design (right).

Most of the model for the LRV 2 frame was constructed from 4-node shell elements. Some variation in the mesh resolution was included in various regions of the model. A relatively uniform mesh and fine mesh resolution in the impact zone of the LRV model was used and contributed to a high quality simulation of the collision behavior. The trucks, ground, rail, and trailing masses were modeled with rigid 8-node brick elements. Beam elements were used in the articulating joint and bolster beam parts.

The rigid body trailing masses were constrained to only allow translation in the direction parallel to the track. Rotations and off-axis translations were not allowed for the trailing masses. The ground and track were modeled as rigid and fully constrained. No other constraints were placed on the model.

LRV 2 was modeled using properties of ASTM A588 steel for most of the car body structure with some 70-ksi High-Strength Low Alloy (HSLA-70) steel in the corner posts and structural shelf. Material properties were supplied for both of the steels and used to develop LS-DYNA material models. The HSLA-70 material was modeled using the *MAT_PLASTIC_KINEMATIC bilinear elastic-plastic model. Additional material characterization data was available for the ASTM A588 steel and as a result it was modeled using the *MAT_PIECEWISE_LINEAR_PLASTICITY constitutive model. The piecewise linear constitutive model was adapted to provide a better characterization of the material behavior in the post-yield regime. The piecewise linear hardening behavior is given in Table 8.

Table 8. Piecewise Linear Yield Curve for ASTM A588

	Plastic Strain	Effective Stress (MPa)
Point 1	0.00E+00	355
Point 2	1.00E-02	386
Point 3	2.00E-02	417
Point 4	3.50E-02	455
Point 5	5.00E-02	485
Point 6	8.00E-02	530
Point 7	1.20E-01	571
Point 8	1.12E+00	1230

Material failure was included through element erosion. If an element reaches its plastic failure strain, it is deleted from the calculation, creating a void and an area for stress concentration in the mesh. Failure criteria for the elastic-plastic materials were chosen based on available material properties and mesh density considerations. Rigid bodies were given generic steel properties and were modeled with the *MAT_RIGID material in LS-DYNA. Material properties used in this study are summarized in Table 9.

Table 9. Material Properties Used in the Collision Analysis

Material	ASTM A588	HSLA-70	Steel (generic)
LS-DYNA Material	24, Piecewise E-P	3, Bi-linear E-P	20, Rigid
Young's Modulus (GPa)	207	200	210
Poisson's Ratio	0.35	0.30	0.30
Yield Strength (MPa)	355	482	N/A
Tangent Modulus (MPa)	n/a	779	N/A
Material Failure Strain	0.30	0.20	N/A

The total LRV 2 mass was calculated as 43 Mg in LSDYNA. Table 10 provides a breakout of component and total modeled LRV 2 masses.

Table 10. Component Masses in the LRV 2 Model

Component	FEA Model (kg)
A-Car	10,508
Motor Bogie	5,336
Trailing Mass (includes B & C-car, Motor Bogie, and center truck)	27,166
Total	43,010

Analysis Results

The compatible collisions analyzed for LRV 2 are at 5, 10, 15, 20, 25, and 30 mph. One vehicle is moving at the collision speed (bullet) and the other is stationary (target). Unless otherwise state, all images show the bullet vehicle on the left and the target vehicle on the right. The collision interface between the two vehicles is shown in Figure 44.

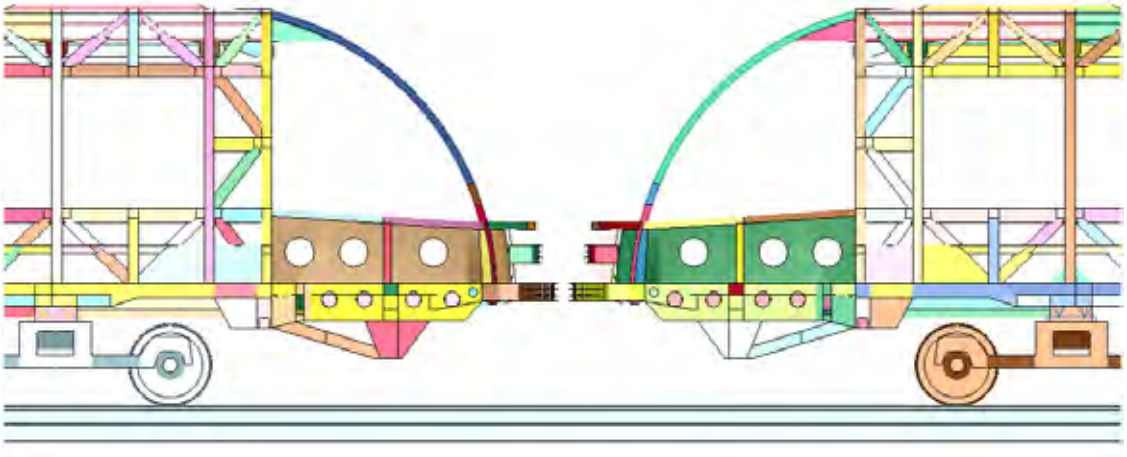

Figure 44. Collision Interface for the LRV 2 Compatible Crash Analysis.

The force crush behaviors calculated for LRV 2 at the various collision closing speeds are shown in Figure 45. The characteristic force-crush behavior shows that the vehicle initially loads up to a crush force of approximately 1.0 MN before any significant crush deformations develop. As the crush progresses the crush forces rapidly increase to a level of over 2.0 MN at a crush deflection of approximately 40 mm. Between 40 and 100 mm of crush the force drops off again then again rises to an approximately steady state crush force of over 2.0 MN.

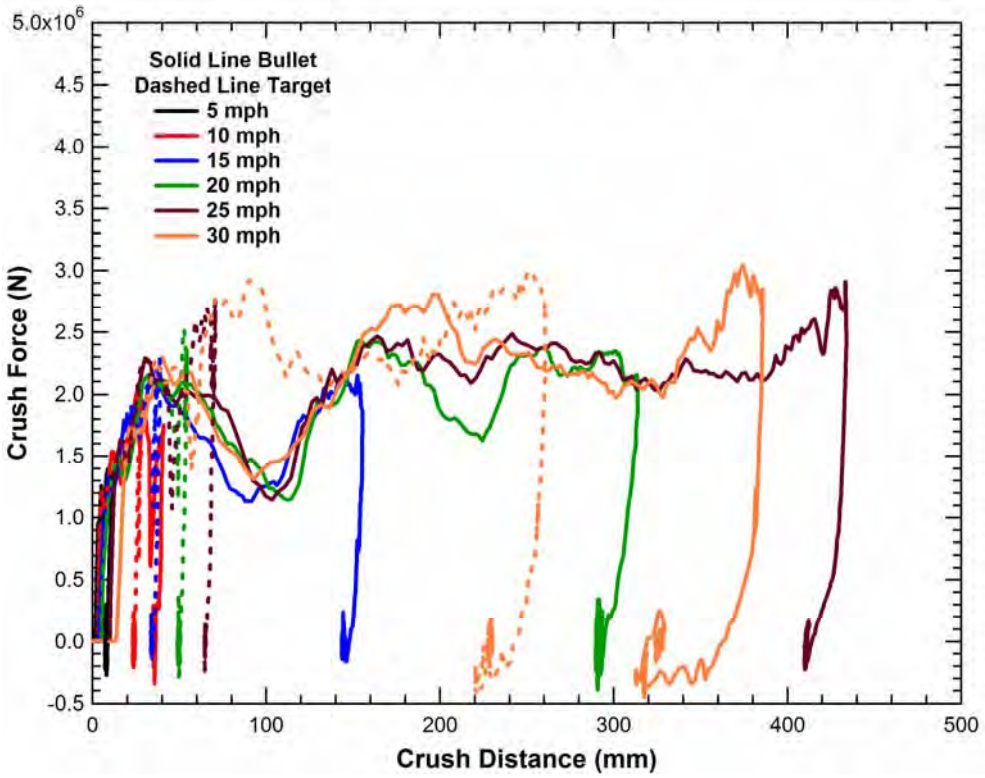

Figure 45. Force-Crush Behavior for all Speeds of the LRV 2 Compatible Crash Analysis.

The crush deformations of LRV 2 at 5 mph were limited to some minor deformations (8 mm) at the nose of the head girder and are therefore not provided in detail. The 5 mph behavior does indicate that a no damage requirement at this collision speed can be easily achieved with some level of energy absorption in either a coupler or bumper assembly on LRV 2.

The crush response of the target LRV 2 vehicle for the 10 mph collision is shown in Figure 46. The crush deformations are located in an energy absorbing crush zone in the nose of the head girder. The fringes of crush for the LRV 2 bullet and target vehicles in the 10 mph collision are shown in Figure 47 and Figure 48, respectively. The average crush in the forward energy absorbers is approximately 50 mm and no significant crush deformations occurred behind the head girders of the LRVs. This crush response is a controlled collapse of the forward crush element as it was designed to deform.

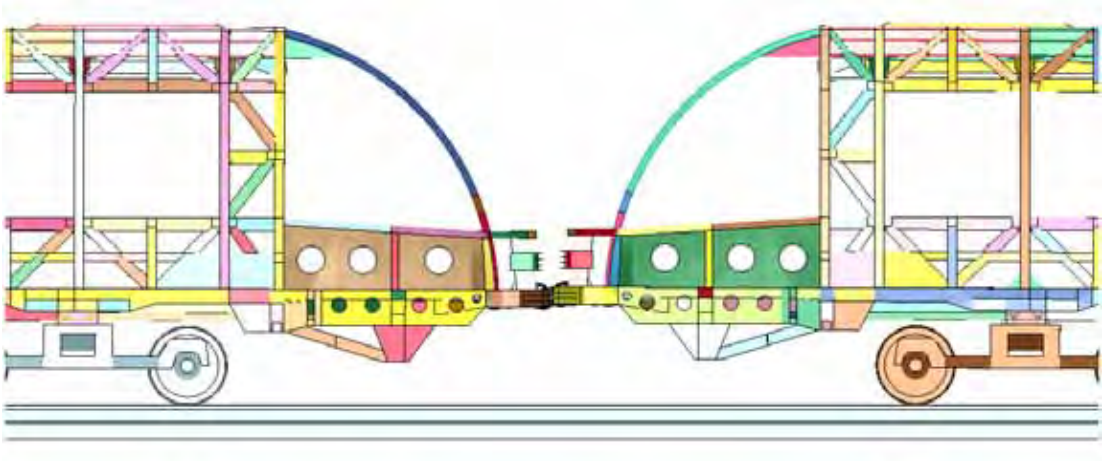

(a) Time = 0.080 s

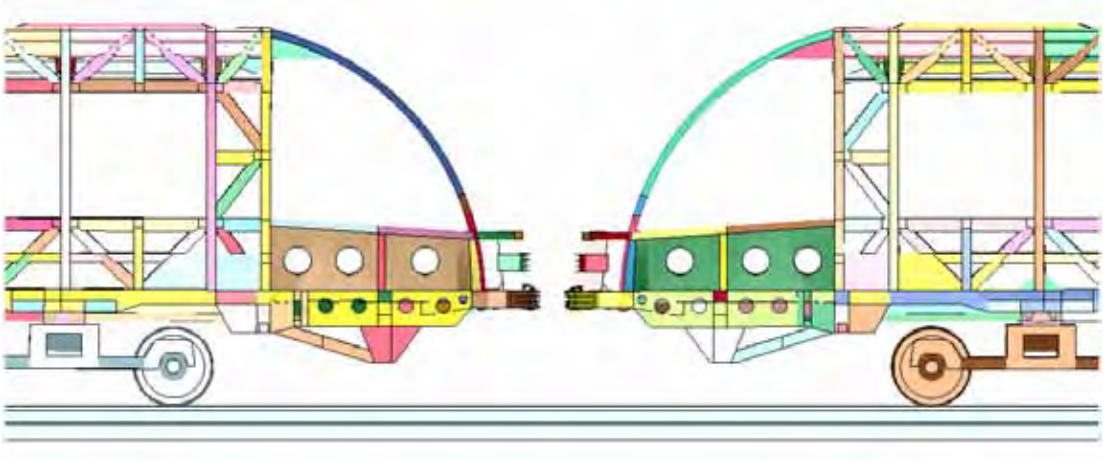

(b) Time = 0.360 s

Figure 46. Simulation of the LRV 2 Compatible Collision at 10 mph.

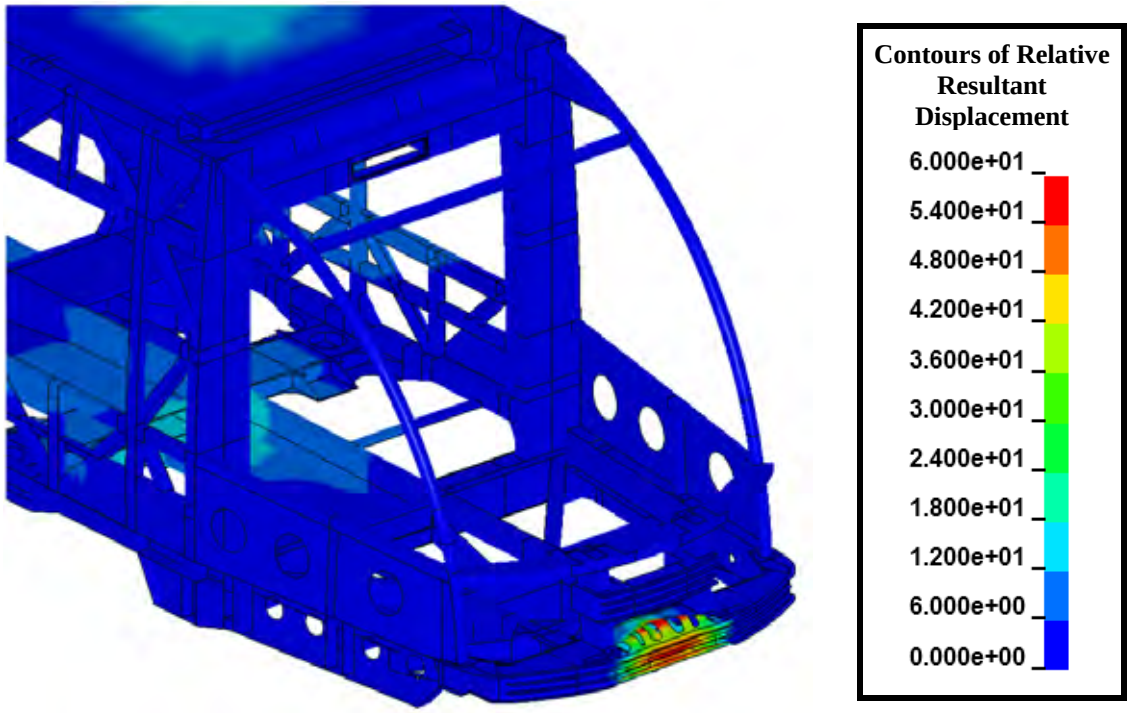

Figure 47. Crush Level (mm) for the LRV 2 Bullet Car in the 10 mph Compatible Collision.

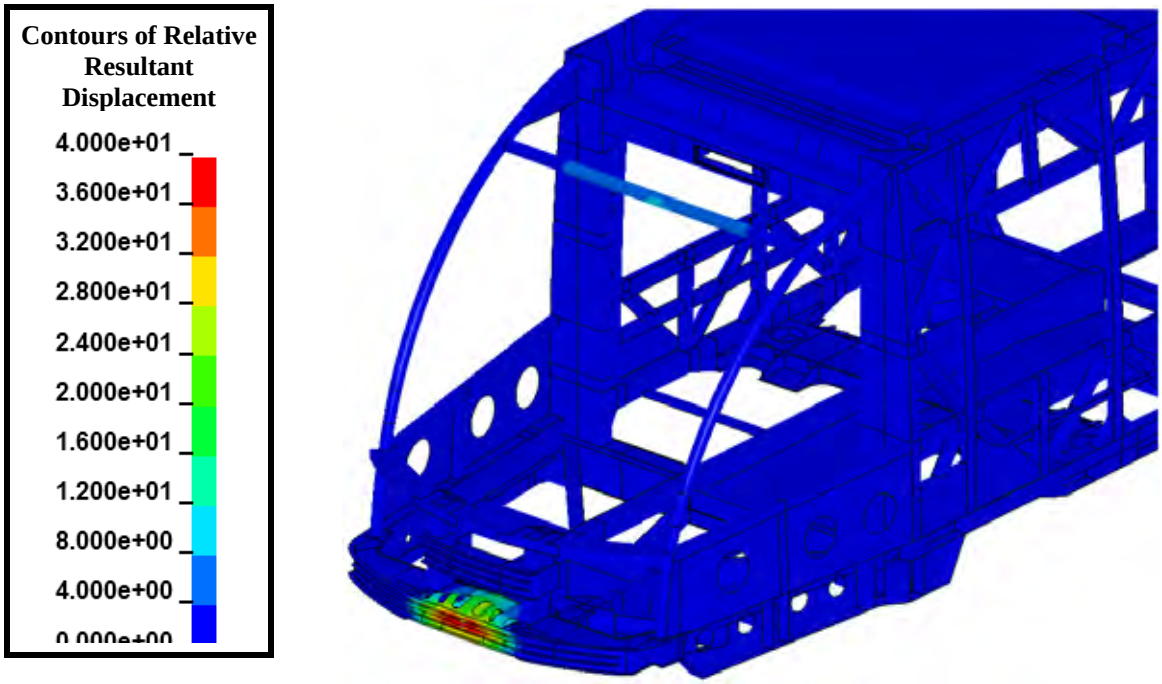

Figure 48. Crush Level (mm) for the LRV 2 Target Car in the 10 mph Compatible Collision.

The crush response of the LRV 2 vehicle for the 15 mph collision is shown in Figure 49. The crush deformations are still located in an energy absorbing crush zone in the nose of the head girder. At the point of maximum crush, the secondary anticlimbers are nearly engaged as seen in Figure 49(a). The fringes of crush for the LRV 2 bullet and target vehicles in the 15 mph collision are shown in Figure 50 and Figure 51, respectively. The average crush in the forward energy absorbers is a bit over 100 mm and no significant crush deformations occurred behind the head girders of the LRVs. This crush response is a controlled collapse of the forward crush element as it was designed to deform.

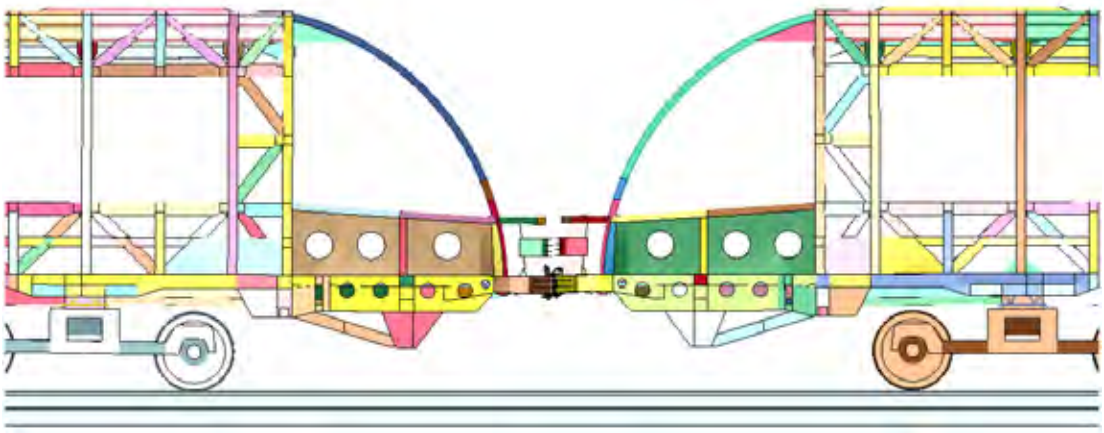

(a) Time = 0.120 s

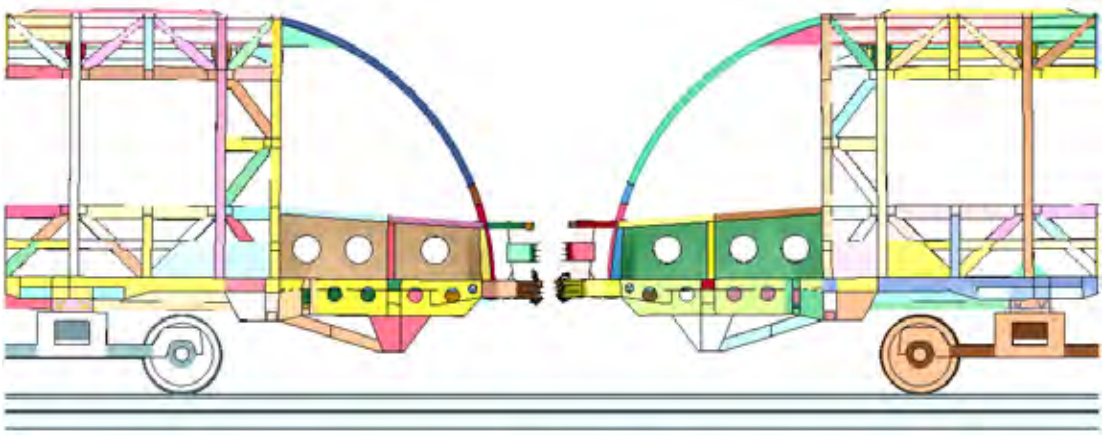

(b) Time = 0.250 s

Figure 49. Simulation of the LRV 2 Compatible Collision at 15 mph.

The distribution of force histories transmitted through the cab structures are shown in Figure 52. The forces are obtained from the cross section definitions that are just aft of the crush zone (refer to Figure 41 for the cross section definitions). The plot shows that the central girders carry approximately 50 percent of the overall collision loads and the remainder is distributed through the other structures (side sills, window belt, underframe cross-bracing).

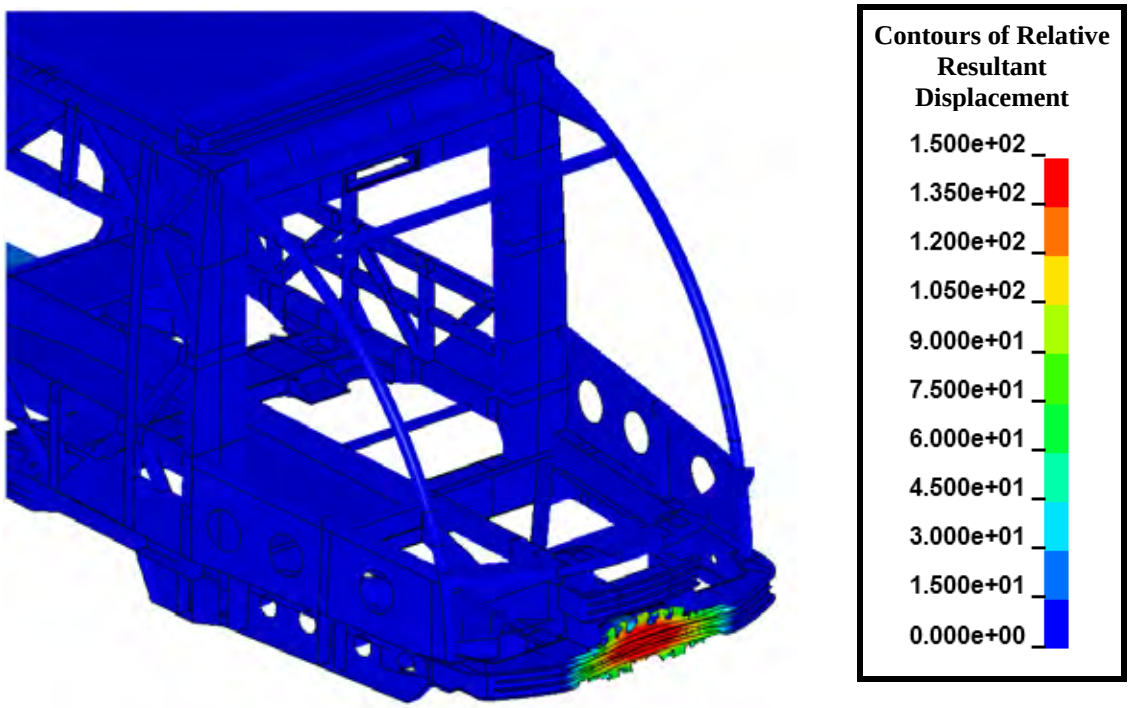

Figure 50. Crush Level (mm) for the LRV 2 Bullet Car in the 15 mph Compatible Collision.

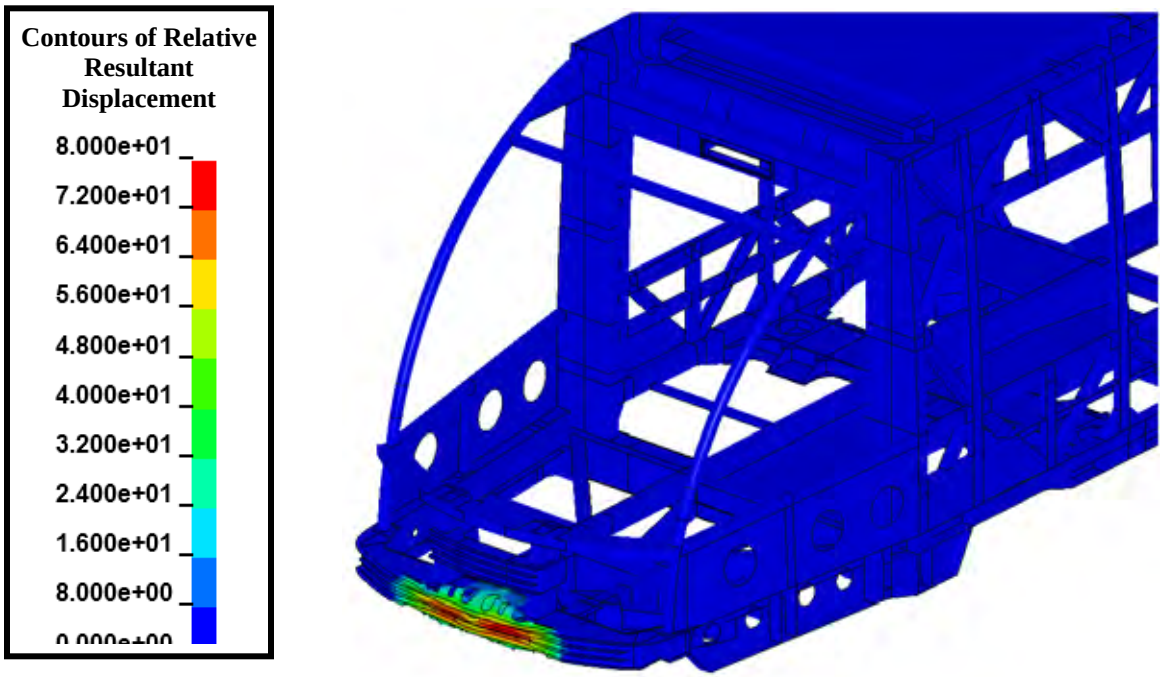

Figure 51. Crush Level (mm) for the LRV 2 Target Car in the 15 mph Compatible Collision.

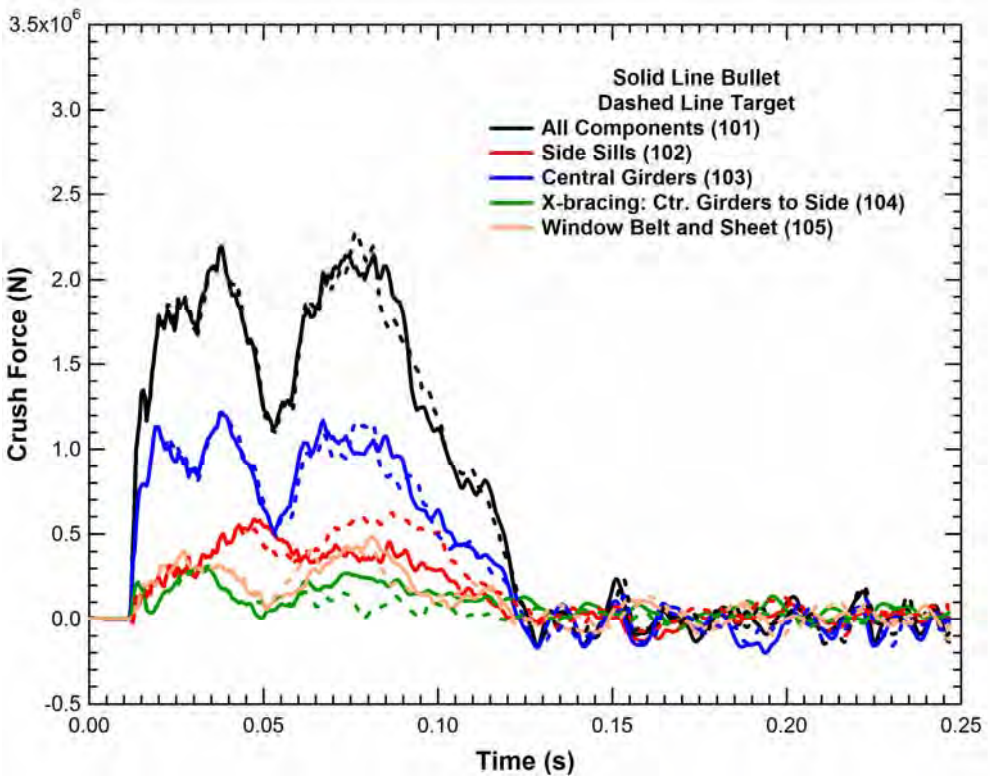

Figure 52. Component Force History of the 15 mph LRV 2 Compatible Crash Analysis.

The response of the LRV 2 vehicles for the 20 mph compatible collision is shown in Figure 53. The crush deformations are still located in an energy absorbing crush zone in the nose of the head girder. At the point of maximum crush the secondary anticlimbers are engaged and the crush has begun in the center sills behind the head girder, as seen in Figure 53(b). The fringes of crush for the LRV 2 bullet and target vehicles in the 15 mph collision are shown in Figure 54 and Figure 55, respectively. The target vehicle has nearly 100 mm of crush in the forward energy absorbers. No significant crush deformations occurred behind the head girder of the LRV. However, the bullet vehicle has a peak crush of approximately 300 mm with 100-150 mm of crush in the central sills behind the head girder. This crush response is a controlled collapse of the forward crush zones as it was designed to deform.

The crush response of the target LRV 2 vehicle for the 25 mph collision is very similar to that of the 20 mph collision described above. The initial crush deformations are still located in an energy absorbing crush zone in the nose of the head girder. At the point of maximum crush, the secondary anticlimbers are engaged and the crush has begun in the center sills behind the head girder of the bullet vehicle.

The calculated crush for the LRV 2 bullet and target vehicles in the 25 mph collision are shown in Figure 56 and Figure 57, respectively. The target vehicle has approximately 100 mm of crush in the forward energy absorbers and no significant crush deformations occurred behind the head girder of the LRV. However, the bullet vehicle has a peak crush of approximately 450 mm with 250-300 mm of crush in the central sills behind the head girder.

This crush response is a controlled collapse of the forward crush zones as it was designed to deform.

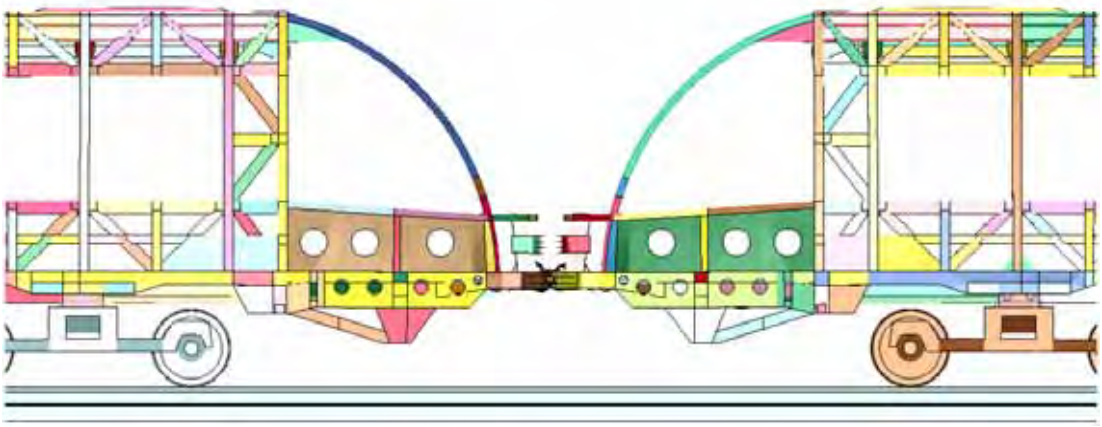

(a) Time = 0.030 s

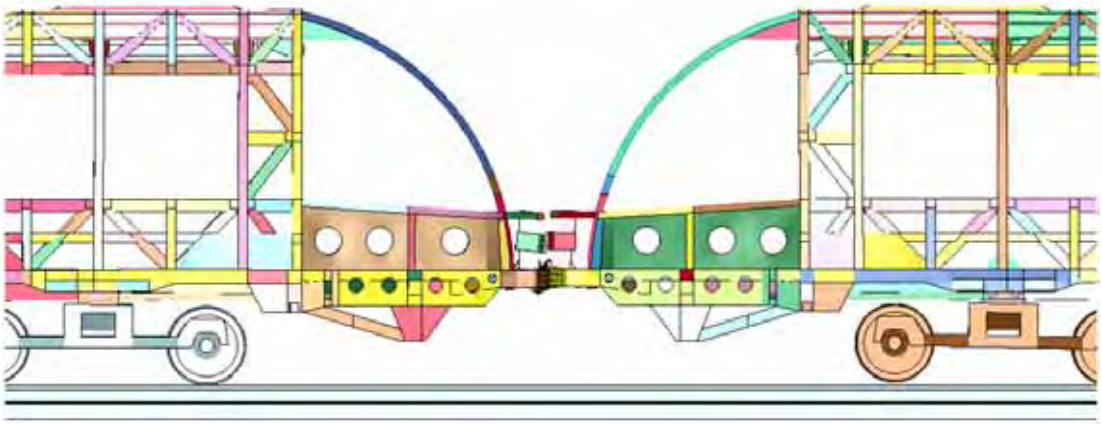

(b) Time = 0.100 s

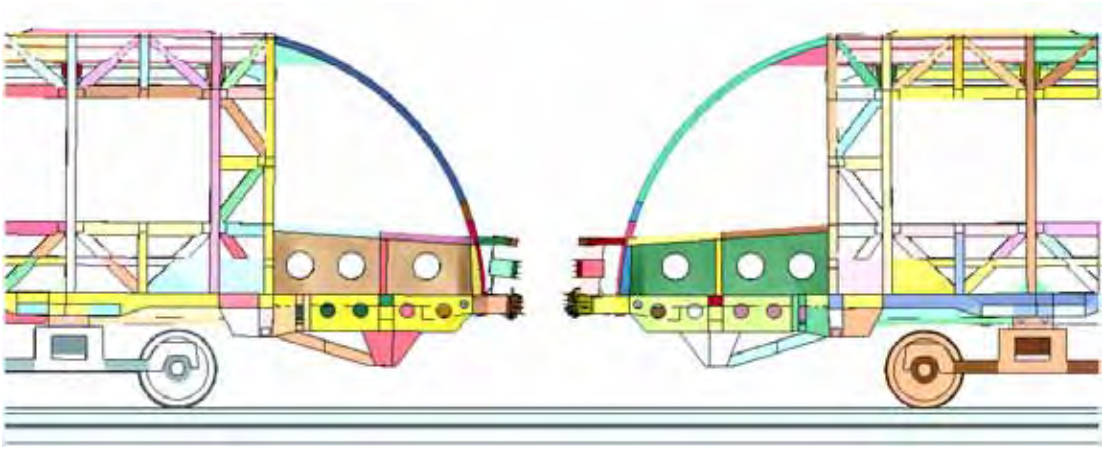

(c) Time = 0.400 s

Figure 53. Simulation of the LRV 2 Compatible Collision at 20 mph.

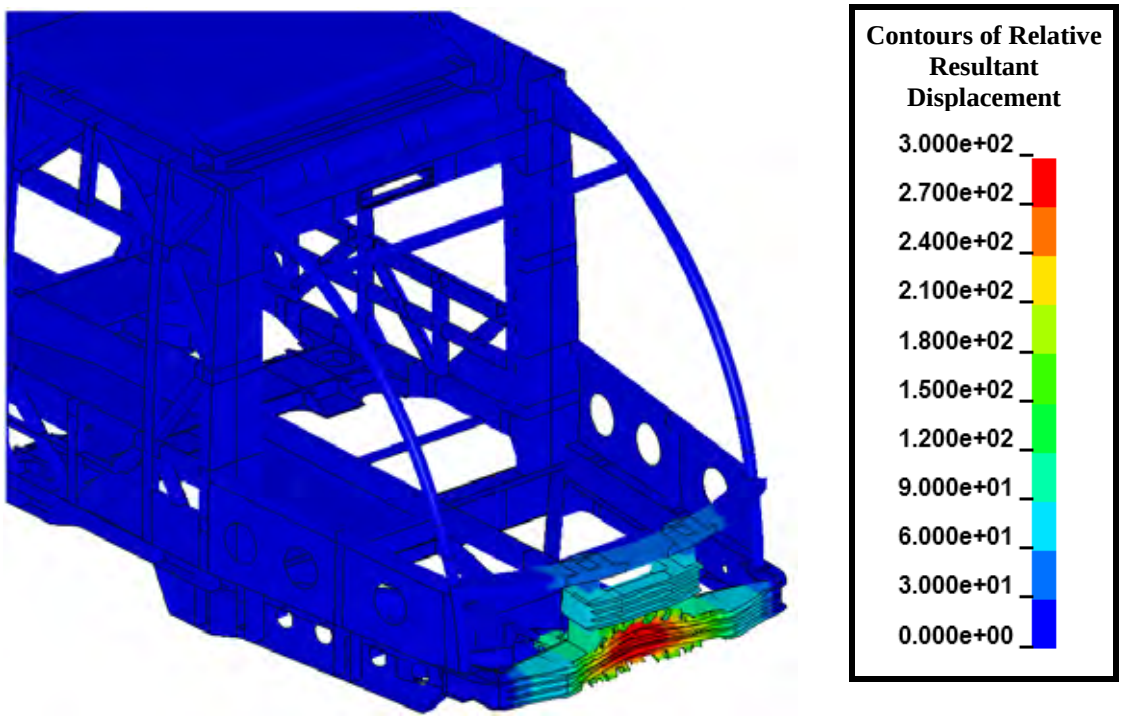

Figure 54. Crush Level (mm) for the LRV 2 Bullet Car in the 20 mph Compatible Collision.

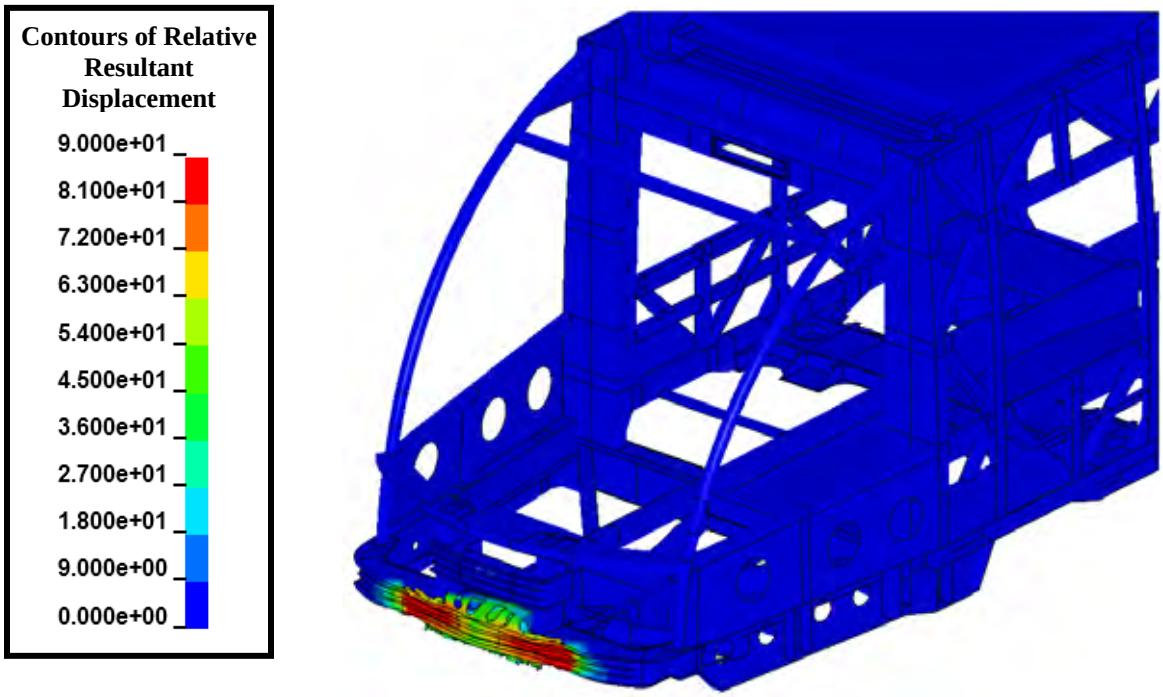

Figure 55. Crush Level (mm) for the LRV 2 Target Car in the 20 mph Compatible Collision.

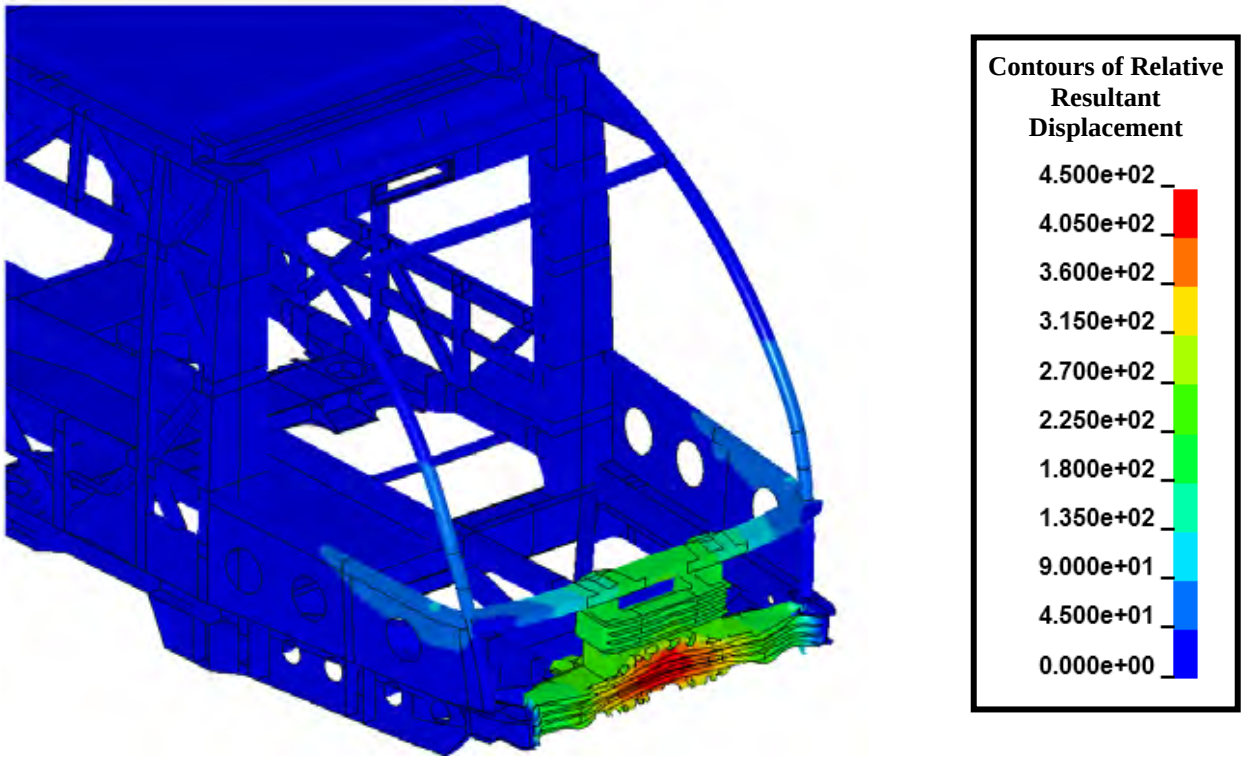

Figure 56. Crush Level (mm) for the LRV 2 Bullet Car in the 25 mph Compatible Collision.

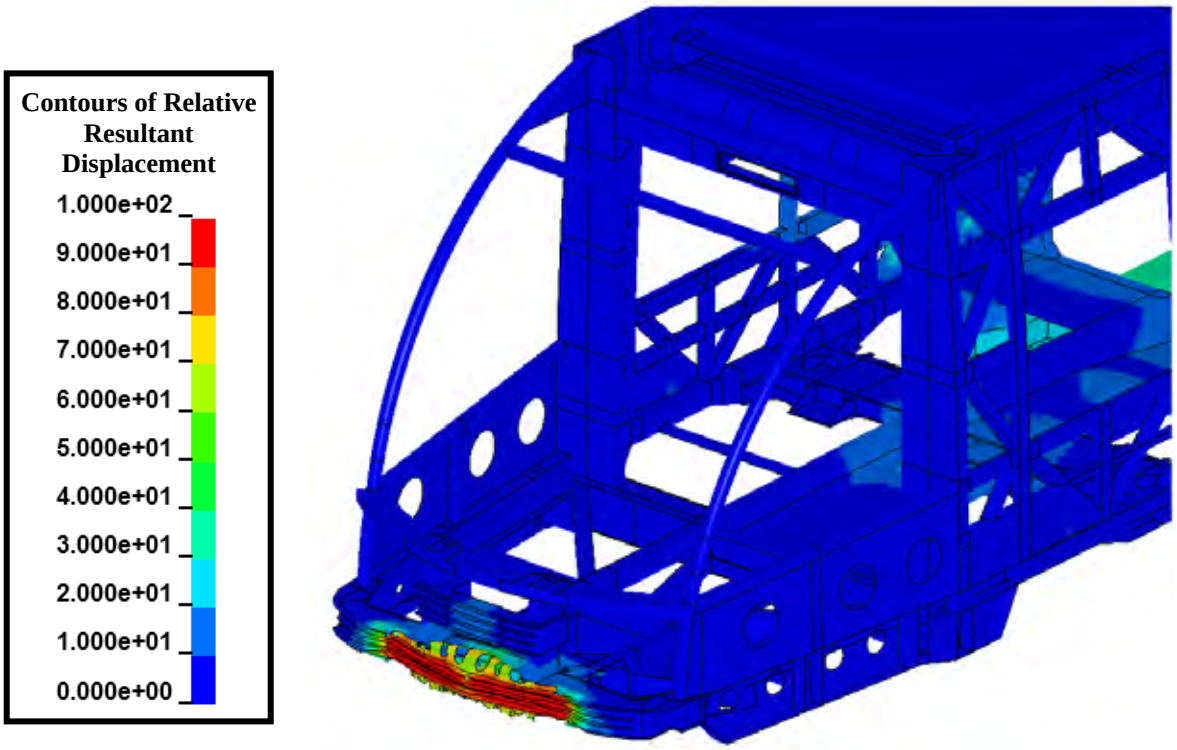

Figure 57. Crush Level (mm) for the LRV 2 Target Car in the 25 mph Compatible Collision.

The response of the LRV 2 vehicles for the 30 mph compatible collision is shown in Figure 58. The crush deformations initiate in the energy absorbing crush zones in the nose of the head girder. At the point of maximum crush, the secondary anticlimbers are engaged and the crush has progresses in the center sills behind the head girder, as seen in Figure 58(b).

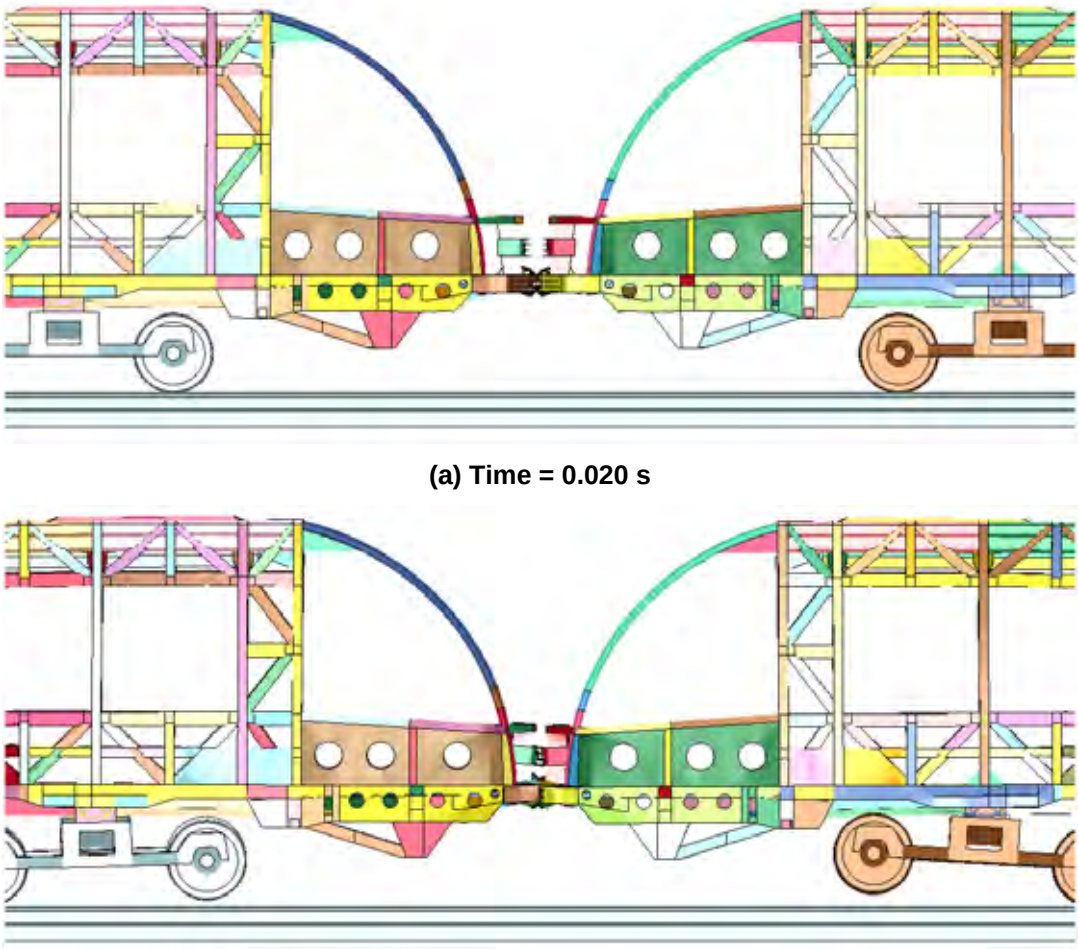

(a) Time = 0.020 s

(b) Time = 0.200 s

Figure 58. Simulation of the LRV 2 Compatible Collision at 30 mph.

The fringes of crush for the LRV 2 bullet and target vehicles in the 30 mph collision are shown in Figure 59 and Figure 60, respectively. The target vehicle has nearly 300 mm of crush in the forward energy absorbers with 100-150 mm of crush in the central sills behind the head girder. Similarly, the bullet vehicle has a peak crush of approximately 350 mm with 150-200 mm of crush in the central sills behind the head girder. This crush response in both vehicles is a controlled collapse of the forward crush zones as it was designed to deform.

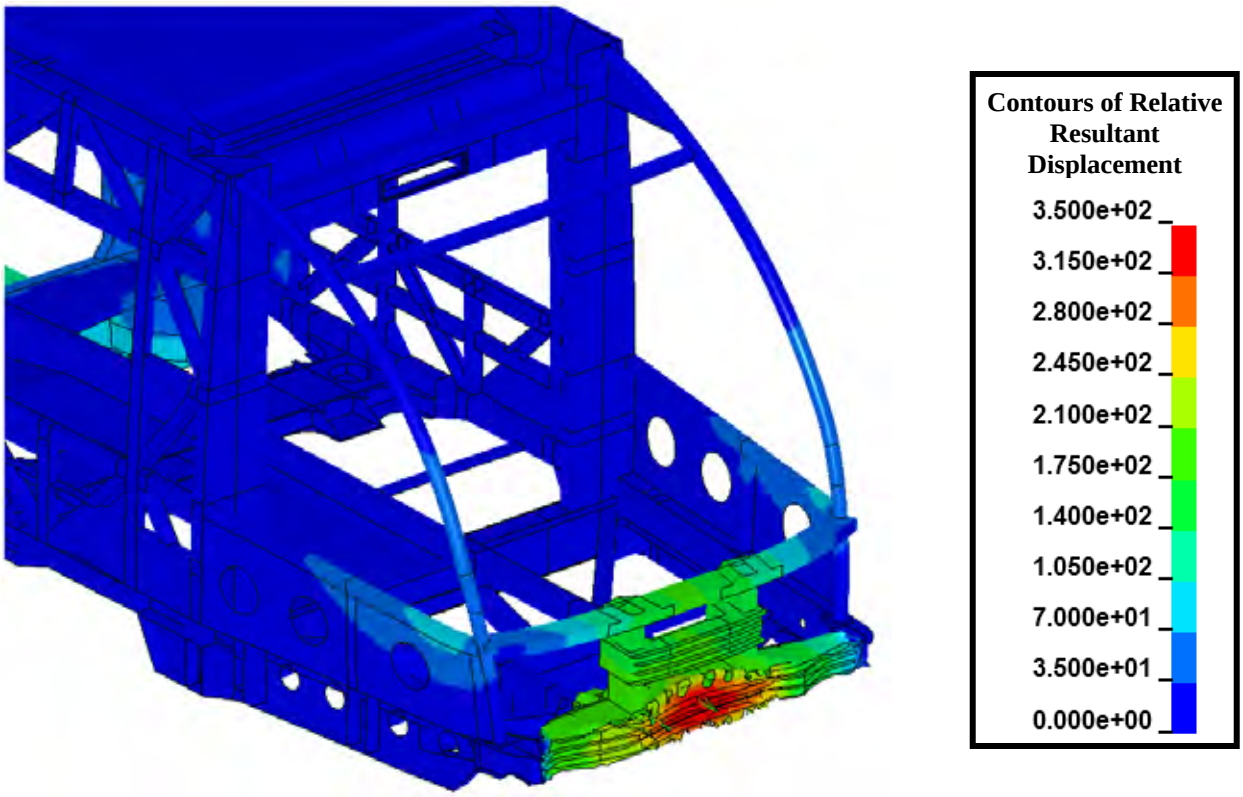

Figure 59. Crush Level (mm) for the LRV 2 Bullet Car in the 30 mph Compatible Collision.

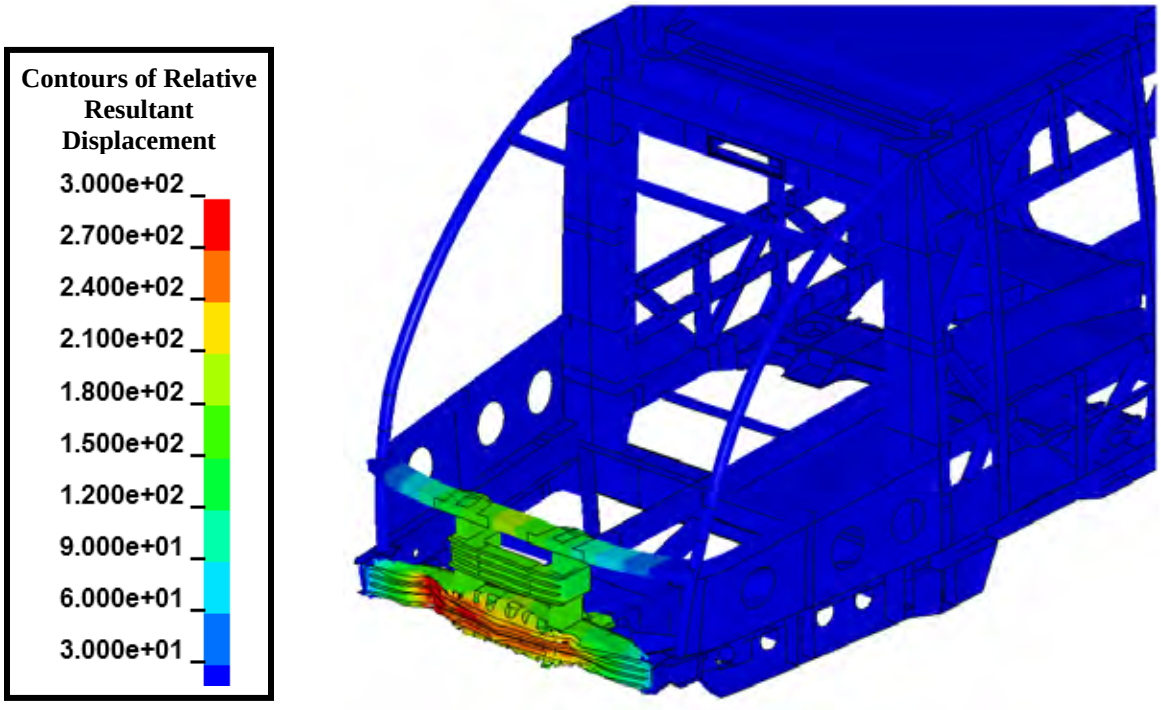

Figure 60. Crush Level (mm) for the LRV 2 Target Car in the 30 mph Compatible Collision.

The longitudinal force-crush curves for the bullet vehicle in the 30 mph compatible collision are shown in Figure 61 (Refer to Figure 41 above for definitions of the cross sections). Note that the central girder components are initially the most heavily loaded members. As the collision progresses, the load is shed to the side sills and window belt components. The corner post force history was substantially lower than the other underframe components and is not displayed in Figure 61.

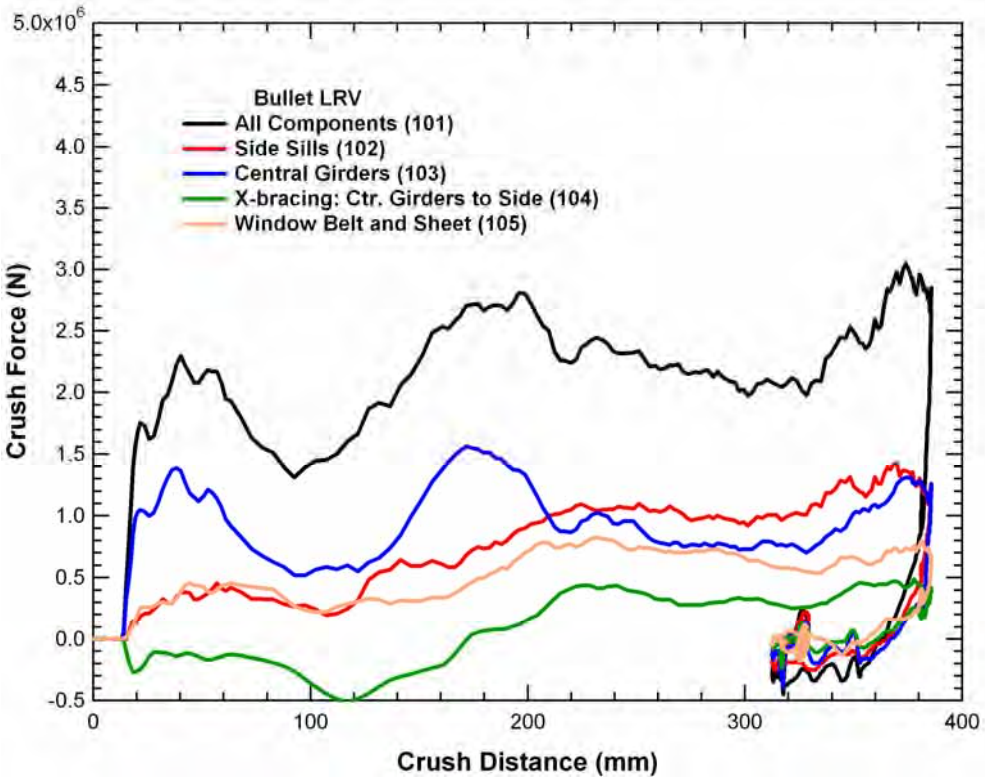

Figure 61. Force-Crush Behavior for the 30 mph LRV 2 Compatible Crash Analysis.

Total force histories at each of the four locations are shown in Figure 62. Note that as the location moves away from the crush zone, the total force is reduced. This is due to less mass in the model acting on that plane. Cross section planes 101 and 107 are close together and the forces are similar. Cross section planes 107 and 108 are relatively close but the force on location 2 is much greater due to the weight of the bogie in addition to the extra car body mass. Basically, only the trailing mass acts on cross section planes 109 and the force through this plane is the lowest. Note that all corresponding force histories exhibited nearly identical behaviors at the various cross sections for both the bullet and target vehicles.

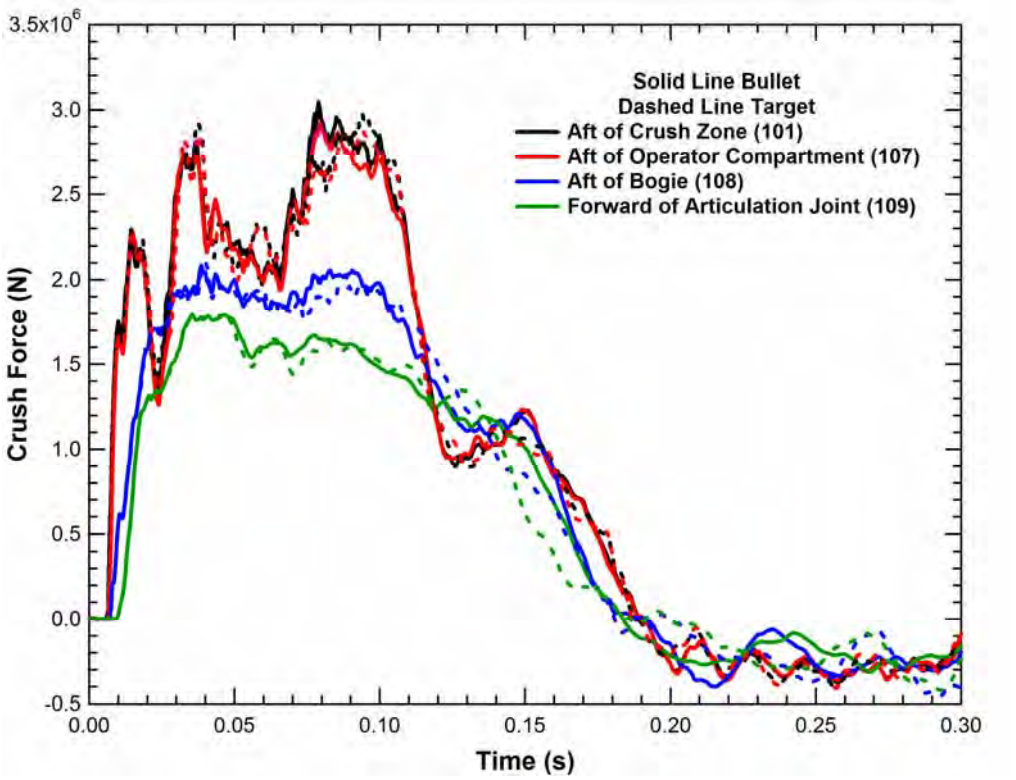

Figure 62. Force History at Four Locations along LRV 2 in the 30 mph Collision.

2.5. LRV 3 Compatible Collisions

LRV 3 Model

The mesh for the LRV 1 model was provided by the manufacturer in ANSYS format and converted to LS-DYNA format. Further input file modifications were made to: (1) identify and assign rigid bodies, (2) add a rail and ground model, (3) assign appropriate shell thickness values, (4) assign material models, (5) prescribe contact algorithms, (6) add gravity, (7) prescribe initial conditions, and (8) perform other miscellaneous edits to run the model in LS-DYNA. The final LS-DYNA model for LRV 3 is shown in Figure 63. As with other models, only the A-car is explicitly modeled. The B and C cars are lumped into a trailing mass coupled to the respective A-car through the articulating joint. The force cross section plane definitions are also indicated in the figure.

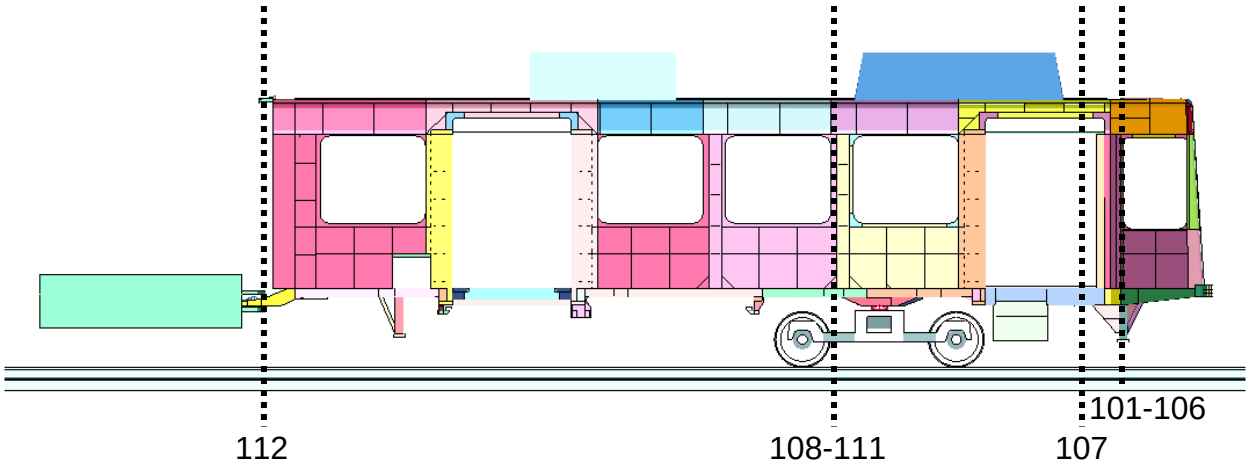

Figure 63. Force Cross Section Plane Locations for the LRV 3 Model.

The collision interface for the compatible LRV collision analyses is shown in Figure 64. The two cars are identical and the impacted car on the right was initially stationary. The wheels on both cars were non-rotating and sliding along the rail to simulate a condition of fully locked brakes such that the wheels slide along the rails with a frictional coefficient of 0.30. The models include the structural members and outer panels which are integral to the LRV structure.

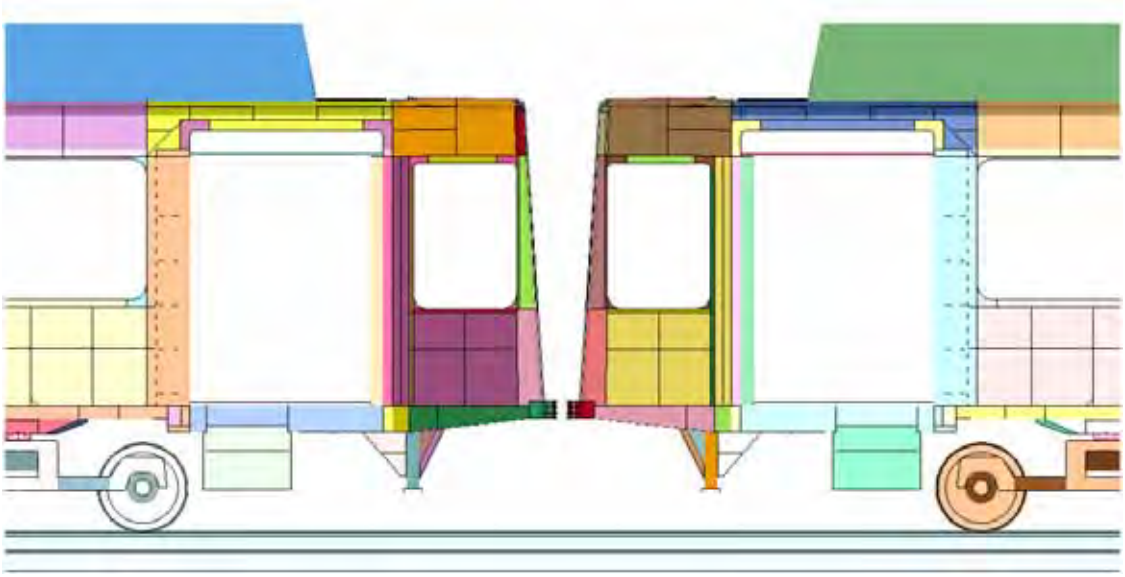

Figure 64. Collision Interface for the LRV 3 Compatible Crash Analysis.

The finite element mesh for LRV 3 was constructed as an assembly of many parts, using a mix of shell, brick, and beam elements. Most of the car model was constructed from 4-node shell elements. Some variation in the mesh resolution was included in various regions of the model. A relatively uniform mesh and fine mesh resolution in the impact zone of the LRV 3 model was used and contributed to a high quality simulation of the collision behavior. The trucks, ground, rail, and trailing masses were modeled with rigid 8-node brick elements. Beam elements were used in the articulating joint and bolster beam parts.

The cars were modeled using properties of Corten-B steel for most of the car body structure with some 70-ksi High-Strength Low Alloy (HSLA-70) steel in the corner posts and structural shelf. These materials were modeled using the bilinear elastic-plastic model *MAT_PLASTIC_KINEMATIC in LS-DYNA. Rigid bodies were given generic steel properties and were modeled with the *MAT_RIGID material in LS-DYNA. Material properties used in this study are summarized in Table 11. Material densities were adjusted by major component group to match the specified vehicle weight.

Material failure was included through element erosion. If an element reaches its plastic failure strain, it is deleted from the calculation, creating a void and an area for stress concentration in the mesh. Failure criteria for the two elastic-plastic materials were chosen based on available material properties and mesh density considerations.

Table 11. Material Properties Used in the LRV 3 Analyses

Material	Corten-B	HSLA-70	Steel (generic)
LS-DYNA Material	3, Bi-linear E-P	3, Bi-linear E-P	20, Rigid
Young's Modulus (GPa)	210	200	210
Poisson's Ratio	0.30	0.30	0.3
Yield Strength (MPa)	355	482	N/A
Tangent Modulus (MPa)	1403	779	N/A
Material Failure Strain	0.28	0.20	N/A

The total LRV 3 mass was calculated as approximately 41 Mg in LSDYNA. Table 12 provides a breakout of component and total modeled LRV 2 masses.

Table 12. Component Masses in the LRV 3 Model

Component	FEA Model(kg)
A-Car	12,763
Motor Bogie	5,573
Trailing Mass (includes B & C-car, Motor Bogie, and center truck)	22,486
Total	40,822

Analysis Results

The compatible collisions analyzed for LRV 3 are at 5, 10, 15, 20, 25, and 30 mph. One vehicle is moving at the collision speed (bullet) and the other is stationary (target). Unless otherwise stated, all images show the bullet vehicle on the left and the target vehicle on the right. The force crush behaviors calculated for LRV 3 at the various collision closing speeds are shown in Figure 65. The characteristic force-crush behavior shows that the vehicle initially loads up to a crush force of approximately 1.0-1.5 MN before the crush initiates. As the initial crush progresses the steady crush forces drop of to a level of approximately 0.8

MN. As the severity of the collision increases and the crush increases from 100 mm up to a level of approximately 700 mm, the characteristic crush curve has a steadily increasing crush force that increases from approximately 0.8MN to 1.8 MN.

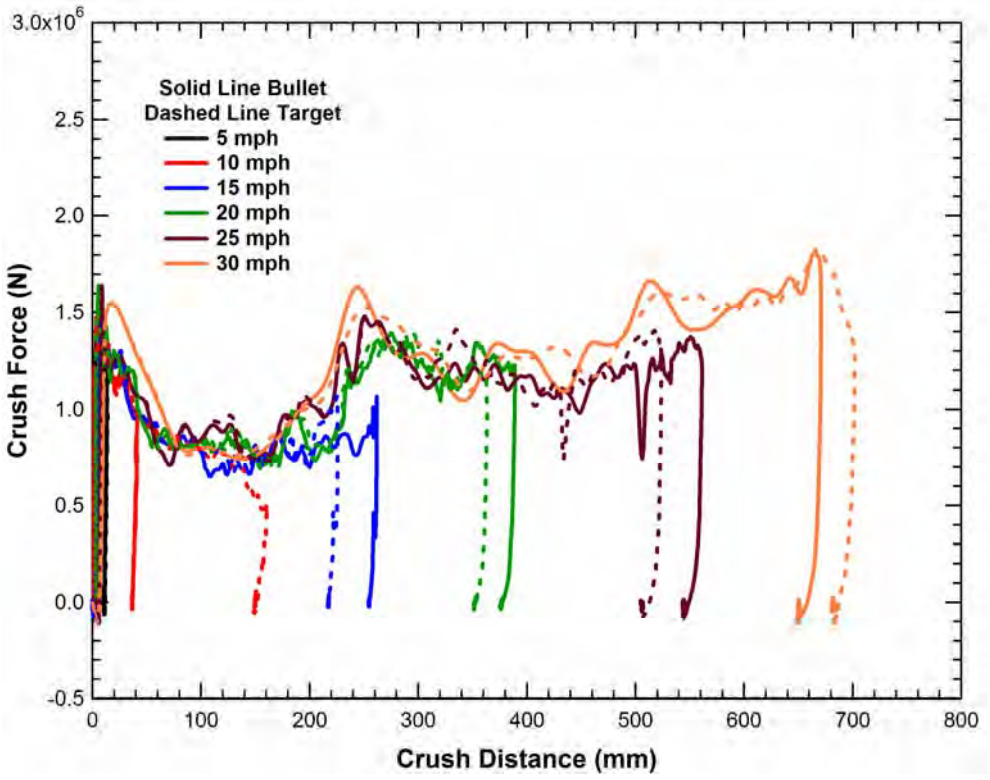

Figure 65. Force-Crush Behavior for all Speeds of the LRV 3 Compatible Crash Analysis.

The crush deformations of LRV 3 at 5 mph were small (11 mm) and limited to some minor deformations at the head girder and are therefore not provided in detail. The 5 mph behavior indicates that a no damage requirement at this collision speed can be easily achieved with some level of energy absorption in either a coupler or bumper assembly.

The calculated crush for the LRV 3 bullet and target vehicles in the 10 mph collision are shown in Figure 66 and Figure 67, respectively. The fringes of crush are referenced to a plane at the back of the cab. There is approximately 40 mm of crush in the bullet LRV and 150 mm of crush in the target vehicle. The crush response is a flattening of the nose and push back of the head girder. This crush response is a controlled collapse that occurs in the desired mode developed during the vehicle design effort.

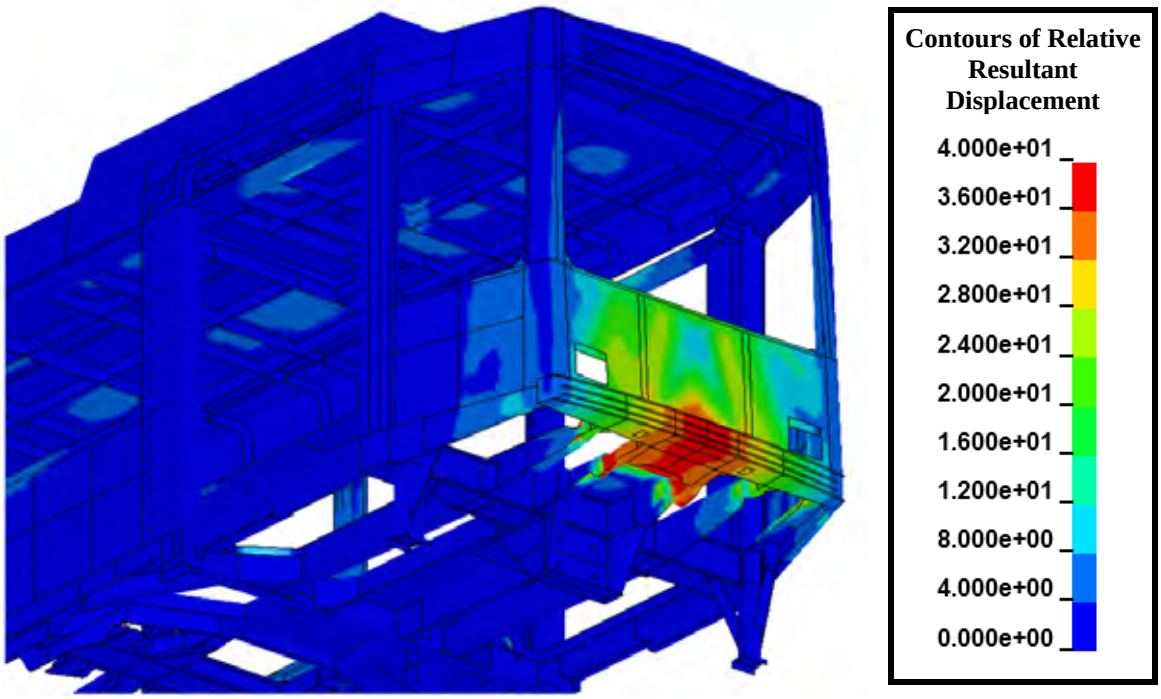

Figure 66. Crush Level (mm) for the LRV 3 Bullet Car in the 10 mph Compatible Collision.

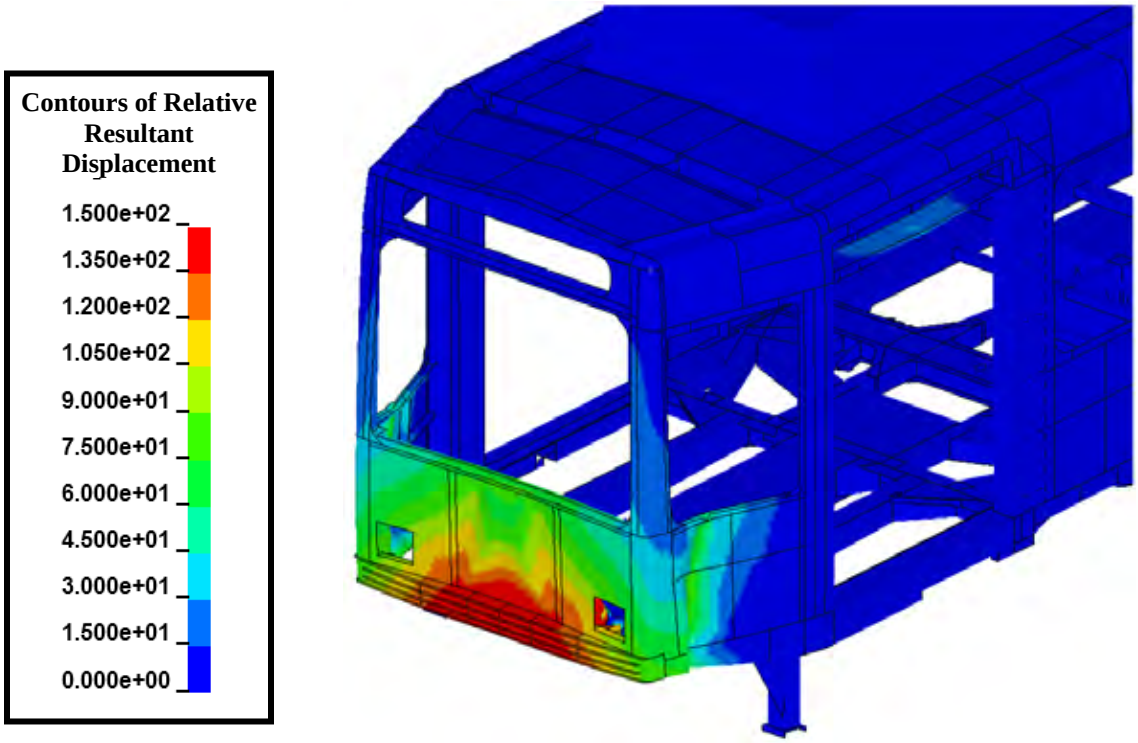

Figure 67. Crush Level (mm) for the LRV 3 Target Car in the 10 mph Compatible Collision.

The calculated 15 mph compatible collision behavior of LRV 3 is shown in Figure 68. The bullet vehicle is shown on the left and the target on the right. The crash response is primarily symmetric. The initial contact and crush is at the underframe level. However, by the time of 0.15 s, shown in Figure 68(b), the maximum crush is reached and the entire ends of the vehicle have engaged.

(a) Time = 0.070 s

(b) Time = 0.150 s

Figure 68. Simulation of the LRV 3 Compatible Collision at 15 mph.

The calculated crush for the LRV 3 bullet and target vehicles in the 15 mph collision are shown in Figure 69 and Figure 70, respectively. The fringes of crush are again referenced to a plane at the back of the cab. There is approximately 300 mm of crush in the bullet LRV and 200 mm of crush in the target vehicle. The crush response is primarily a push back of the head girder at the underframe level. The crush magnitude at the top of the cab is very small as a result of the tapered profile at the end of the LRV.

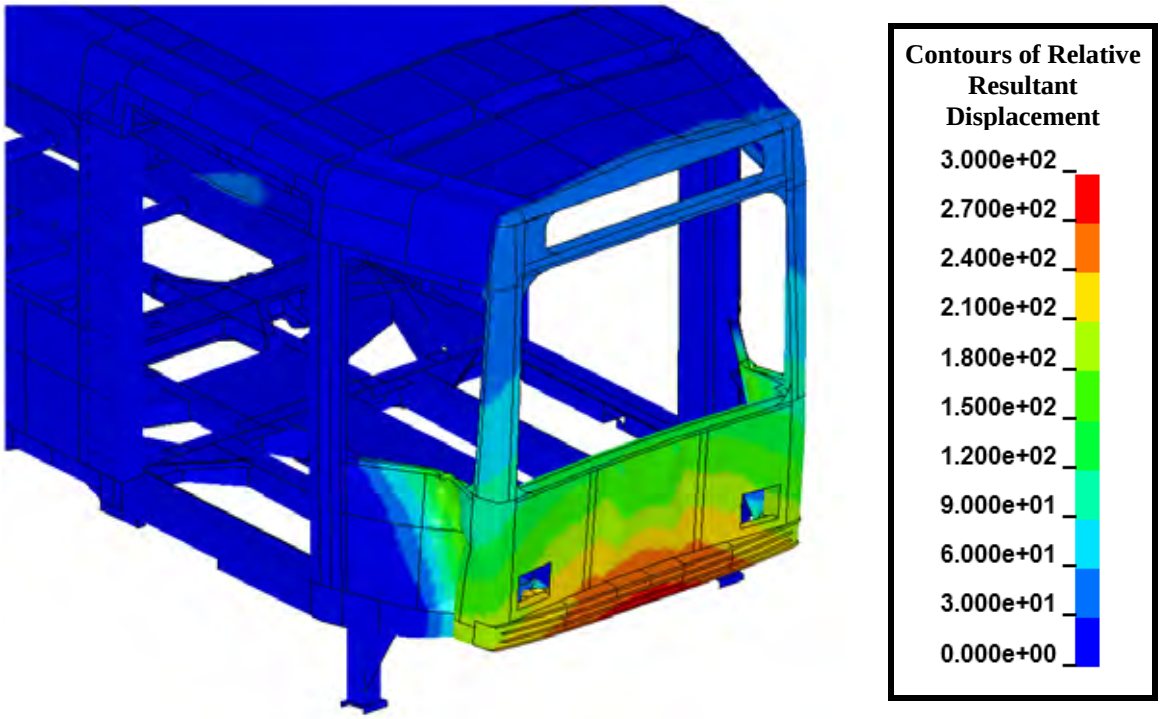

Figure 69. Crush Level (mm) for the LRV 3 Bullet Car in the 15 mph Compatible Collision.

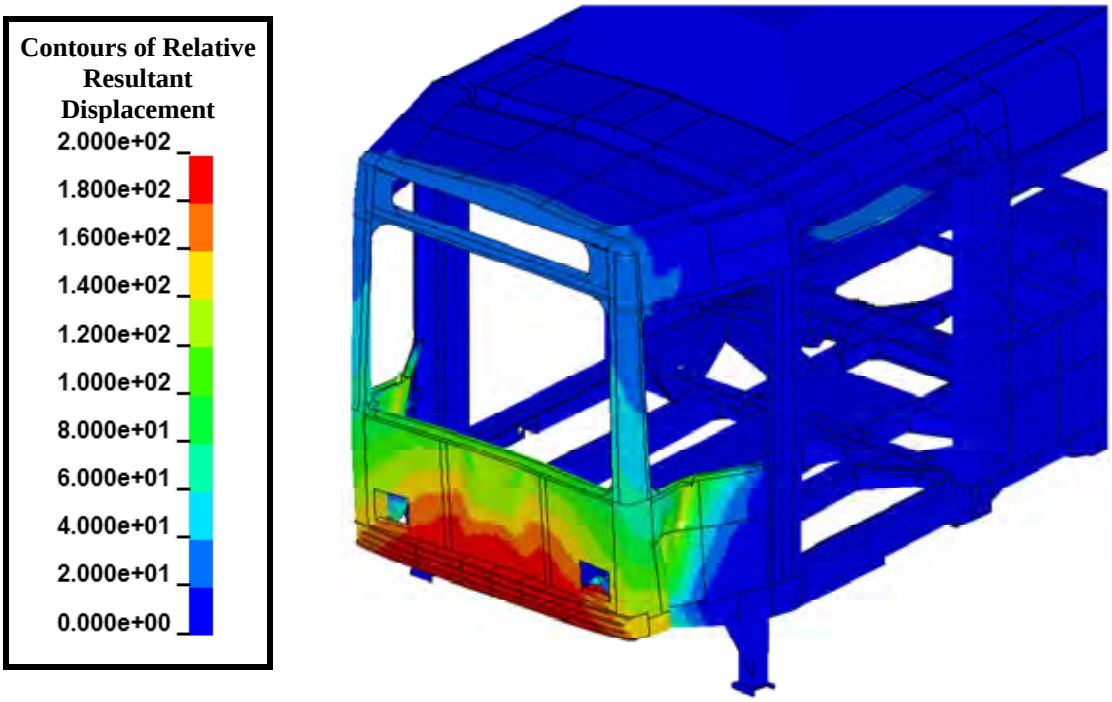

Figure 70. Crush Level (mm) for the LRV 3 Target Car in the 15 mph Compatible Collision.

The calculated 20 mph compatible collision response of LRV 3 is shown in Figure 71. The bullet vehicle is shown on the left and the target on the right. The initial crush response to a time of 0.1 seconds is very symmetric as the ends of the vehicle collide and come into

contact over the full height of the vehicle face as seen in Figure 71(a). As the collision continues, the crush at the underframe remains symmetric but a slight asymmetry in crush develops in the LRV structures near the vehicle roof, as seen in Figure 71(b). By the time of 0.3 seconds, the collision is complete and the vehicles have rebounded from each other.

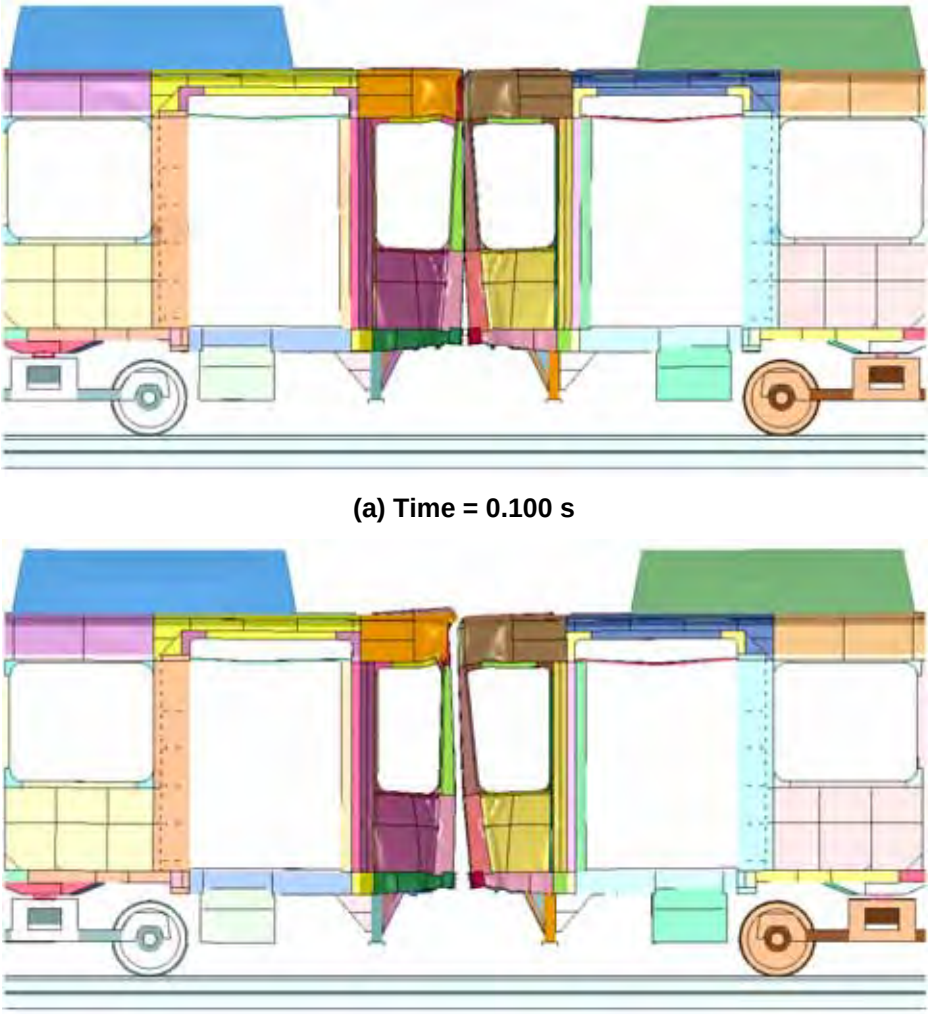

(a) Time = 0.100 s

(b) Time = 0.300 s

Figure 71. Simulation of the LRV 3 Compatible Collision at 20 mph.

The calculated crush for the LRV 3 bullet and target vehicles in the 20 mph collision are shown in Figure 72 and Figure 73, respectively. The fringes of crush are again referenced to a plane at the back of the cab. There is approximately 350 mm of crush in the target LRV and 400 mm of crush in the bullet vehicle. The crush of both vehicles is developed through a push back of the head girder and a corresponding crush of the underframe immediately aft of the head girder. Despite the small asymmetry of the vehicle responses near the roof structures, the crush responses are controlled collapse that occurs in a desirable mode.

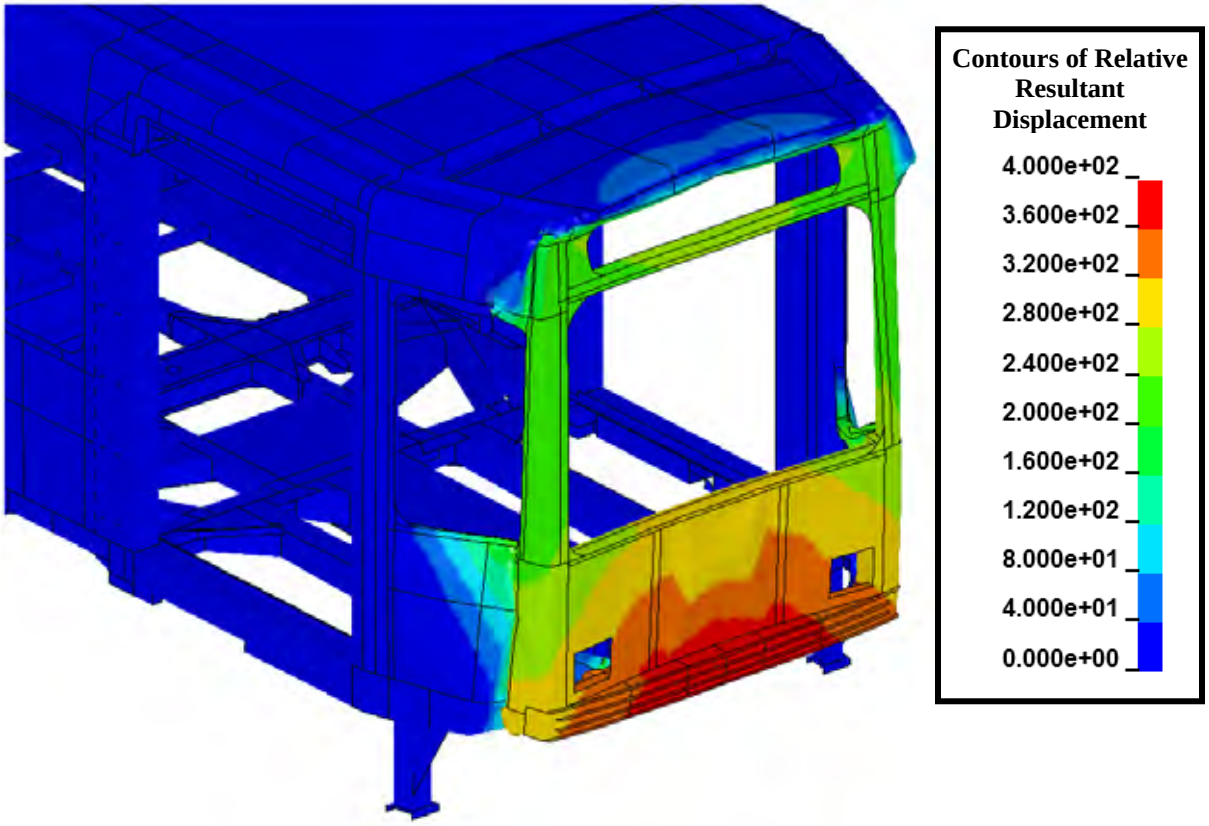

Figure 72. Crush Level (mm) for the LRV 3 Bullet Car in the 20 mph Compatible Collision.

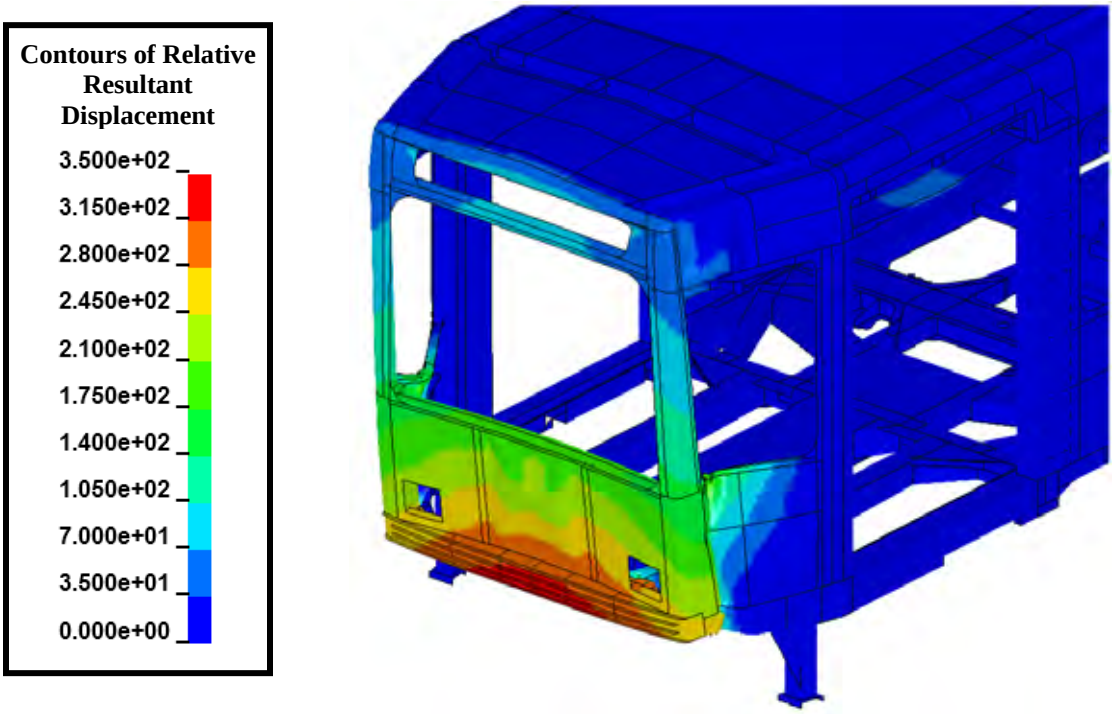

Figure 73. Crush Level (mm) for the LRV 3 Target Car in the 20 mph Compatible Collision.

The calculated 25 mph compatible collision response of LRV 3 is shown in Figure 74. The bullet vehicle is shown on the left and the target on the right. The crush response is very similar to that of the 20 mph collision but with larger crush displacements to dissipate the energy. The crush at the underframe remains symmetric but an asymmetry in crush is observed in the LRV structures near the vehicle roof.

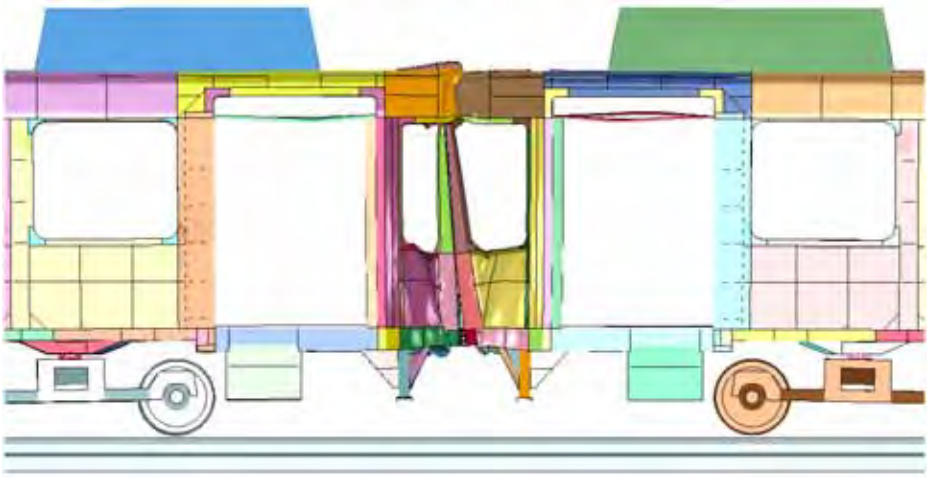

Figure 74. Simulation of the LRV 3 Compatible Collision at 25 mph.

The calculated crush for the LRV 3 bullet and target vehicles in the 25 mph collision are shown in Figure 75 and Figure 76, respectively. The fringes of crush are again referenced to a plane at the back of the cab. There is approximately 500 mm of crush in the target LRV and 600 mm of crush in the bullet vehicle. The crush of both vehicles is developed through a push back of the head girder and a corresponding crush of the underframe immediately aft of the head girder. The primary difference in the two vehicles is the larger crush displacements at the top of the cab forward wall in the bullet vehicle. Despite the asymmetry of the vehicle responses near the roof structures, the crush responses are both a controlled collapse that occurs in a desirable mode.

The longitudinal force-crush curves for the LRV 3 vehicles in the 25 mph compatible collision are shown in Figure 77 (Refer to Figure 63 above for definitions of the cross sections). Note that the central girder components are initially the most heavily loaded members and carry almost all of the collision forces. As the collision progresses beyond the initial 50 mm of crush, a significant portion of the load is shed to the side sills and other structural components.

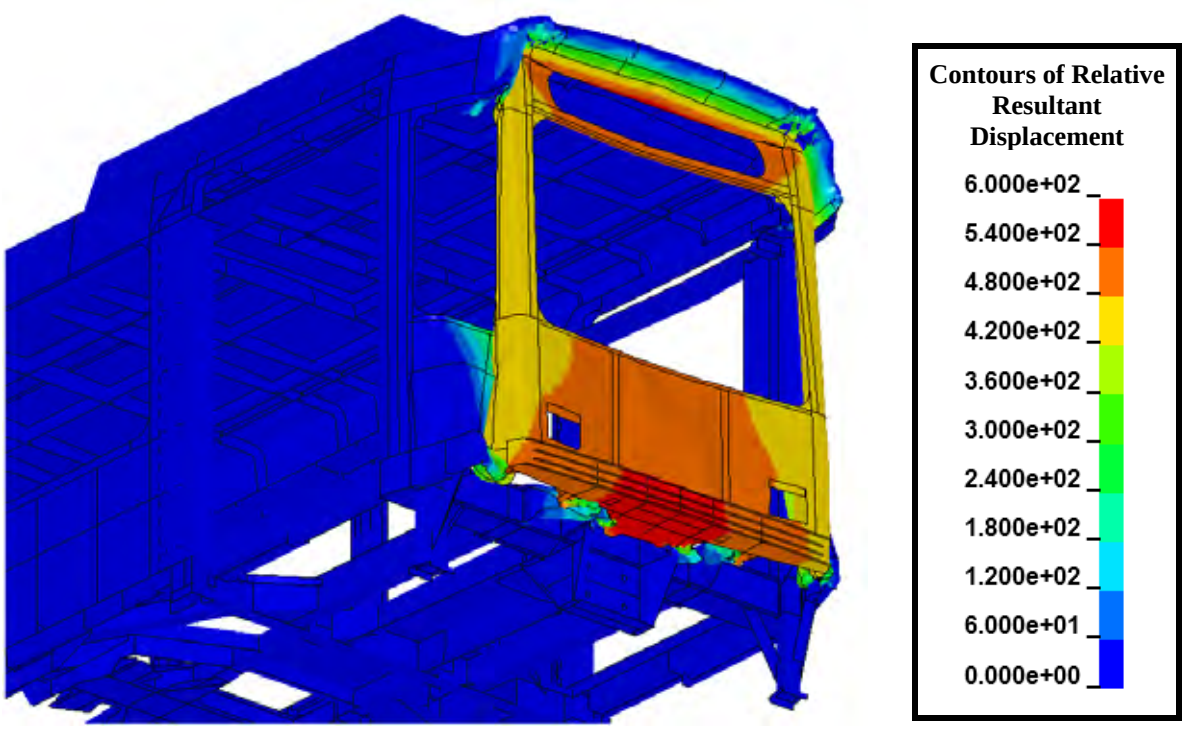

Figure 75. Crush Level (mm) for the LRV 3 Bullet Car in the 25 mph Compatible Collision.

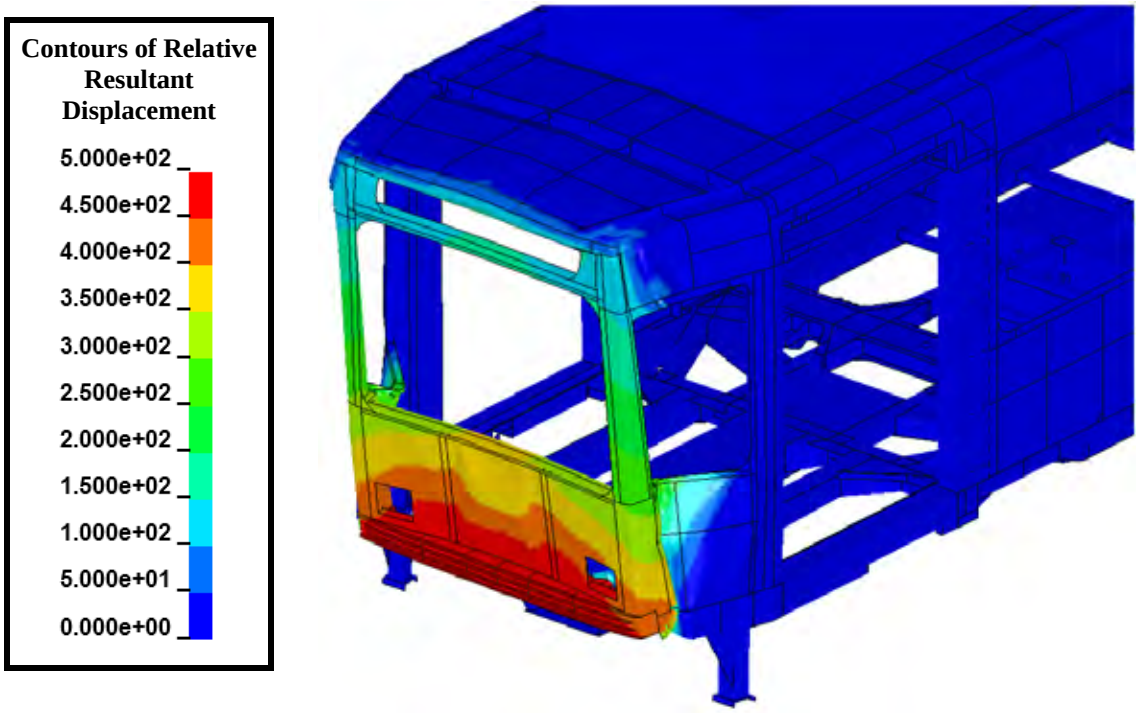

Figure 76. Crush Level (mm) for the LRV 3 Target Car in the 25 mph Compatible Collision.

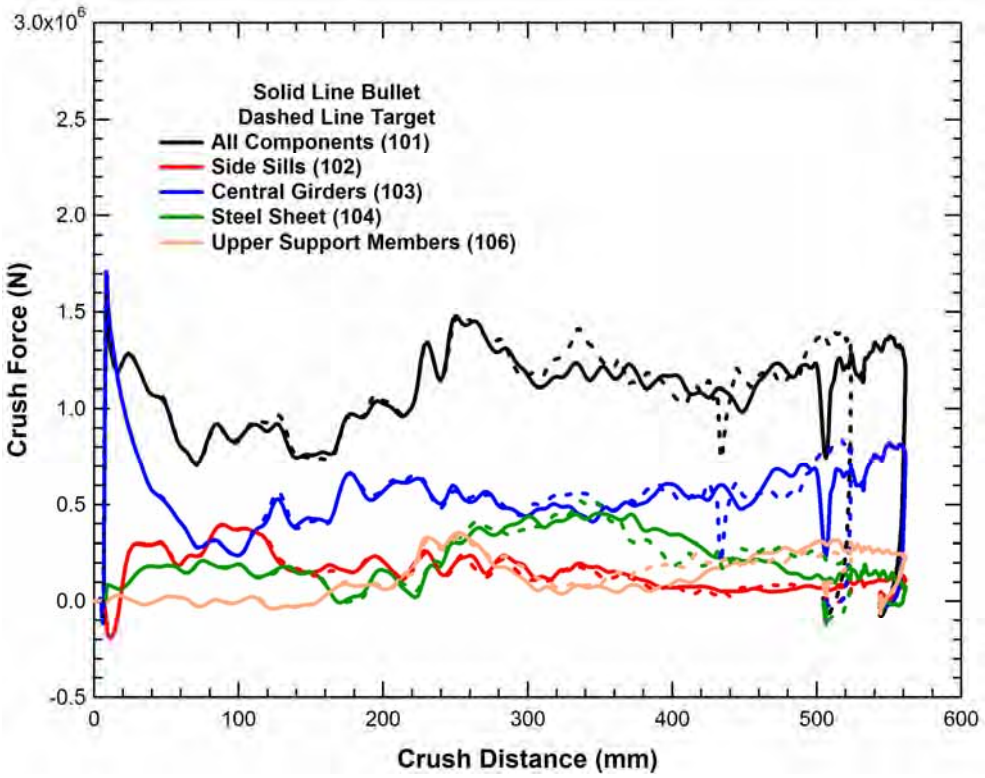

Figure 77. Force-Crush Behavior for the 25 mph LRV 3 Compatible Crash Analysis.

The calculated 30 mph compatible collision response of LRV 3 is shown in Figure 78. The bullet vehicle is shown on the left and the target on the right. The crush displacements at this collision speed are relatively balanced on either side of the collision interface. The calculated crush for the LRV 3 bullet and target vehicles in the 30 mph collision are shown in Figure 79 and Figure 80, respectively. The fringes of crush are again referenced to a plane at the back of the cab. There is a peak crush displacement of approximately 750 mm on both vehicles. However, at these displacements, there is an initiation of a lateral rotation of the collision interface with both vehicles having a larger amount of crush on the left side of the cab underframe. Despite this rotation, the crush of both vehicles is developed through a push back of the head girder and a corresponding crush of the underframe aft of the head girder. The crush displacements at the top of the cab forward wall in both vehicles is also very symmetric for this higher collision speed. Despite the lateral rotation of the collision interface, the crush response of both LRVs is a controlled collapse that occurs in a desirable mode.

(a) Time = 0.060 s

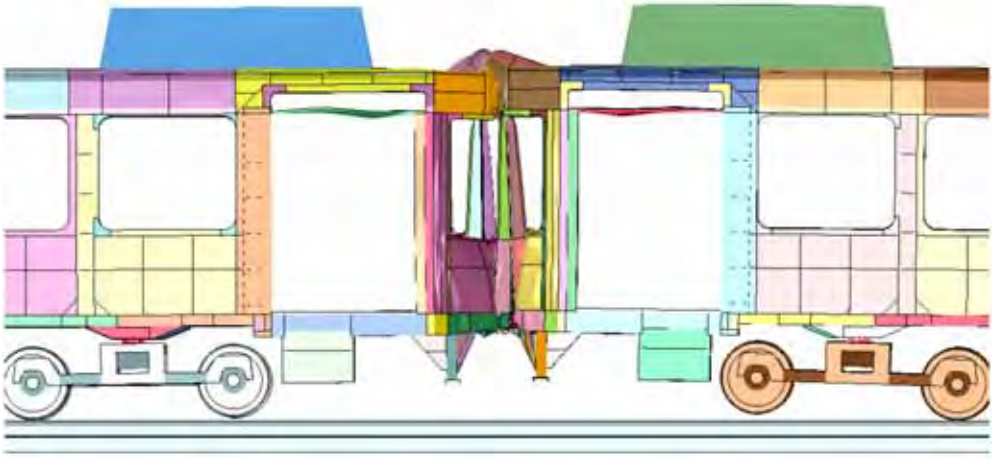

(b) Time = 0.250 s

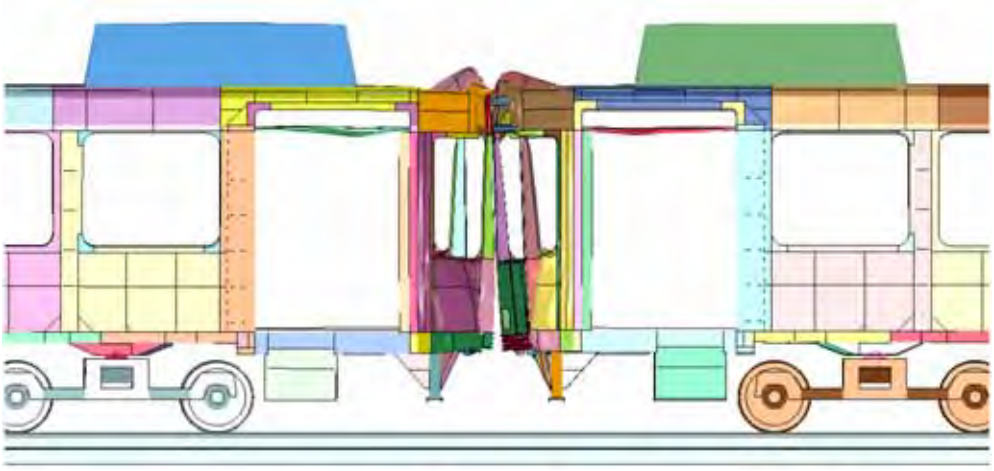

(c) Time = 0.600 s

Figure 78. Simulation of the LRV 3 Compatible Collision at 30 mph.

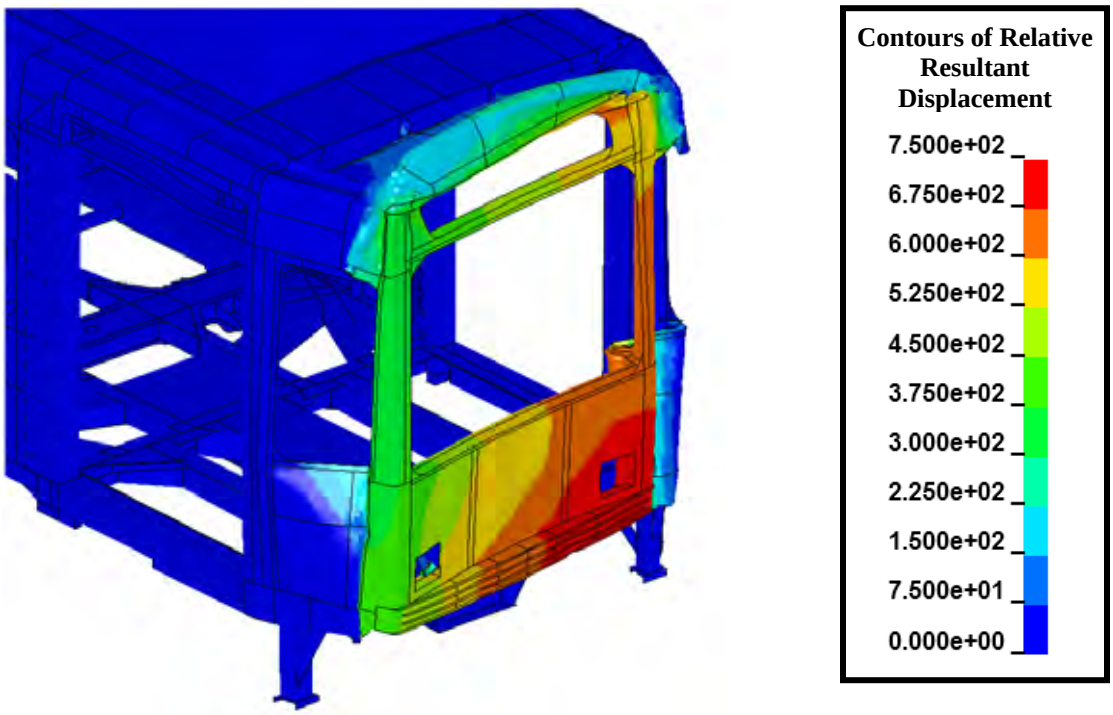

Figure 79. Crush Level (mm) for the LRV 3 Bullet Car in the 30 mph Compatible Collision.

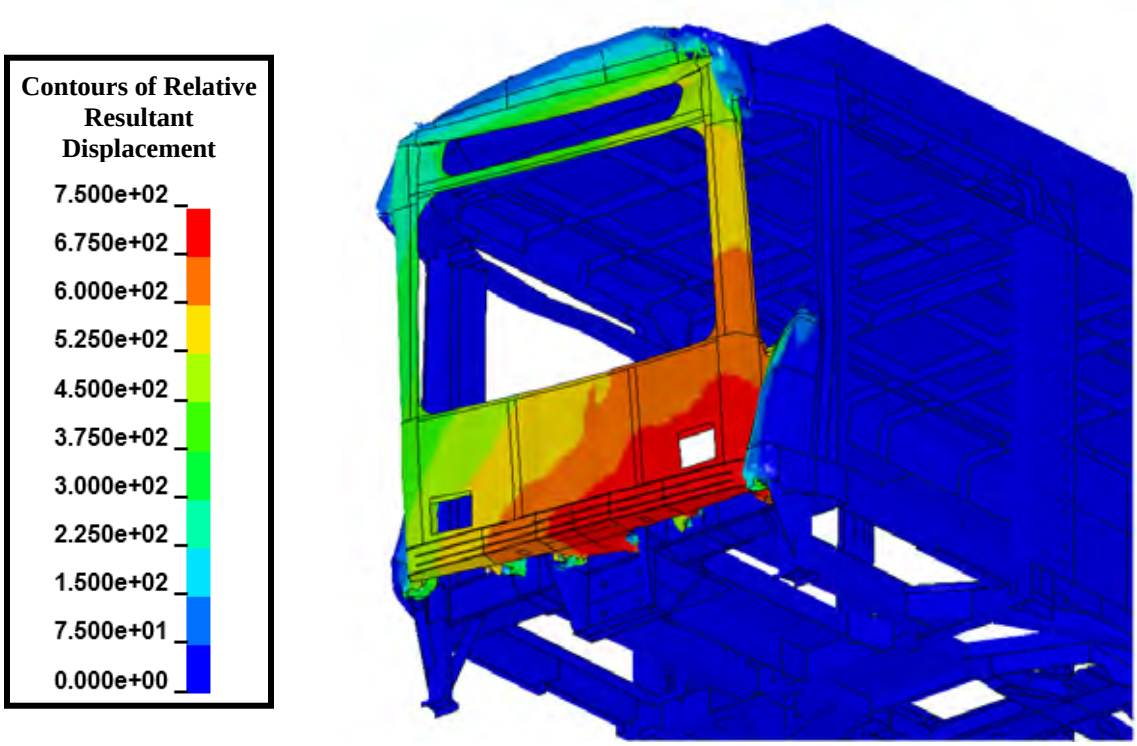

Figure 80. Crush Level (mm) for the LRV 3 Target Car in the 30 mph Compatible Collision.

2.6. LRV 4 Compatible Collisions

LRV 4 Model

The analysis methodologies for LRV 4 were identical to those used in the previous LRV 1-3 analyses. The model for the LRV 4 was already in LS-DYNA format and ready for crash analyses. Modifications were made to: (1) add force cross-section plane definitions, (2) reflect the vehicle for compatible collision scenarios, (3) add new rail and ground model, and (4) prescribe initial conditions.

Only the forward section of the LRV is explicitly modeled. The remainder of the vehicle is modeled using a rigid body attached to the structures aft of the articulating joint as shown in Figure 81. Only the primary structural members are included in the cab model; no outer panels, auxiliary equipment, or interior fitments are included. In the occupant compartment, the model includes some of the side and roof sheeting that are integral to the structure, as well as floor panels. However, other nonstructural components such as doors and windows were not included. The locations that force-cross sections were added to the model are also indicated in the figure.

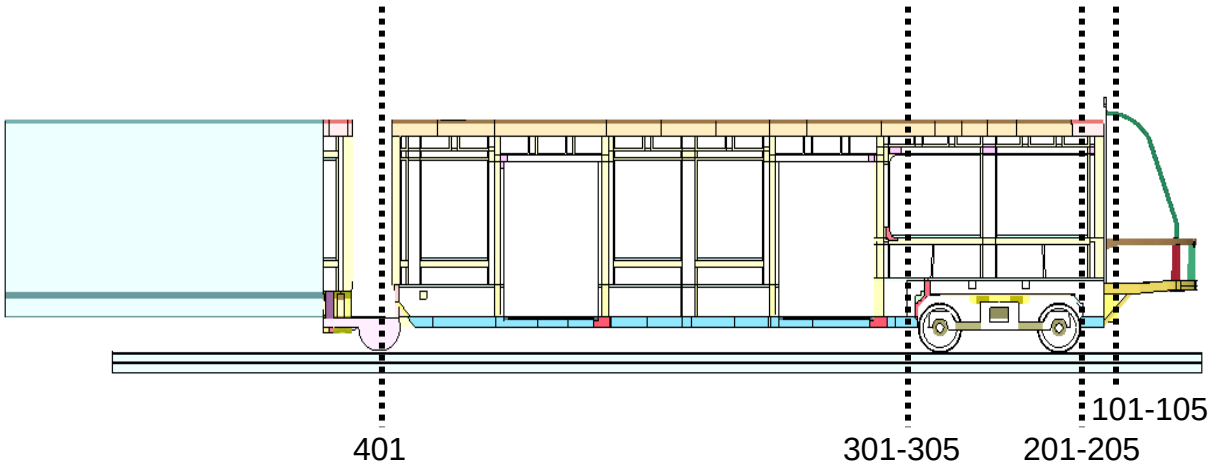

Figure 81. Force Cross Section Plane Locations for the LRV 4 Model.

The finite element mesh for LRV 4 was constructed as an assembly of many parts, using a mix of shell and brick elements. Most of the car model was constructed from 4-node shell elements. A relatively uniform mesh and fine mesh resolution in the impact zone of the LRV 4 model was used and contributed to a high quality simulation of the collision behavior. The trucks, ground, rail, and trailing masses were modeled with rigid 8-node brick elements.

The collision interface between the two colliding vehicles is shown in Figure 82. The wheels on both cars were non-rotating and sliding along the rail to simulate a condition of fully locked brakes such that the wheels slide along the rails with a frictional coefficient of 0.30.

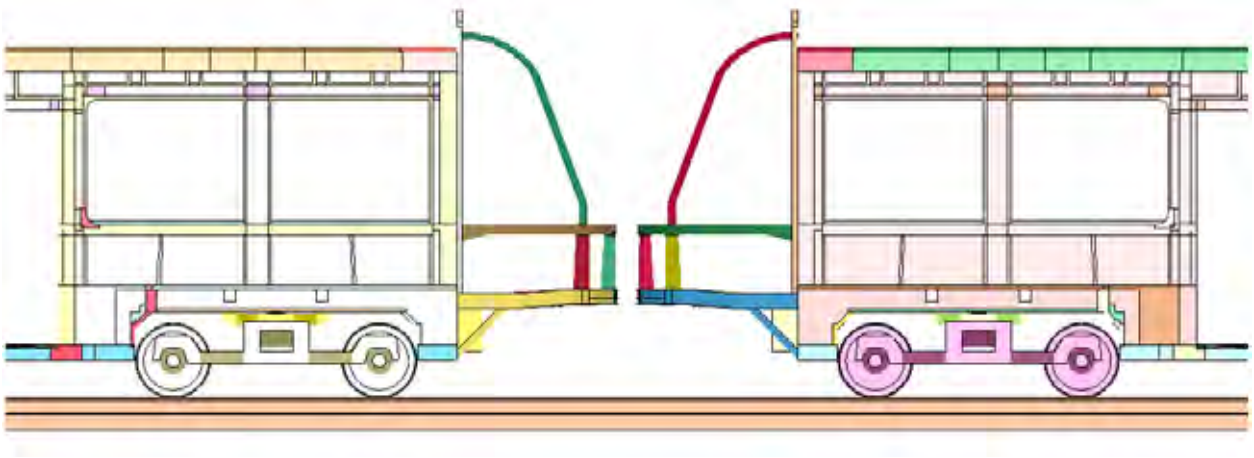

Figure 82. Collision Interface for the LRV 4 Compatible Crash Analysis.

The cars were modeled with a bilinear elastic-plastic behavior using the *MAT_PIECEWISE_LINEAR_PLASTICITY constitutive model in LS-DYNA. Properties for the two primary structural materials are provided in Table 13. Material 1 was used for most components in the structural frame and Material 2 was used for the side and roof panels in the passenger compartment. Additional deformable materials were used for specific components such as the floor panels or the articulating joint. However, these materials did not contribute significantly to the observed crash responses and energy dissipation. Rigid bodies were given generic steel properties and were modeled with the *MAT_RIGID material in LS-DYNA. Material densities were previously adjusted by major component group to match the specified vehicle weight.

Material failure was included through element erosion. If an element reaches its plastic failure strain, it is deleted from the calculation, creating a void and an area for stress concentration in the mesh. Failure criteria for the two elastic-plastic materials were chosen based on available material properties and mesh density considerations. For the primary structural materials failure was assumed to occur at a plastic strain level of 25%.

Table 13. Material Properties Used in the LRV 4 Analyses

Material	Material 1	Material 2
LS-DYNA Material	Material Model 24, Piecewise Linear Elastic-Plastic	
Young's Modulus (GPa)	207	193
Poisson's Ratio	0.30	0.33
Yield Strength (MPa)	358	379
Tangent Modulus (MPa)	662	1248
Material Failure Strain	0.25	0.25

The total LRV 4 mass was calculated as approximately 46 Mg in LSDYNA. Table 14 provides a breakout of component and total modeled LRV 2 masses.

Table 14. Component Masses in the LRV 4 Model

Component	FEA Model (kg)
A-Car	17,344
Motor Bogie	5,377
Trailing Mass (includes B & C-car, Motor Bogie, and center truck)	23,663
Total	46,384

Analysis Results

The compatible collisions analyzed for LRV 4 are at 10, 15, 20, 25, and 30 mph. One vehicle is moving at the collision speed (bullet) and the other is stationary (target). Unless otherwise stated, all images show the bullet vehicle on the left and the target vehicle on the right. The collision force time histories for the various collision speeds are shown in Figure 83.

The collision pulses have an initial rise to a level of 1.8 to 2.0 MN before dropping off to an initial crush force level of approximately 1.4 MN. For more severe collisions, there is a subsequent rise in crush force levels with a peak force of 3.0 MN for the 30 mph collision. The duration of the collisions vary from approximately 120 ms for the 10 mph collision up to approximately 240 ms for the 30 mph collision. When the crush forces are plotted against the crush distance, as shown in Figure 84, the LRV is again shown to have a characteristic force-crush behavior that is reproduced in the different collision speeds.

The calculated crush of the LRV 4 bullet and target vehicles in the 20 mph collision are shown in Figure 85 and Figure 86, respectively. There is approximately 300 mm of crush in the bullet LRV and 200 mm of crush in the target LRV. The crush response is a flattening of the nose in the underframe and collapse of the buckle initiators in the forward crush zone. This crush response is a controlled collapse that occurs in the desired mode developed during the vehicle design effort.

As the collision speed increases, the crush progresses from the front of the cab in a similar mode. The crush response of the target LRV 4 vehicle for the 25 mph collision is shown in Figure 87. There is approximately 300 mm of crush in the target LRV. The crush response is very similar to that of the bullet vehicle in the 20 mph collision with the exception that the larger crush distance has resulted in a small amount of deformation in the secondary buckle initiators in the central girder. This crush response has developed to a point where the primary crush zone in the nose of the cab has been completely exhausted and the axial crush forces in the structures increases to the maximum level of approximately 3 MN. Beyond this level of response, the crush was still observed to progress from the front of the cab aft. However, the mode of crush was less controlled and localization of deformations resulted in failure of structural members at some locations. This crush response is again a controlled collapse that occurs in the desired mode developed during the vehicle design effort.

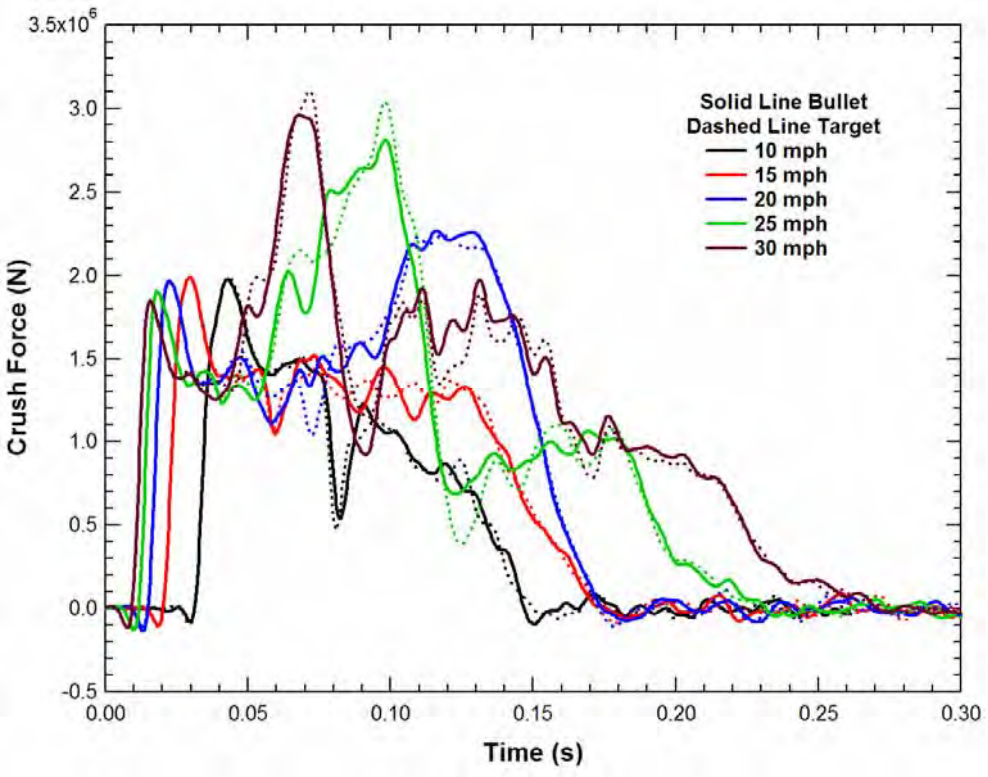

Figure 83. Component Force History for all Speeds of the LRV 4 Compatible Crash Analysis.

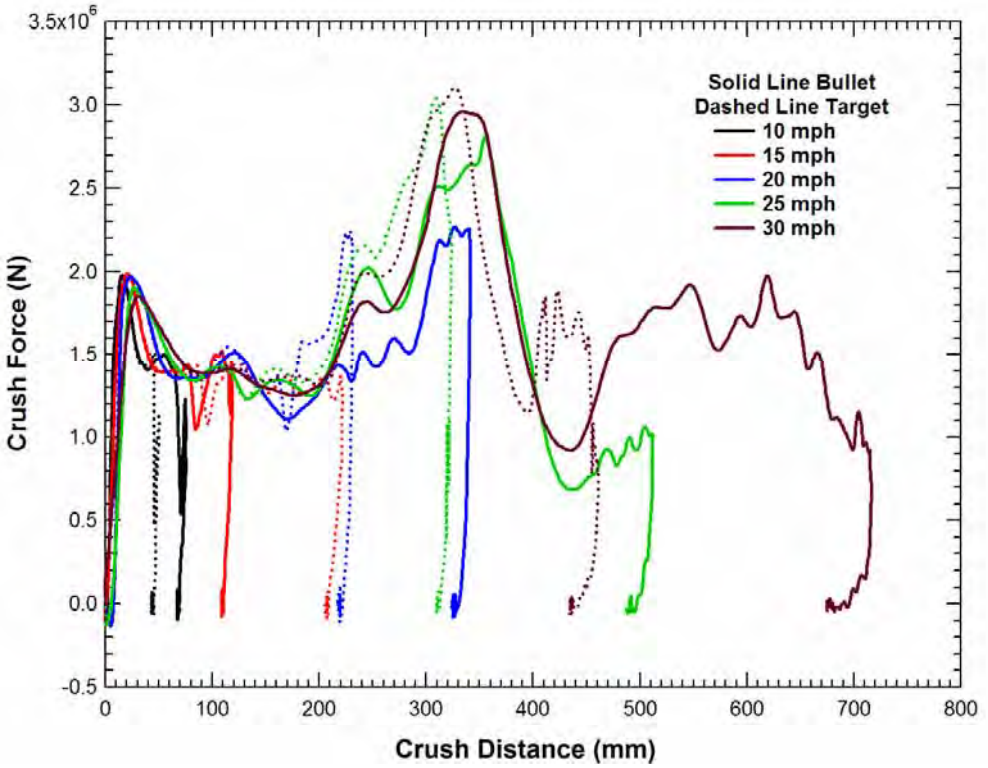

Figure 84. Force-Crush Behavior for all Speeds of the LRV 4 Compatible Crash Analysis.

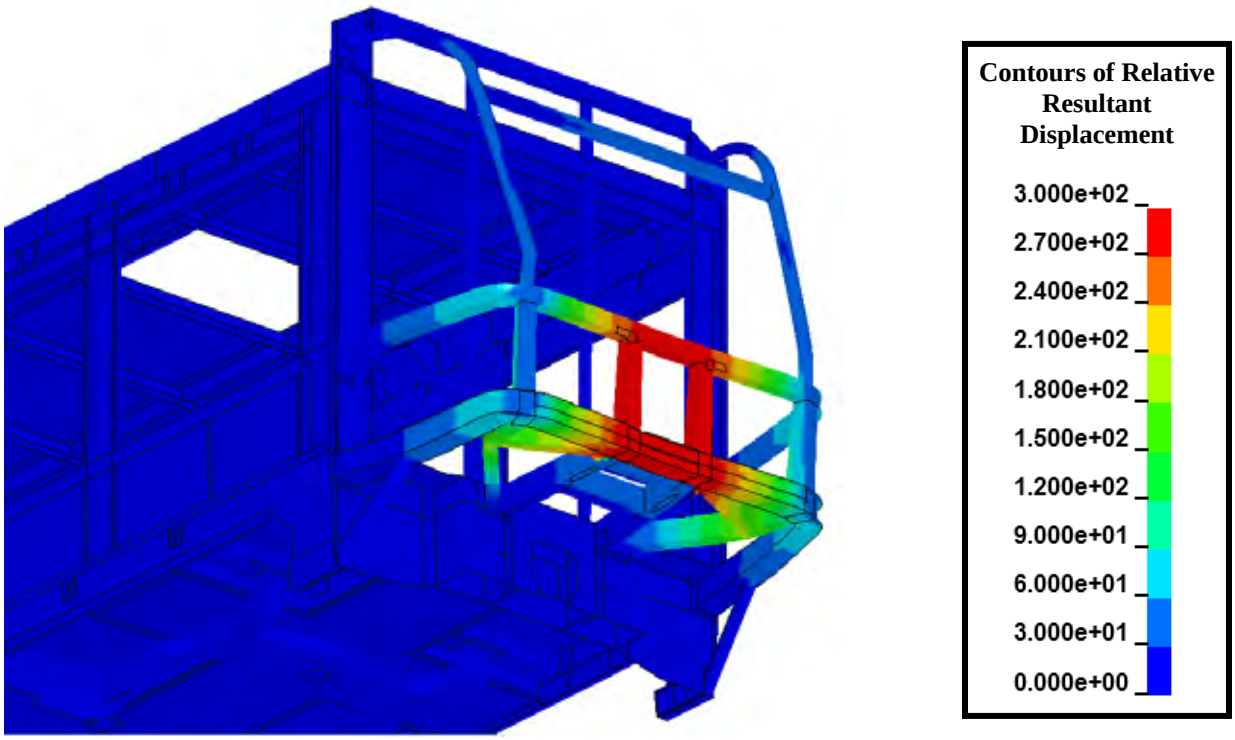

Figure 85. Crush Level (mm) for the LRV 4 Bullet Car in the 20 mph Compatible Collision.

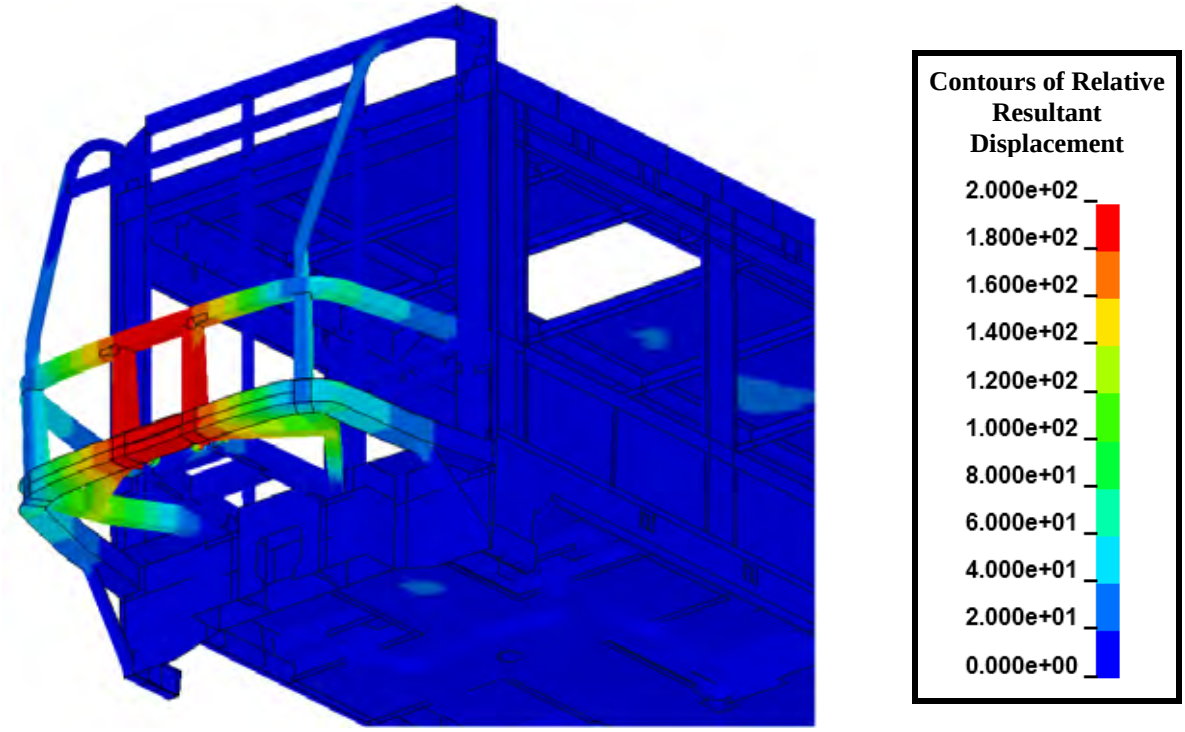

Figure 86. Crush Level (mm) for the LRV 4 Target Car in the 20 mph Compatible Collision.

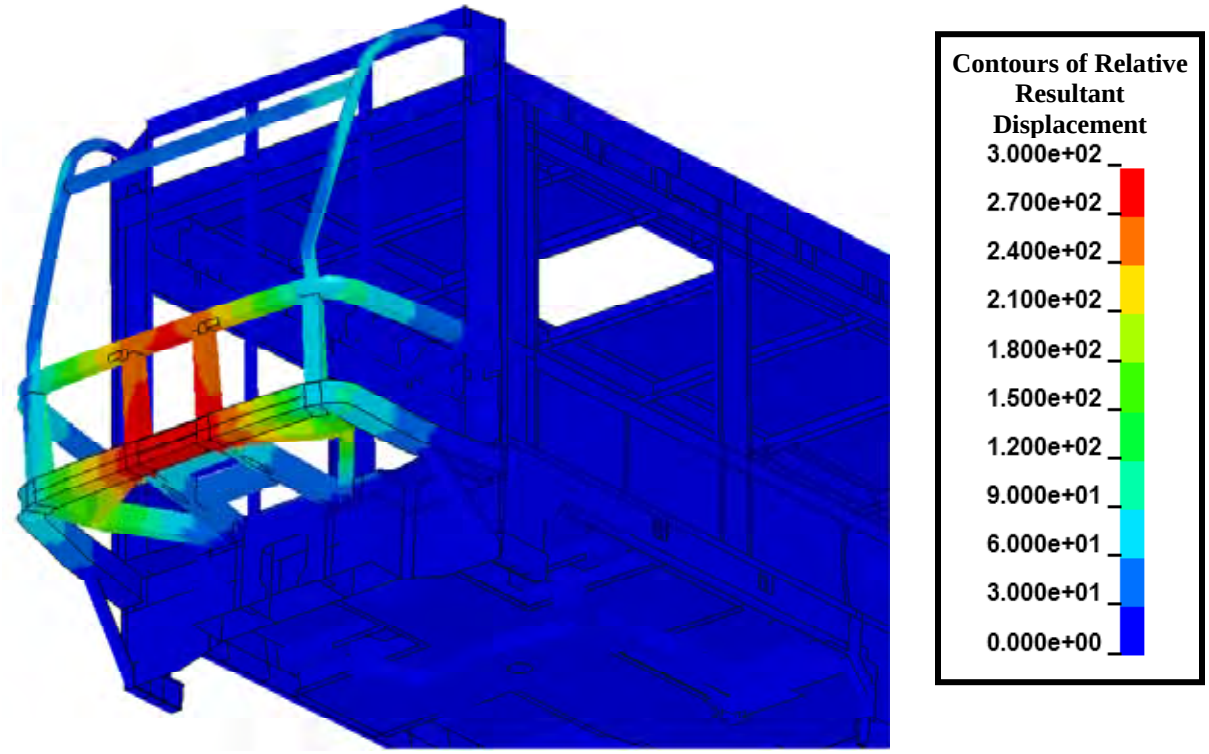

Figure 87. Crush Level (mm) for the LRV 4 Target Car in the 25 mph Compatible Collision.

As the collision speed increases further, the crash energy and crush magnitude becomes larger than considered as part of the crashworthy design effort. The crush response of the target LRV 4 vehicle for the 30 mph collision is shown in Figure 88. There is approximately 400 mm of crush in the target LRV and the collapse has progressed into the secondary buckle initiators in the central girder are also beginning to initiate. This crush response has developed to a point where the primary crush zone in the nose of the cab has been completely exhausted and the axial crush forces in the structures increases to the maximum level of approximately 3 MN. Beyond this level of response, the crush was still observed to progress from the front of the cab aft. However, the mode of crush was less controlled and localization of deformations resulted in failure of structural members at some locations.

The distribution of forces through the cab structures as the crush develops for LRV 4 is shown in Figure 89. The side sills carry a relatively uniform load of approximately 1.0 MN until the crush length exceeds approximately 400 mm. The central girders and cross bracing in the underframe carry an initial load of approximately 750 kN until the buckling initiates and the load drops off. As the crush length approaches 400 mm, the underframe deformations begin to lock up and the forces transmitted through these structures increases to approximately 1.4 MN before the load again drops off in a secondary crushing response. The structural shelf and window sills carry a relatively small load during the early portions of the crush response but develop a maximum load of 500-600 kN at approximately 300 mm crush.

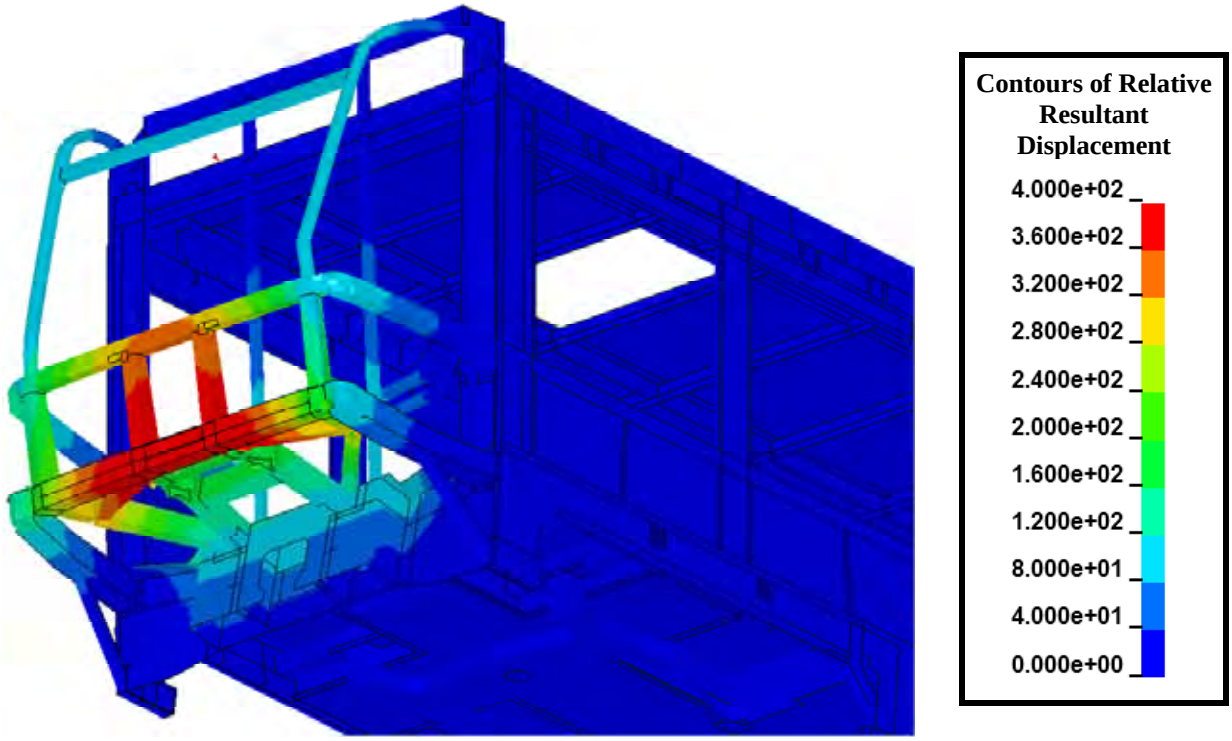

Figure 88. Crush Level (mm) for the LRV 4 Target Car in the 30 mph Compatible Collision.

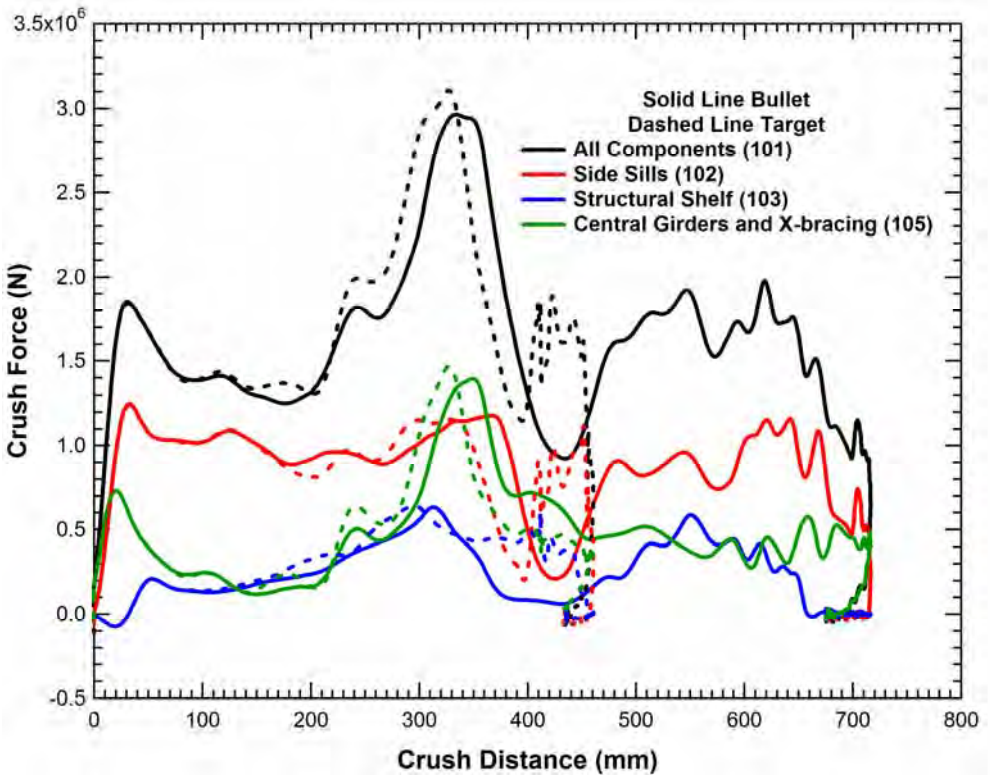

Figure 89. Force-Crush Behavior for the 30 mph LRV 4 Compatible Crash Analysis.

2.7. Summary of Analysis Results for Incompatible LRV Collisions

The second set of LRV collision calculations performed were the incompatible collisions between different LRV designs (Phase II Task 3). These analyses are important for understanding the issues associated with the compatibility of vehicles built to a new standard with existing vehicles. To assess compatibility concerns, we need to establish the compatibility of the current fleet of vehicles that could be operating together as well as the compatibility of different vehicles built to the same specification under the current state of practice.

In the incompatible collision simulations, the two different LRVs were both initialized to be moving in opposite directions at one-half of the desired collision speed. Thus the pitching effects of the breaking forces are equivalent in the two vehicles. This eliminates any bias in the crash response that could be introduced by the assignment of the moving and stationary LRVs. Impact simulations were performed for a range of collision closing speeds (e.g. 5, 10, 15, 20, 25, and 30 mph). The analyses of different severity collisions allowed for the assessment of the range of outcomes for different collision conditions. Fully dynamic nonlinear analysis methodologies were applied. The explicit nonlinear dynamic finite element code LS-DYNA was used.

The details of the individual LRV models and collision analyses were provided in the previous report sections on compatible collision analyses. Here we present a summary of the incompatible collision behaviors and the influence on potential CEM requirements.

The first set of incompatible collision analyses was performed with the two designs with the overall lowest average crush strength (LRV 1 and LRV 3). The corresponding force crush behavior of these two vehicles from the 30 mph compatible collision analyses is shown in Figure 90. The comparison shows that during the initial 200 mm of crush, LRV 1 is significantly stronger than LRV 3. Subsequently, the two have similar crush strengths. However, the high initial crush strength of LRV 1 is higher than the entire curve of LRV 3 out to the crush displacements of 700 mm.

A summary of vehicle force-crush behaviors for the vehicles in the LRV 1 to LRV 3 incompatible collisions is shown in Figure 91. The LRV 1 to LRV 3 incompatible collisions were performed at closing speeds between 5 and 25 mph. The crush curves clearly indicate that the vast majority of the crush occurred in LRV 3 with very little damage to LRV 1. In addition, a comparison of the LRV 3 crush curves from the compatible and incompatible collisions (Figure 90 and Figure 91) show that the overall crush force for small crush distances (0-200 mm) are quite similar. However for large crush distances (500 mm and greater) the LRV 3 crush forces are significantly lower in the incompatible collision. This probably results from the fact that only the underframe of LRV 3 is deforming in the incompatible collision. In the compatible collision, the entire ends of the LRV 3 vehicles engage and additional forces are produced by the crushing of the vehicle side walls and roof structures.

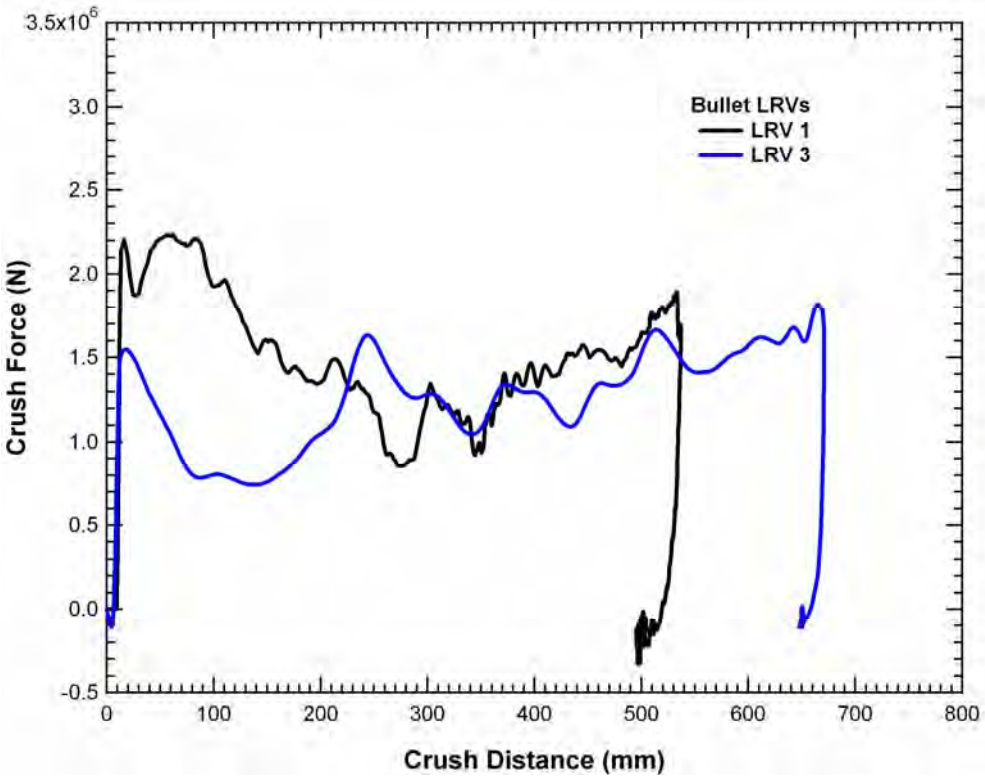

Figure 90. Force-Crush Plots for LRV 1 and LRV 3 in the 30 mph Compatible Collisions.

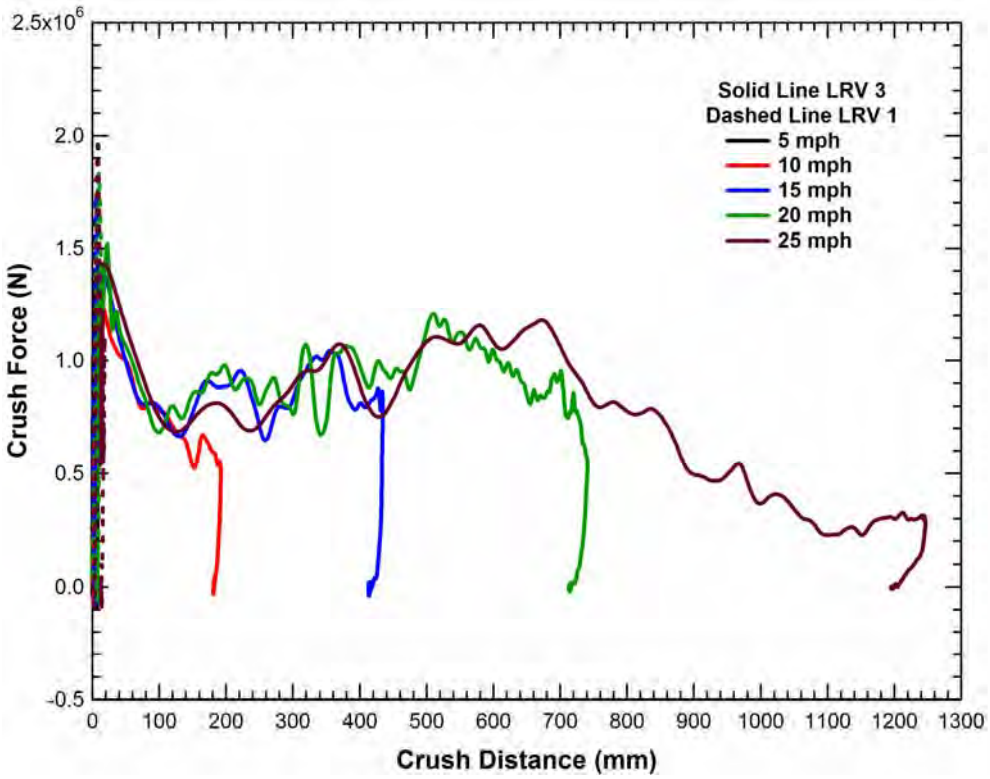

Figure 91. Force-Crush Behaviors for the LRV 1 to LRV 3 Incompatible Crash Analysis.

A summary of vehicle crush lengths for the various incompatible collisions is presented in Table 15. The LRV 1 to LRV 3 collisions are presented in the top half of the Table. The crush distances clearly indicate that the vast majority of the crush occurred in LRV 3 with very little damage to LRV 1. Even at the 25 mph closing speed the LRV 1 damage was limited to 14 mm of crush in the nose of the head girder. A similar behavior would be expected for collisions of either LRV 2 or LRV 4 against LRV 3 based on the comparison of the crush curves and the relatively high strengths of the other vehicles compared to LRV 3.

Table 15. Summary of Vehicle Crush Lengths (in mm) for the Incompatible Collision Analyses.

Vehicle Crush (in mm)	Collision Speed					
	5 mph	10 mph	15 mph	20 mph	25 mph	30 mph
LRV 1	1	2	4	7	14	—
LRV 3	7	182	414	714	1195	—
Average	**4**	**92**	**209**	**360**	**605**	**—**
LRV 2	—	—	—	150	168	223
LRV 4	—	—	—	282	519	713
Average	**—**	**—**	**—**	**216**	**343**	**468**

The subsequent set of incompatible collision analyses was performed with the other two designs (LRV 2 and LRV 4). These two vehicles were designed with very similar specifications on crash safety including both a 2g buff strength and a compatible crash scenario at a closing speed of 15-20 mph. The corresponding force crush behavior of these two vehicles from the 30 mph compatible collision analyses is shown in Figure 92. The comparison shows that the two vehicles have both a similar strength in the initial portion of the crush response and the peak crush forces that occur between 300 and 400 mm of crush. However, between 100 and 300 mm of crush, LRV 2 is the stronger of the two vehicles.

A summary of vehicle force-crush behaviors for the vehicles in the LRV 2 to LRV 4 incompatible collisions is shown in Figure 93. These analyses were performed at closing speeds between 20 and 30 mph. The crush curves indicate that LRV 2 absorbs part of the energy in a crush length of approximately 200 mm and the remainder of the crush is in LRV 4. For the higher collision speeds, the crush in LRV 4 is significantly larger than in LRV 2.

A summary of the LRV crush lengths for the LRV 2 to LRV 4 incompatible collisions presented in the bottom half of Table 15. The crush distances are more balanced than in the LRV 1 and LRV 3 incompatible collisions. However, there is still significantly greater crush in LRV 4 than in LRV 2.

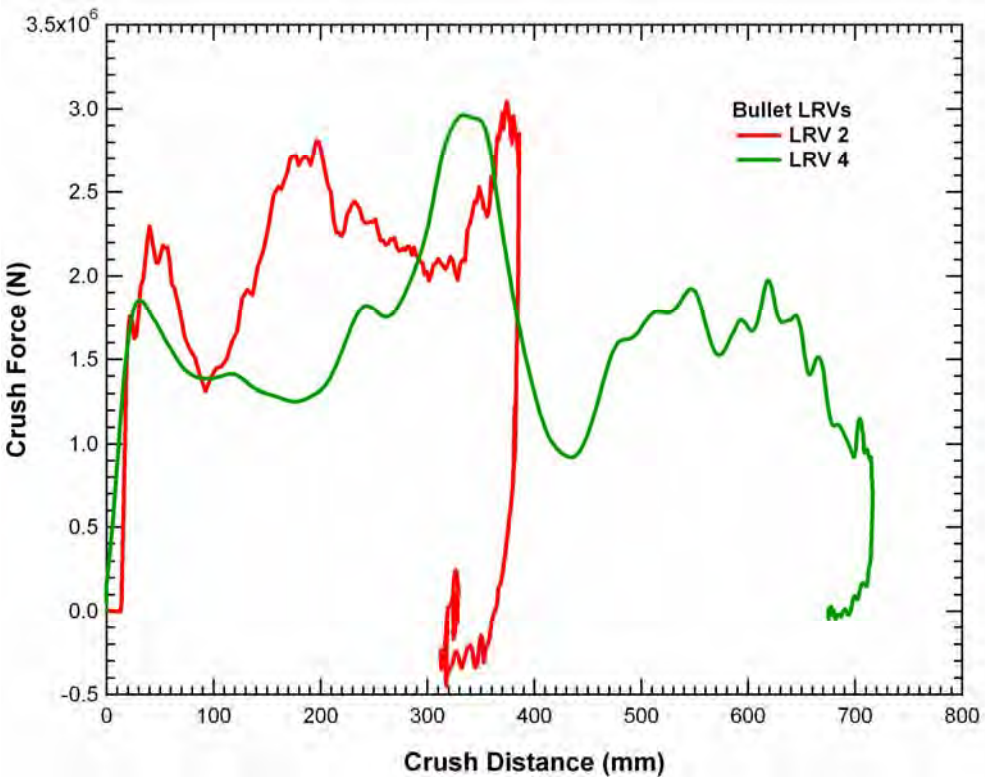

Figure 92. Force-Crush Plots for LRV 2 and LRV 4 in the 30 mph Compatible Collisions.

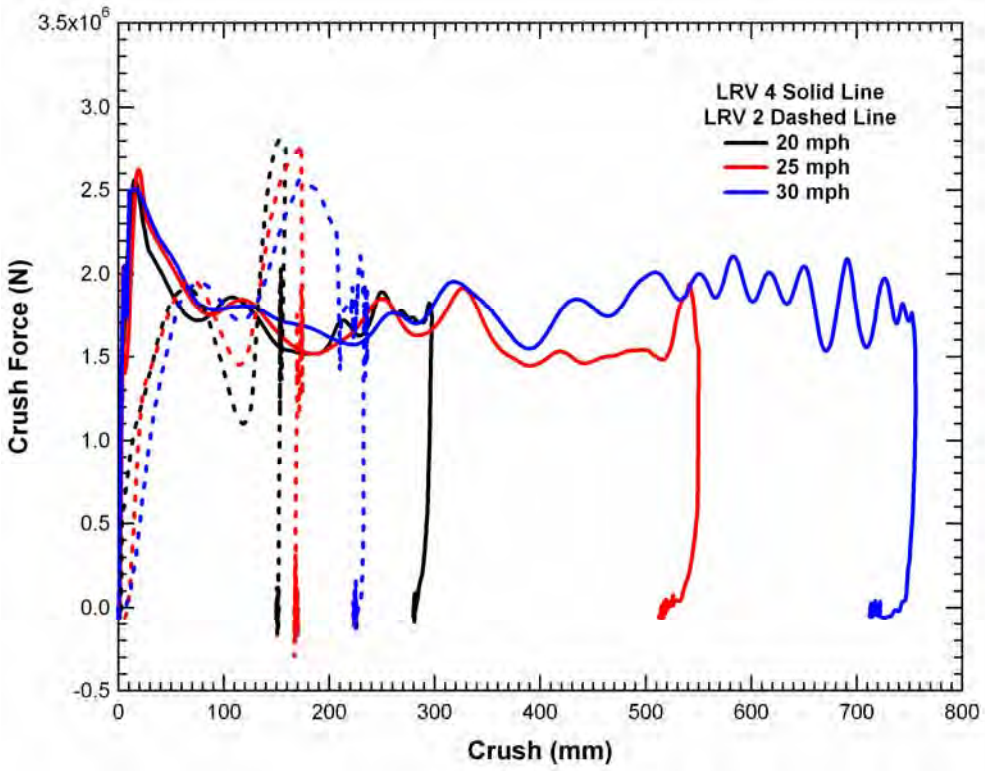

Figure 93. Force-Crush Behavior for the LRV 2 to LRV 4 Incompatible Crash Analysis.

The above summary of the incompatible crash analyses show that the current fleet of LRVs, including vehicles designed to very similar crush strengths, are not sufficiently compatible to obtain a balanced crush in both colliding vehicles. In fact, several of the compatible LRV collision analyses had unbalanced levels of crush in the colliding vehicles. In many of these collisions, the unbalanced crush does not necessarily mean that the collision behaviors obtained are undesirable or result in a greater risk of injuries. However, in some cases, the larger crush in one of the vehicles would put the occupants of the cab at a greater risk of injuries.

If compatibility of crush in LRV collisions is the ultimate goal of the standard, the crush strengths will need to be closely controlled and the progressive collapse behavior needs to be developed with a steadily increasing crush force. However, there has been no LRV collisions identified that demonstrate the incompatibility of LRVs pose a safety risk. As a result, it is difficult to justify a tightly controlled crush force specification. In addition, the analyses of compatible collisions at different speeds should improve the overall compatibility of the collision behaviors.

Some additional details of the incompatible collision analyses are provided in the following sections.

Analysis of LRV 1 – LRV 3 Incompatible Collisions

Incompatible collisions were simulated between LRV 1 and LRV 3, at 5, 10, 15, 20, and 25 mph. In these simulations, both vehicles were moving, each at half the collision speed. The collision interface between the two vehicles is shown in Figure 94. LRV 3 is on the left hand side of the image and LRV 1 is on the right hand side. LRV 3 was raised 86 mm so the anticlimbers would be compatible.

The calculated crash response between LRV 1 and LRV 3 for the 10 mph incompatible collision is shown in Figure 95. The crush response of LRV 3 in the collision is a push back of the head girder and crush of the underframe structures at the car end. The LRV 3 crush in the 10 mph incompatible collision is shown in Figure 96. The fringes of crush are referenced to a plane at the back of the cab. The crush response is a flattening of the nose and push back of the head girder. There is approximately 200 mm of crush in the central girders and 100 mm of crush in the side sills. This crush response is a controlled collapse that occurs in a desirable mode. The behavior looks very similar to the crush response of the compatible LRV 3 collision response at low collision speeds.

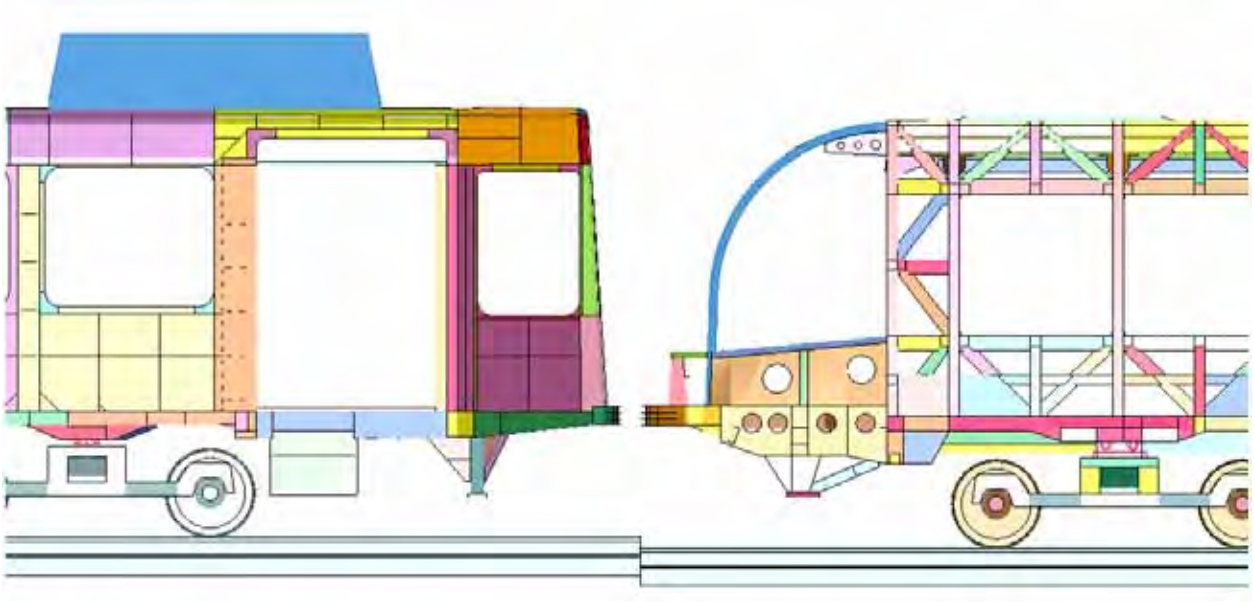

(a) Side view

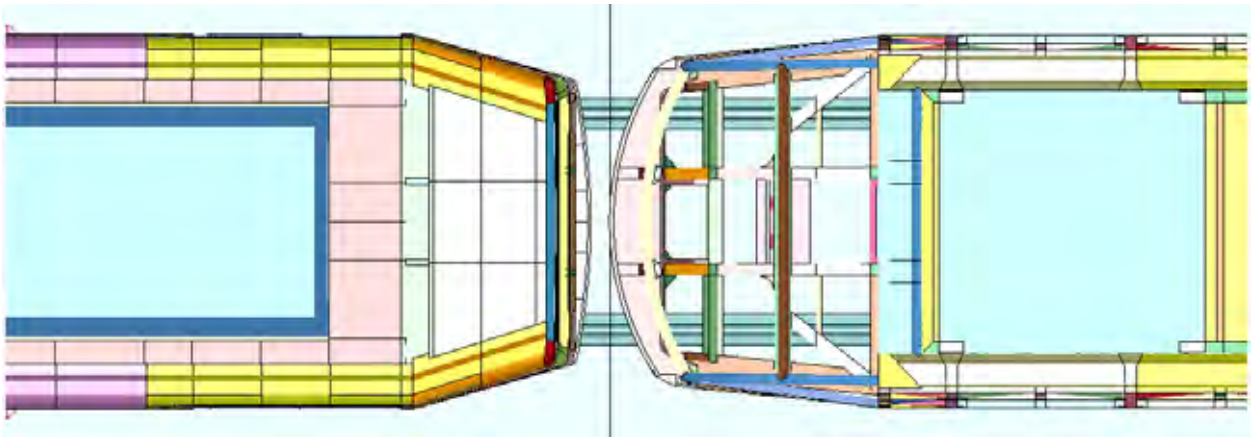

(b) Top view

Figure 94. Collision Interface for the Incompatible Crash Analysis between LRV 1 and LRV 3.

The calculated crash response between LRV 1 and LRV 3 for the 15 mph incompatible collision is shown in Figure 97. The crush response of LRV 3 in the collision is a push back of the head girder and crush of the underframe structures at the car end. The crush at the underframe level is sufficient to create a noticeable inward rotation of the end wall.

The LRV 3 crush in the 15 mph incompatible collision is shown in Figure 98. The fringes of crush are referenced to a plane at the back of the cab. The crush response is a push back of the head girder and crushing of the forward underframe structures. There is approximately 450 mm of crush in the underframe with no damage at the upper cab structures. This underframe crush response is still a controlled collapse that occurs in a desirable mode.

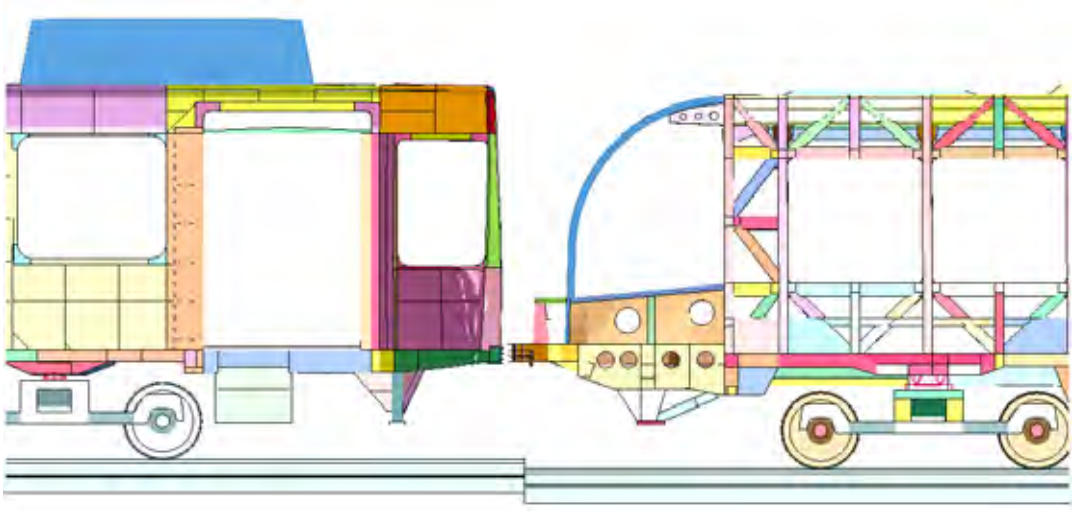

time = 0.500 s

Figure 95. Simulation of the Incompatible Collision between LRV 3 and LRV 1 at 10 mph.

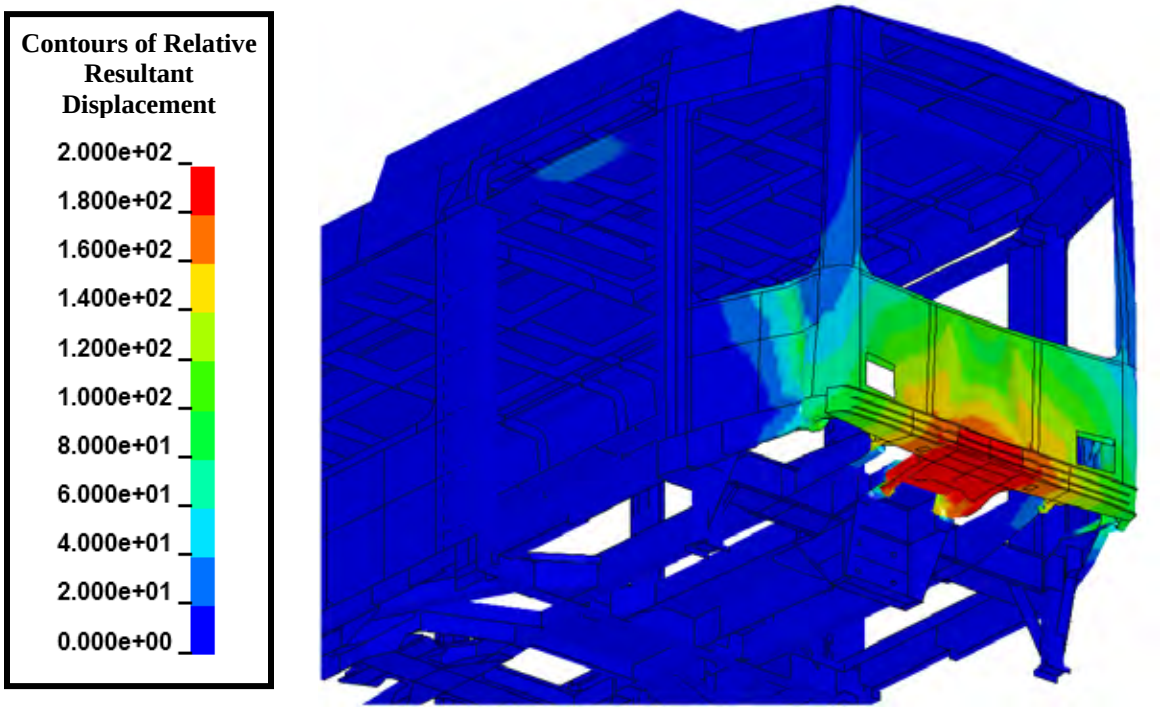

Figure 96. Crush Level (mm) for LRV 3 in the 10 mph Incompatible Collision.

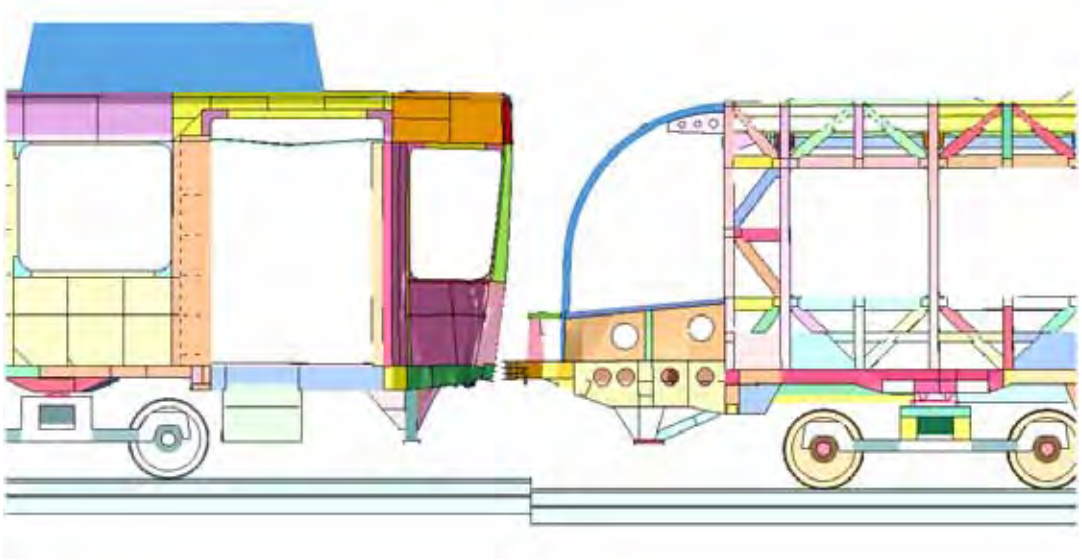

time = 0.400 s

Figure 97. Simulation of the Incompatible Collision between LRV 3 and LRV 1 at 15 mph.

The calculated crash response between LRV 1 and LRV 3 for the 20 mph incompatible collision is shown in Figure 99. The crush response of LRV 3 in the collision is a push back of the head girder and crush of the underframe structures at the car end. The crush at the underframe level is sufficient to create a significant inward rotation of the end wall that is starting to produce an upward lifting of the head girder.

The LRV 3 crush in the 20 mph incompatible collision is shown in Figure 100. The fringes of crush are reference to a plane at the back of the cab. The crush response is a push back of the head girder and crushing of the forward underframe structures. There is approximately 800 mm of crush in the underframe with no damage at the upper cab structures. This underframe crush response is still a controlled collapse of the forward underframe.

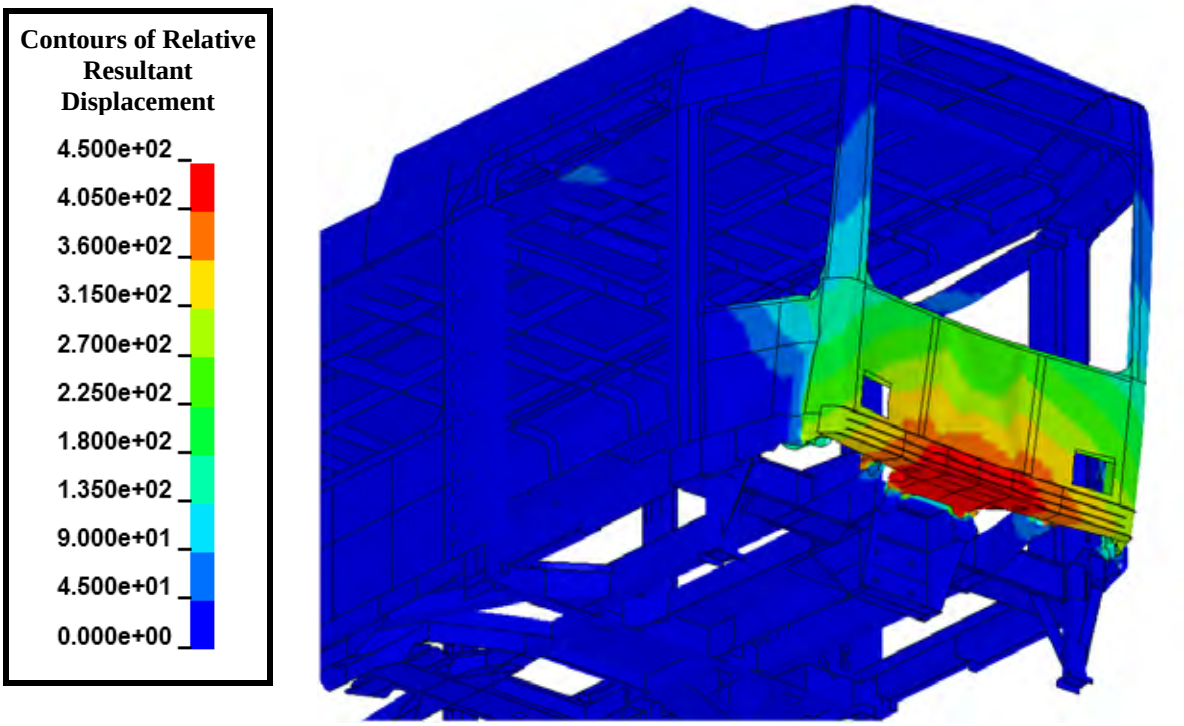

Figure 98. Crush Level (mm) for LRV 3 in the 15 mph Incompatible Collision.

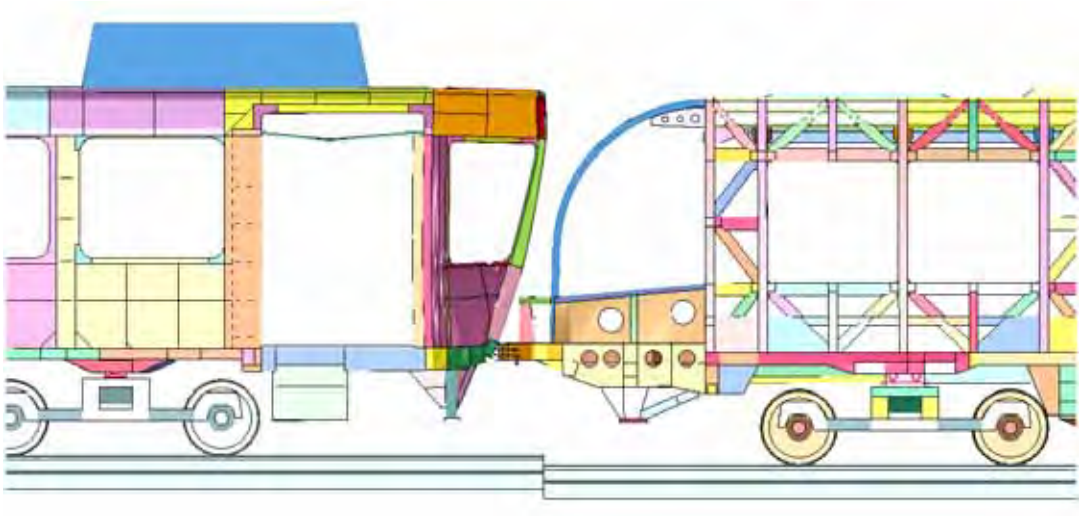

time = 0.350 s

Figure 99. Simulation of the Incompatible Collision between LRV 3 and LRV 1 at 20 mph.

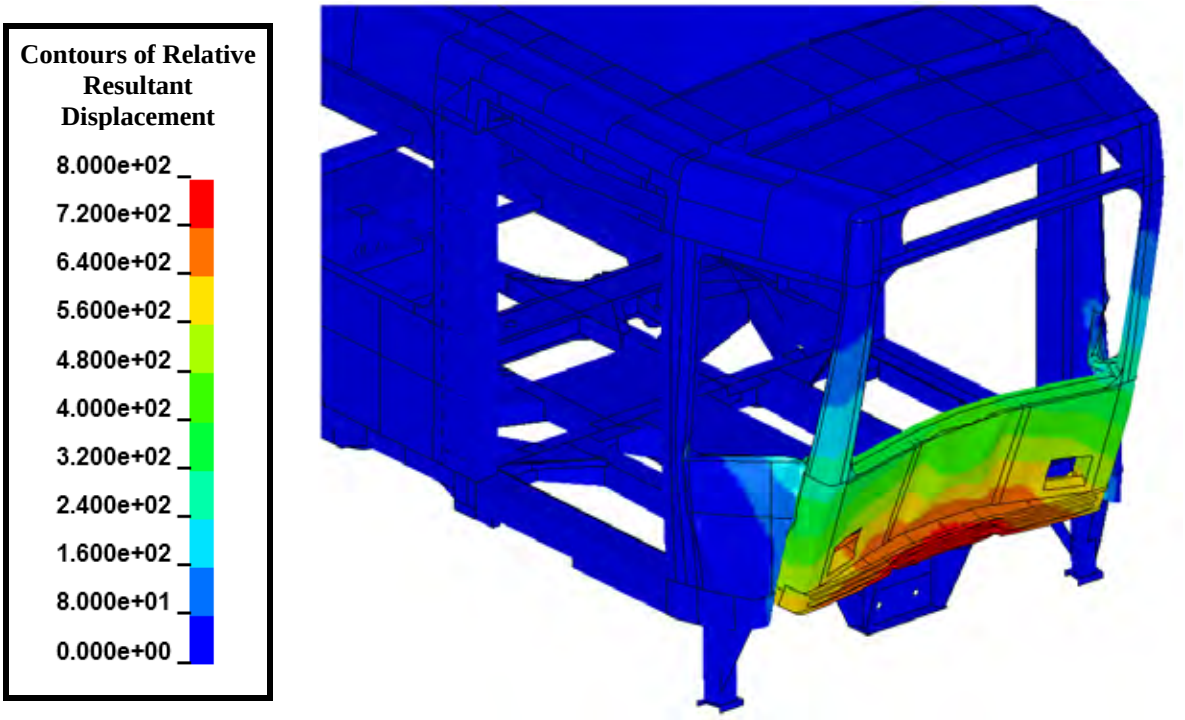

Figure 100. Crush Level (mm) for LRV 3 in the 20 mph Incompatible Collision.

The calculated crash response between LRV 1 and LRV 3 for the 25 mph incompatible collision is shown in Figure 101. The crush response of LRV 3 in the collision is a push back of the head girder and crush of the underframe structures at the car end. The crush at the underframe level is sufficient to create a large inward rotation of the end wall that produces a significant upward lifting of the head girder. This lifting behavior results in a crush mode that is less controlled and more unstable than in the compatible collisions.

The LRV 3 crush in the 25 mph incompatible collision is shown in Figure 102. The crush response is a push back and upward of the head girder and crushing of the forward underframe structures. There is approximately 1.3 m of crush in the underframe with no damage at the upper cab structures. This underframe crush response is nearly a complete collapse of the cab underframe.

The calculated crush of LRV 1 in the 25 mph incompatible collision is shown in Figure 103. Even in this relatively severe collision there is very little damage to LRV 1 with the structural crush displacements of approximately 15 mm.

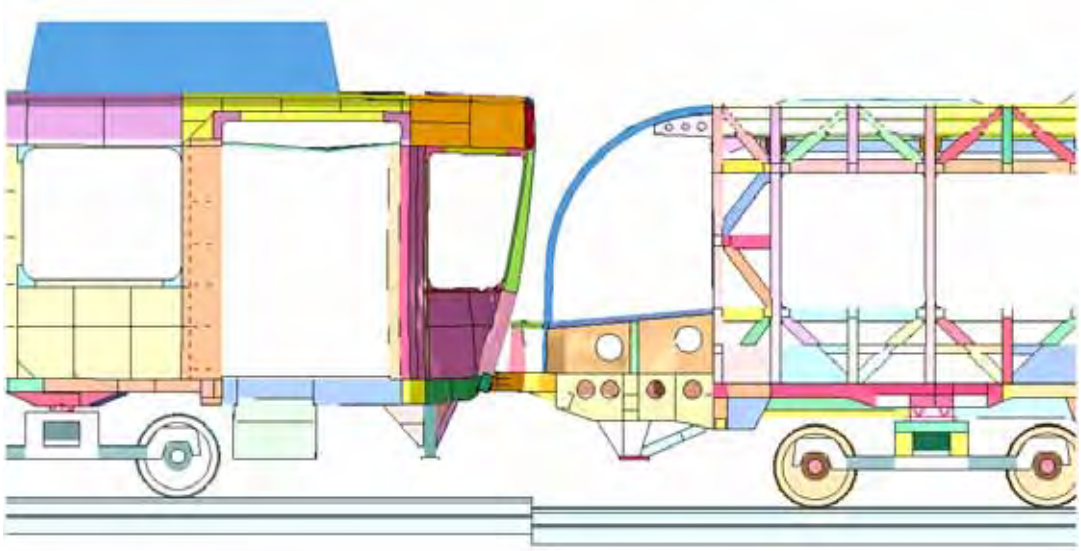

time = 0.090 s

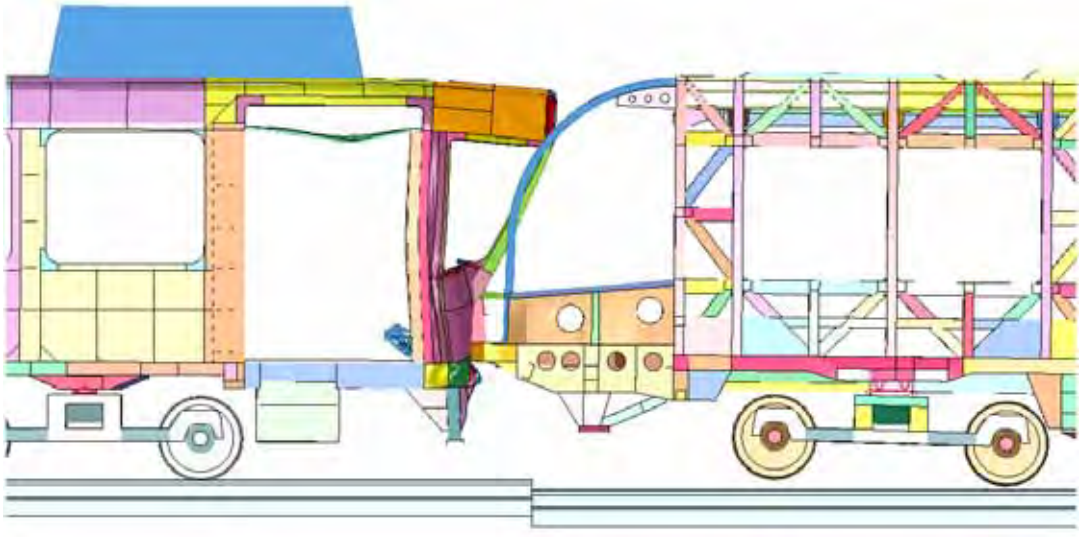

time = 0.700 s

Figure 101. Simulation of the Incompatible Collision between LRV 3 and LRV 1 at 25 mph.

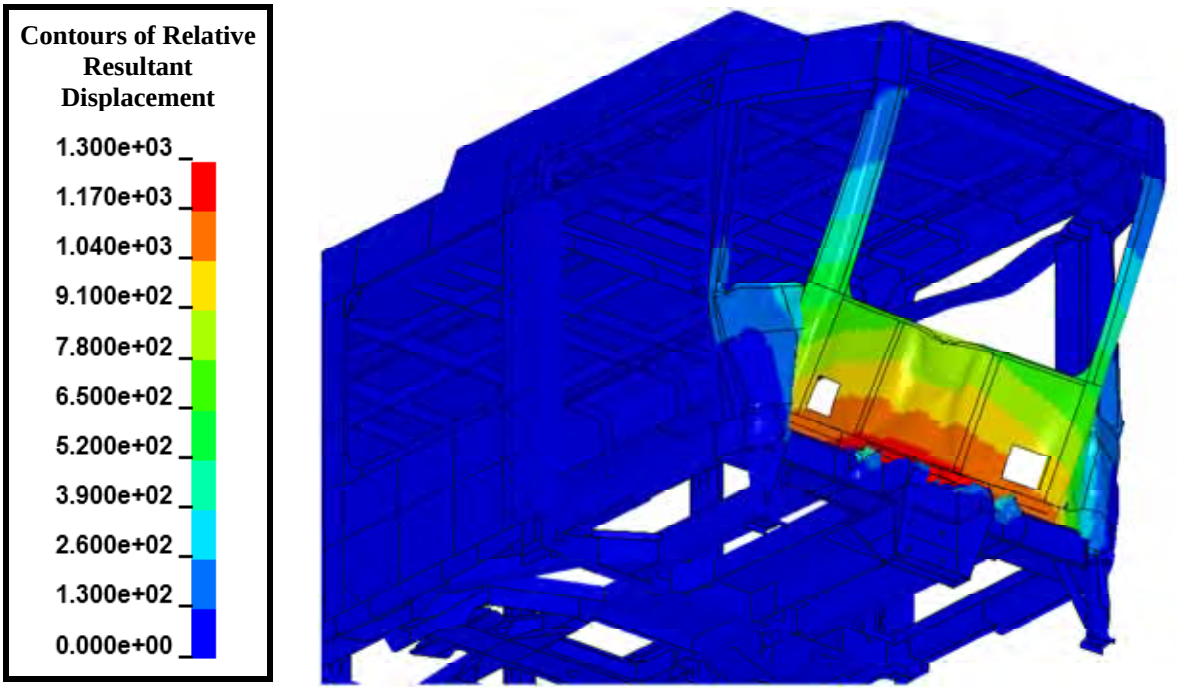

Figure 102. Crush Level (mm) for LRV 3 in the 25 mph Incompatible Collision.

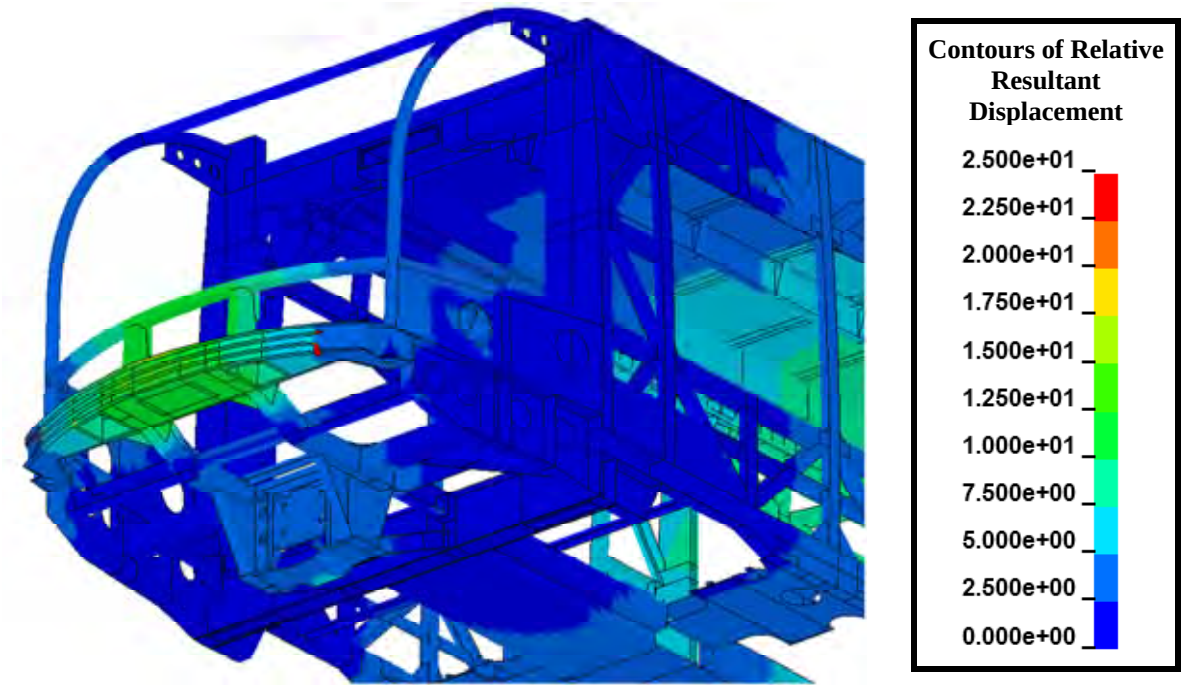

Figure 103. Crush Level (mm) for LRV 1 in the 25 mph Incompatible Collision.

Analysis of LRV 2 – LRV 4 Incompatible Collisions

Incompatible collision were simulated between LRV 2 and LRV 4, at 20, 25, and 30 mph. In these simulations, both vehicles were moving, each at half the collision speed. The collision interface between the two vehicles is shown in Figure 104. LRV 4 is on the left side of the image and LRV 2 is on the right side.

The LRVs were adjusted so the anticlimbers would be compatible. These two vehicles were designed with very similar specifications on crash safety including both a 2g buff strength and a compatible crash scenario at a closing speed of 15-20 mph. They also both have a design with a sloped profile of the cab and variations in the height of the cab floor from the head girder to the back of the cab. However, the structural design approaches used to develop a controlled progressive collapse of the structures are significantly different in the two designs.

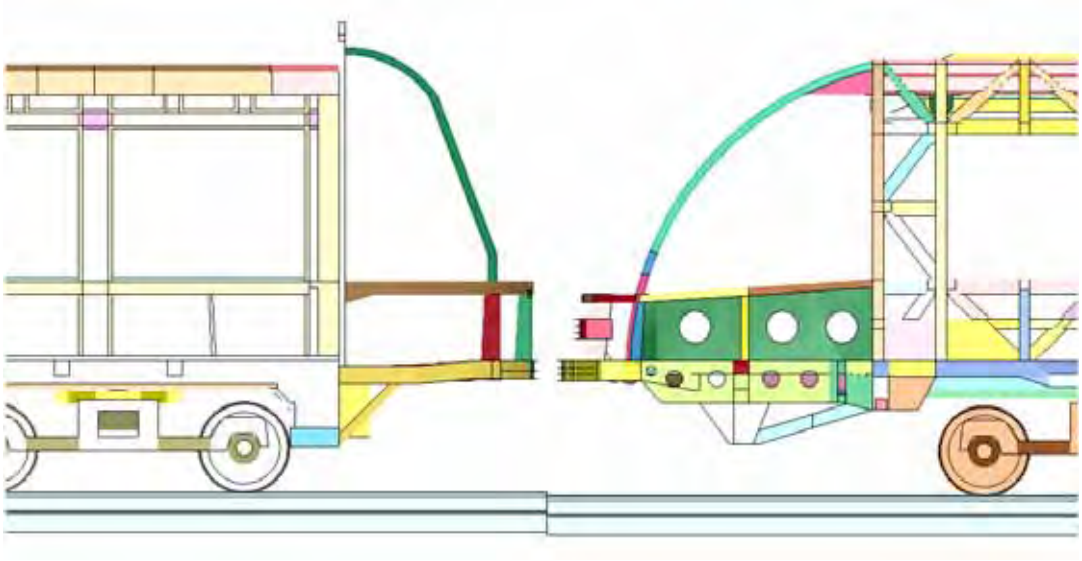

(a) Side view

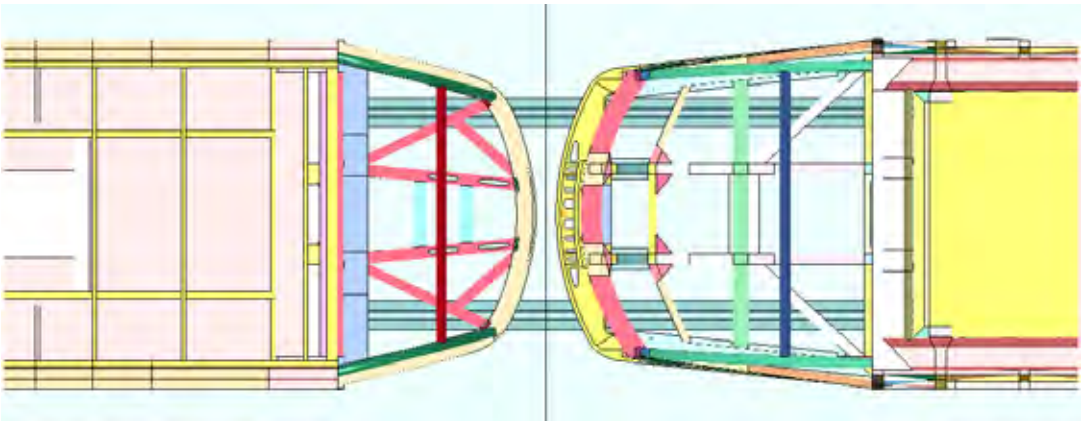

(b) Top view

Figure 104. Collision Interface for the Incompatible Crash Analyses between LRV 4 and LRV 2.

The calculated crash response between LRV 2 and LRV 4 for the 20 mph incompatible collision is shown in Figure 105. The initial stage of the response is the crushing of the energy absorbing zone in the LRV 2 head girder as seen in Figure 105(a). The subsequent response is primarily a controlled crushing of the energy absorbing zone in the nose of LRV 4 as seen in Figure 105(b).

The crush in the 20 mph incompatible collision for LRV 2 and LRV 4 are shown in Figure 106 and Figure 107, respectively. The fringes of crush are referenced to planes at the back of the cabs. The crush response of LRV 2 is primarily the collapse of the energy absorbing structures in the nose of the head girder with a crush magnitude of approximately 100 mm. The crush response of LRV 4 is a crushing of the forward underframe structures in a stable controlled collapse mode as developed for this design. There is approximately 300 mm of crush in the LRV 4 underframe, all located in the forward nose of the vehicle. The crush responses of both vehicles occur in desirable modes that were developed as part of the vehicle crashworthiness design strategies.

The calculated crash response between LRV 2 and LRV 4 for the 25 mph incompatible collision is shown in Figure 108. The initial stage of the response is the crushing of the energy absorbing zone in the LRV 2 head girder as seen in Figure 108 (a). The subsequent response is primarily a controlled crushing of the energy absorbing zone in the nose of LRV 4 as seen in Figure 108 (b).

The crush in the 25 mph incompatible collision for LRV 2 and LRV 4 are shown in Figure 109 and Figure 110, respectively. The crush response of LRV 2 is primarily the collapse of the energy absorbing structures in the nose of the head girder with a crush magnitude of approximately 200 mm. A small amount of crush is initiating in the underframe structures immediately aft of the LRV 2 head girder. The crush response of LRV 4 is a crushing of the forward underframe structures in a stable controlled collapse mode as developed for this design. There is approximately 500 mm of crush in the LRV 4 underframe, all located in the forward cab underframe. The crush responses of both vehicles occur in desirable modes that were developed as part of the vehicle crashworthiness design strategies.

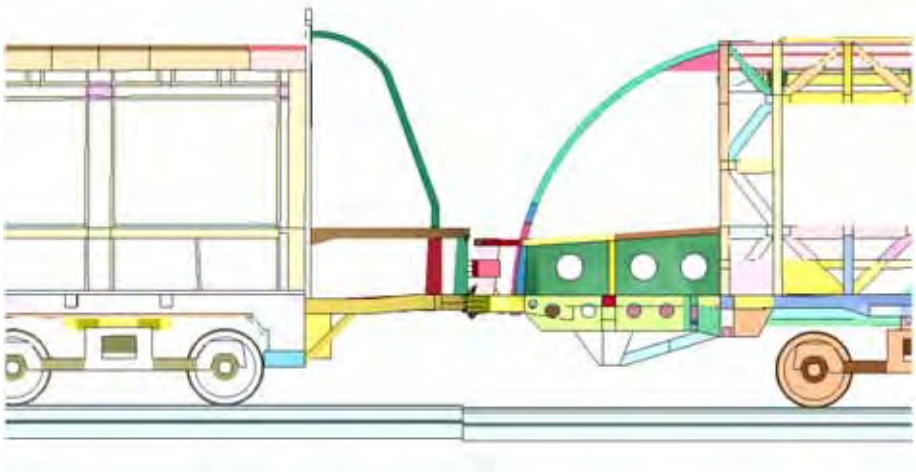

(a) time = 0.040 s

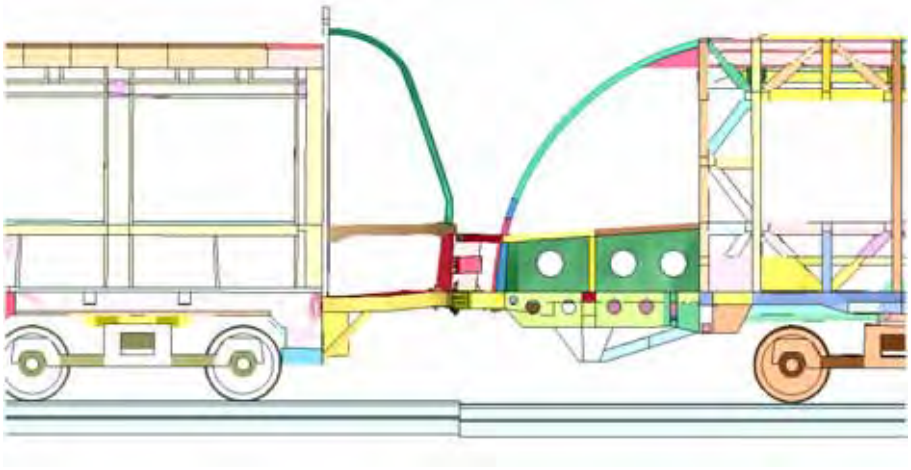

(b) time = 0.140 s

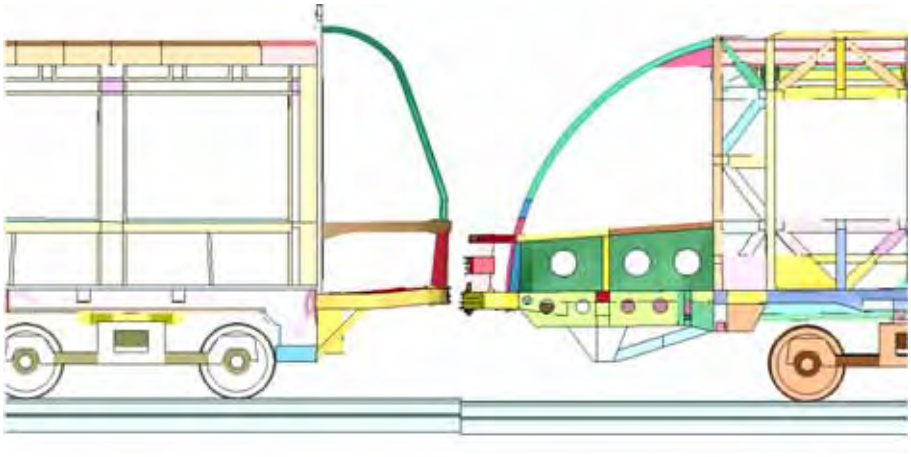

(c) time = 0.300 s

Figure 105. Simulation of the Incompatible Collision between LRV 4 and LRV 2 at 20 mph.

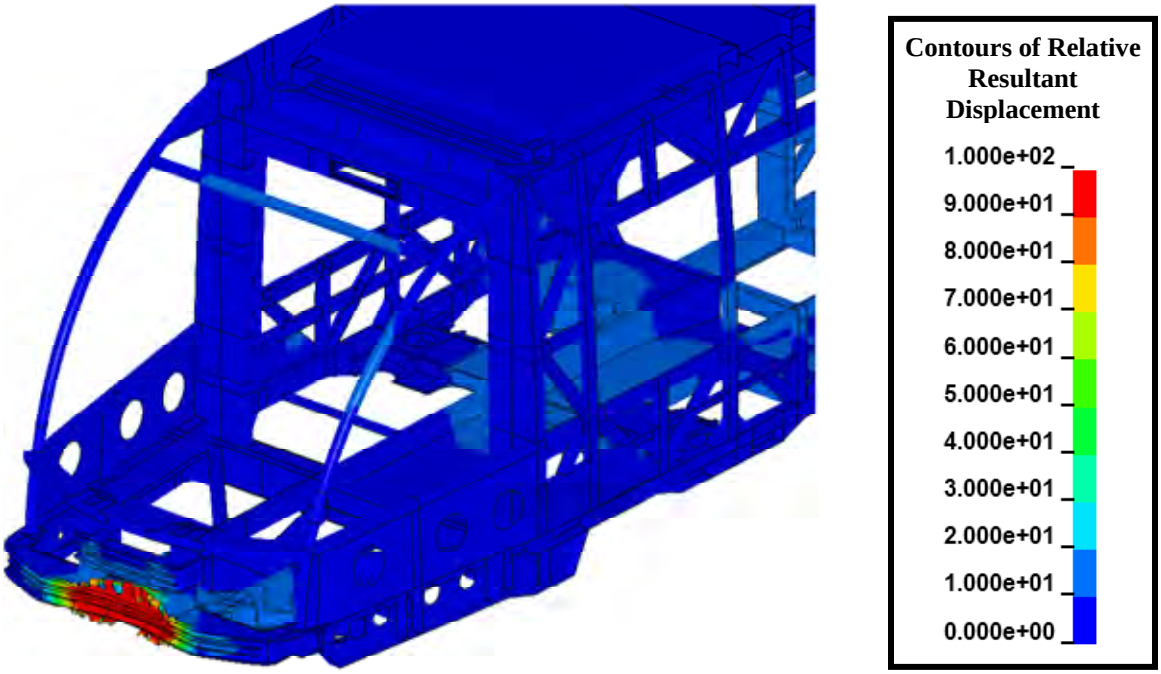

Figure 106. Crush Level (mm) for LRV 2 in the 20 mph Incompatible Collision.

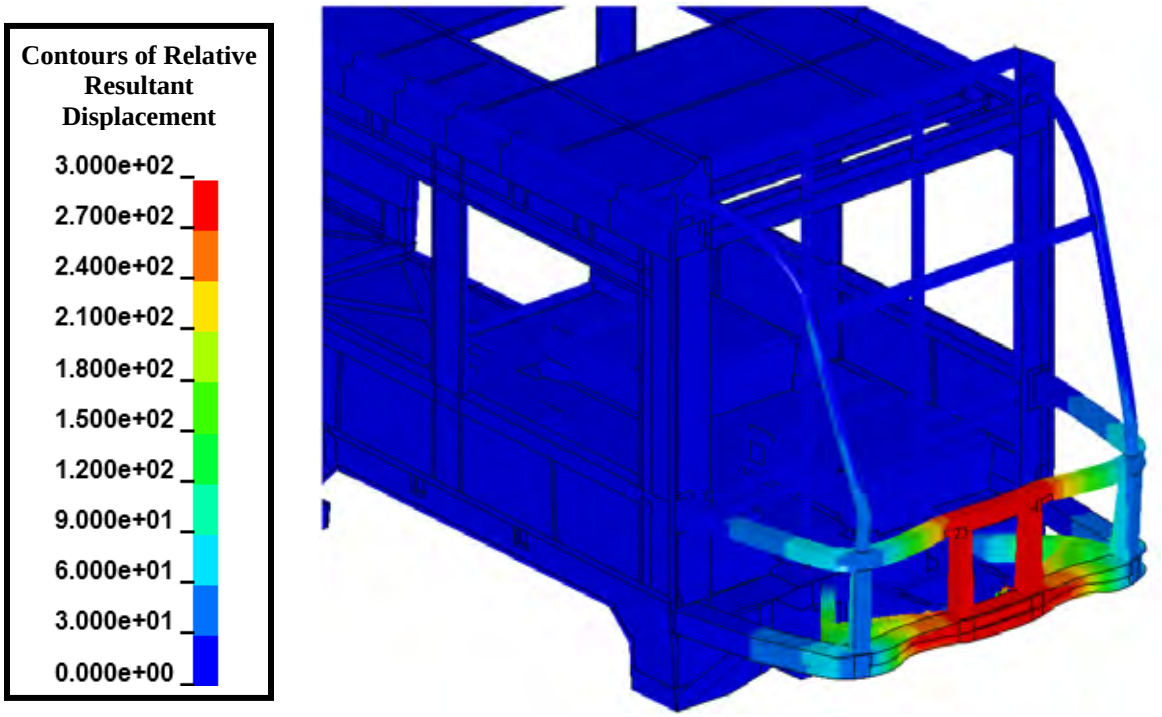

Figure 107. Crush Level (mm) for LRV 4 in the 20 mph Incompatible Collision.

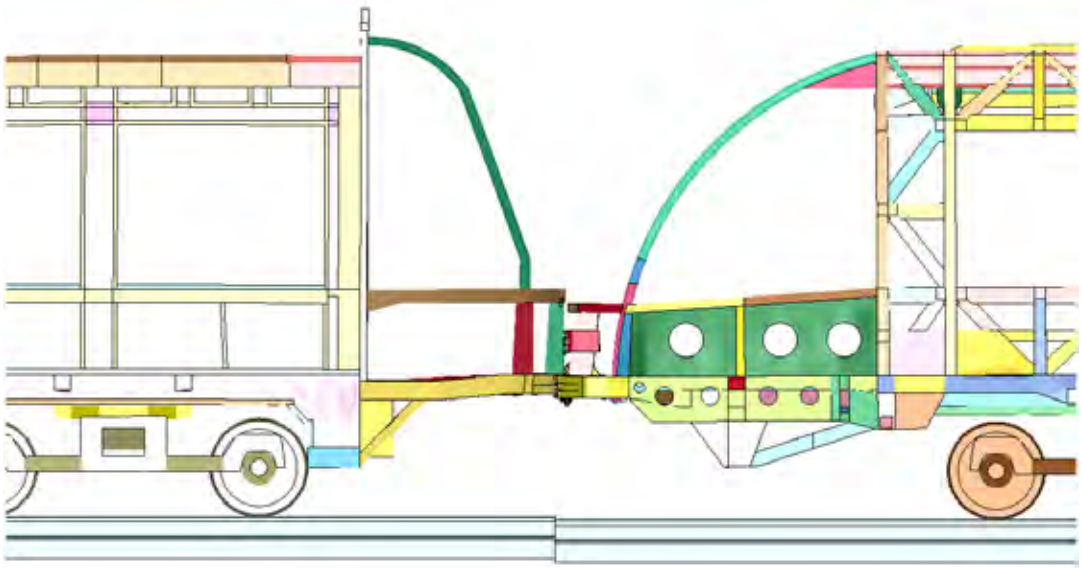

(a) time = 0.040 s

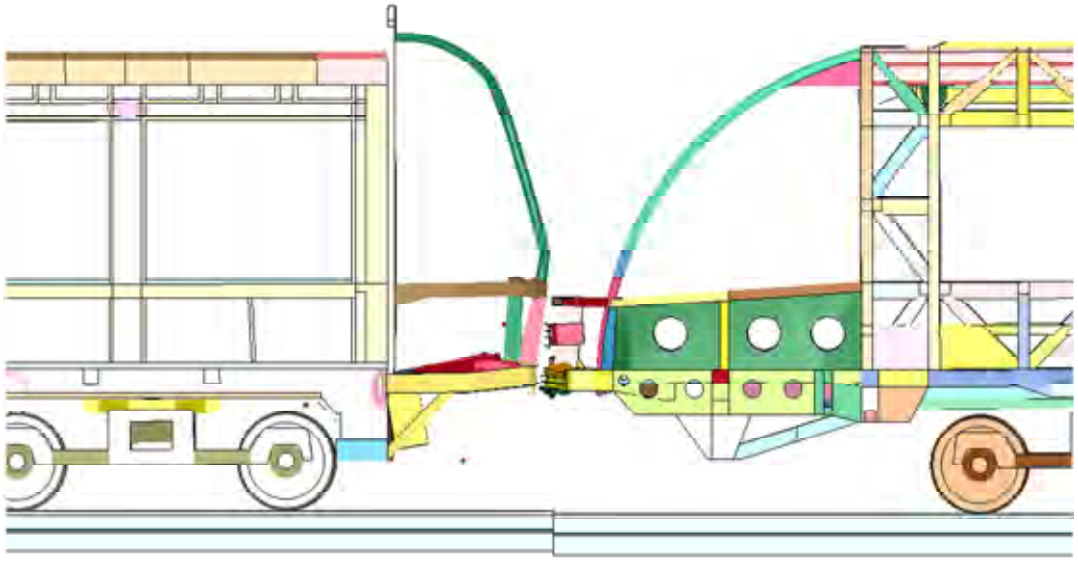

(b) time = 0.350 s

Figure 108. Simulation of the Incompatible Collision between LRV 4 and LRV 2 at 25 mph.

The calculated crash response between LRV 2 and LRV 4 for the 30 mph incompatible collision is shown in Figure 111. The initial stage of the response is the crushing of the energy absorbing zone in the LRV 2 head girder, as seen in Figure 111(a). The subsequent response is primarily a controlled crushing of the energy absorbing zone in the nose of LRV 4, as seen in Figure 111(b).

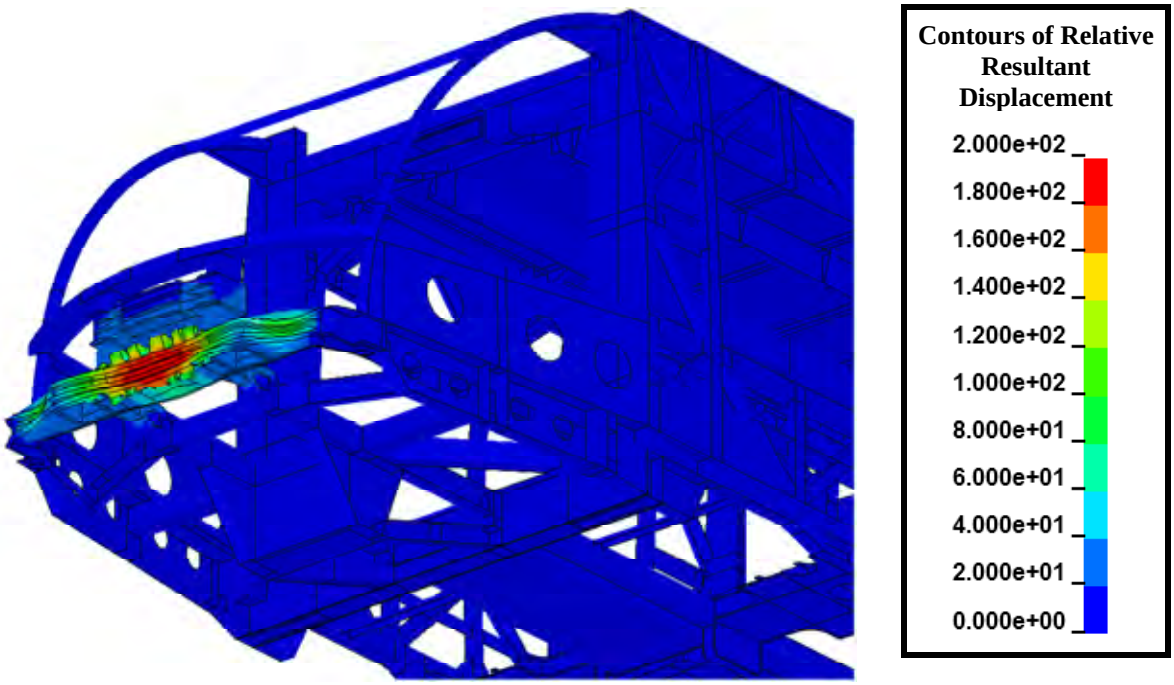

Figure 109. Crush Level (mm) for LRV 2 in the 25 mph Incompatible Collision.

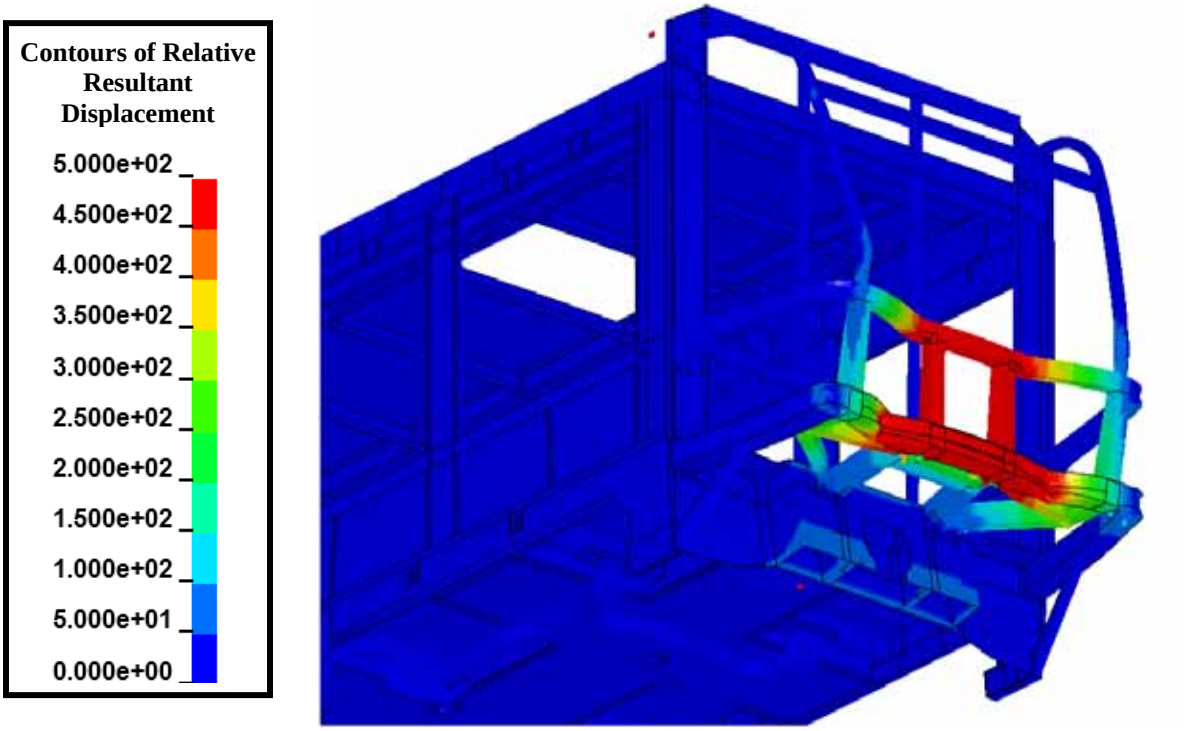

Figure 110. Crush Level (mm) for LRV 4 in the 25 mph Incompatible Collision.

The crush in the 30 mph incompatible collision for LRV 2 and LRV 4 are shown in Figure 112 and Figure 113, respectively. The crush response of LRV 2 has a peak crush magnitude of approximately 200 mm that is spit between the collapse of the energy absorbing structures in the nose of the head girder and crush of the underframe structures immediately aft of the LRV 2 head girder. The crush response of LRV 4 is a crushing of the forward underframe structures that initiates in a stable controlled collapse mode, as developed for this design. There is approximately 800 mm of crush in the LRV 4 underframe all located in the cab underframe. The large magnitude of crush at this high severity collision resulted in the failure of specific LRV 4 frame members that are deformed beyond their design capacities.

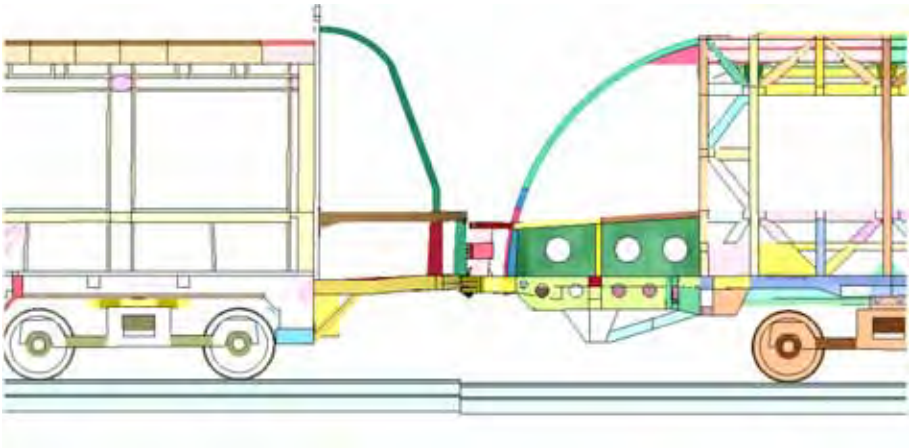

(a) time = 0.030 s

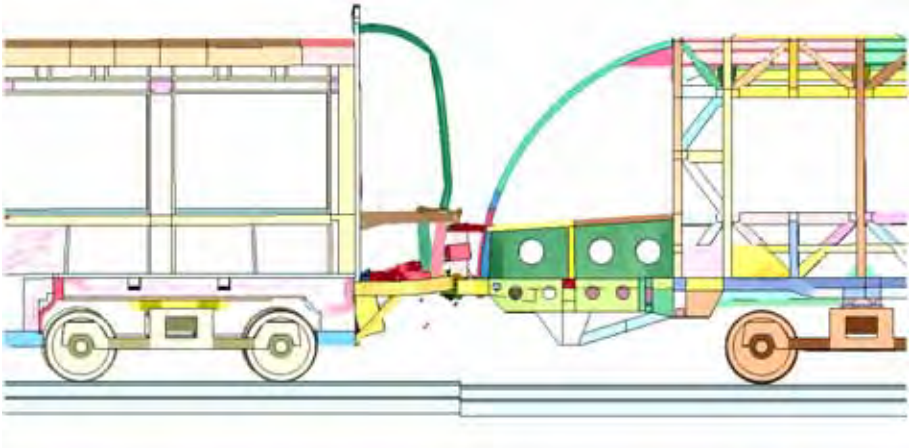

(b) time = 0.350 s

Figure 111. Simulation of the Incompatible Collision between LRV 4 and LRV 2 at 30 mph.

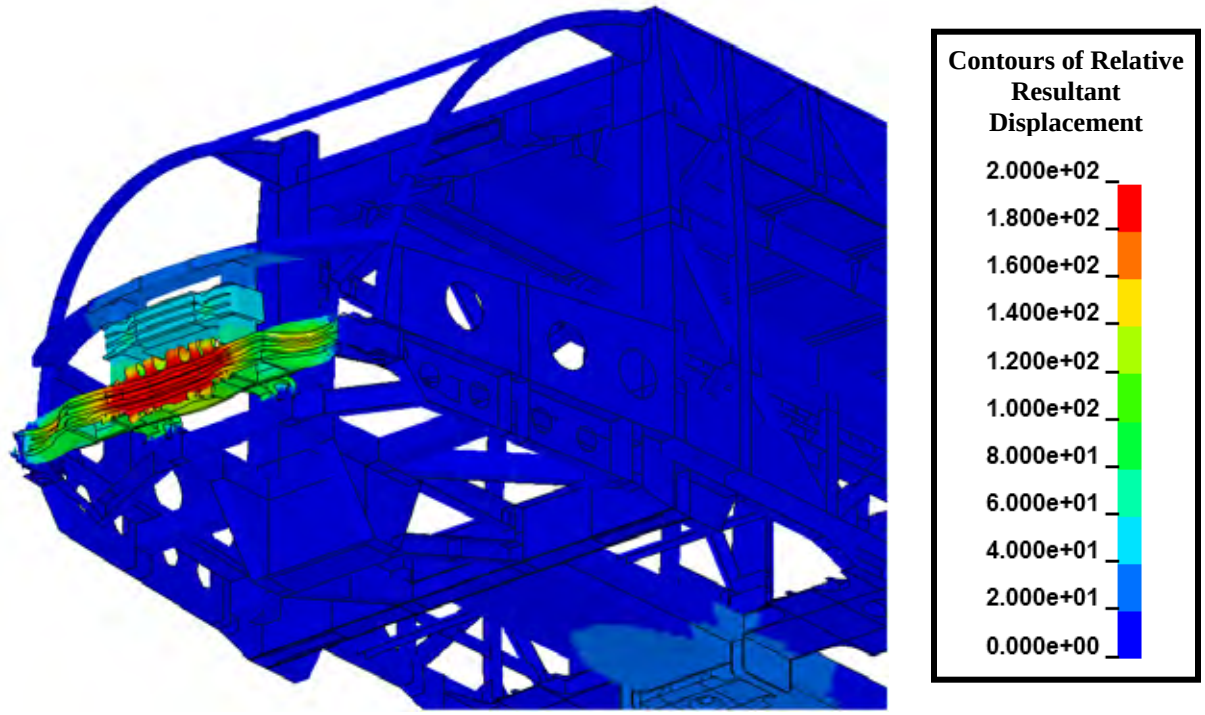

Figure 112. Crush Level (mm) for LRV 2 in the 30 mph Incompatible Collision.

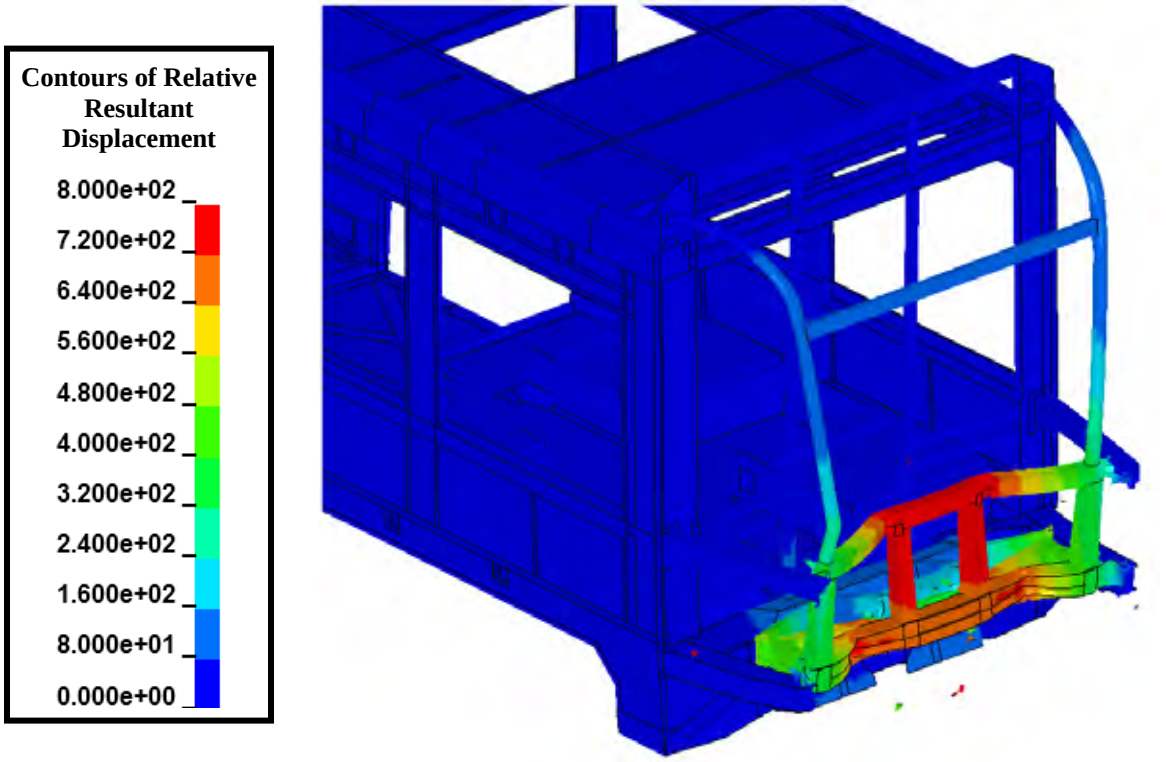

Figure 113. Crush Level (mm) for LRV 4 in the 30 mph Incompatible Collision.

2.8. Development of a 1G LRV Design

The objective of Tasks 4 and 5 in the Phase II research plan was to modify one of the LRV models, designed with a 2g buff load requirement, to be representative of an LRV with 1g buff load capacity. The original and modified models were subsequently used to evaluate the significance of the modified buff strength requirement on the crash behaviors. The results from this effort are described in this section.

Modifications to LRV designs to reduce the buff load capacity were estimated from structural considerations. Typical LRV structures in the underframe that are dominated by the buff load requirement are the center sills and supporting longitudinal underframe structures. The controlling locations are commonly at bends or connections to other members where local stress concentrations exist and the members are subjected to localized bending moments. Due to bending, the peak stresses are at the outer or inner surfaces of the structural sections and typically scale inversely to the square of the thickness of these members. Thus, reducing these members to 70% of their original thickness would reduce the static proof load capacity of the critical members to 50% of their original design levels.

This approach was first applied to LRV 2 to reduce the thicknesses of the primary longitudinal members in the cab structure. For this first effort, no changes were made to the vehicle structures aft of the cab. The corresponding crush behaviors of the original and modified LRV 2 model in a 20 mph collision are shown in Figure 114. The comparison shows an overall similar gross crush strength profile with a reduction in the average crush strength of between 15% and 20%. These differences are considerably smaller than the differences observed in different vehicle designs as described in Section 2.2.

The design changes to LRV 2 were made and evaluated in collaboration with the vehicle designer. In addition to the crash analyses described above, static analyses were performed to confirm the relative stress magnitudes in the modified structural elements designed to meet the different static proof load levels. When the evaluation was performed on the modified LRV 2 it was found that the reduced section thicknesses were still able to withstand all of the original static proof loads, including the 2g buff load requirement. Investigation into this result indicated that all of the critical structures in the cab were sized to obtain a desirable behavior in the two different collision scenarios that were evaluated in the development of the design. As a result, the buff load requirement was a trivial load case in terms of controlling the structural design of this vehicle. The structural design controlled primarily by the two collision scenarios resulted in a vehicle with a buff strength significantly greater than 2g.

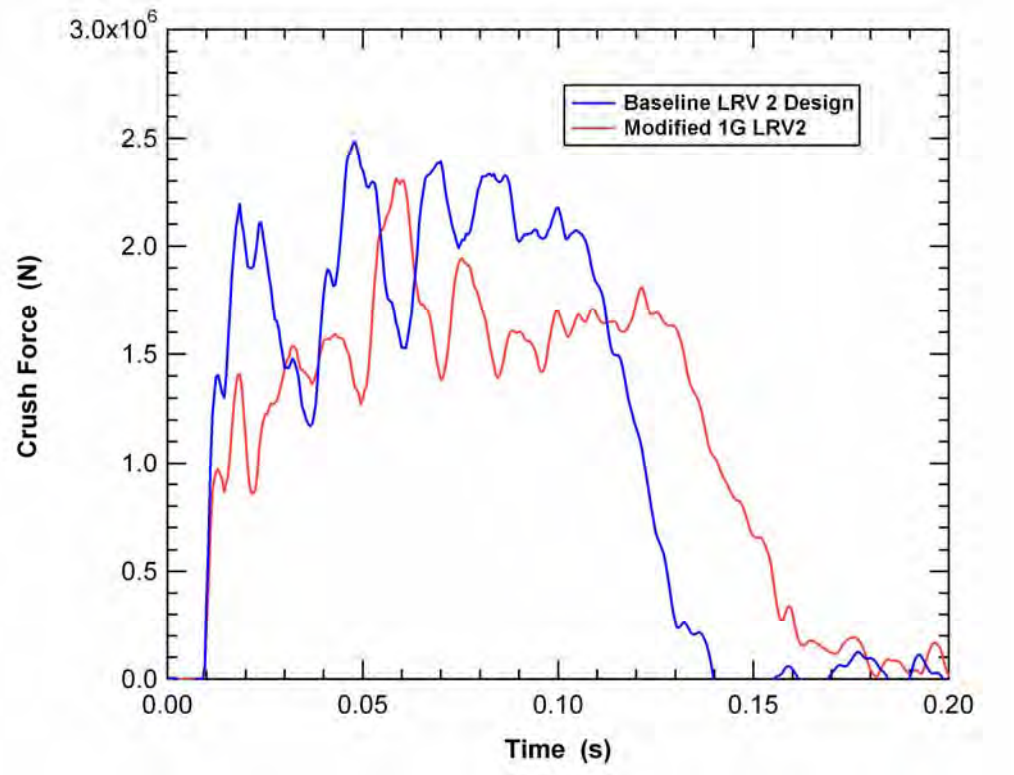

Figure 114. Comparison of the Original and Modified Crush Strengths for LRV 2.

The conclusions from this preliminary LRV 2 redesign effort were:

1) The change in buff strength requirement will result in a significantly smaller change in the vehicle crush strength. In this example, an approximately 50% reduction in the cab structure buff load capacity resulted in a 15-20% reduction in the crush strength.
2) The design of this specific LVR was not controlled by the buff load requirement. As a result, it is not an ideal LRV design for use in this effort to reduce a 2g design to a 1g design.
3) When the reduced buff load requirement is applied only to the design of the cab, a relatively small amount of weight savings will be achieved. In this example, the total weight reduction in the cab was approximately 150 kg (total savings of 300 kg with a cab at each end of the LRV). This corresponds to significantly less than a one percent weight reduction for the LRV.

Subsequently, the approach was applied to LRV 1 to reduce the thicknesses of the primary structural members throughout the vehicle. The entire car body was modified to investigate the possible reductions in weight with the lowered buff load requirement. Using the modified car design, the static proof load cases were evaluated. All of the load cases were maintained at the original design levels with the exception of the buff load requirement which was reduced to 1g. The static analyses determined that the modified design was

acceptable. The total weight savings for the LRV was approximately 2800 kg or a 6% reduction of the total mass.

Following the static assessment of the modified car body structure, the vehicle was analyzed for the 20 mph compatible LRV collision scenario (the collision scenario that was the original CEM requirement in the design specification). The modified LRV 1 design with a 1g buff strength performed very poorly in the collision scenario. Six subsequent design iterations were performed where various structural components in the modified car body were reinforced, many approaching or equal to their original dimensions. A satisfactory behavior was not obtained with sufficient design variations from the original dimensions in the 2g design.

The primary conclusion that was obtained from the redesign effort is that the buff strength requirement is much less important for the crash behaviors than the CEM requirements in the design. In LRV 2, all of the primary longitudinal members in the cab were sized to meet the crash performance of the collision scenarios and the vehicle had significantly greater strength than required by the 2g buff load requirement. In addition, the analyses demonstrated that a 50% reduction in the buff strength results in approximately a 20% reduction in crush strength if the buff strength dominated the design. This variation is much less than the variation in strength seen in various 2g LRV designs.

In LRV 1, the strength required to meet the collision scenario was closer to that of the 2g buff load requirement in some of the primary structural members. However, a 20 mph compatible collision requirement was a much more stringent constraint on the design than the buff load specification. As a result, relaxing the buff load requirement without a corresponding reduction in the CEM requirement did not allow for significant design changes.

2.9. Analysis of Collisions with Highway Vehicles

Another very important aspect of crash safety for LRVs is collisions with highway vehicles. The transit crash statistics show that the vast majority of injuries and fatalities result from collisions between an LRV and automobiles [2-5]. A significant portion of the fatalities and serious injuries attributed to transit operation is to the occupants of the highway vehicles. Incorporating features that can enhance the crash safety in these collision scenarios can result in large overall improvements to transit system safety.

The concern over aggressivity of LRVs, trams, and streetcars colliding with highway vehicles is not new [15]. Many older streetcar designs included bumpers or other devices to protect pedestrians and automobiles in collisions [16]. Similarly, bumpers and crash compatibility features are being incorporated in modern US LRV designs. The Houston METRO vehicle has a retractable coupler and fully enclosed front end. The Phoenix LRV design is fully enclosed with an energy absorbing bumper with 100-150 mm of stroke before the anticlimber elements engage [17].

Primary modifications that can be made to improve compatibility in collisions with automobiles are to eliminate features in the LRV front end geometry that make it aggressive. These measures include (1) adopting retractable or fold-away couplers at the ends of the LRV, (2) enclosing the front end of the vehicle and having a sufficiently low nose to prevent override of cars, and (3) including energy absorbing elements in the front-end designs of LRVs.

A collision where the LRV overrides an automobile, as seen in Figure 115, can produce negative consequences compared to a similar severity collision where the automobile is deflected [18]. First, the override behavior results in significantly greater crush intrusions into the automobile and a higher potential for severe injuries to the automobile occupants. Second, the override collision has the potential to produce much more extensive damage to the LRV and greatly increase the repair costs and time before the vehicle is placed back in service. Finally, the override collision has a much higher potential to derail the LRV or create higher crash decelerations that can result in higher injury potential to the LRV occupants.

Figure 115. Example Collisions between LRVs and Automobiles.

Simulations of collisions between automobiles and LRVs were used in this effort to quantify the potential safety improvements that can be obtained by adding appropriate crash safety features to the LRV. The base LRV model used for the collision analyses was LRV 2. The strength of LRVs are sufficiently large compared to highway vehicles that there is no significant damage to the LRV. Therefore, we expect little difference in the results if one of the other LRV models was substituted as the bullet LRV. One possible exception is LRV 3, which has a cab with more square profile. This profile could potentially have caused more damage to the highway vehicles in the oblique impact scenarios.

Two different highway vehicles were used in the collision analyses. Highway vehicle 1 (HV 1) is the Dodge Neon, as shown in Figure 116. The Dodge Neon was selected to be representative of a small passenger vehicle which would potentially have a higher risk in a collision with an LRV as a result of the greater height and weight differences. Highway vehicle 2 (HV 2) is the Ford Explorer, as shown in Figure 117. The Ford Explorer was selected to be representative of the light truck and sport utility vehicle (SUV) class of passenger vehicles which are very common in the highway vehicle fleet. The SUV could potentially have a lower risk in a collision with an LRV as a result of the greater height and weight than the Dodge Neon.

The collisions were performed at a range of speeds between 10 mph and 30 mph. Two different impact orientations were used. The first is a normal (90 degree) impact of the LRV into the side of the highway vehicle passenger compartment, as seen in Figure 118. The second is an oblique impact of the corner of the LRV into the highway vehicles at a 45 degree angle relative to the LRV axis, as shown in Figure 119.

A side view of the impact interface between HV 1 and LRV 2 with no modifications to the front end geometry is shown in Figure 120. The impact geometry clearly illustrates the potential geometric incompatibility of the two vehicles that would be expected to introduce a significant injury risk to the occupants of the highway vehicle. The impact point of the head girder is close to the bottom of the side window. Such an impact would result in large intrusions close to the upper thorax of an occupant, leading to a high potential of a head impact against the LRV front end structures.

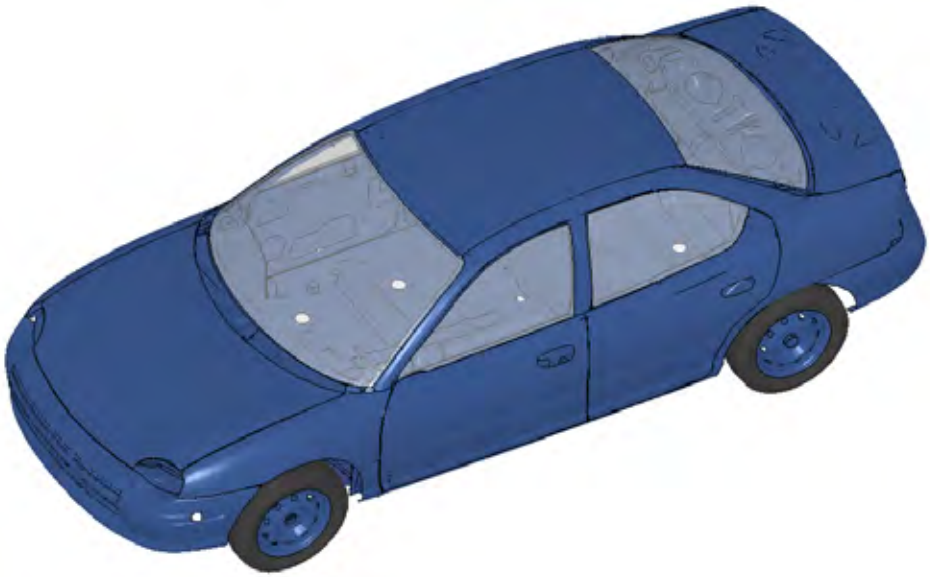

Figure 116. Finite Element Model for Highway Vehicle 1.

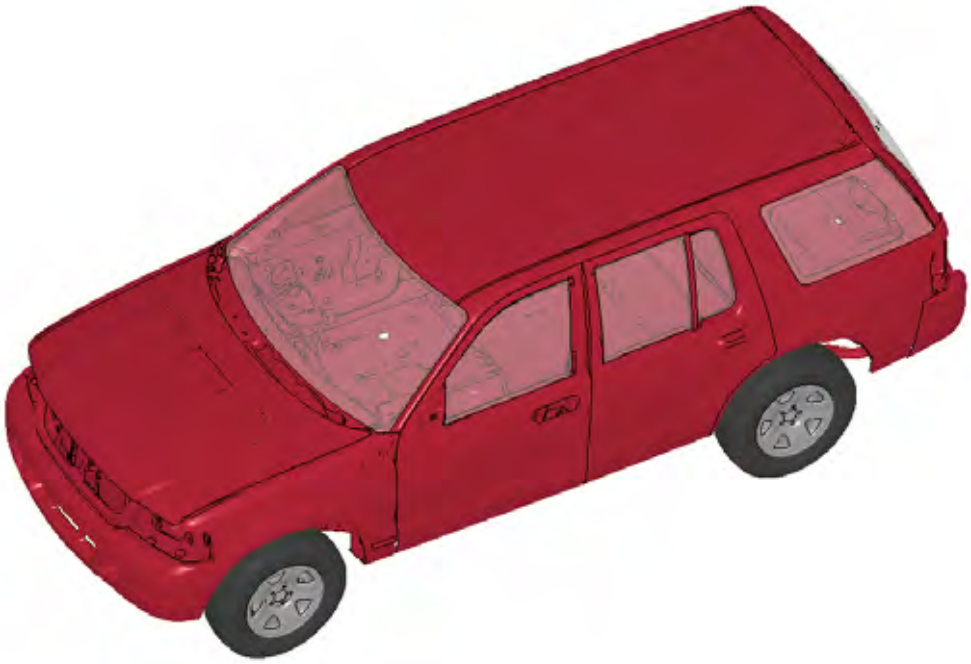

Figure 117. Finite Element Model for Highway Vehicle 2.

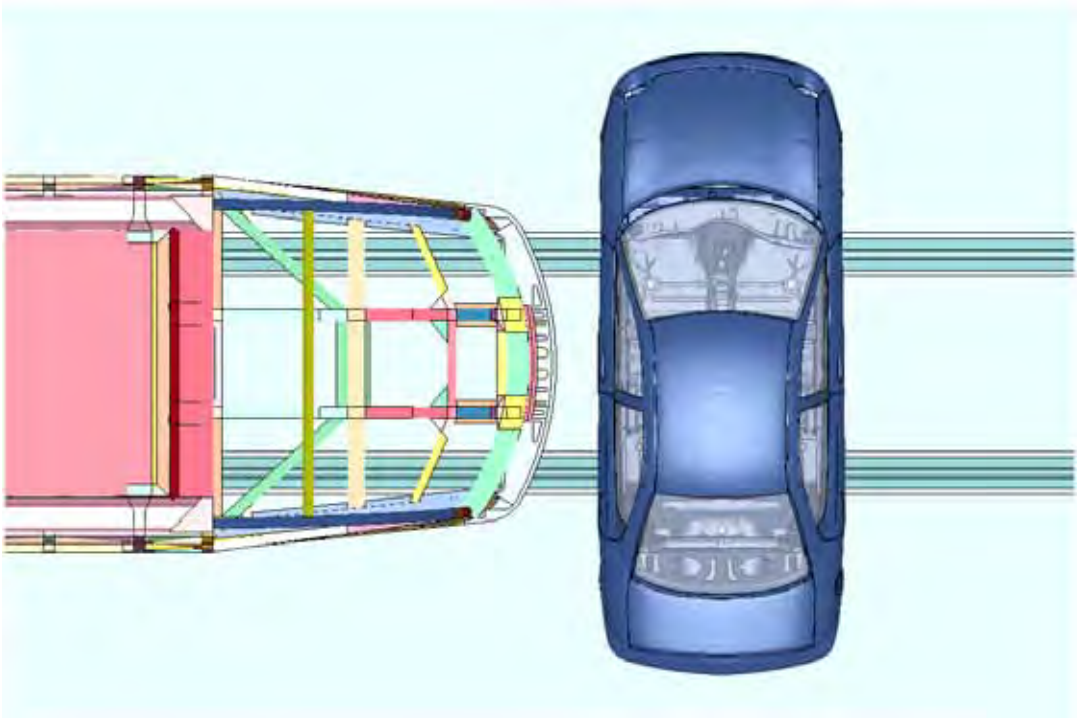

Figure 118. 90 degree Collision Interface for LRV 2 and Highway Vehicle 1.

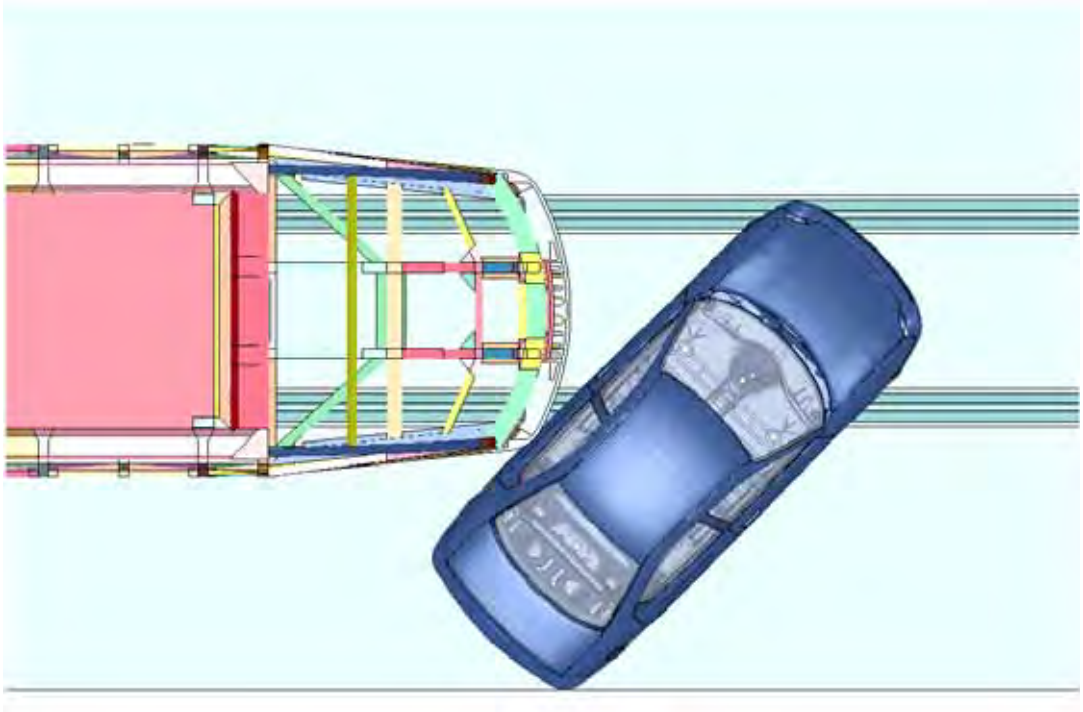

Figure 119. 45 degree Collision Interface for LRV 2 and Highway Vehicle 1.

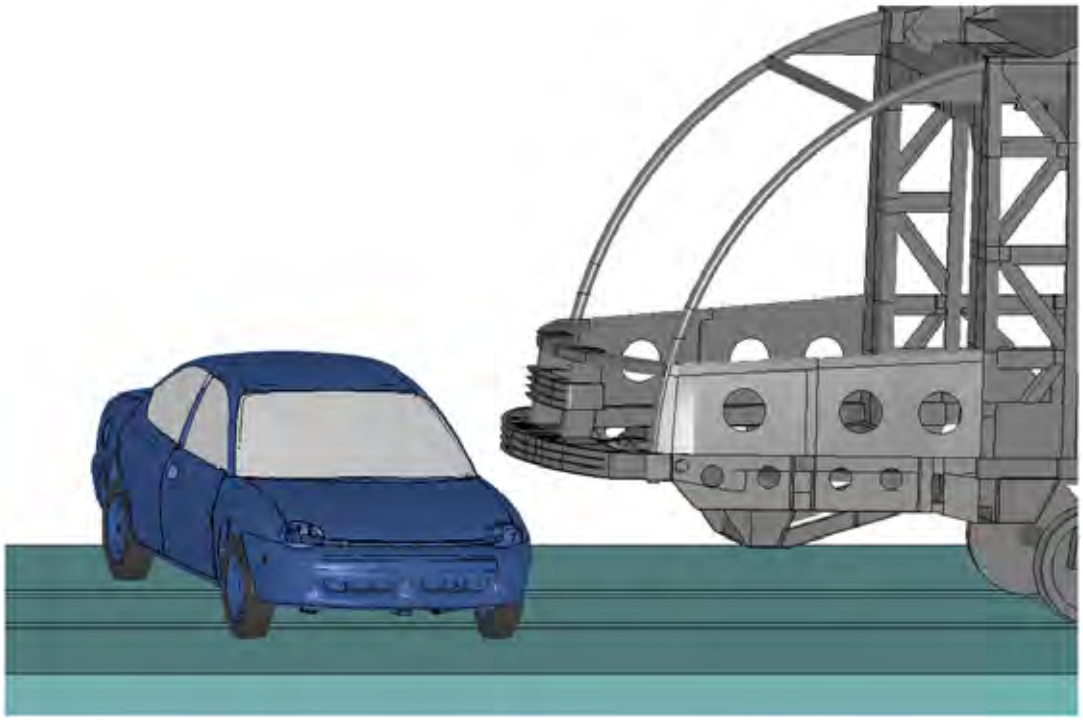

Figure 120. Collision Interface without LRV Front End Safety Features.

One common modification to LRVs to protect highway vehicles in a collision is a bumper or similar enclosure on the front of the LRV [16]. The collision interface of the LRV fitted with a bumper enclosure and HV 1 is shown in Figure 121. The bumper enclosure extends in height from approximately 300 mm to slightly over a meter above top of rail. The addition of the bumper enclosure results in a significant improvement of the geometric compatibility. The enclosure applies the collision loads more evenly and lower on the automobile structure where the collision energy can be more efficiently dissipated.

The calculated 20 mph crash behavior of the LRV without any front end safety features into the side of HV 1 (90 degree) is shown in Figure 122 and Figure 123 for the side and top views, respectively. The head girder overrides much of the HV 1 side protective structures and intrudes significantly into the occupant volume. The high location of the impact also rotates the struck HV 1 lifting the wheels on the impact side off the ground.

The calculated 20 mph crash behavior of the LRV with a bumper enclosure into the side of HV 1 (90 degree) is shown in Figure 124 and Figure 125 for the side and top views, respectively. The bumper engages much of the HV 1 side protective structures and the crash response is significantly modified. The lower impact forces, as seen in Figure 124, pushes HV 1 laterally in the direction of the LRV movement. The motion is primarily a translation without the large roll of HV 1 seen when impacted without the bumper. Similarly, from the comparison of the top views of the collision behaviors, seen in Figure 123 and Figure 125, the bumper significantly reduces the crush intrusions of the LRV into HV 1.

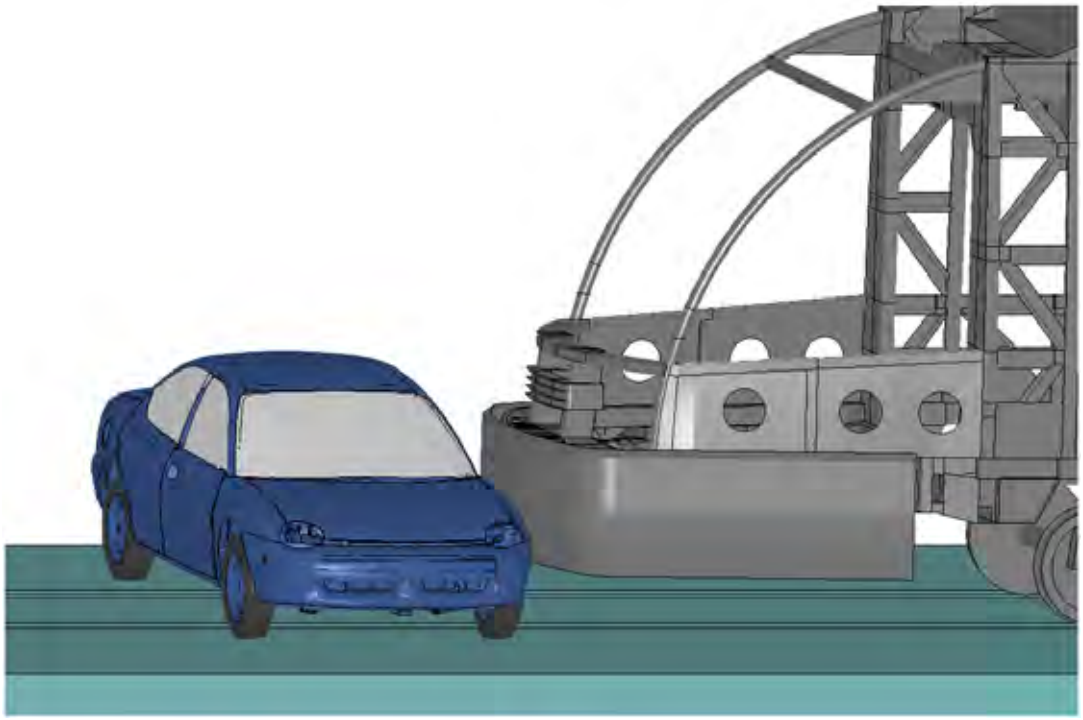

Figure 121. Geometric Compatibility with Bumper

The corresponding crush intrusions in the Dodge Neon for the 20 mph collisions without and with the bumper enclosure are shown in Figure 126. The differences in the crush intrusions are significant. The maximum crush without the bumper enclosure was approximately 670 mm and located relatively high on the occupant compartment of the car. With the bumper enclosure, the maximum crush in the occupant compartment was reduced to approximately 450 mm and is more uniform over the center portion of the door.

The level of automobile injury potential resulting from inclusion of the bumper enclosure can be estimated from research on side impact safety of automobiles provided by the National Automotive Sampling System (NASS), which reports statistics of injury. We use this data to estimate the effect of broadening the load distribution across the automobile and directing the principal contact point lower on the automobile structure. Data from NASS correlates injury probability to the physical intrusion into the vehicle, as shown in Figure 127 [6]. As a result of adding bumpers, the probability of a fatal injury is reduced from approximately 75% without the bumper enclosure down to approximately 35% with the enclosure. Similarly the probabilities of serious injuries are reduced from above 90% to approximately 70%.

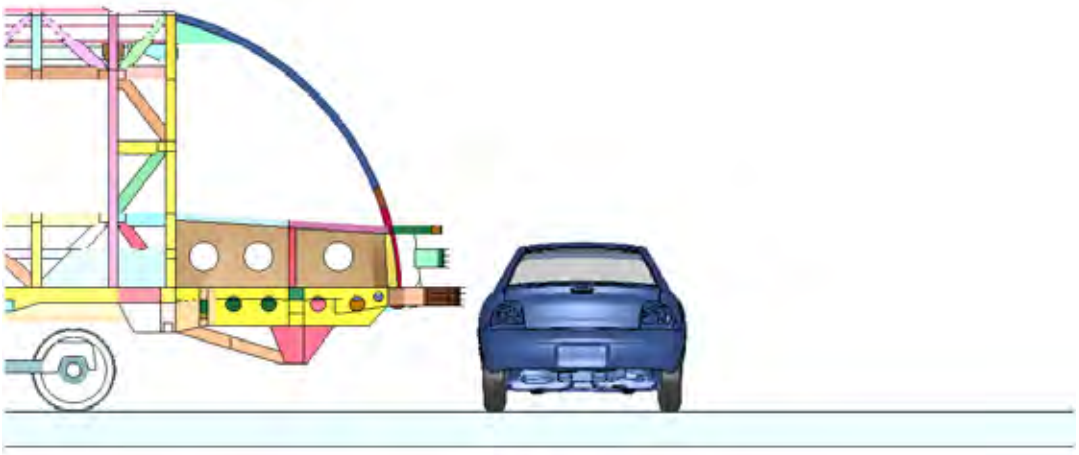

(a) Time = 0.00 s

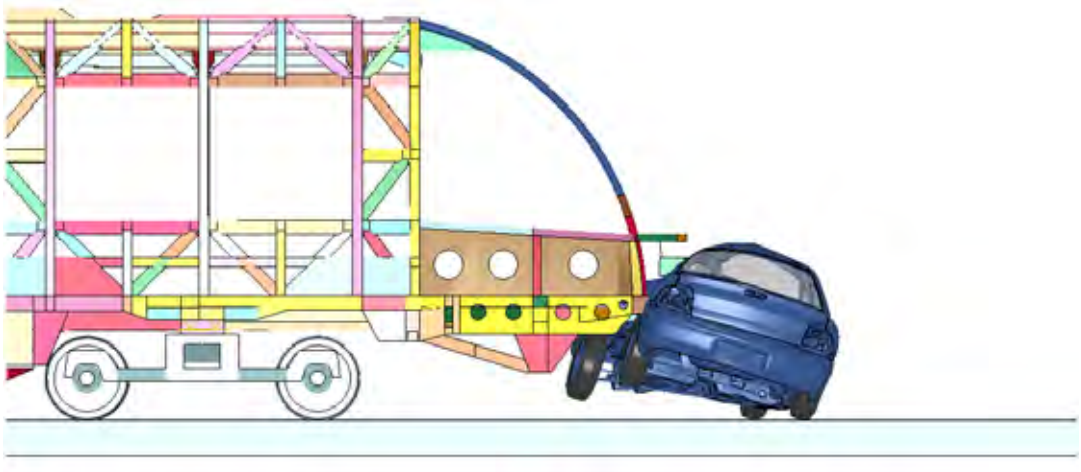

(b) Time = 0.25 s

Figure 122. Simulation of the 90 degree, 20 mph Collision with HV 1 (Side View – LRV without a Bumper).

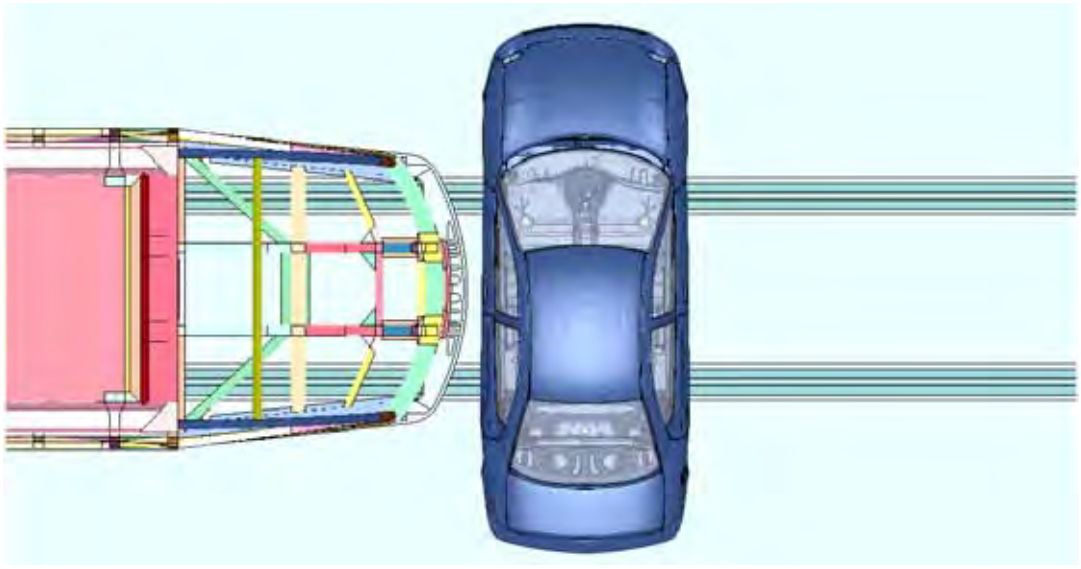

(a) Time = 0.00 s

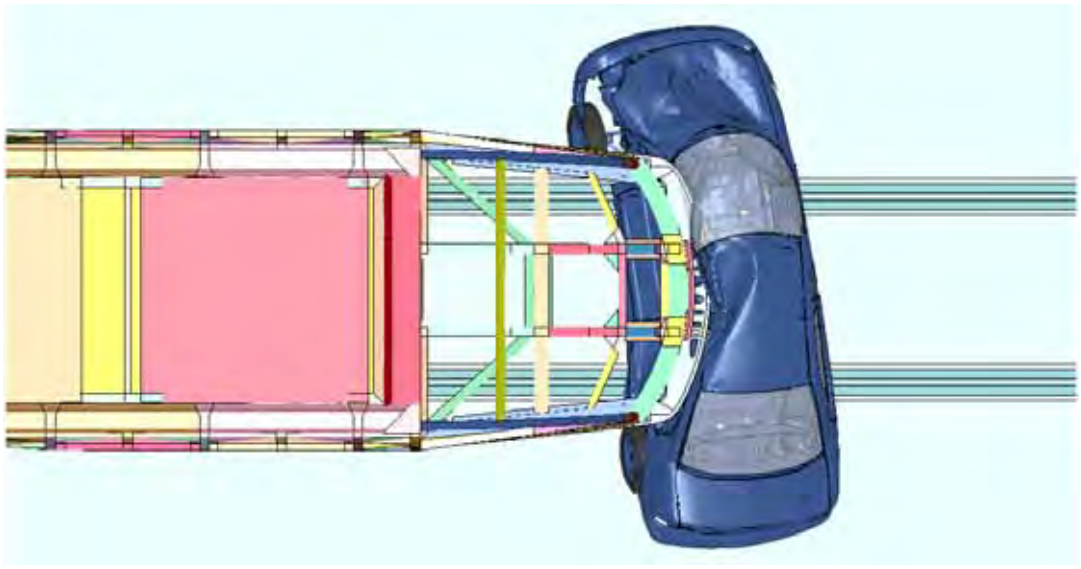

(b) Time = 0.25 s

Figure 123. Simulation of the 90 degree, 20 mph Collision with HV 1 (Top View – LRV without a Bumper).

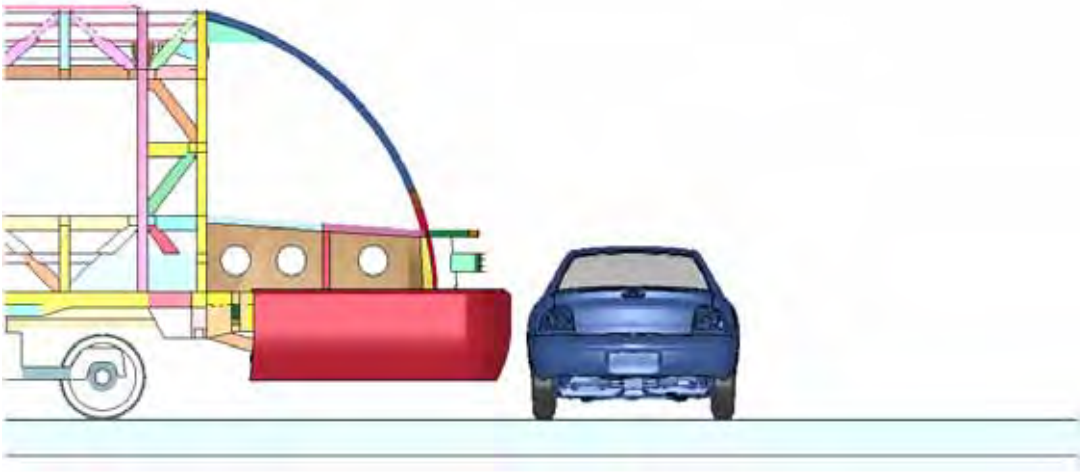

(a) Time = 0.00 s

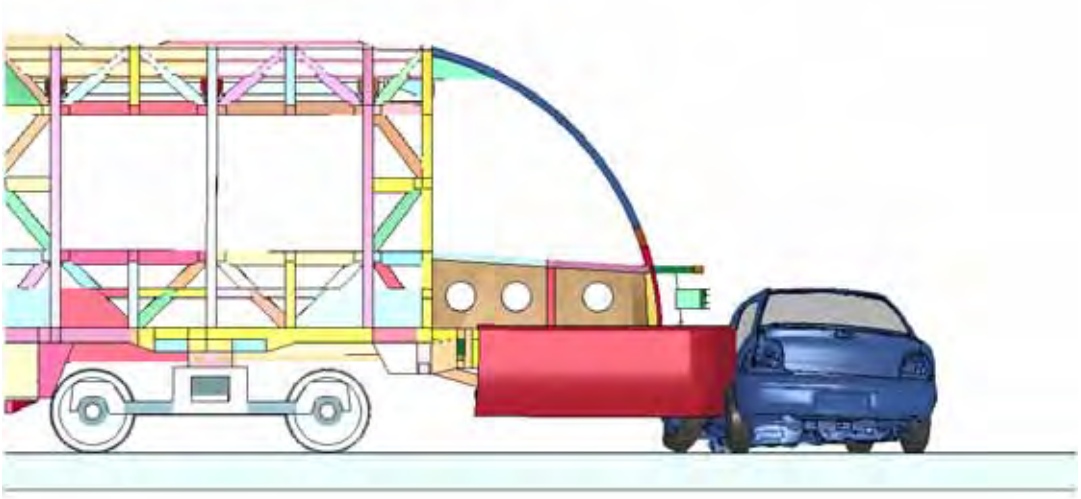

(b) Time = 0.22 s

Figure 124. Simulation of the 90 degree, 20 mph Collision with HV 1 (Side View – LRV Fitted with a Bumper).

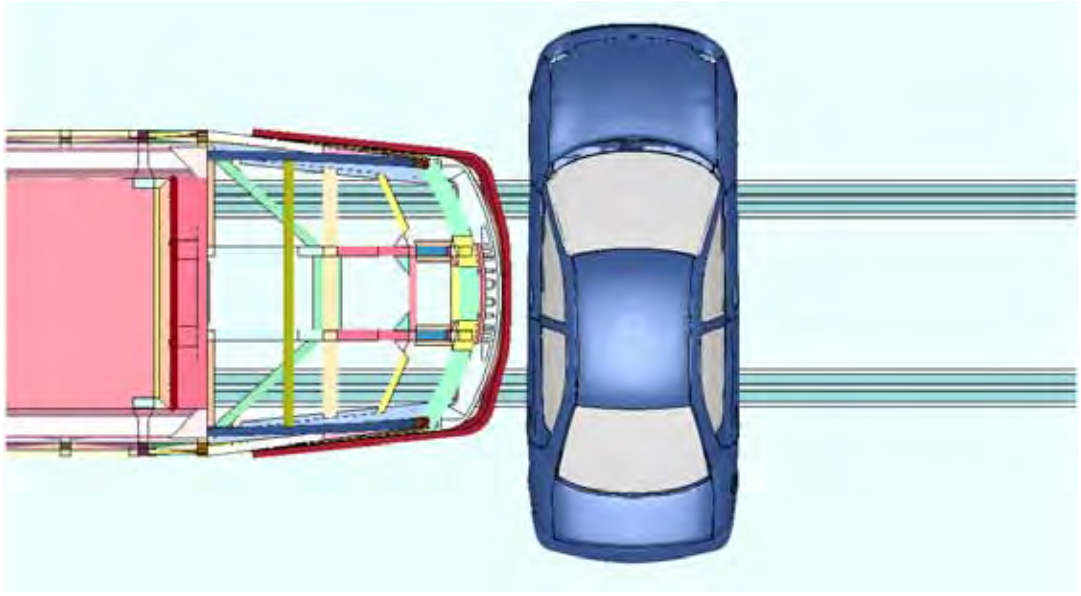

(a) Time = 0.00 s

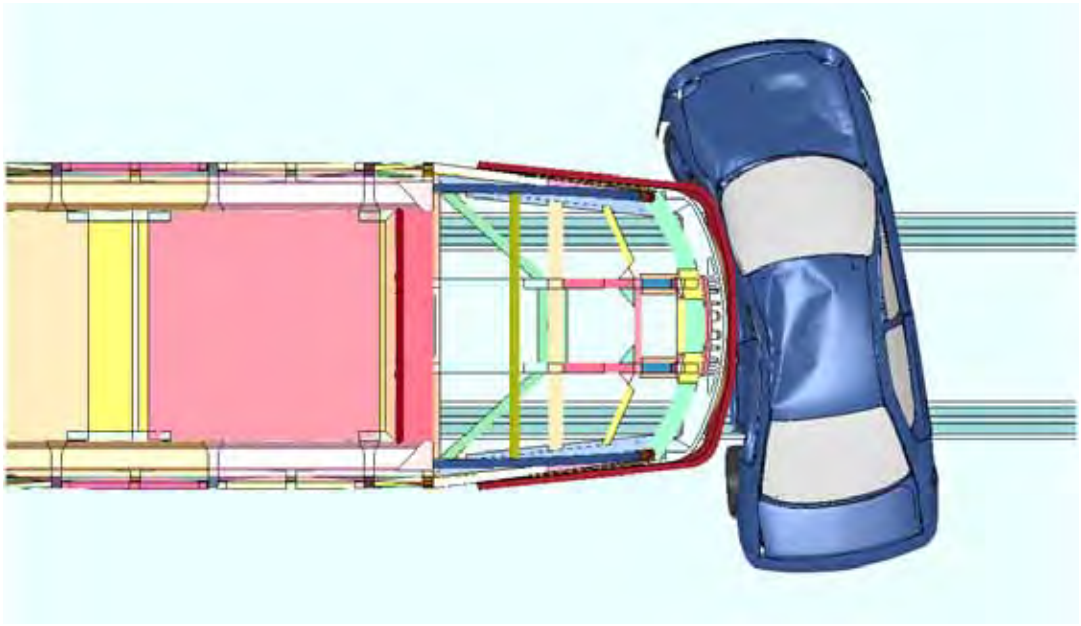

(b) Time = 0.22 s

Figure 125. Simulation of the 90 degree, 20 mph Collision with HV 1 (Top View – LRV Fitted with a Bumper).

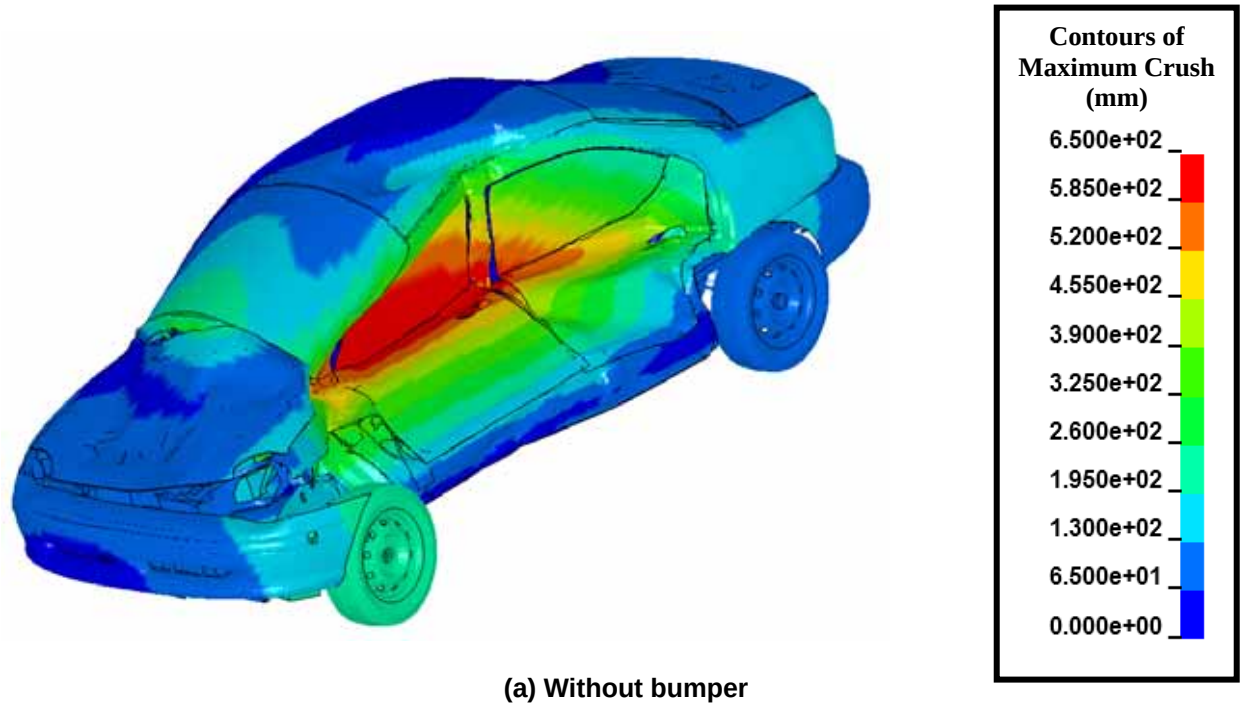

(a) Without bumper

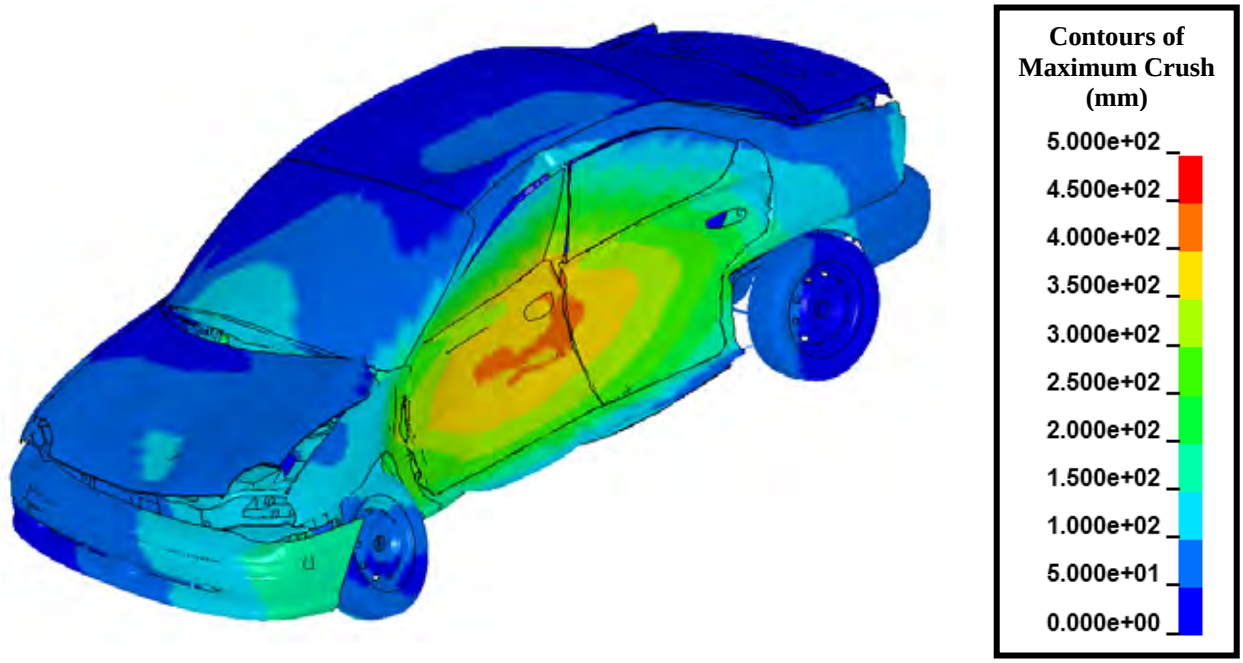

(b) With bumper

Figure 126. Calculated Crush for HV 1 in the 90 degree, 20 mph Collisions.

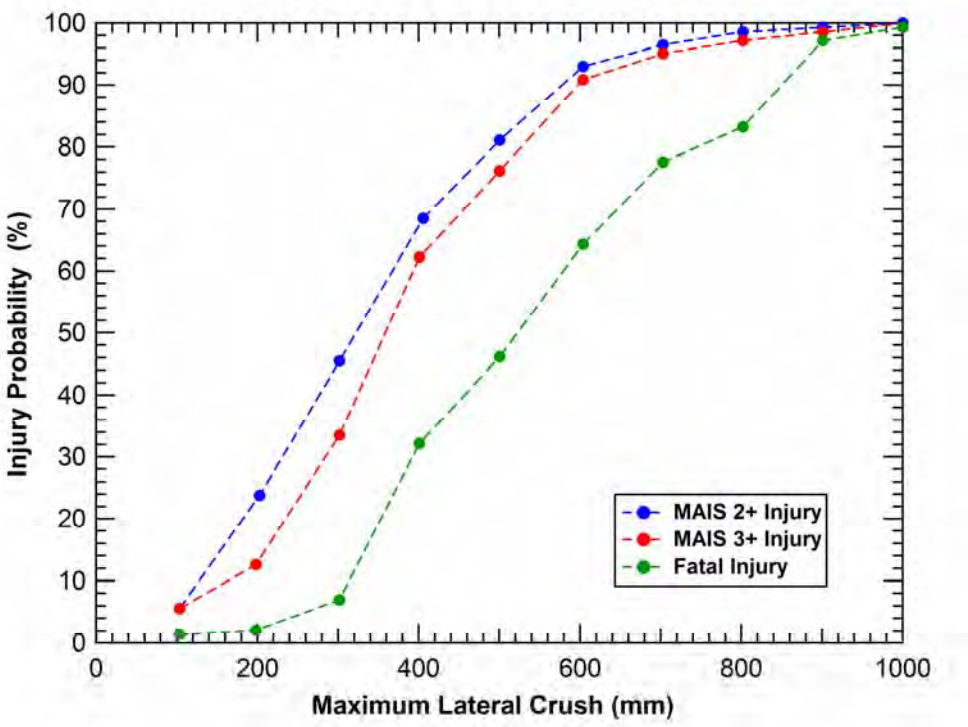

Figure 127. Injury Probability as a Function of Maximum Lateral Crush.

For some transit systems, a fully enclosed front end may be difficult to accomplish given the operating requirements. To address this issue an additional simulation was performed where a thin pilot beam was added to the LRV instead of the bumper system. The collision interface for the LRV fitted with the pilot beam is shown in Figure 128. The center height of the pilot beam is approximately 480 mm above top of rail. The primary pilot beam structure is constructed with a steel box section tube approximately 80 mm in height and width. This is a narrow profile for a pilot beam and would not be expected to provide an optimum level of protection compared to a pilot beam that has a greater height and extending lower toward the top of the rail.

The corresponding crush in the Dodge Neon for the 20 mph collisions with the pilot beam is shown in Figure 129. The maximum crush with the pilot beam was approximately 490 mm and located close to the bottom of the doors. By comparison to the maximum crush without a bumper (670 mm) and the crush with a bumper (450 mm) the pilot beam is approximately 20% less effective than the bumper at reducing the maximum intrusion into the occupant compartment for this scenario. This would suggest that with some minor design modifications, the pilot beam concept could be nearly as effective at reducing injury potential as the bumper enclosure.

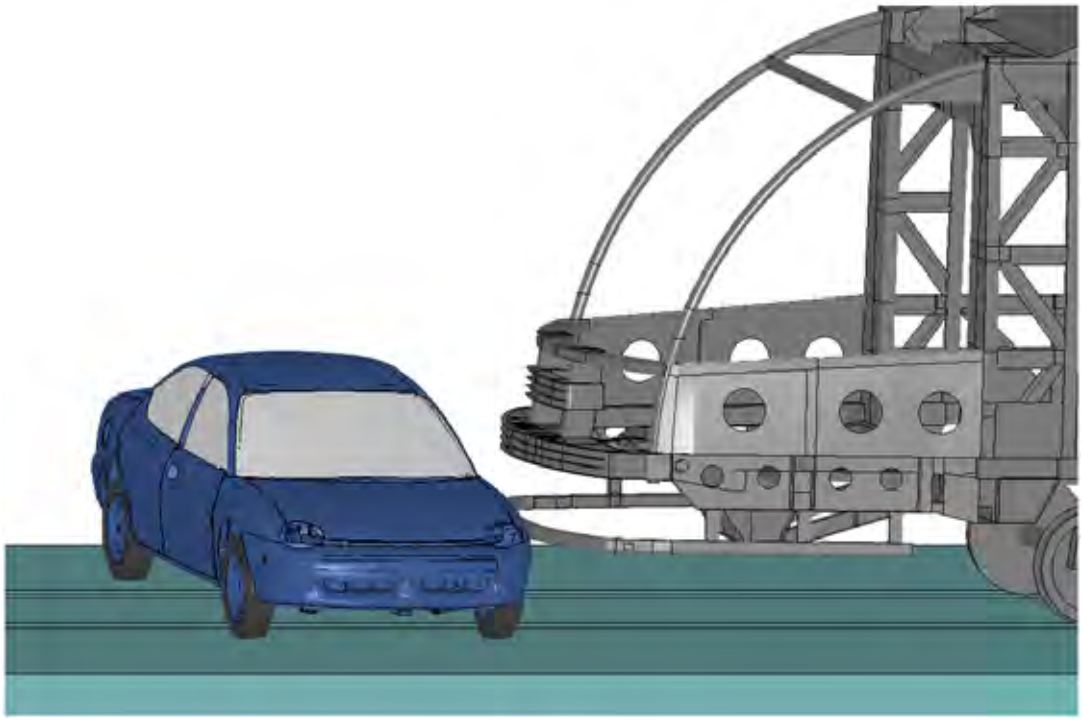

Figure 128. Geometric Compatibility with Thin Pilot Beam.

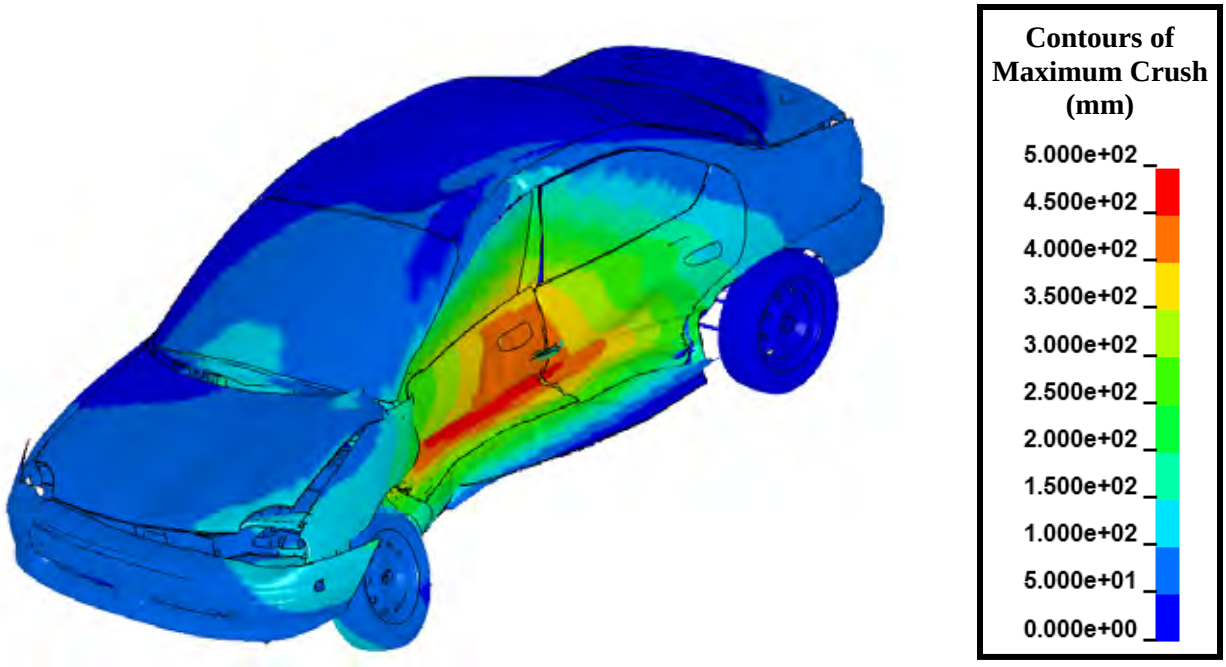

Figure 129. Calculated Crush for HV 1 in the 90 degree, 20 mph Collision with a Pilot Beam.

The crush intrusions in HV 1 for the 20 mph oblique (45 degree) collisions with and without the bumper enclosure are shown in Figure 126. The differences in the crush intrusions for this case are less significant. The maximum crush both with and without the bumper enclosure was approximately 640 mm. However, the appearance of the crush pattern and the height of the

maximum intrusion are significantly different. The crush without the bumper enclosure is located on the B-pillar which is relatively high on the occupant compartment of the car. The true value of the intrusion in this case was probably larger than recorded by the structural crush since the driver window was pushed into the car and the head girder penetrated through the window opening. With the bumper enclosure, the maximum crush in the occupant compartment was located close to the door handle and is more uniform over the side of the vehicle.

The maximum crush for both configurations indicate a high probability of serious injuries (greater than 90%) and fatalities (approximately 70%). From accident data, the collision scenario on the right front corner of the LRV is quite common with highway vehicles making a left turn across the LRV tracks. However, as a result of the combination of the moving highway vehicle and the braking efforts of the LRV operator, the 20 mph closing speed assumed for this collision may be higher than in the majority of these collisions.

A second set of the oblique collisions was performed at a 10 mph closing speed between the LRV and HV 1. The crush profiles on the impacted vehicles are shown in Figure 131. The maximum crush without the bumper enclosure was approximately 500 mm and located on the B-pillar relatively high on the occupant compartment of the car. With the bumper enclosure, the maximum crush in the occupant compartment was reduced to approximately 260 mm and is more uniform over the center portion of the door.

From the NASS injury curves, shown in Figure 127, the collision without the bumper has approximately a 45% chance of being fatal and a 75% probability of serious injuries. As a result of adding the bumper enclosure, the probability of a fatal injury is reduced to approximately 5% and the probability of a serious injury is reduced to approximately 25%. The comparison shows a big improvement in protection of the highway vehicle occupants by adding the bumper.

Collision analyses with the Ford Explorer model (HV 2) found very similar trends. The calculated 20 mph crash behavior of the LRV without any front-end safety features into the side of HV 2 (90 degree) is shown in Figure 132. The head girder overrides much of the HV 2 side protective structures and intrudes significantly into the occupant volume. The high location of the impact also rotates the HV 2 lifting the wheels on the impact side off the ground. The corresponding intrusions of the LRV into HV 2 can be seen in the top view at the end of the collision as shown in Figure 133.

The calculated 20 mph crash behavior of the LRV with a bumper enclosure into the side of HV 2 (90 degree) is shown in Figure 134 and Figure 135, for the side and top views, respectively. The bumper engages much of the HV 2 side protective structures and the crash response is significantly modified. The lower impact forces, as seen in Figure 134, pushes HV 2 laterally in the direction of the LRV movement and the motion is primarily a translation without the large roll seen when impacted without the bumper. Similarly, from the comparison of the top views of the collision behaviors, shown in Figure 133 and Figure 135, the bumper significantly reduces the crush intrusions of the LRV into HV 2.

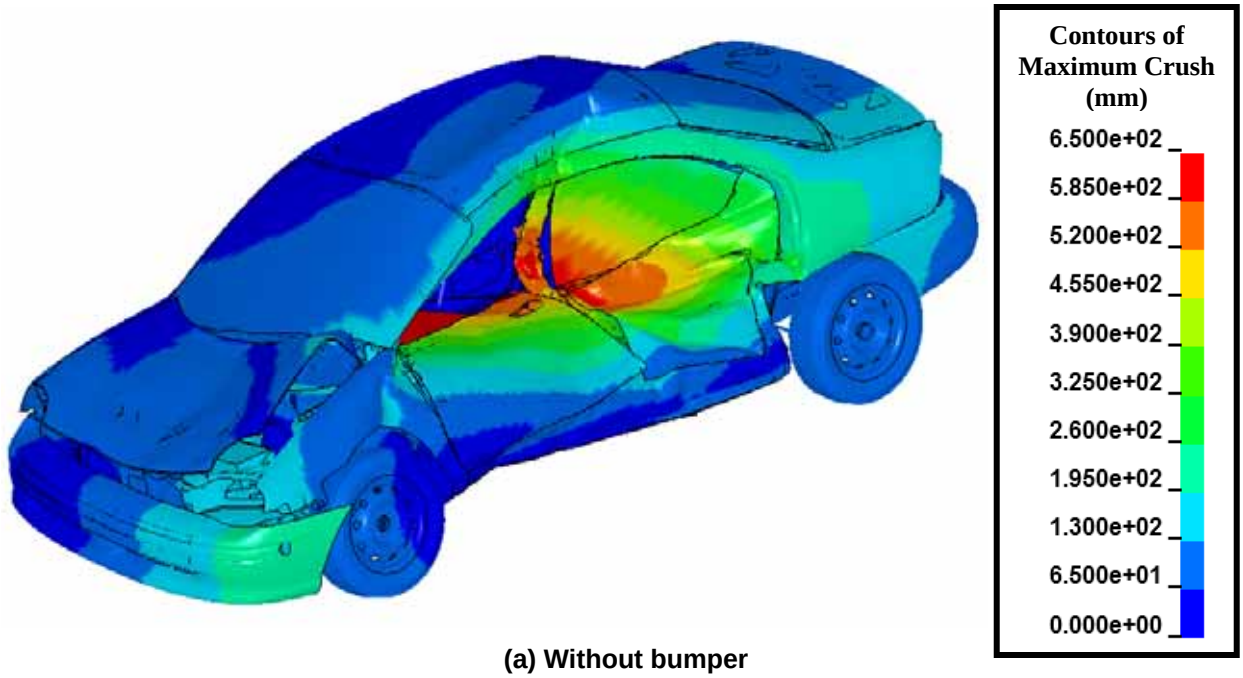

(a) Without bumper

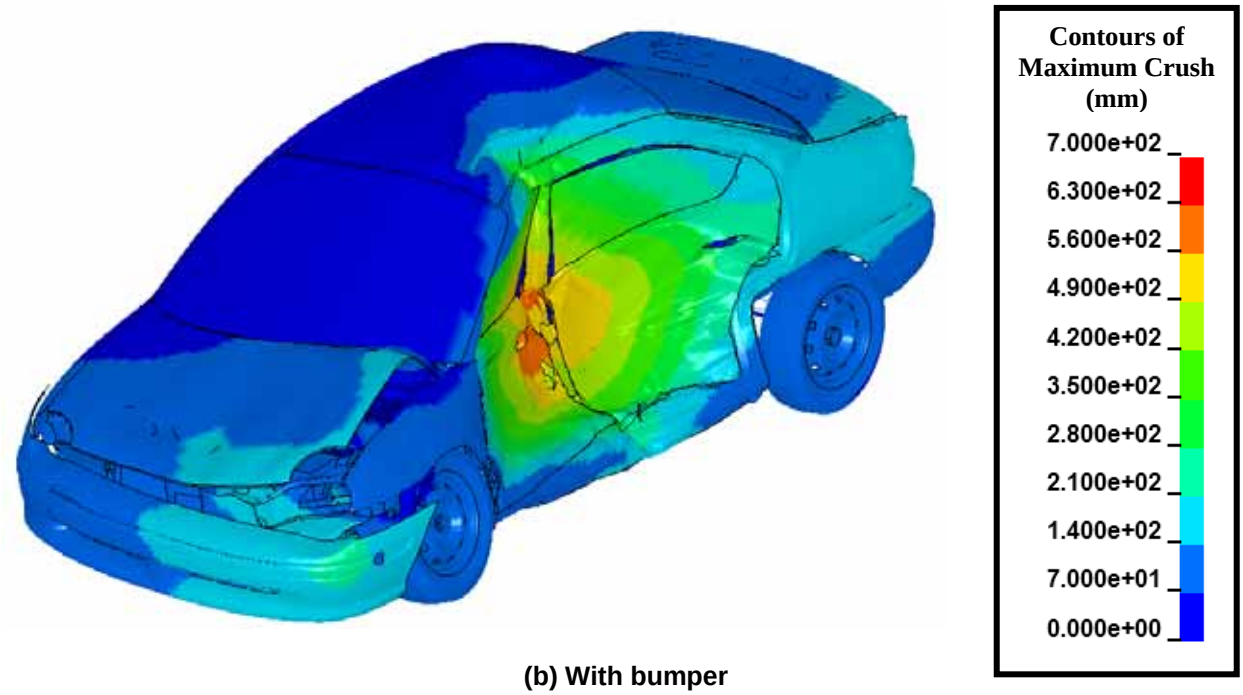

(b) With bumper

Figure 130. Crush in HV 1 after a 45 degree, 20 mph Collision with LRV 2 both with and without a Bumper.

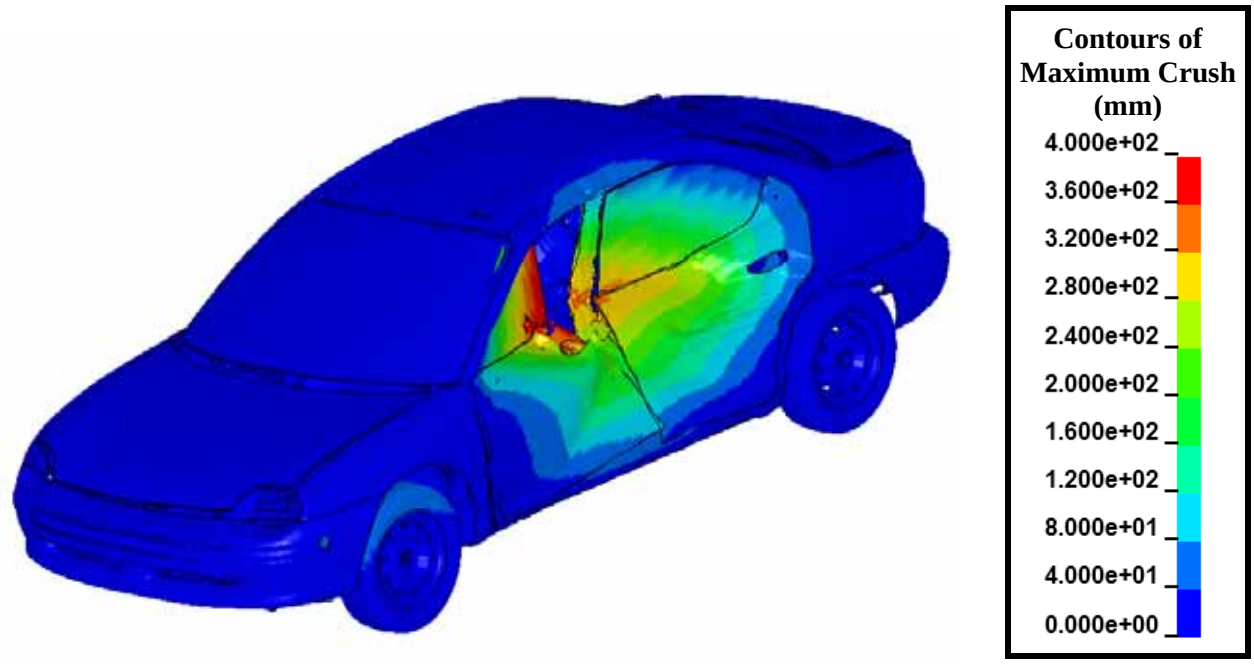

(a) Without bumper

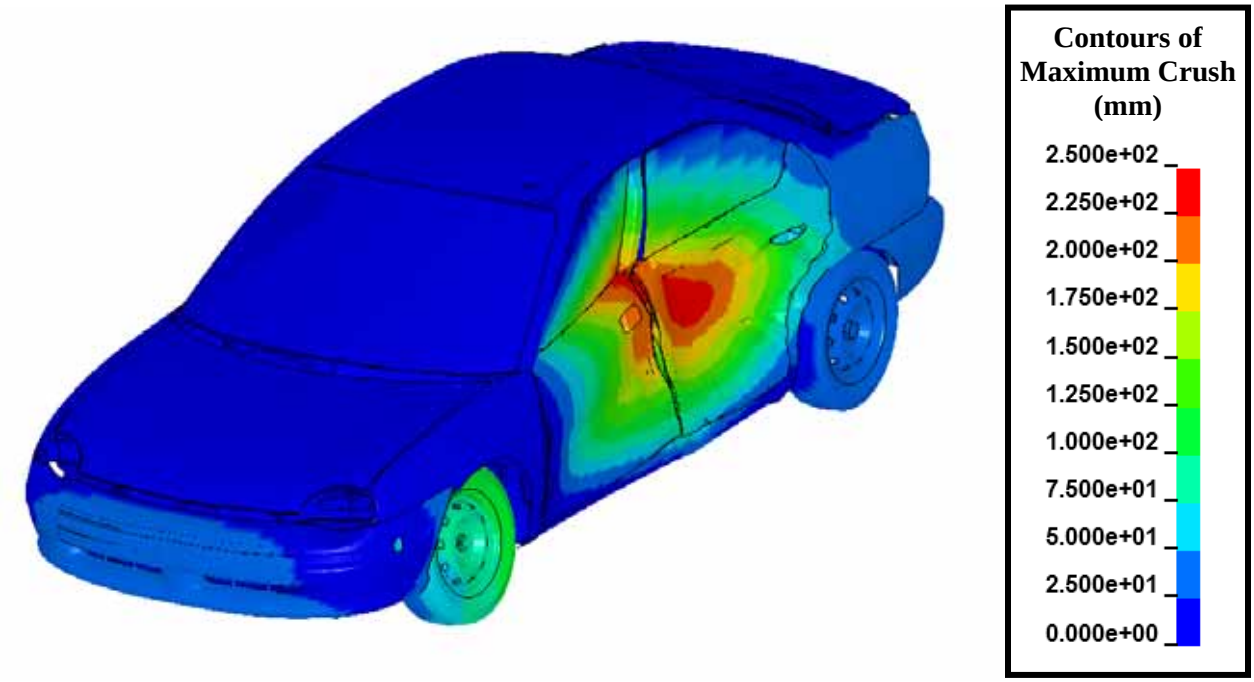

(b) With bumper

Figure 131. Calculated Crush in HV 1 from the 45 degree, 10 mph Collisions.

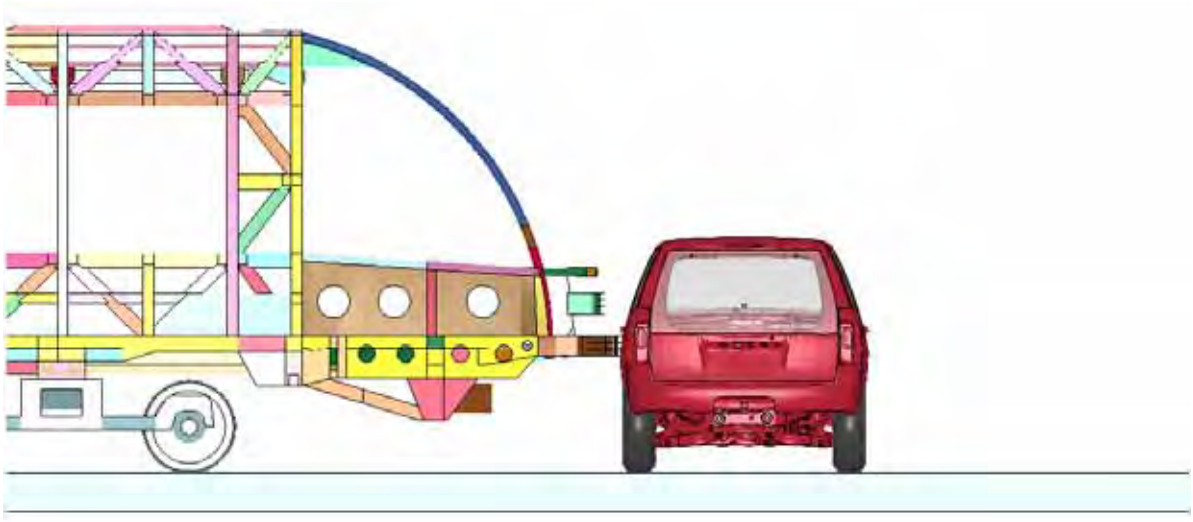

(a) Time = 0.00 s

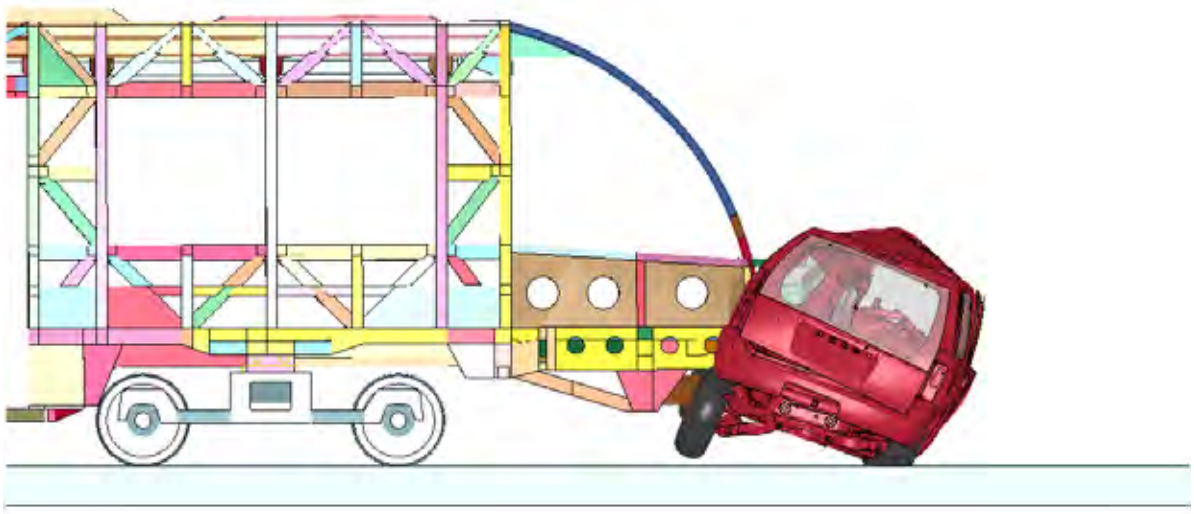

(b) Time = 0.18 s

Figure 132. Simulation of the 90 degree, 20 mph Collision with HV 2 (Side View – LRV without a Bumper).

The corresponding crush intrusions in the Ford Explorer for the 20 mph collisions with and without the bumper enclosure are shown in Figure 136. The differences in the crush intrusions are significant. The maximum crush without the bumper enclosure was approximately 940 mm and located relatively high on the occupant compartment of the car. With the bumper enclosure, the maximum crush in the occupant compartment was reduced to approximately 490 mm and is more uniform over the door. It is interesting to note that these crush intrusions are larger than those for a similar impact condition on HV 1. This is in part a result of the fact that the impact against the heavier highway vehicle requires greater crash energy absorption.

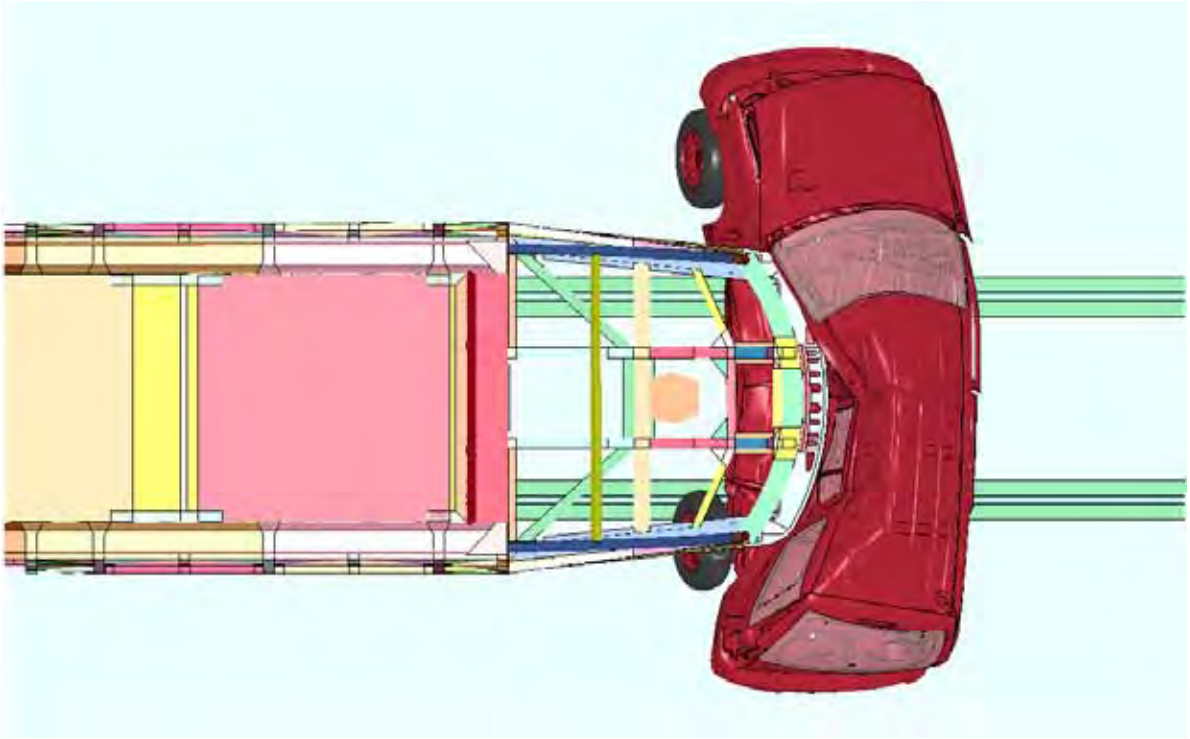

Figure 133. Simulation of the 90 degree, 20 mph Collision with HV 2 (Top View – LRV without a Bumper).

The injury potential resulting from the side impact damage on HV 2 can again be obtained from the NASS injury curves shown in Figure 127. The collision without any safety features has a probability of a fatality of 98% and a probability of serious injury of 99%. As a result of adding bumpers, the probability of a fatal injury is reduced to 45% and the probabilities of serious injuries are reduced to 75%. Thus, the addition of the bumpers has reduced the probability that this collision scenario will be fatal by more than a factor of two and significantly reduced the potential for serious injuries.

One other configuration of interest is the effect of an extended coupler on the collision risk. The extended coupler can be a potential crash hazard since it is extended from the front of the LRV and can potentially concentrate the crash loads on a smaller section of the car and localize the crush. The coupler could also have a beneficial effect since the coupler contacts lower on the side of the highway vehicle where the resistance to crush penetrations is greater. To investigate the effect of the coupler, an additional 20 mph collision analysis was performed using HV 2 and a model of the LRV with a coupler extended, as shown in Figure 137.

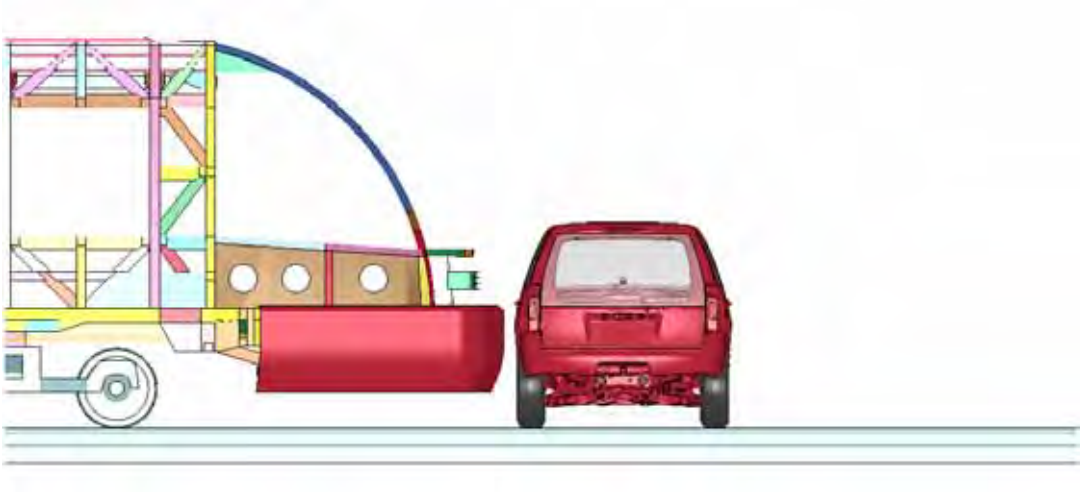

(a) Time = 0.00 s

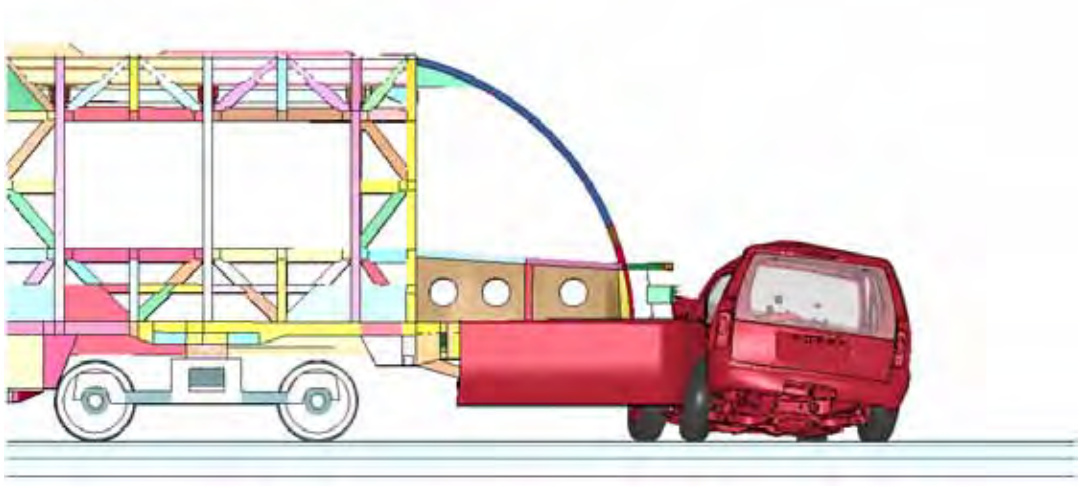

(b) Time = 2.00 s

Figure 134. Simulation of the 90 degree, 20 mph Collision with HV 2 (Side View – LRV Fitted with a Bumper).

The calculated 20 mph crash behavior of the LRV with an extended coupler into the side of HV 2 (90 degree) is shown in Figure 138. The coupler strikes the lower side of HV 2 near the bottom of the B-pillar. The low location of the impact results in primarily a translation of HV 2 after the collision. The corresponding intrusions of the LRV into HV 2 can be seen in the top view at the end of the collision as shown in Figure 139. The majority of the crush is localized to a narrow region around the B-pillar, centered on the coupler impact point.

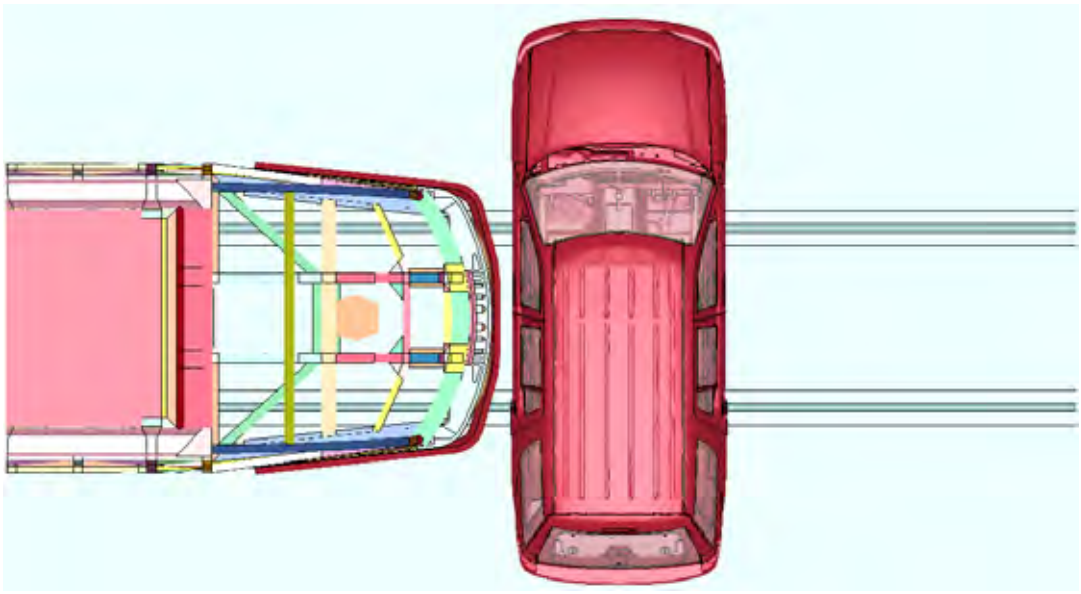

(a) Time = 0.00 s

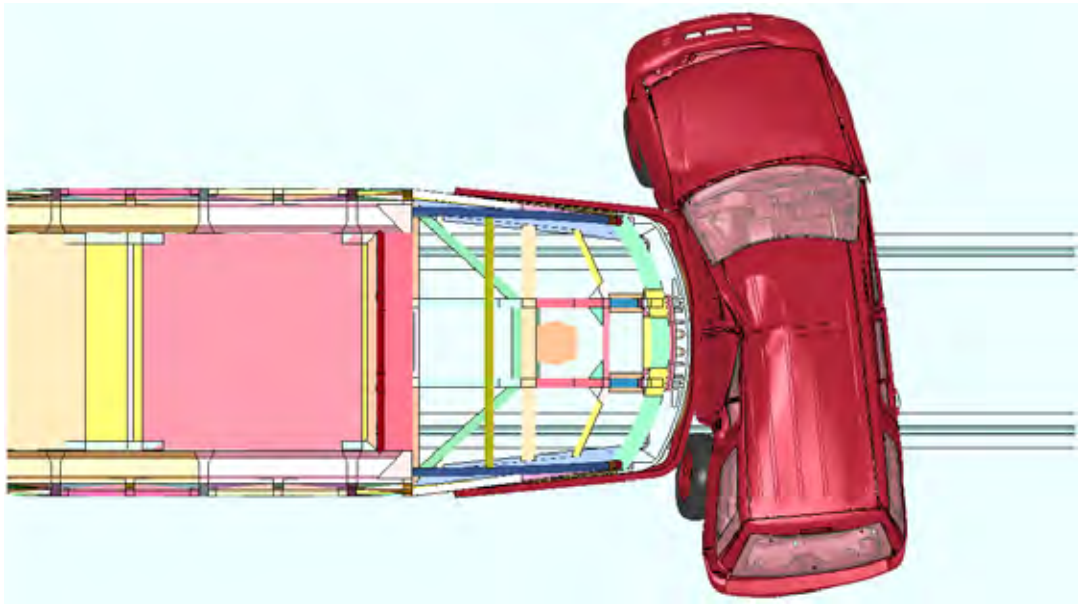

(b) Time = 2.00 s

Figure 135. Simulation of the 90 degree, 20 mph Collision with HV 2 (Top View – LRV Fitted with a Bumper).

The corresponding crush intrusions in HV 2 for the 20 mph collisions with the extended coupler are shown in Figure 140. The maximum crush in the collision is 590 mm (compared to 940 mm without the coupler and 490 mm with the bumper). Thus, the extended coupler in this collision has a lower injury risk than if the coupler is retracted or folded away. However, the coupler is not as effective as the bumper enclosure for protecting the occupants of HV 2.

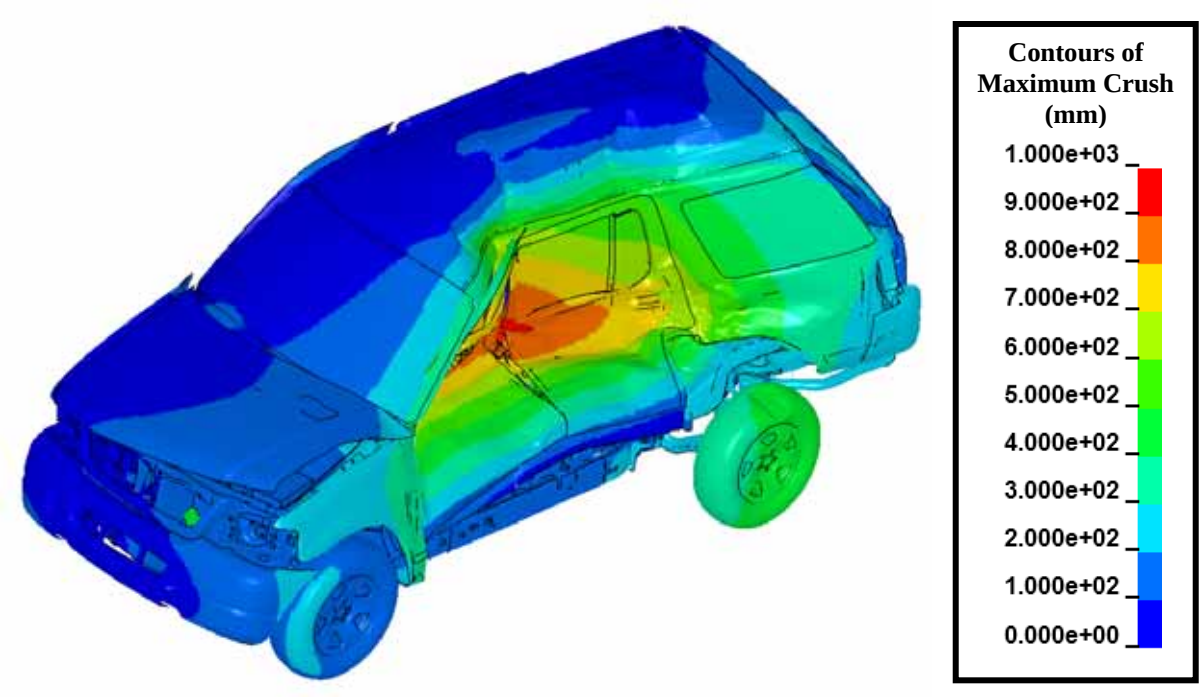

(a) Without bumper

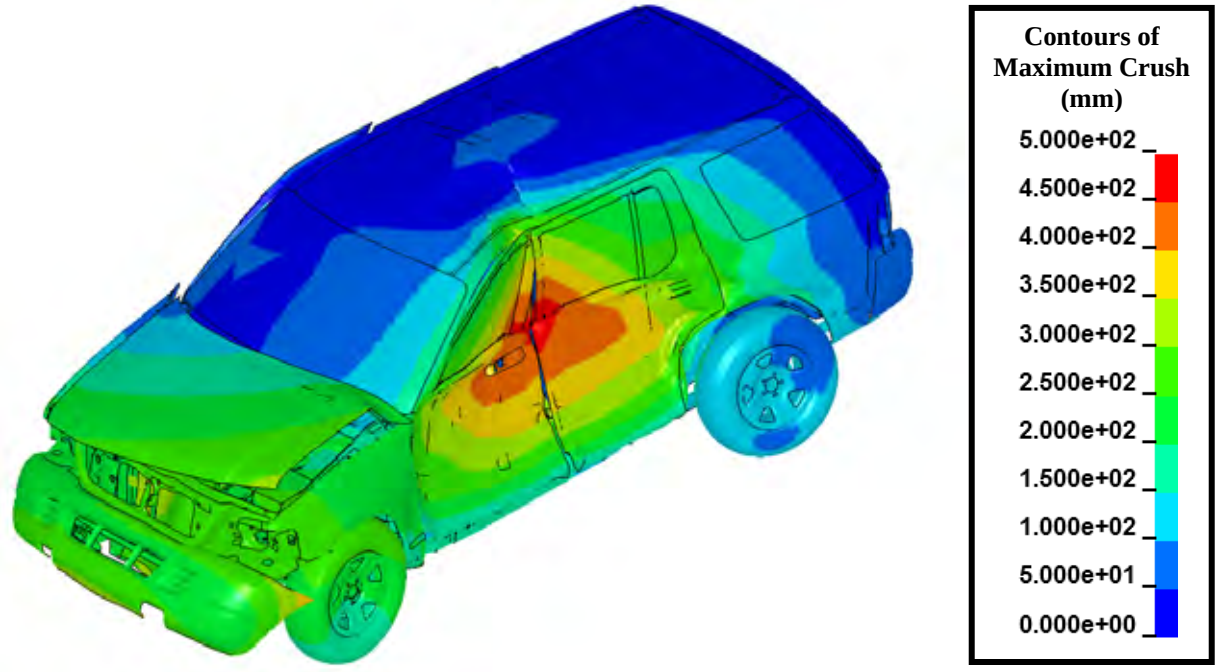

(b) With bumper

Figure 136. Crush in HV 2 after a 90 degree, 20 mph Collision with LRV 2 both with and without a Bumper.

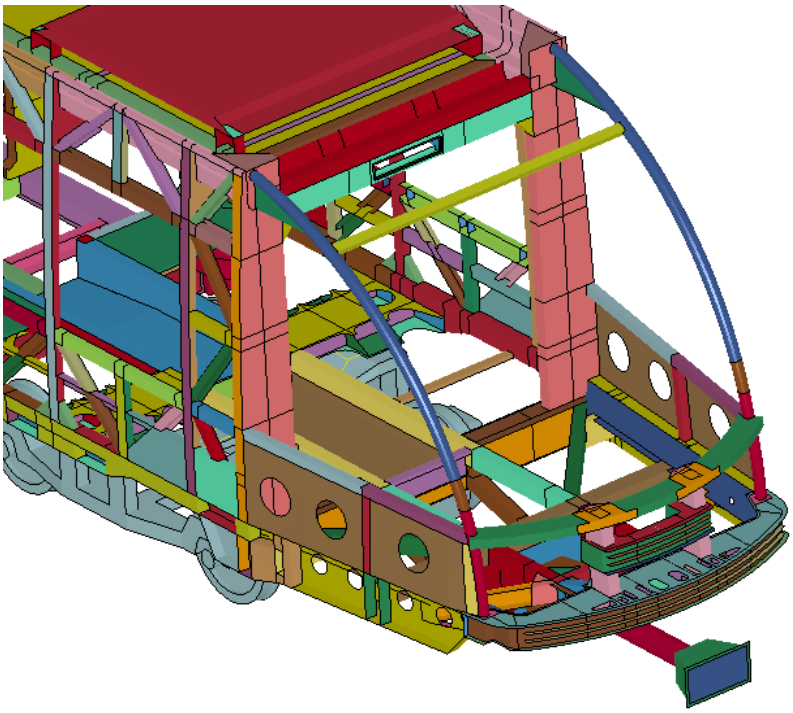

Figure 137. LRV 2 Front-End with an Extended Coupler Model.

A summary of the calculated crash responses for LRVs colliding with highway vehicles are provided in Table 16 through Table 18. Table 16 summarizes the maximum crush intrusion in the occupant volume of the highway vehicles for the different impact speeds, orientations, LRV configurations, and highway vehicle type. Table 17 and Table 18 summarize the corresponding probabilities of fatalities or injuries based on the calculated crush intrusions and the NASS injury database.

The data in Table 16 through Table 18 illustrate that for survivable collisions, the addition of a rigid bumper enclosure greatly improves the geometric compatibility and significantly reduces the probabilities of fatalities or serious injuries. Alternative features such as a pilot beam can contribute to safety, but some additional design work would be beneficial to optimize the performance. The pilot beam should be lowered as much as possible to engage the lower structures on the highway vehicle and the profile of the pilot beam should be wider to apply a more uniformly distributed crash load. In addition, the pilot beam needs to consider the necessary clearances for the coupler operation.

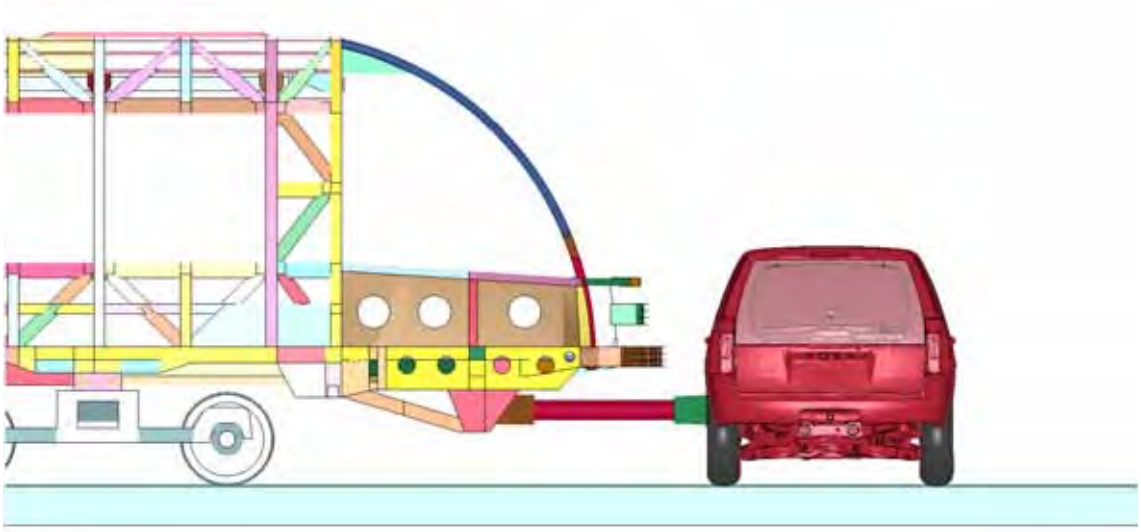

(a) Time = 0.000 s

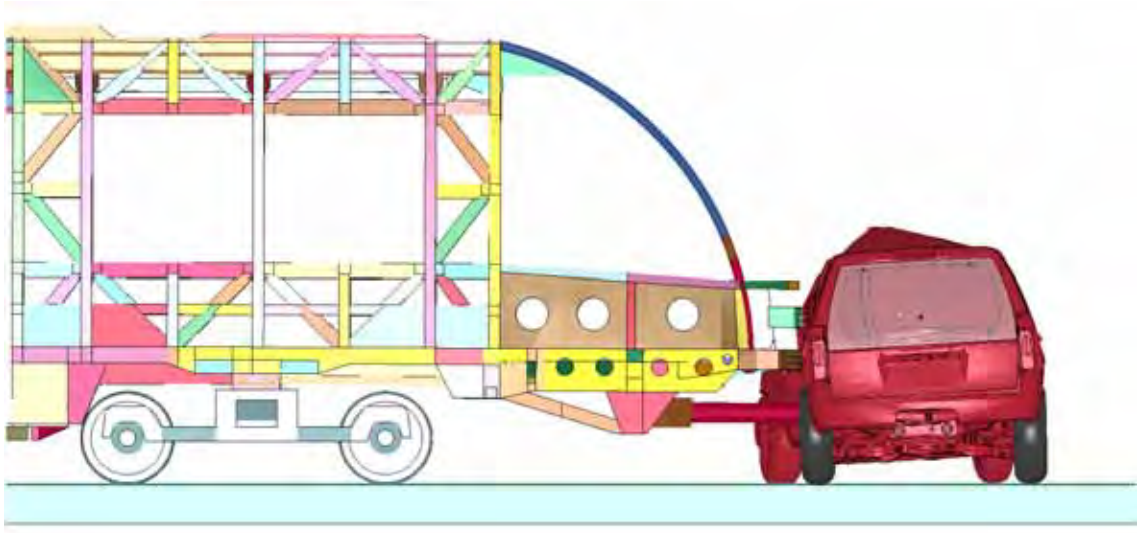

(b) Time = 0.135 s

Figure 138. Simulation of the 90 degree, 20 mph Collision with HV 2 (Side View – LRV Fitted with a Coupler).

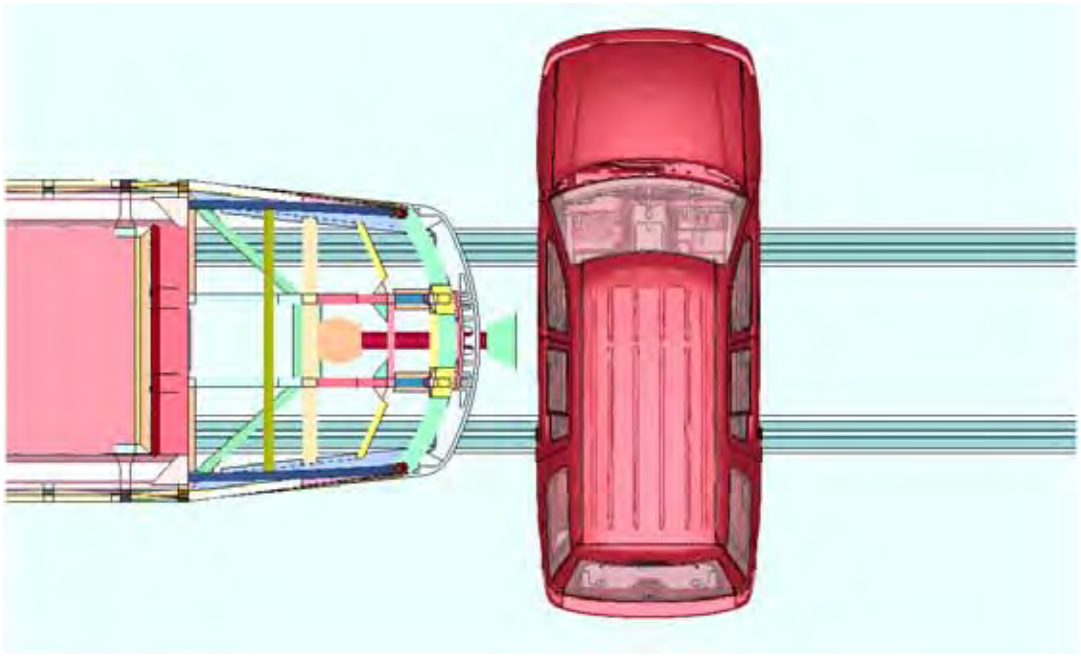

(a) Time = 0.000 s

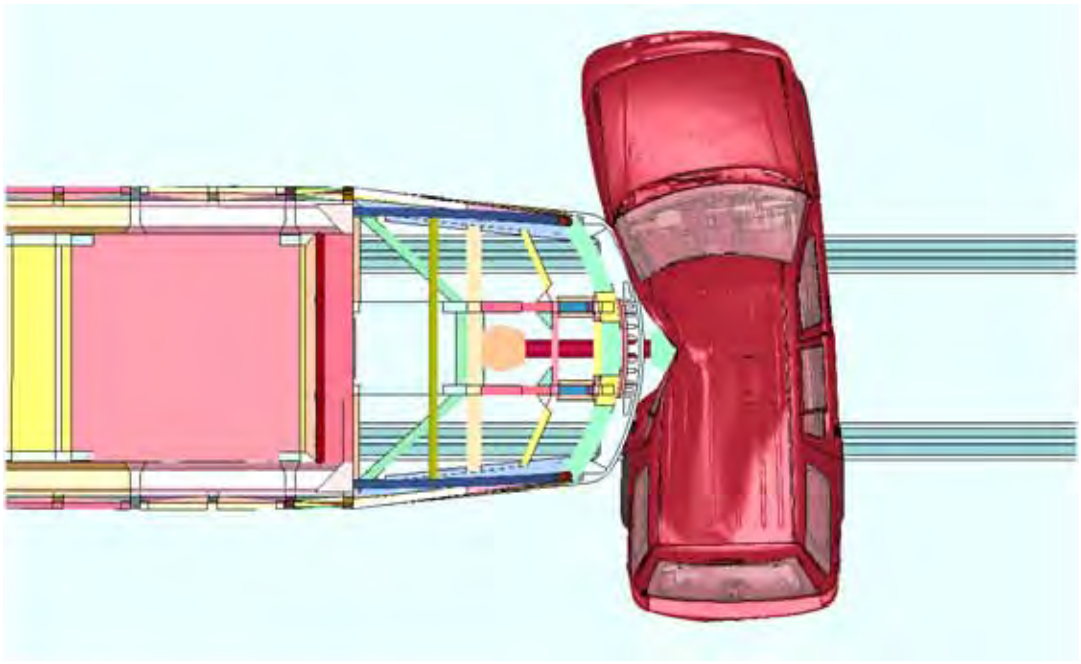

(b) Time = 0.135 s

Figure 139. Simulation of the 90 degree, 20 mph Collision with HV 2 (Top View – LRV Fitted with a Coupler).

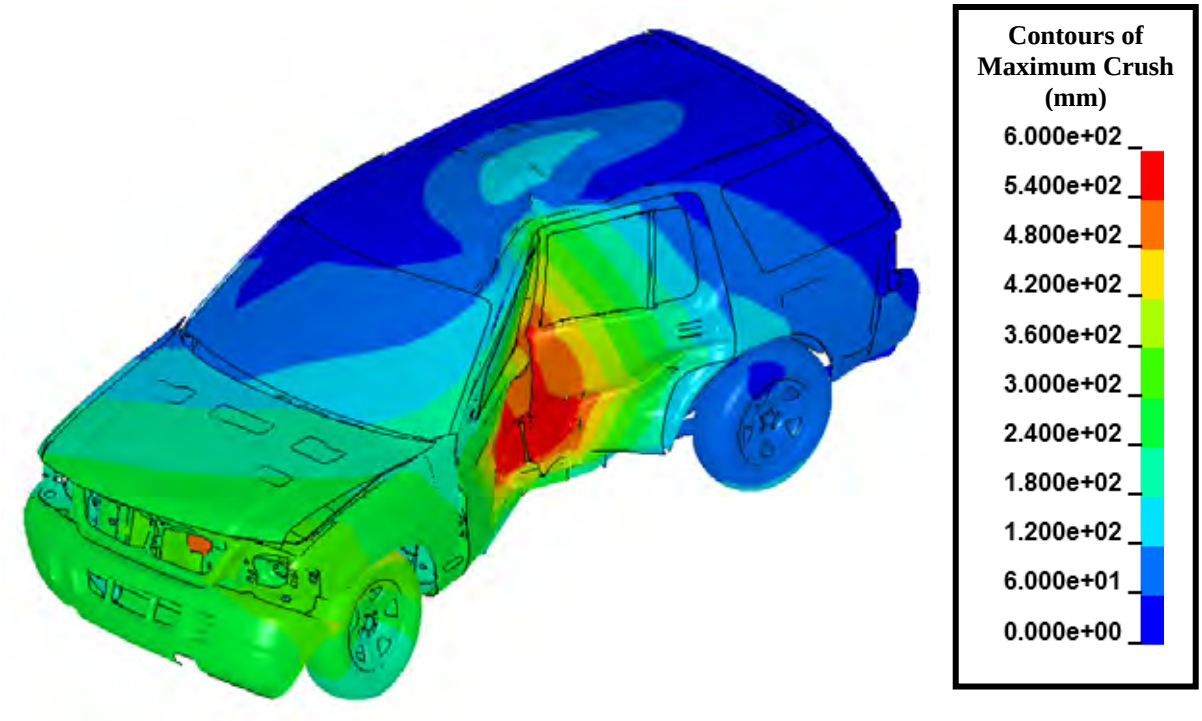

Figure 140. Calculated Crush in HV 2 after a 90 degree, 20 mph Collision with a Coupler.

Table 16. Calculated Crush in Side Impacts of Highway Vehicles

Collision Scenario	90 degrees			45 degrees		
	15 mph	20 mph	30 mph	10 mph	20 mph	30 mph
LRV Not Fitted with a Bumper/Coupler						
HV 1 Crush (mm)	480	670	970	500	640	930
HV 2 Crush (mm)	—	940	1050	—	690	—
LRV Fitted with a Bumper						
HV 1 Crush (mm)	360	450	760	260	650	910
HV 2 Crush (mm)	—	490	—	—	660	—
LRV Fitted with a Pilot Beam						
HV 1 Crush (mm)	—	490	—	—	—	—
HV 2 Crush (mm)	—	—	—	—	—	—
LRV Fitted with a Coupler						
HV 1 Crush (mm)	—	—	—	—	—	—
HV 2 Crush (mm)	—	590	—	—	—	—

Table 17. Calculated Fatality Probabilities in Side Impacts of Highway Vehicles

Collision Scenario	90 degrees			45 degrees		
	15 mph	20 mph	30 mph	10 mph	20 mph	30 mph
LRV Not Fitted with a Bumper/Coupler						
HV 1	43%	73%	99%	46%	69%	98%
HV 2	—	98%	100%	—	76%	—
LRV Fitted with a Bumper						
HV 1	22%	39%	81%	5%	69%	97%
HV 2	—	45%	—	—	72%	—
LRV Fitted with a Pilot Beam						
HV 1	—	45%	—	—	—	—
HV 2	—	—	—	—	—	—
LRV Fitted with a Coupler						
HV 1	—	—	—	—	—	—
HV 2	—	62%	—	—	—	—

Table 18. Calculated Injury Probabilities (MAIS 3+) in Side Impacts of Highway Vehicles

Collision Scenario	90 degrees			45 degrees		
	15 mph	20 mph	30 mph	10 mph	20 mph	30 mph
LRV Not Fitted with a Bumper/Coupler						
HV 1	73%	94%	100%	76%	92%	99%
HV 2	—	99%	100%	—	95%	—
LRV Fitted with a Bumper						
HV 1	51%	69%	96%	25%	92%	99%
HV 2	—	75%	—	—	93%	—
LRV Fitted with a Pilot Beam						
HV 1	—	75%	—	—	—	—
HV 2	—	—	—	—	—	—
LRV Fitted with a Coupler						
HV 1	—	—	—	—	—	—
HV 2	—	89%	—	—	—	—

Bumper Energy Absorption Analyses

Another potential safety feature of the LRV front end is to make the bumper structures be energy absorbing. A common approach is to specify force, stroke, and energy absorbing levels that are appropriate for a 5 mph collision between two similar LRVs. If we consider a symmetric collision between two identical LRVs, the crash energy that needs to be dissipated in each vehicle is

$$E = \frac{1}{8} M_1 V_o^2$$

where V_o is the LRV closing speed and M_1 is the mass of a single LRV. For a collision between two 45,000 kg (100,000 lb) LRVs both equipped with bumpers capable of dissipating 30 KJ, the closing speed can be as high as 8.3 kph (5.1 mph) with no damage to either vehicle. Thus, the 30 KJ energy dissipating bumper system is the minimum requirement for the first level of CEM for LRV to LRV collisions.

The bumper characteristics from the Phoenix LRV specification were designed to prevent any vehicle structural damage for collision speeds of up to 8 km/hr (5 mph). They adopted a more conservative design approach where the entire kinetic energy of the LRV at 5 mph could be dissipated by the bumper system resulting in approximately 115 kJ of energy absorption capacity [17]. Additional Phoenix LRV bumper specifications were:

- The bumper design shall provide for a bumper travel in the range of 100 mm (4 in) to 150 mm (6 in) before the struck vehicle's anticlimber elements come into contact with the colliding vehicle or object.
- The bumper shall be a minimum of 300 mm (11.8 in) high and extend across the entire front of the vehicle. This bumper shall be mounted so as to provide the best match with automobile and heavy highway vehicle bumpers, 355 to 762 mm (14 to 26 in) above top of rail. Note that this is compatible with the bumper heights for a range of passenger highway vehicles, as shown in Figure 141 [19].

If we assume a bumper travel of 125 mm for this system and the 115 KJ of energy absorption, the average force for the bumper is 920 KN. If the energy absorption requirements are reduced to 30 KJ and the bumper travel is increased to 150 mm, the average bumper force is reduced to 200 KN. This is a minimum force level that would allow a bumper to be effective for the 5 mph LRV-LRV collision without significantly increasing the bumper travel.

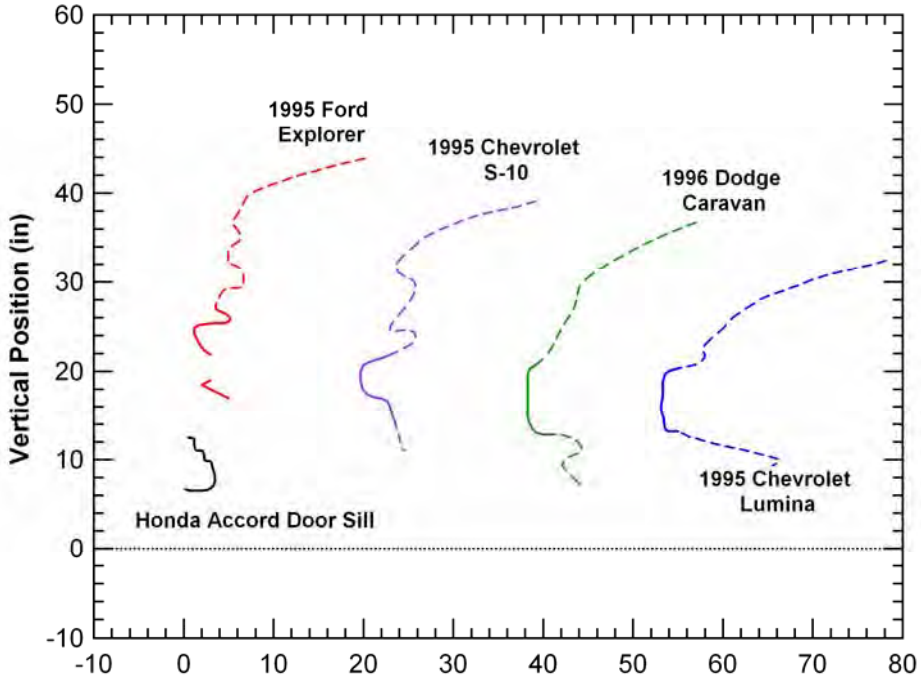

Figure 141. Front profile measurements for various highway vehicles [19].

We next need to consider the bumper energy absorption characteristics that are compatible with a collision between an LRV and a highway vehicle. The calculated average energy dissipation for the various collisions between the LRV and the highway vehicles is summarized in Table 19. The total energy dissipation requirements are 26, 43, and 86 KJ for 90 degree impacts of HV 1 at 15, 20, and 30 mph, respectively. Similarly the crash energy dissipation for 90 degree impacts of HV 2 at 20 and 30 mph are 76 and 176 KJ, respectively. The higher energy absorption requirements for HV 2 (nearly double those of HV 1 at a given collision speed) are a direct result of the higher vehicle weight. The energy levels for the collisions at 30 mph or above are of lesser interest since their potential survivability is quite low.

Table 19. Calculated Energy Dissipation in Side Impacts of Highway Vehicles

Energy Dissipation (kJ)	Velocity in mph					
	90 degrees			45 degrees		
	15	20	30	10	20	30
HV 1	26	43	86	9	40	91
HV 2	—	76	176	—	71	—

The best methodology to determine effective bumper energy absorbing characteristics to protect occupants of automobiles struck by an LRV is to evaluate the force-crush characteristics of the highway vehicles impacted with the rigid bumper system. The force-crush characteristics for both HV 1 and HV 2 impacted at 20 mph by the LRV with the rigid bumper system at 90 degree

and 45 degree orientations are shown in Figure 142. For the 90 degree collisions, the crush forces remain below approximately 100 KN until a crush intrusion of 300-400 mm. The forces then increase to a maximum of 150 KN for HV1 and 220 KN for HV 2 at crush intrusions between 400 and 500 mm. For the 45 degree collisions, the crush forces remain below approximately 40 KN for HV 1 and 75 KN for HV 2 until a crush intrusion of greater than 500 mm. The peak crush force for either vehicle in the 45 degree collisions remains below 100 KN.

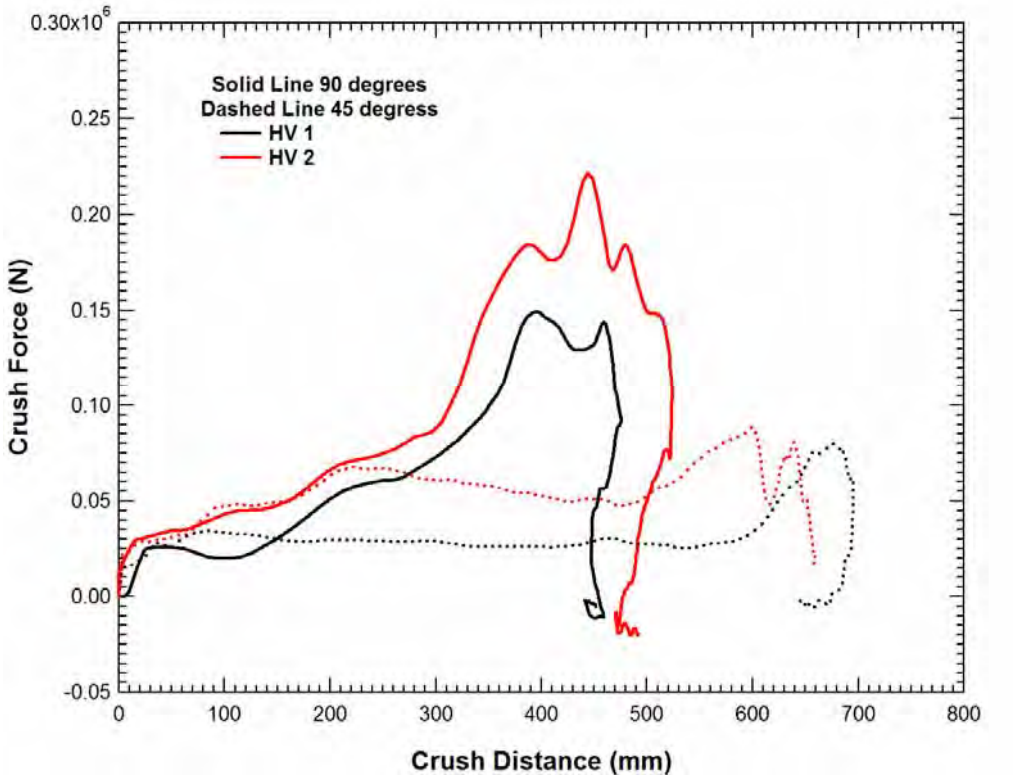

Figure 142. Force-Crush Profiles for the 45 and 90 degree, 20 mph Collisions (LRV Fitted with Bumper)

The comparison of the highway vehicle force-crush behaviors illustrates the difficulty of defining an energy-absorbing bumper for LRVs that reduces injury to automobile occupants and is still effective for LRV operations. Unless the force for bumper activation is significantly below 100 KN, the energy absorption mechanisms will not be activated in oblique impacts. If the system has 200 mm of travel at an average force of 50 KN, the energy absorbed would be 10 KJ. In the 90 degree impacts at 20 mph, this would reduce the crush by approximately 15%. By comparison, the addition of the rigid bumper enclosure reduced the crush by approximately 35 % in HV 1 and nearly 50% in HV 2.

In addition, the 15 KJ of energy is only about half of the energy dissipation needed for the 5 mph collision between two similar LRVs. As a result, it is difficult to develop a bumper system that will both dissipate a significant amount of energy in collisions with automobiles but still be suitable for preventing damage in the 5 mph collision between two identical LRVs. However,

the simulations show that simply adding a rigid bumper enclosure can significantly reduce the injury probability for many collision scenarios between LRVs and highway vehicles.

Analysis of a SUV impacting the side of an LRV

A major objective in the development of LRV safety standards is to provide sufficient strength of the passenger compartment to preserve volume in the passenger compartment during collisions. There has been a concern in the LRV crash safety community that the past design practices may not be sufficient to protect against impacts by large SUVs or trucks against the LRV side, particularly for vehicle regions with a low floor. It is especially important due to the growing trends of lowering floors in newly designed LRVs combined with the increase in the US automotive fleet of larger, heavier, and higher trucks and SUVs.

Current practice to protect against this collision scenario is the application of static design loads on the side wall. Under this load case, the acceptance criterion is that no yielding of car body structure occurs. The objective of this task is to use a SUV or a pickup truck model to assess possible penetration into the passenger residual space and the effectiveness of the current practice for these collisions.

In this task, simulations were completed for the case of HV 2 impacting LRV 2. The impact point on the LRV was centered between the two doors in a low-floor section on the left side of the LRV. Impact velocities for the HV 2 were 20 mph and 35 mph. Figure 143 shows the top view of the collision interface for these simulations.

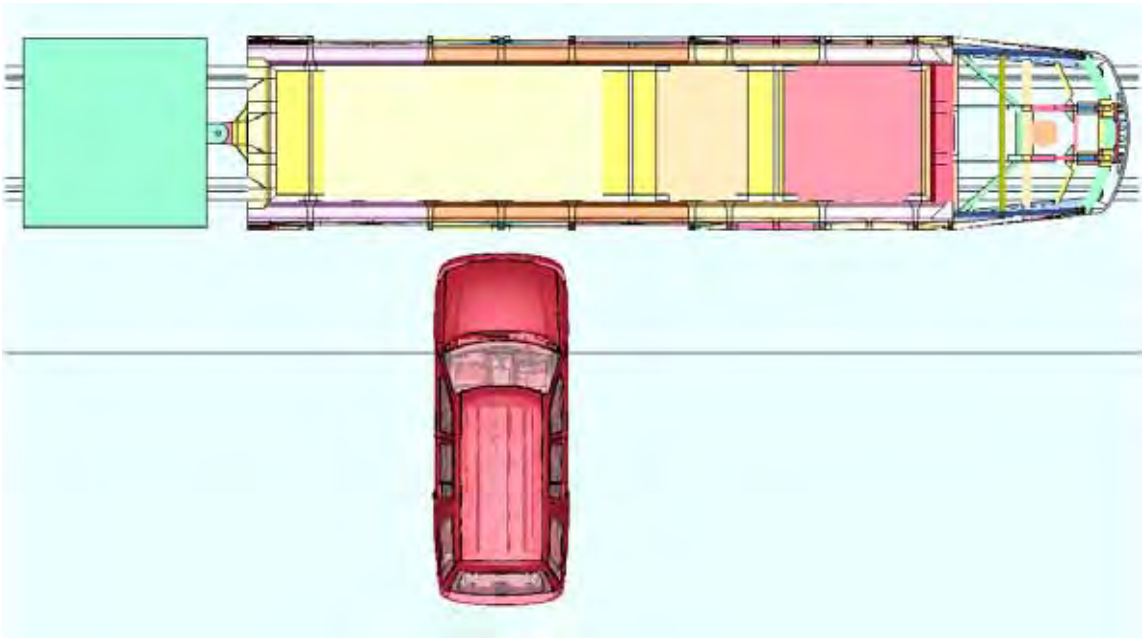

Figure 143. Collision Interface for the 90 degree Impact of HV 2 into LRV 2.

One concern with the simulations performed for this task is that none of the LRV models were developed with the expectation that this collision scenario would be evaluated. The mesh in the side of the LRV model is acceptable for the assessment. However, none of the other surrounding structures (doors, windows, seat frames, floor panels, external siding, internal wall panels, etc.) were added to the model. Although none of these components are designed to be primary structural members, they would all contribute to the side impact resistance of the LRV. As a result, the LRV model is probably more compliant to this type of loading condition than the actual LRV in operation.

A side view of the collision analysis at 35 mph is shown in Figure 144. The calculated response shows that the crush displacements are increasing in both HV 2 and the LRV during the collision. This indicates that the crush strengths of the SUV front end and the side structures in the LRV model are of similar levels. This can be further demonstrated by comparing the crush displacements of HV 2, shown in Figure 145, and the crush of the LRV, shown in Figure 146, for both collision speeds. The crush in the SUV is approximately 100 mm and 300 mm for the 20 and 35 mph collision speeds, respectively. Similarly, the crush in the LRV is approximately 150 mm and 400 mm for the 20 and 35 mph collision speeds, respectively.

Figure 147 shows the maximum displacement in the LRV due to a 90 degree impact from HV 2 at 20 mph and 35 mph. The maximum displacement was measured at the impact point and occurs at approximately the height where seats would be located in the LRV.

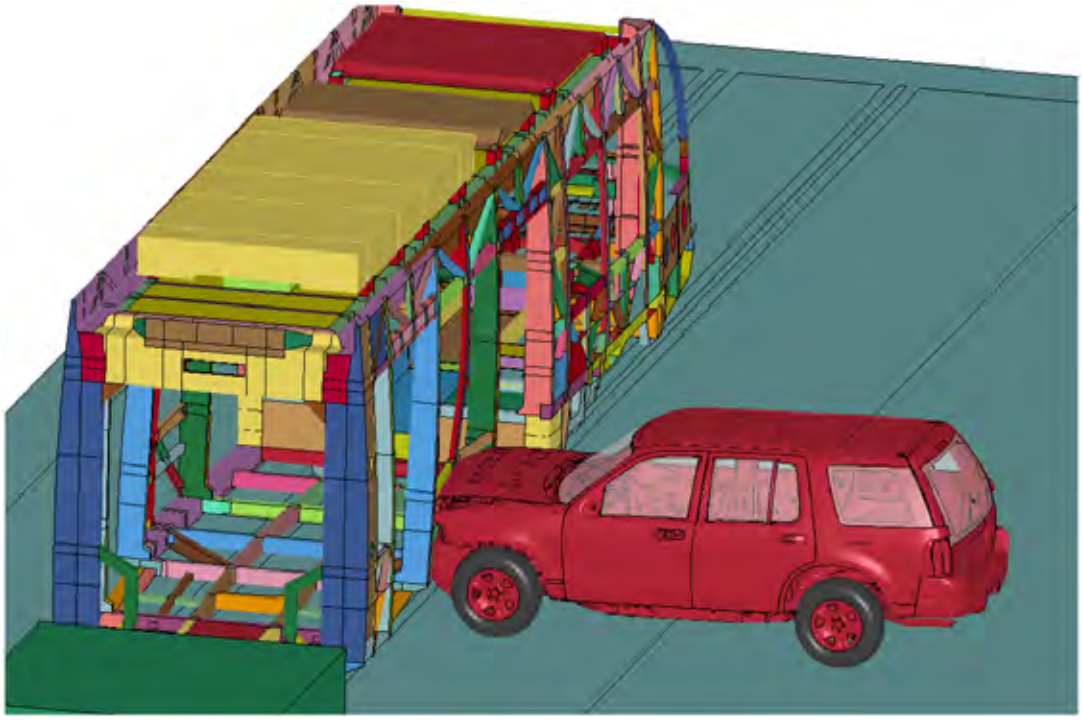

(a) t = 0.03 s

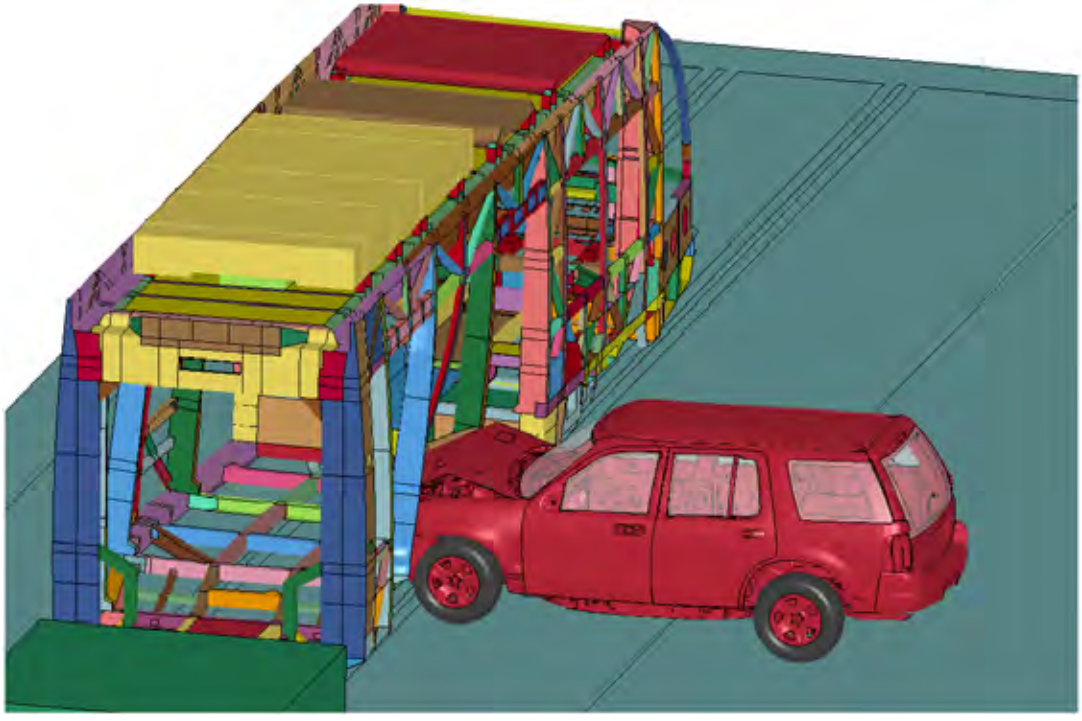

(b) t = 0.09 s

Figure 144. Side View of the Simulation of the HV 2 into LRV 2 90 degree, 35 mph Collision.

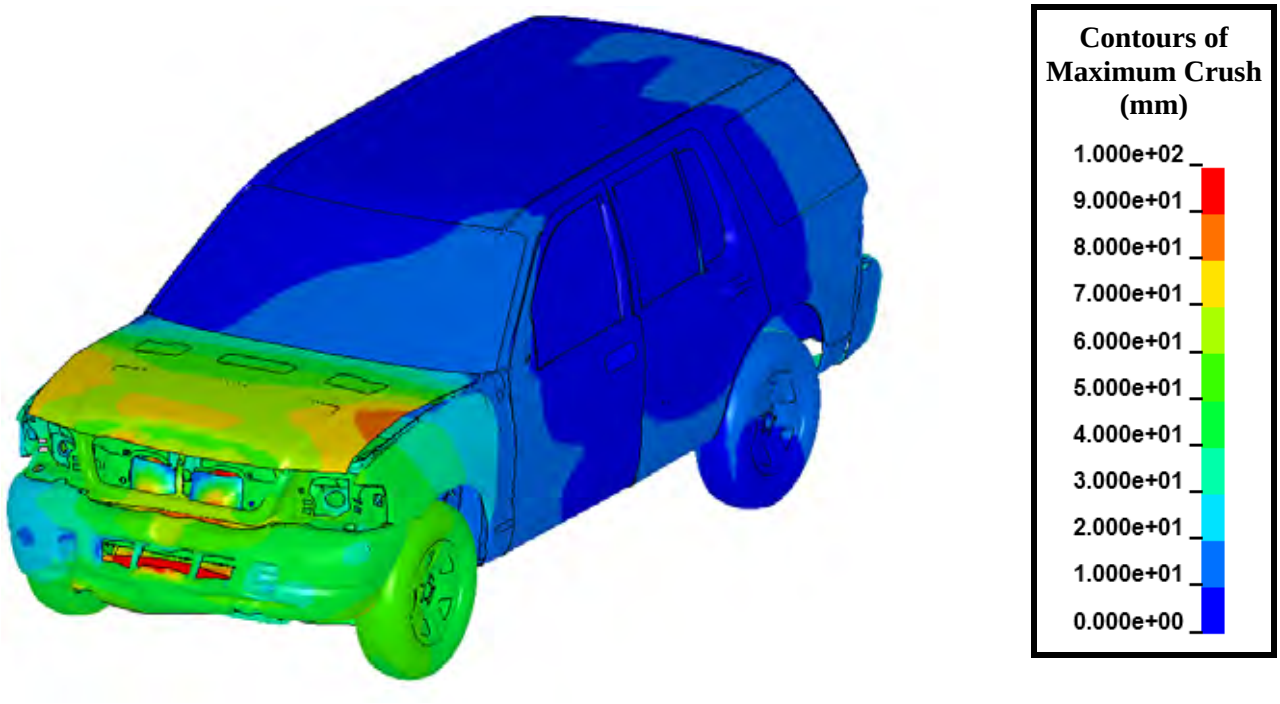

(a) 20 mph Collision

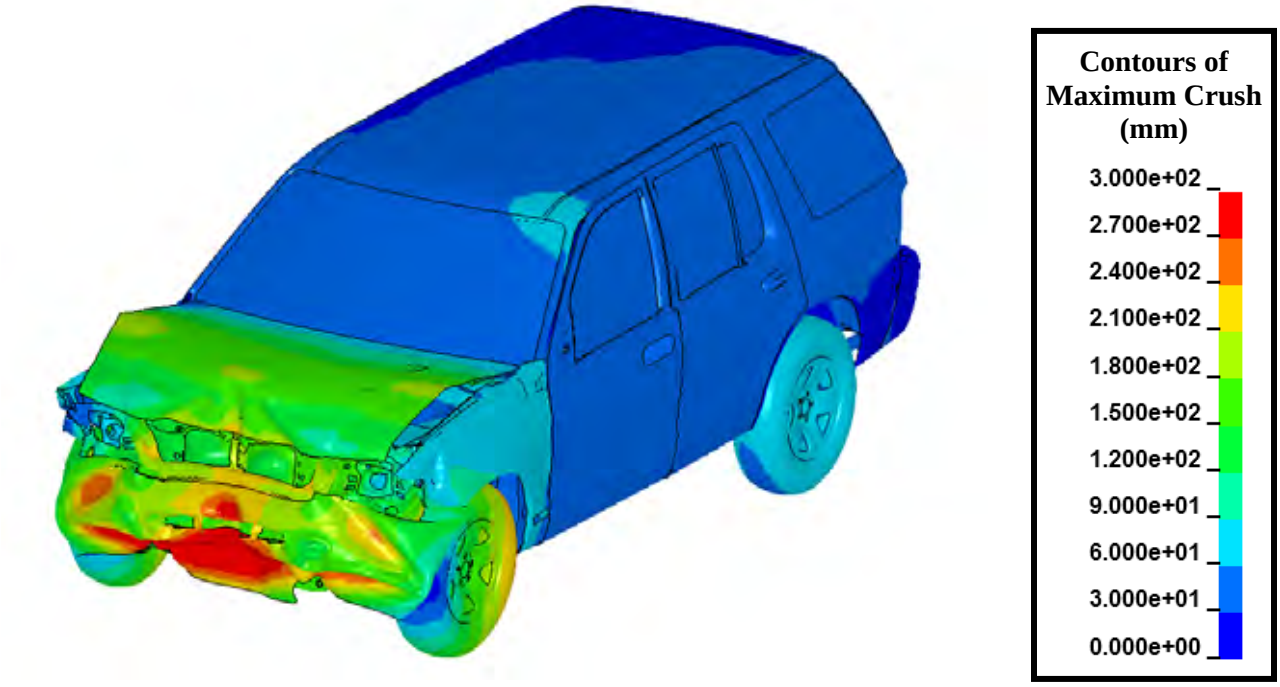

(b) 35 mph Collision

Figure 145. Calculated Crush of HV 2 due to 90 degree Side Impacts into LRV 2.

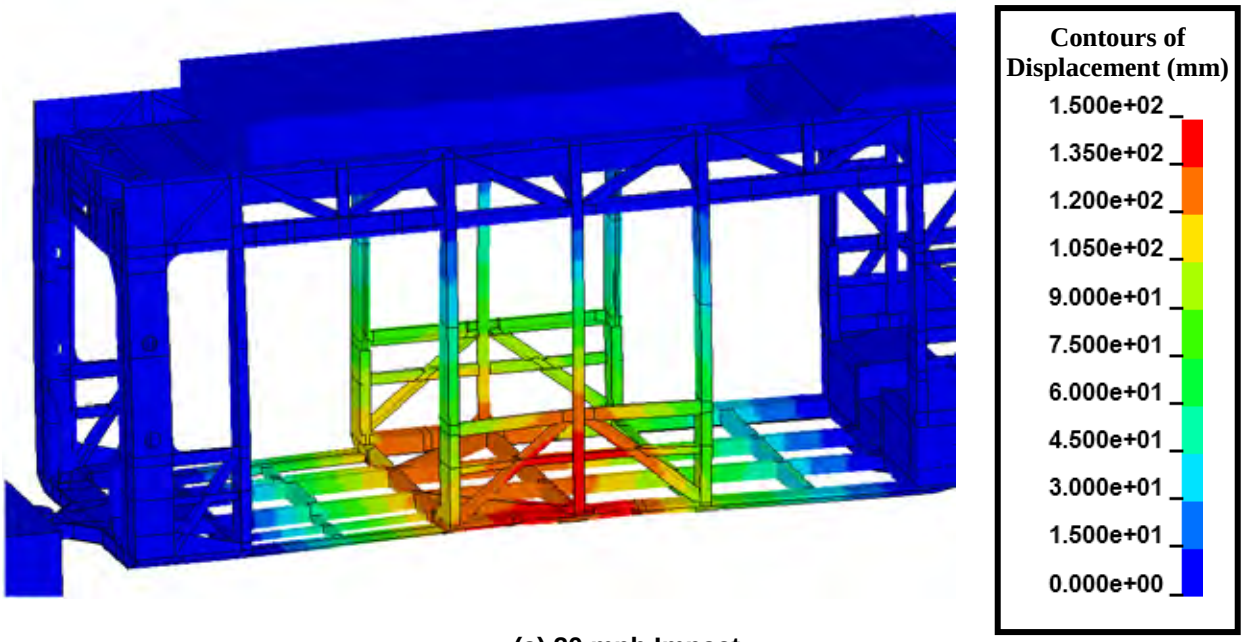

(a) 20 mph Impact

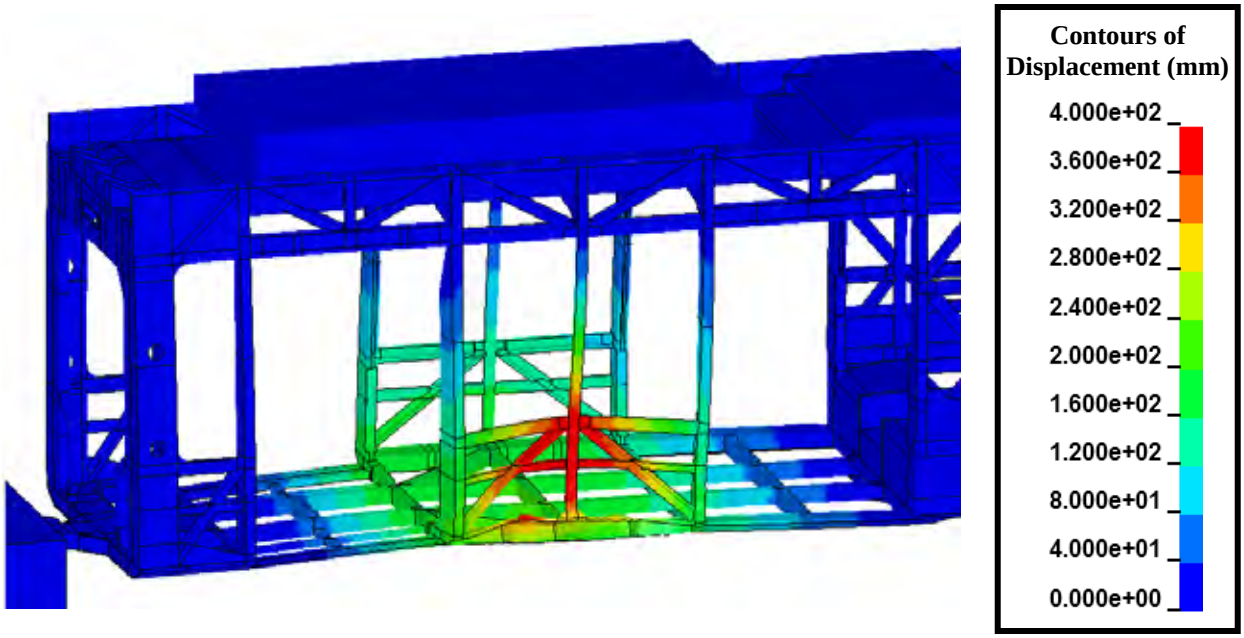

(b) 35 mph Impact

Figure 146. Calculated Crush in LRV 2 after 90 degree Side Impacts from HV 2.

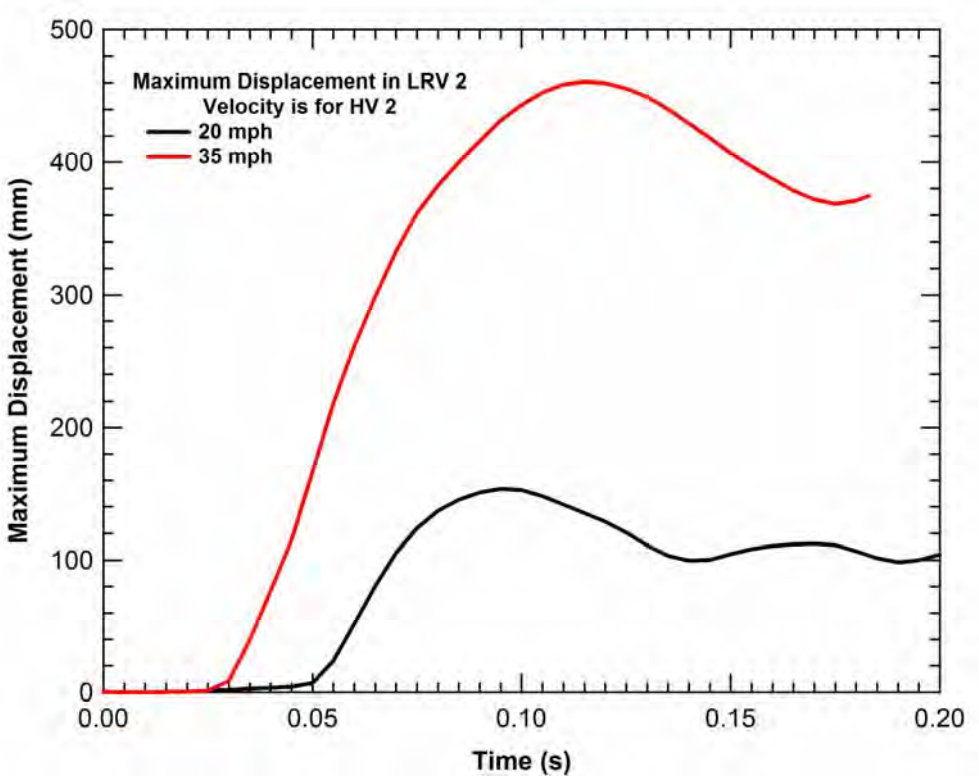

Figure 147. Crush Displacement Histories of LRV 2 during the 90 degree Impact from HV 2 at 20 and 35 mph.

2.10. Data Analysis of Collisions between LRVs and Automobiles

Accident statistics show that the vast majority of collisions involving an LRV do not involve another LRV. An automobile or truck was involved in 62% of cases reported to the Transit Cooperative Research Program [1], and pedestrians and cyclists were involved in 38% of cases. Slightly more pedestrians/cyclists than occupants of highway vehicles were killed. LRV to LRV collisions are so rare that they do not even figure in the statistics. It is probable that they do happen, but at relatively low speeds in the maintenance facility, when no passengers are on board.

An analysis method was identified to evaluate approaches for addressing the collisions with automobiles in the RT-1 Standard. In order to quantify the relationship between highway vehicle design and collision fatalities, automotive researchers defined the "aggressivity index" [7]. This index is the ratio of 'Driver Fatalities in Collision Partners' to 'Number of Crashes of Subject Vehicle'.

In this task, we attempted to apply the same statistical analysis methodology to determine the relative safety of different LRV designs in collisions with automobiles. The transit accident data collected in the US over the last decade has provided the type of information necessary to perform an assessment of the aggressivity of different LRV designs [1-5]. We can compare the aggressivity of LRVs with an enclosed front end design (e.g. Houston, Phoenix, Portland Streetcar) with that of LRVs with open front end designs and exposed couplers (e.g. Denver, Sacramento, San Jose), or those of hybrid geometry, such as Minneapolis, that have an enclosed rounded front end, but an exposed coupler. Using the relative aggressivity of different designs with the overall crash statistics of the industry would allow an assessment of the potential reduction in fatalities by modifying the standards on the vehicle front end profiles. We believe this analysis of the crash data would be helpful in developing LRV front end standards to include in RT-1.

The transit safety data is collected as part of the State Safety Oversight program [4]. The objective of the program is to collect data on collision incidents, injuries, and fatalities for different modes of transit and operations. The annual reports from this program do not split out the data sufficiently for the assessment of aggressivity. As part of this research effort, the data was obtained split out by the individual transit authorities. A summary of the data is provided in Table 20.

Table 20. Statistical Fatality Rates for LRV Incidents.

Fatality Rate per 100					
System	Incidents	Major Incidents	Fatalities	Rate per 100 Incidents	Rate per 100 Major Incidents
Dallas	55	54	3	5.5	5.6
Utah	31	31	0	0.0	0.0
San Francisco	113	62	2	1.8	3.2
Los Angeles	24	4	0	0.0	0.0
Houston	67	62	1	1.5	1.6
Southeastern PA	229	1	0	0.0	0.0
Seattle	22	8	0	0.0	0.0
MA Bay Transit	38	36	0	0.0	0.0
New Orleans	101	57	2	2.0	3.5
Allegheny County, PA	270	31	3	1.1	9.7
Sacramento	42	42	0	0.0	0.0
Cleveland	49	48	0	0.0	0.0
Tri-County District of OR	29	19	1	3.4	5.3

To develop valid conclusions on the aggressivity of different vehicle designs requires having sufficient data to be statistically significant. It also requires good quality data with similar data collection and reporting methodologies applied across different transit authorities. Both of these requirements are in question in the data that was collected. The highest number of fatalities for any of the systems during the reporting period is 3 and more than half of the transit systems had no fatalities. Similarly, there are characteristics of the data that indicate that the collection and reporting methodologies are inconsistent, making a comparison of the vehicle aggressivity invalid. However, they identify some of the issues with the State Safety Oversight program and suggest possibilities for future accident investigation work. Some additional training of the personnel in the transit systems collecting the accident data is needed. In addition, more detailed information on each of the major incidents should be collected. These include estimates of the impact conditions (orientation and speed) and an assessment of the damage to the highway vehicles from the collision. Standard methods for data collection can be developed from research programs looking at accidents and injuries in highway vehicle collisions and established accident reconstruction methodologies. Collecting more detailed data would allow for analyses of safety given the much smaller number of incidents that occur for LRV operations.

CHAPTER 3. Summary and Conclusions

In the initial phase of the study, available data was collected on LRV crashworthiness and safety. The accident data clearly indicated that the vast majority of the injuries and fatalities associated with LRV collisions were a result of collisions between LRVs and highway vehicles (and to a lesser extent with pedestrians and bicyclists).

Most of the experts contributing to the development of a safety standard for LRVs agree that the collisions between two LRVs represent a severe collision condition that can't be neglected. However, the accident data and collision analyses in this study indicate that the CEM requirements with the highest potential for safety improvements is in the specification of the LRV front-end characteristics to reduce the aggressivity in collisions with highway vehicles.

A statistical analysis was performed on the available collision data in order to assess the impact of LRV design features on crash safety. The quantity and quality of the data in the current accident reporting database was not sufficient to draw any meaningful conclusions at this time. However, this type of assessment has been very useful for other transit modes. A recommendation of this study is that additional efforts be made to improve the future accident reporting to support future LRV safety studies. This would include improved training to standardize accident reporting practice across different transit systems and more detailed accident reconstruction for the severe collisions.

In the remainder of this study, detailed crash analyses were performed for various LRV designs and collision conditions to evaluate the crashworthiness of current equipment and develop supporting information for the development of an LRV safety standard. The first series of these analyses was the evaluation of the collision response for compatible collisions between two identical LRVs at various collision speeds. These analyses establish the expected range of collision behaviors of current equipment. This range of collision behaviors can be used to guide the selection of crash scenarios (e.g. closing speeds) and acceptable outcomes (e.g. crush lengths) in the development of the CEM requirements in the LRV safety standard. Some specific findings from these compatible collisions include:

(1) The various LRV designs that are currently in use have a significant range of crush strengths and collision behaviors. Even vehicles that were designed to nearly identical specifications can have significantly different crush strengths. As a result, current design practice in the United States does not ensure crash compatibility in the existing LRV fleet. The type of incompatibility described here refers to the possibility that most or all of the crush deformation is localized to one of the colliding LRVs. This type of incompatibility is not necessarily a problem for many collisions if the damage remains in unoccupied regions of the vehicle. However, it can lead to higher injury potential in a more severe collision when the available crush zones in the lower strength vehicle are exhausted.

(2) Some of the LRV designs resulted in asymmetric crush lengths in the two vehicles in the compatible collision scenarios. Greater stability of the crush behavior could be obtained by including specifications on the compatibility of the two LRV crush lengths for these collision scenarios. The most common approach to meet this requirement is to design a crush response with an increasing crush load for larger crush distances. This crush profile is more stable and has been shown to be a favorable behavior for crash safety of rail vehicles. However, the complexity of the LRV cab structures and variations in LRV designs (e.g. rounded cab end structures and variable floor heights) makes the development of a steadily increasing crush strength profile much more difficult than for other rail vehicle types. Given the low probability of these severe LRV collisions the additional requirements on the crush profile may not be justified.

(3) The CEM design approach of modeling the collision of a moving LRV colliding with a stationary LRV with the brakes applied is capable of determining the crush modes, force-deflection characteristics, energy dissipation, and stability of the crush behaviors. Simplified analyses that apply the idealized collision of a single LRV colliding with a rigid wall do not allow for the development of asymmetric crush behaviors across the collision interface and may suppress some potential unstable crush modes. Therefore, it is recommended that CEM requirements in an LRV safety standard include collision analysis between moving and stationary LRVs (brakes applied on both) at various collision speeds.

(4) All of the vehicles had minimal damage at the 5 mph collision speed with damage limited to the anticlimber ribs and head girder. This suggests that a 5 mph collision requirement that results in no permanent damage to the vehicle is acceptable. Any energy dissipation requirements at this collision speed could be managed with existing coupler technologies or energy-absorbing bumper systems.

(5) All of the vehicles analyzed had crush behaviors that were generally acceptable up to a collision closing speed above 25 mph. The crush behaviors were all limited to a forward zone in the operator cabin and the average crush lengths in each LRV were approximately 400 mm. This suggests that a 25 mph collision scenario is an achievable level for a high-severity CEM requirement in a safety standard.

The last finding relates to the addition of a high-severity CEM requirement in the LRV safety standard. The associated costs and benefits of this requirement are under consideration within the LRV safety community. This requirement would certainly be beneficial for the design in the event that a future high-speed collision between two LRVs were to occur. Evaluating the high-speed collision behavior would also improve the robustness of the design for crashworthiness of collisions between LRVs at lower speeds. Plus, this study indicates that the higher speed collision scenario will not require large changes for most modern LRV designs (assuming that the acceptance criteria are not overly restrictive).

The arguments against the addition of the high speed collision scenario are that it is a more severe requirement than previously adopted in other international standards. In addition, the addition of this high-speed CEM requirement makes it more difficult to reduce the weight of the LRV designs. These costs become more are more difficult to justify since the past accident data indicates that a collision at a closing speed on the order of 25 mph is a very low probability.

To address the influence of buff strength requirements on the collision response, a vehicle design study was performed to modify an LRV with a 2g buff strength design into a vehicle with a 1g buff strength. The design study found that the 50% reduction in the buff strength requirement is expected to produce less than a 20% reduction in the crush strength. This variation in crush strength is significantly less than the difference in strengths typically seen between two different LRV designs with equivalent buff strengths. More importantly, the design study demonstrated that the CEM specifications (collisions at various speeds and acceptable outcomes) provided a much more stringent set of constraints on the crush behavior and vehicle design than the buff load specification. Thus if appropriate CEM requirements are included in a safety specification, the selection of the buff load requirement will have a negligible influence on the crash safety of the resulting LRVs.

A set of incompatible collisions (i.e. between different LRV designs) were also analyzed. These analyses confirmed the expected result that when two vehicles with different crush strengths collide, the weaker vehicle will have a significantly larger crush length and dissipate the majority of the collision energy. In extreme cases, the weaker vehicle will contribute most of the crush response. Again, this incompatibility is not necessarily a problem for many collisions if the damage remains in unoccupied regions of the vehicle. To ensure compatible behavior, much tighter controls on the acceptable force-crush behaviors would be required. Developing these tightly controlled crush behaviors would be very difficult for many existing LRV designs and would add significant cost (and potentially weight) to the LRV designs.

The final series of collision scenarios analyzed were between LRVs and highway vehicles. These are important collisions to evaluate since they represent the vast majority of LRV collisions and result in the majority of injuries and fatalities for LRV operations. Some specific findings from these collision analyses include:

(1) The addition of a bumper enclosure, resulting in a smooth LRV front-end profile and lower contact zone between the LRV and the automobile, has a significant potential for reducing injuries and fatalities in side collisions. Although further research into methodologies and equipment to protect automobile occupants in these collisions would be warranted, the analyses in this study suggest that modifications to the LRV geometric profile has the greatest potential for reducing the number of fatalities and severity of injuries in these collisions.

(2) In scenarios where a bumper enclosure is not compatible with the operational requirements, a pilot beam or other structures to engage the highway vehicle at a lower position in a collision was shown to have a significant safety benefit.

(3) An energy-absorbing bumper system that protects against a 5 mph LRV collision does not appear to offer much advantage in collisions with automobiles over the performance of a rigid bumper enclosure. The side crush strengths of automobiles, particularly for the oblique impact conditions, are sufficiently low that the energy absorbers would not be activated. Designing an energy-absorbing bumper to protect the automobile would require low force levels and a large stroke length for significant safety improvements.

(4) A bumper with an enclosed geometry that is less aggressive in collisions with automobiles and energy absorption be designed for the 5 mph LRV collision scenario combined would be an effective CEM requirement. This recommendation results from the significant safety improvements achieved in collisions with highway vehicles by the changes in the LRV front-end geometry and the difficulty in developing an energy-absorbing bumper system that will be universally effective for all collision scenarios.

REFERENCES

1. Transit Cooperative Research Program (TCRP) Report 69, Light Rail Service: Pedestrian and Vehicular Safety, National Academy Press, 2001.
2. Safety Management Information Statistics (SAMIS) 1997 Annual Report, U.S. Department of Transportation, Report No. FTA-MA-26-5002-99-01, DOT-VNTSC-FTA-99-3, March 1999.
3. National Transit Database (NTD) Data, http://www.ntdprogram.com/, Annual Data Tables.
4. Federal Transit Administration (FTA) State Safety Oversight Program, http://www.transit-safety.volpe.dot.gov/, 2003 Annual Report.
5. Bureau of Transportation Statistics (BTS), National Transportation Statistics 2005, http://www.bts.gov/publications/national_transportation_statistics/2005/, U.S. Department of Transportation (USDOT)
6. R.A. Arbelaez, B.C. Baker, J.M. Nolan, “Delta Vs for IIHS Side Impact Crash Tests and their Relationship to Real-World Crash Severity,” Insurance Institute for Highway Safety, Paper Number 05-0049.
7. Gabler, H.C. and Hollowell, W.T., “The Aggressivity of Light Trucks and Vans in Traffic Crashes”, Society of Automotive Engineers Paper No. 980908. February 1998.
8. LS-DYNA Keyword User’s Manual, Version 970, Livermore Software Technology Corporation, 2004.
9. Hallquist, J.O., “DYNA3D User’s Manual (Nonlinear, Dynamic Analysis of Solids in Three Dimensions),” University of California, Lawrence Livermore National Laboratory, Report UCID 19156, Revision 2, 1986.
10. “LS-DYNA Theoretical Manual,” Livermore Software Technology Corporation, May 1998.
11. S.W. Kirkpatrick and R.A. MacNeill, "Development of a Computer Model for Prediction of Collision Response of a Railroad Passenger Car,” Proceedings of: JRC2002, The 2002 ASME/IEEE Joint Rail Conference, April 23-25, 2002, Washington D.C.
12. S. Summers, A. Prasad, W.T. Hollowell, “NHTSA’s Compatibility Research Program Update,” Paper No. 01B-257, Society of Automotive Engineers, Warrendale, PA, 2000.
13. Severson, K., Tyrell, D., Perlman, A.B., “Collision Safety Comparison of Conventional and Crash Energy Management Passenger Rail Car Designs,” American Society of Mechanical Engineers, Paper No. JRC2003-1657, April 2003.
14. M. Carolan, A.B. Perlman, and D. Tyrell, "Performance Efficiency of a Crash Energy Management System," Proceedings of the 2007 ASME/IEEE Joint Rail Conference & Internal Combustion Engine Spring Technical Conference, JRCICE2007-40064, March 2007..
15. R. Grzebieta, C. Tingvall, and G. Rechnitzer, “Geometric Compatibility in Near Side Impact Crashes,” Monash University Accident Research Centre, Monash University, Clayton, Australia, Paper number 243.
16. John Swanson, “Light Rail Vehicles and Running Safety 2,” APTA Commuter Rail/Rail Transit Conference, June 2002
17. John D. Swanson, “Establishing the Needs - What Must We Design For?” Presentation to the RT-1 CEM Subcommittee Meeting, Colorado Springs, CO, September 30-October 2, 2003
18. Sacramento Bee, October 20, 2004, “Light Rail Train Crushes Automobile That Gets in the Way; Four Injured.”
19. S. Summers, A. Prasad, W.T. Hollowell, “NHTSA’s Vehicle Compatibility Research Program,” SAE Paper No. 1999-01-0071.